

UNIVERSITY OF NAPLES FEDERICO II
POLYTECHNIC AND BASIC SCIENCES SCHOOL

DEPARTMENT OF CHEMICAL SCIENCES



PH.D. IN CHEMICAL SCIENCES

SYNTHESIS AND BIOLOGICAL EVALUATION OF NOVEL
THERAPEUTIC CANDIDATES FOR THE TREATMENT
OF INFECTIOUS AND RARE DISEASES

ANNA ESPOSITO

XXXIII CYCLE 2018-2020

SUPERVISOR: PROF. ANNALISA GUARAGNA

*A mia madre,
per avermi mostrato che puoi farcela,
anche quando sembra impossibile*

UNIVERSITY OF NAPLES FEDERICO II

Polytechnic and Basic Sciences School

Ph.D. in Chemical Sciences – XXXIII Cycle



Ph.D. Student: Anna Esposito

Supervisor: Prof. Annalisa Guaragna

SYNTHESIS AND BIOLOGICAL EVALUATION OF NOVEL THERAPEUTIC CANDIDATES FOR THE TREATMENT OF INFECTIOUS AND RARE DISEASES

In the current PhD thesis, novel synthetic routes were developed and exploited for the synthesis of novel compounds with the aim to identify therapeutic candidates for the treatment of rare and infectious diseases. Particular attention was devoted to the synthesis of *N*-alkyl D- and L-deoxyiminosugars and their lipophilic conjugates, as well as of corticosteroid derivatives and nucleoside analogues for their use in the treatment of Cystic Fibrosis, a rare disease, and of bacterial and viral infections.

CYSTIC FIBROSIS

Cystic Fibrosis is a genetic rare disorder characterized by chronic infections and inflammation of the airways that represent the primary cause of mortality in CF patients.^{1,2} Accordingly, increasing attention is currently devoted to development of novel anti-inflammatory therapies aimed to ameliorate CF lung pathology. In search for novel targets and pathways involved in the inflammatory response in CF airway lung disease, a key role of the non-lysosomal glucosidase 2 (GBA2-encoded NLGase) in pro-inflammatory state characterizing CF cells has been recently highlighted.^{3,4} As matter of fact, Miglustat®, an *N*-alkylated D-iminosugar (D-NBDNJ, *N*-butyl-D-deoxynojirimycin, **2**) has been found to reduce the inflammatory response in *P. aeruginosa* infected CF bronchial cells, showing an interesting therapeutic potential of iminosugars (sugar analogues having an amino function in place of the endocyclic oxygen atom of the corresponding carbohydrate) in CF lung disease treatment.^{5,6} However, as widely reported, the poor *in vivo* selectivity of D-iminosugars hampers their long-term use as therapeutics.^{7,8} Conversely, their non-superimposable mirror image, L-iminosugars have shown higher selectivity acting as inhibitors or enhancers of glycosidases and glycosyltransferases.⁹ Based on these findings, in order to explore the role of iminosugar configuration on the therapeutic potential of these molecules in the treatment of CF lung inflammation, herein a novel synthetic procedure for the preparation of L-NBDNJ (*ent*-**2**), i.e. the enantiomer of the iminosugar drug Miglustat, and the *N*-alkylated iminosugars *ent*-**3-6** was studied (FIGURE 1).¹⁰

Particularly, use of polymer-supported triphenylphosphine/iodine (PS-TPP/I₂) system was conceived for the assembly of the alkyl chains on the unnatural L-DNJ (*ent*-**1**), in turn obtained from a *de novo* procedure.¹¹ *N*-alkyl L-deoxyiminosugars (*ent*-**2-6**) were evaluated *in vitro* for their inhibitory effect on NLGase and for their effect on the inflammatory response to *P.*

aeruginosa (the most predominant lung infection in CF), either alone or in synergistic combination with their D-enantiomers.

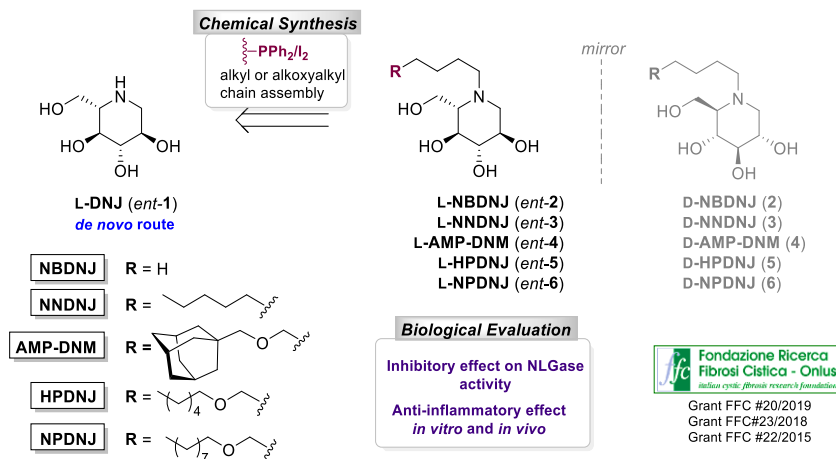


FIGURE 1. Synthesis of *N*-alkyl L-imosugars and biological evaluation for application in CF.

The anti-inflammatory effect of L-NBDNJ (*ent-2*) was also assessed in murine models of *P. aeruginosa* lung infection revealing a promising potential of this compound as anti-inflammatory agent in CF. In addition, an unexpected antibacterial activity of *ent-2* was observed *in vivo* leading us to explore the antibacterial potential of L-NBDNJ, as well as of the other *N*-alkyl L-imosugars.

This work was funded by Italian Cystic Fibrosis Research Foundation grants number FFC #20/2015, FFC #23/2018 and FFC#20/2019.

BACTERIAL INFECTIONS

Bacterial infections represent a serious threat to public health due to the emergence of antibiotic-resistant pathogens. In addition, bacteria ability to form biofilms increases the difficulties to eradicate pathogens leading to chronic and resistant infections. Therefore, development of novel candidates active against bacteria in planktonic state, as well as growing in biofilm, represents an important issue. In this context, our interest in the development of novel small molecules endowed with biological activity led us to identify two classes of compounds, *N*-alkyl-D- and L-imosugars and corticosteroid derivatives (FIGURES 2 and 3) as novel potential antibacterial and antibiofilm agents.

***N*-alkyl-D- and L-deoxyimosugars and their lipophilic derivatives.** Due to their ability to interact with carbohydrate-processing enzymes, iminosugars have displayed therapeutic potential against a broad range of diseases including malignancies, viral infections and genetic disorders.^{5,12,13} Conversely, only rarely they have been considered for their antibacterial activity showing, however, interesting pharmacological potential.^{14,15} On these bases, herein the therapeutic potential of *N*-alkyl deoxyimosugars as antibacterial agents was evaluated.

Particularly we evaluated the inhibition of *S. aureus* ATCC 29213 growth by D- and L-DNJ (**1**) and their *N*-alkyl derivatives (**2-6**; **FIGURE 1**),¹⁶ as well as of the cholesterol-bearing iminosugars **7** and **8** (**FIGURE 2**) in order to evaluate the role of both the chirality and of lipophilicity on the eventual anti-bacterial activity of these molecules.

The established PS-TPP/I₂ activating system was exploited for the conjugation of the iminosugars with the cholesteryl moiety enabling to obtain the target compounds in a one-pot procedure.¹⁷ All the iminosugars were screened against *S. aureus* ATCC 29213 as preliminary evaluation of the antimicrobial potential of these molecules.

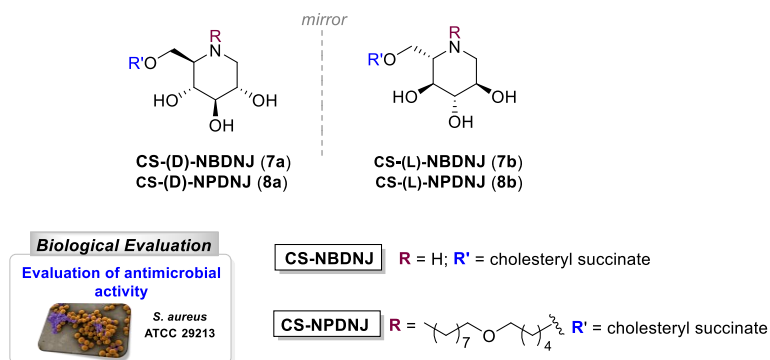


FIGURE 2. D- and L-DNJ and its *N*-alkyl derivatives as antimicrobial agents against *S. aureus*.

Deflazacort and its synthetic precursors. The excellent biological properties of the corticosteroid drug Deflazacort (DFZ, **9**, currently marketed for its anti-inflammatory and immunosuppressive activity and endowed with high efficacy and good tolerability)¹⁸ led us to develop a novel synthetic protocol for its preparation¹⁹ and to evaluate its activity against both Gram-positive and Gram-negative bacteria, as well as of some of its synthetic precursors²⁰⁻²² (**FIGURE 3**). Herein a fast and expeditious route to DFZ was explored, starting from 9-bromotriene acetate **10**, enabling a straightforward access to DFZ in only five reaction steps.

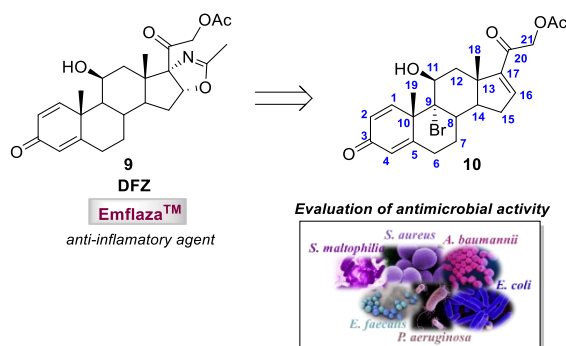


FIGURE 3. Synthesis and antimicrobial evaluation of Deflazacort and its precursors.

Biological assays were provided to assess the ability of DFZ and its synthetic precursors against Gram-positive and Gram-negative bacteria responsible for drug-resistant infections including *S. aureus*, *E. faecalis*, *A. baumannii*, *P. aeruginosa*, *E. coli*, *S. maltophilia* revealing an interesting activity as antibacterial and antibiofilm agent, not by DFZ but for one of its precursor.^{20–22}

VIRAL DISEASES

Over the past years, remarkable advancements have been achieved in antiviral drug discovery (about 90 antiviral drugs have been formally approved till 2016),²³ Nonetheless, viral diseases still represent a serious threat to public health. Hepatitis B (HBV), C (HCV) and the human immunodeficiency virus (HIV) even today cause millions of deaths every year,²⁴ while several outbreaks of (re-)emerging viruses for which no licensed treatments or vaccines exist, such as Dengue, Zika, Ebola, Chikungunya, West Nile, Yellow fever viruses, or the newly emerged coronavirus SARS-CoV-2 responsible for the ongoing COVID-19 pandemic, continue to affect the global health.^{25,26} Among the antiviral drugs currently available, nucleoside analogues (NAs) hold a privileged position becoming cornerstones of treatment of viral infections and still now, many efforts are devoted to the identification of more potent, selective and less toxic NAs.^{27,28} In this context, the synthesis of three classes of NAs has been herein explored.

D- and L-Cyclohexenyl Nucleosides and their ProTide derivatives. Cyclohexenyl nucleosides (FIGURE 4) represent well-known biomimetic agents, working as bioactive NAs, either at monomeric and oligomeric level, or as substrates/templates for enzymatic replication.²⁹ These properties are due to the capacity by the cyclohexenyl ring to act as a conformational bioisostere of natural deoxyribose. Indeed, the flexible nature of cyclohexenyl nucleosides, rapidly fluctuating between the low energy ²H₃ and ³H₂ conformations, enables a close resemblance with the bioactive sugar ring pucker (²T₃ and ³T₂) of natural nucleosides.

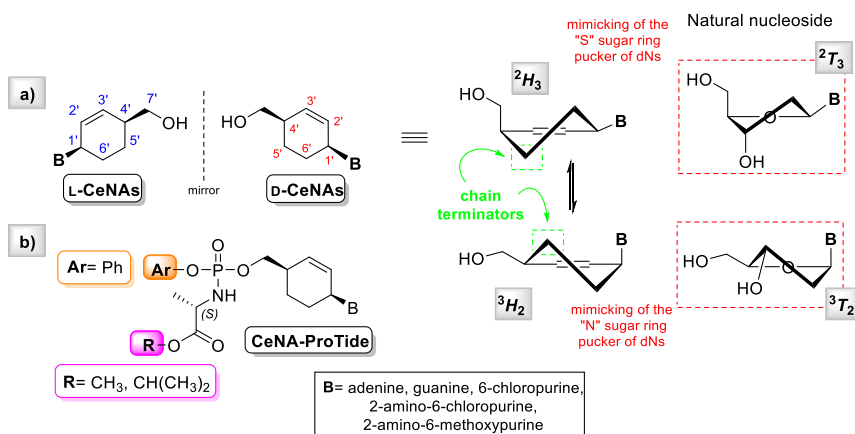


FIGURE 4. a) CeNAs as conformational mimetics of natural nucleosides. b) Application of ProTide Technology to CeNAs.

With the aim to expand the repertoire of these bioactive nucleosides, we synthesized novel cyclohexenyl nucleosides **D-CeNAs** and **L-CeNAs** (**FIGURE 4**) lacking the OH group at C5' position and therefore being conceived to act as antiviral agents by chain termination mechanism.^{27,30}

Different CeNA derivatives, bearing pyrimidine nucleobases, were herein synthesized (**FIGURE 4a**) along with early examples of their corresponding ProTides (**FIGURE 4b**) with the aim to explore the potential of this technology applied to our nucleosides in terms of biological activity. Preliminary biological evaluation of synthesized nucleosides was also provided in order to assess their antiviral properties against DNA and RNA viruses.

Piperidine-based Nucleosides. At the basis of the design of efficient NAs, there is the idea of obtaining molecules acting as conformational mimics of natural nucleosides.³¹ Indeed, it is widely recognized that the conformation adopted by sugar unit of NAs plays a crucial role in the enzyme-substrate recognition phase. In this context a successful strategy relies on the replacement of natural furanose ring with a six-membered sugar moiety leading to conformationally restricted nucleoside analogues.^{32,33} On these bases and considering the excellent properties exhibited by the iminosugar-based nucleosides, a synthetic approach aimed at the preparation of novel aza-*C*-nucleosides, **11** and **12**, has been herein studied. These compounds have been conceived as analogues of the bioactive Immucillin A,^{34,35} mimicking its structure and conformational properties (**FIGURE 5**).

Particularly in early studies, nucleoside **11**, bearing the natural adenine as nucleobase, was synthesized in order to tune up the synthetic strategy aimed at the preparation of the more complex analogues equipped with the unnatural 9-deazapurine nucleobase (e.g. **12**), as well as to study the conformational behavior of this piperidine-based nucleosides. Indeed, these analogues were conceived to be frozen in a ¹C₄ conformation closely related to the bioactive ₃E conformation of Immucillins (**FIGURE 5**). Piperidine nucleosides **11** and **12** will be evaluated for their potential as RNA polymerase inhibitors against a wide range of RNA viruses including SARS-CoV-2.

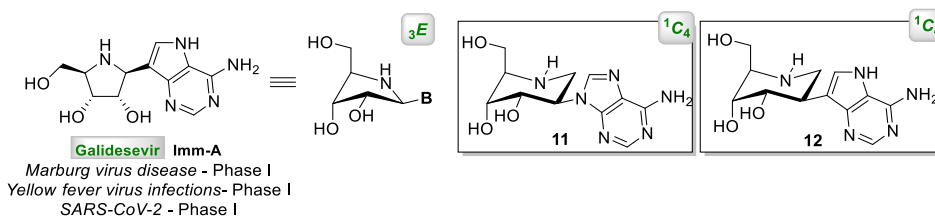


FIGURE 5. Imm-A and the corresponding piperidine-based analogues **11** and **12**.

Propargylated Purine Nucleosides. Pathogenesis of most viruses-caused diseases is poorly understood because of limited knowledge about life cycle and host-interaction of most viruses; therefore, viral DNA/RNA labelling strategies are indispensable to develop novel therapeutic candidates for the treatment of viral diseases.³⁶ Other than to their antiviral potential, also in this context, NAs hold an important position. Indeed, over the last years, they have been successfully applied to elucidate the biology of several viruses.³⁷ However, the major limitation of these techniques is often the lack of selectivity for tracking of viral replication.³⁸ With the aim to obtain

virus-specific nucleoside analogues for *in vivo* replication visualization, a set of novel propargyl-containing nucleosides (**13-20**; **FIGURE 6**) was herein prepared with the aim to obtain clickable nucleoside analogues, which would be selectively incorporated into the viral genome without causing off-target labelling of cellular DNA/RNA.

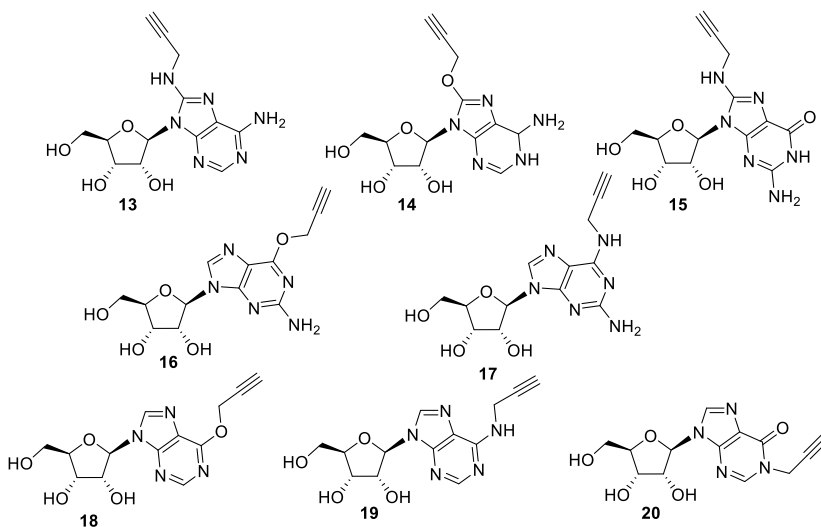


Figure 6.4 Propargyl-containing nucleosides for visualization of viral RNA replication.

Particularly, propargyl moiety was introduced at C8 or C6 position of the nucleobase through either C-N or C-O bond, starting from adenosine, guanosine and inosine. Preliminary biological data to assess the cell cytotoxicity and antiviral properties of the compounds against Zika virus (ZKV, as an example of *Flaviviruses*) were also provided.

This study is part of a research project developed by Prof. Arthur Van Aerschot (Medicinal Chemistry, Rega Institute for Medical Research, Department of Pharmaceutical and Pharmacological Sciences, KU Leuven) and therefore, was carried out under his supervision, at Rega Institute, KU Leuven in Belgium.

REFERENCES

- (1) Cutting, G. R. Cystic Fibrosis Genetics: From Molecular Understanding to Clinical Application. *Nat. Rev. Genet.* **2015**, *16* (1), 45–56. <https://doi.org/10.1038/nrg3849>.
- (2) Elborn, J. S. Cystic Fibrosis. *Lancet* **2016**, *388* (10059), 2519–2531. [https://doi.org/10.1016/S0140-6736\(16\)00576-6](https://doi.org/10.1016/S0140-6736(16)00576-6).
- (3) Loberto, N.; Tebon, M.; Lampronti, I.; Marchetti, N.; Aureli, M.; Bassi, R.; Giri, M. G.; Bezzerri, V.; Lovato, V.; Cantù, C.; Munari, S.; Cheng, S. H.; Cavazzini, A.; Gambari, R.; Sonnino, S.; Cabrini, G.; Dehecchi, M. C. GBA2-Encoded β -Glucosidase Activity Is Involved in the Inflammatory Response to *Pseudomonas Aeruginosa*. *PLoS One* **2014**, *9* (8), e104763. <https://doi.org/10.1371/journal.pone.0104763>.
- (4) Chiricozzi, E.; Loberto, N.; Schiumarini, D.; Samarani, M.; Mancini, G.; Tamanini, A.; Lippi, G.;

- Dehecchi, M. C.; Bassi, R.; Giussani, P.; Aureli, M. Sphingolipids Role in the Regulation of Inflammatory Response: From Leukocyte Biology to Bacterial Infection. *J. Leukoc. Biol.* **2018**, *103* (3), 445–456. <https://doi.org/10.1002/JLB.3MR0717-269R>.
- (5) Esposito, A.; D'Alonzo, D.; De Fenza, M.; De Gregorio, E.; Tamanini, A.; Lippi, G.; Dehecchi, M. C.; Guaragna, A. Synthesis and Therapeutic Applications of Iminosugars in Cystic Fibrosis. *Int. J. Mol. Sci.* **2020**, *21* (9), 3353. <https://doi.org/10.3390/ijms21093353>.
- (6) Dehecchi, M. C.; Nicolis, E.; Norez, C.; Bezzerri, V.; Borgatti, M.; Mancini, I.; Rizzotti, P.; Ribeiro, C. M. P.; Gambari, R.; Becq, F.; Cabrini, G. Anti-Inflammatory Effect of Miglustat in Bronchial Epithelial Cells. *J. Cyst. Fibros.* **2008**, *7* (6), 555–565. <https://doi.org/10.1016/j.jcf.2008.06.002>.
- (7) Compain, Philippe; Martin, O. *Iminosugars: From Synthesis to Therapeutic Applications*; Compain, P., Martin, O. R., Eds.; John Wiley & Sons, Ltd: Chichester, UK, 2007. <https://doi.org/10.1002/9780470517437>.
- (8) Nash, R. J.; Kato, A.; Yu, C. Y.; Fleet, G. W. Iminosugars as Therapeutic Agents: Recent Advances and Promising Trends. *Future Med. Chem.* **2011**, *3* (12), 1513–1521. <https://doi.org/10.4155/fmc.11.117>.
- (9) D'Alonzo, D.; Guaragna, A.; Palumbo, G. Glycomimetics at the Mirror: Medicinal Chemistry of L-Iminosugars. *Curr. Med. Chem.* **2009**, *16* (4), 473–505. <https://doi.org/10.2174/092986709787315540>.
- (10) De Fenza, M.; D'Alonzo, D.; Esposito, A.; Munari, S.; Loberto, N.; Santangelo, A.; Lampronti, I.; Tamanini, A.; Rossi, A.; Ranucci, S.; De Fino, I.; Bragonzi, A.; Aureli, M.; Bassi, R.; Tironi, M.; Lippi, G.; Gambari, R.; Cabrini, G.; Palumbo, G.; Dehecchi, M. C.; Guaragna, A. Exploring the Effect of Chirality on the Therapeutic Potential of N-Alkyl-Deoxyiminosugars: Anti-Inflammatory Response to Pseudomonas Aeruginosa Infections for Application in CF Lung Disease. *Eur. J. Med. Chem.* **2019**, *175*, 63–71. <https://doi.org/10.1016/j.ejmech.2019.04.061>.
- (11) D'Alonzo, D.; De Fenza, M.; Porto, C.; Iacono, R.; Huebecker, M.; Cobucci-Ponzano, B.; Priestman, D. A.; Platt, F.; Parenti, G.; Moracci, M.; Palumbo, G.; Guaragna, A. N-Butyl-l-Deoxynojirimycin (l-NBDNJ): Synthesis of an Allosteric Enhancer of α -Glucosidase Activity for the Treatment of Pompe Disease. *J. Med. Chem.* **2017**, *60* (23), 9462–9469. <https://doi.org/10.1021/acs.jmedchem.7b00646>.
- (12) Alonzi, D. S.; Scott, K. A.; Dwek, R. A.; Zitzmann, N. Iminosugar Antivirals: The Therapeutic Sweet Spot. *Biochem. Soc. Trans.* **2017**, *45* (2), 571–582. <https://doi.org/10.1042/BST20160182>.
- (13) Winchester, B. G. Iminosugars: From Botanical Curiosities to Licensed Drugs. *Tetrahedron Asymmetry* **2009**, *20* (6–8), 645–651. <https://doi.org/10.1016/j.tetasy.2009.02.048>.
- (14) Hasan, S.; Singh, K.; Danisuddin, M.; Verma, P. K.; Khan, A. U. Inhibition of Major Virulence Pathways of Streptococcus Mutans by Quercitrin and Deoxynojirimycin: A Synergistic Approach of Infection Control. *PLoS One* **2014**, *9* (3), 1–12. <https://doi.org/10.1371/journal.pone.0091736>.
- (15) Greimel, P.; Spreitz, J.; Stutz, A.; Wrodnigg, T. Iminosugars and Relatives as Antiviral and Potential Anti-Infective Agents. *Curr. Top. Med. Chem.* **2005**, *3* (5), 513–523. <https://doi.org/10.2174/1568026033452456>.
- (16) De Gregorio, E.; Esposito, A.; Vollaro, A.; De Fenza, M.; D'Alonzo, D.; Migliaccio, A.; Iula, V. D.; Zarrilli, R.; Guaragna, A. N-Nonyloxypentyl-l-Deoxynojirimycin Inhibits Growth, Biofilm Formation and Virulence Factors Expression of Staphylococcus Aureus. *Antibiotics* **2020**, *9* (6), 362. <https://doi.org/10.3390/antibiotics9060362>.
- (17) Esposito, A.; D'Alonzo, D.; D'Errico, S.; De Gregorio, E.; Guaragna, A. Toward the Identification of Novel Antimicrobial Agents: One-Pot Synthesis of Lipophilic Conjugates of N-Alkyl d- and l-Iminosugars. *Mar. Drugs* **2020**, *18* (11), 572. <https://doi.org/10.3390/md18110572>.
- (18) Parente, L. Deflazacort: Therapeutic Index, Relative Potency and Equivalent Doses versus Other Corticosteroids. *BMC Pharmacol. Toxicol.* **2017**, *18* (1), 1–8. <https://doi.org/10.1186/s40360-016-0111-8>.
- (19) Esposito, A.; De Gregorio, E.; De Fenza, M.; D'Alonzo, D.; Satawani, A.; Guaragna, A. Expedient Synthesis and Preliminary Antimicrobial Activity of Deflazacort and Its Precursors. *RSC Adv.* **2019**, *9* (37), 21519–21524. <https://doi.org/10.1039/C9RA03673C>.
- (20) Esposito, A.; Vollaro, A.; Esposito, E. P.; D'Alonzo, D.; Guaragna, A.; Zarrilli, R.; De Gregorio,

- E. Antibacterial and Antivirulence Activity of Glucocorticoid PYED-1 against *Stenotrophomonas Maltophilia*. *Antibiotics* **2020**, *9* (3), 105. <https://doi.org/10.3390/antibiotics9030105>.
- (21) Vollaro, A.; Esposito, A.; Antonaki, E.; Iula, V. D.; D'Alonzo, D.; Guaragna, A.; De Gregorio, E. Steroid Derivatives as Potential Antimicrobial Agents against *Staphylococcus Aureus* Planktonic Cells. *Microorganisms* **2020**, *8* (4), 468. <https://doi.org/10.3390/microorganisms8040468>.
- (22) Vollaro, A.; Esposito, A.; Esposito, E. P.; Zarrilli, R.; Guaragna, A.; De Gregorio, E. PYED-1 Inhibits Biofilm Formation and Disrupts the Preformed Biofilm of *Staphylococcus Aureus*. *Antibiotics* **2020**, *9* (5), 240. <https://doi.org/10.3390/antibiotics9050240>.
- (23) De Clercq, E.; Li, G. Approved Antiviral Drugs over the Past 50 Years. *Clin. Microbiol. Rev.* **2016**, *29* (3), 695–747. <https://doi.org/10.1128/CMR.00102-15>.
- (24) Leoni, M. C.; Ustianowski, A.; Farooq, H.; Arends, J. E. HIV, HCV and HBV: A Review of Parallels and Differences. *Infect. Dis. Ther.* **2018**, *7* (4), 407–419. <https://doi.org/10.1007/s40121-018-0210-5>.
- (25) Ji, X.; Li, Z. Medicinal Chemistry Strategies toward Host Targeting Antiviral Agents. *Med. Res. Rev.* **2020**, *40* (5), 1519–1557. <https://doi.org/10.1002/med.21664>.
- (26) Hu, B.; Guo, H.; Zhou, P.; Shi, Z. L. Characteristics of SARS-CoV-2 and COVID-19. *Nat. Rev. Microbiol.* **2020**, No. December. <https://doi.org/10.1038/s41579-020-00459-7>.
- (27) Seley-Radtke, K. L.; Yates, M. K. The Evolution of Nucleoside Analogue Antivirals: A Review for Chemists and Non-Chemists. Part I: Early Structural Modifications to the Nucleoside Scaffold. *Antiviral Res.* **2018**, *154* (March), 66–86. <https://doi.org/10.1016/j.antiviral.2018.04.004>.
- (28) Yates, M. K.; Seley-Radtke, K. L. The Evolution of Antiviral Nucleoside Analogues: A Review for Chemists and Non-Chemists. Part II: Complex Modifications to the Nucleoside Scaffold. *Antiviral Res.* **2019**, *162* (October 2018), 5–21. <https://doi.org/10.1016/j.antiviral.2018.11.016>.
- (29) Herdewijn, P. The Interplay between Antiviral Activity, Oligonucleotide Hybridisation and Nucleic Acids Incorporation Studies. *Antiviral Res.* **2006**, *71* (2-3 SPEC. ISS.), 317–321. <https://doi.org/10.1016/j.antiviral.2006.04.004>.
- (30) De Clercq, E.; Neyts, J. Antiviral Agents Acting as DNA or RNA Chain Terminators. *Handb. Exp. Pharmacol.* **2009**, *189*, 53–84. https://doi.org/10.1007/978-3-540-79086-0_3.
- (31) Burai Patrascu, M.; Malek-Adamian, E.; Damha, M. J.; Moitessier, N. Accurately Modeling the Conformational Preferences of Nucleosides. *J. Am. Chem. Soc.* **2017**, *139* (39), 13620–13623. <https://doi.org/10.1021/jacs.7b07436>.
- (32) Verheggen, I.; Van Aerschot, A.; Toppet, S.; Snoeck, R.; Janssen, G.; Balzarini, J.; De Clercq, E.; Herdewijn, P. Synthesis and Antih herpes Virus Activity of 1,5-Anhydrohexitol Nucleosides. *J. Med. Chem.* **1993**, *36* (14), 2033–2040. <https://doi.org/10.1021/jm00066a013>.
- (33) Herdewijn, P. *Nucleic Acids with a Six-Membered “carbohydrate” Mimic in the Backbone*; 2010; Vol. 7. <https://doi.org/10.1002/cbdv.200900185>.
- (34) Evans, G. B.; Tyler, P. C.; Schramm, V. L. Immucillins in Infectious Diseases. *ACS Infect. Dis.* **2018**, *4* (2), 107–117. <https://doi.org/10.1021/acsinfecdis.7b00172>.
- (35) Taylor, R.; Kotian, P.; Warren, T.; Panchal, R.; Bavari, S.; Julander, J.; Dobo, S.; Rose, A.; El-Kattan, Y.; Taubenheim, B.; Babu, Y.; Sheridan, W. P. BCX4430 - A Broad-Spectrum Antiviral Adenosine Nucleoside Analog under Development for the Treatment of Ebola Virus Disease. *J. Infect. Public Health* **2016**, *9* (3), 220–226. <https://doi.org/10.1016/j.jiph.2016.04.002>.
- (36) Liu, X.; Ouyang, T.; Ouyang, H.; Ren, L. Single Particle Labeling of RNA Virus in Live Cells. *Virus Res.* **2017**, *237* (March), 14–21. <https://doi.org/10.1016/j.virusres.2017.05.007>.
- (37) Müller, T.; Sakin, V.; Müller, B. A Spotlight on Viruses—Application of Click Chemistry to Visualize Virus-Cell Interactions. *Molecules* **2019**, *24* (3), 481. <https://doi.org/10.3390/molecules24030481>.
- (38) Ligasová, A.; Liboska, R.; Friedecký, D.; Mičová, K.; Adam, T.; Ozdian, T.; Rosenberg, I.; Koberna, K. Dr Jekyll and Mr Hyde: A Strange Case of 5-Ethynyl-2'-Deoxyuridine and 5-Ethynyl-2'-Deoxycytidine. *Open Biol.* **2016**, *6* (1). <https://doi.org/10.1098/rsob.150172>.

LIST OF ABBREVIATIONS

Ac	Acetyl group
ACV	Acyclovir
AMP-DNM	<i>N</i> -(5-adamantane-1-yl-methoxypentyl)-deoxynojirimycin
Bn	Benzyl
Boc	<i>t</i> -Butoxycarbonyl group
BuLi	<i>n</i> -Butyllithium
BVDU	Brivudin
Bz	Benzoyl
CeNA	Cyclohexenyl Nucleoside Analogue
Cer	Ceramide
CerGlcT	Ceramide GlucosylTransferase
CF	Cystic Fibrosis
CFTR	Cystic Fibrosis Transmembrane Conductance Regulator
CMV	Citomegalovirus
<i>m</i> -CPBA	<i>m</i> -chloroperbenzoic acid
DBU	1,8-diazobicyclo[5.4.0]undec-7-ene
DEAD	Diethyl azodicarboxylate
DGJ	Deoxygalactonojirimycin
DIAD	Diisopropyl azodicarboxylate
DIPEA	Diisopropylethylamine
DMAP	Dimethylaminopyridine
DCM	Dichloromethane
DMF	<i>N,N</i> - dimethylformamide
DMP	Dimethoxypropane
DMSO	Dimethyl Sulfoxide
DNA	Deoxyribonucleic Acid

DNJ	Deoxy-nojirimycin
EC ₅₀	Half maximal effective concentration
<i>ee</i>	Enantiomeric excess
ER	Endoplasmic Reticulum
Et ₂ O	Diethyl ether
EtOAc	Ethyl acetate
FDA	Food and Drug Administration
GAA	Scid α -glucosidase
GCS	Ceramide glucosyltransferase
GCV	Ganciclovir
HBV	Hepatitis B Virus
HCV	Hepatitis C Virus
HHV	Human Herpes Viruses
HIV	Human Immunodeficiency Virus
HPDNJ	<i>N</i> -[5-(Hexoxy)pentyl]-deoxynojirimycin
HSV-1	Herpes Simplex Virus - Type 1
HSV-2	Herpes Simplex Virus -Type 2
IC ₅₀	Half maximal inhibitory concentration
IL-8	Interleukin-8
J	Coupling constant
LSD	Lysosomal Storage Disorder
Me	Methyl
MeOH	Methanol
MeONa	Sodium Methoxyde
NAs	Nucleoside Analogues
Ni/Ra	Raney Nickel
NLGase	Non-lysosomal β -glucosidase 2

NJ	Nojirimycin
NMR	Nuclear Magnetic Resonance Spectroscopy
NBDNJ	<i>N</i> -Butyl-deoxynojirimycin
NPDNJ	<i>N</i> -[5-(Nonyloxy)pentyl]deoxynojirimycin
NNDNJ	<i>N</i> -Nonyl-deoxynojirimycin
PD	Pompe Disease
PNP	Purine Nucleoside Phosphorylase
PPh ₃	Triphenylphosphine
Ppm	Parts per million
PS-TPP	Polymer-supported triphenylphosphine
Py	Pyridine
rhGAA	Recombinant human acid α -glucosidase
RNA	Ribose Nucleic Acid
RT	Reverse Transcriptase
TBAF	Tetrabutylammonium fluoride
TBDMS	<i>t</i> -butyldimethylsilyl group
TEA	Triethylamine
THF	Tetrahydrofuran
TLC	Thin Layer Chromatography
TPP	Triphenylphosphine
VZV	Varicella Zoster Virus

TABLE OF CONTENTS

PREFACE	1
CYSTIC FIBROSIS	2
1 N-ALKYL-DEOXYIMINOSUGARS AS ANTI-INFLAMMATORY AGENTS FOR APPLICATION IN CYSTIC FIBROSIS	4
1.1 INTRODUCTION	4
1.1.1 CYSTIC FIBROSIS	4
1.1.1.1 THERAPEUTIC APPROACHES FOR CYSTIC FIBROSIS TREATMENT	5
1.1.2 IMINOSUGARS: POWERFUL GLYCOMIMETICS.....	6
1.1.2.1 PHARMACOLOGICAL APPLICATIONS OF IMINOSUGARS	8
1.1.2.2 IMINOSUGARS IN CYSTIC FIBROSIS	9
1.1.2.3 IMPROVING ENZYMATIC SELECTIVITY OF IMINOSUGARS: ROLE OF THE LIPOPHILICITY AND OF CONFIGURATION	11
1.2 RESULTS AND DISCUSSION.....	14
1.2.1 SYNTHESIS OF <i>N</i> -ALKYL L-DEOXYIMINOSUGARS	15
1.2.2 BIOLOGICAL EVALUATION	17
1.3 CONCLUDING REMARKS	20
1.4 EXPERIMENTAL SECTION.....	21
1.5 BIBLIOGRAPHY	26
BACTERIAL INFECTIONS.....	34
2 N-ALKYL-DEOXYIMINOSUGARS AND THEIR LIPOPHILIC CONJUGATES AS NOVEL ANTIBACTERIAL AGENTS.....	36
2.1 INTRODUCTION.....	36
2.1.1 ANTIMICROBIAL RESISTANCE: A GLOBAL THREAT.....	36
2.1.2 ANTIBIOTIC RESISTANT PATHOGENS	37
2.1.3 IMINOSUGARS AS ANTIBACTERIAL AND ANTIBIOFILM AGENTS.....	39
2.2 RESULTS AND DISCUSSION.....	40
2.2.1 SYNTHESIS OF LIPOPHILIC CONJUGATES OF <i>N</i> -ALKYL IMINOSUGARS.....	41
2.2.2 BIOLOGICAL EVALUATION	44
2.3 CONCLUDING REMARKS	47
2.4 EXPERIMENTAL SECTION.....	48
2.5 BIBLIOGRAPHY	50
3 SYNTHESIS AND ANTIBACTERIAL ACTIVITY OF DEFLAZACORT AND ITS SYNTHETIC PRECURSORS.....	54
3.1 INTRODUCTION.....	54

3.1.1	PHARMACOLOGICAL PROPERTIES OF NATURAL AND SYNTHETIC CORTICOSTEROIDS	.54
3.1.2	DEFLAZACORT: A POWERFUL GLUCOCORTICOID	55
3.1.2.1	SYNTHETIC APPROACHES TO DEFLAZACORT	56
3.1.2.1	ANTIBACTERIAL ACTIVITY OF CORTICOSTEROIDS	57
3.2	RESULTS AND DISCUSSION	58
3.2.1	SYNTHETIC APPROACH TO DEFLAZACORT	58
3.2.2	BIOLOGICAL EVALUATION	62
3.3	CONCLUDING REMARKS	68
3.4	EXPERIMENTAL SECTION	68
3.5	BIBLIOGRAPHY	72
	VIRAL DISEASES	76
4	SYNTHESIS OF CYCLOHEXENYL NUCLEOSIDES AND THEIR PROTIDE DERIVATIVES AS NOVEL ANTIVIRAL AGENTS	78
4.1	INTRODUCTION	78
4.1.1	NUCLEOSIDE ANALOGUES AS ANTIVIRAL AGENTS	78
4.1.2	SUGAR-MODIFIED NUCLEOSIDES	79
4.1.2.1	CARBOCYCLIC NUCLEOSIDES	80
4.1.2.2	BRIEF OVERVIEW ON THE SYNTHETIC APPROACHES FOR THE SYNTHESIS OF CARBOCYCLIC NUCLEOSIDES	81
4.1.2.3	CYCLOHEXENYL NUCLEOSIDES	83
4.1.3	FROM NUCLEOSIDE ANALOGUES TO THEIR PRODRUGS: THE PROTIDE APPROACH	85
4.2	RESULTS AND DISCUSSION	88
4.2.1	SYNTHESIS OF D- AND L-CYCLOHEXENYL NUCLEOSIDES	89
4.2.1.1	ENANTIOSELECTIVE SYNTHESIS OF THE CYCLOHEXENYL MOIETY	89
4.2.1.2	NUCLEOSIDE SYNTHESIS: TSUJI-TROST REACTION	90
4.2.2	SYNTHESIS OF CYCLOHEXENYL NUCLEOSIDE PROTIDE	94
4.2.3	BIOLOGICAL EVALUATION OF CYCLOHEXENYL NUCLEOSIDES	97
4.3	CONCLUDING REMARKS	100
4.4	EXPERIMENTAL SECTION	101
4.5	BIBLIOGRAPHY	113
5	SYNTHESIS OF PIPERIDINE-BASED NUCLEOSIDES: MIMICKING THE BIOACTIVE CONFORMATION OF IMMUCILLIN-A	117
5.1	INTRODUCTION	117
5.1.1	THE ROLE OF SUGAR CONFORMATION IN THE ACTIVITY OF NUCLEOSIDE ANALOGUES	117
5.1.2	C-NUCLEOSIDES	120
5.1.2.1	PYRROLIDINE-BASED NUCLEOSIDE ANALOGUES: IMMUCILLINS	121
5.1.2.1	SYNTHETIC ROUTES TO IMMUCILLINS	122

5.2	RESULTS AND DISCUSSION.....	124
5.2.1	SYNTHESIS OF PIPERIDINYL NUCLEOSIDES AS ANALOGUES OF BIOACTIVE IMMUCILLIN A	124
5.2.2	SYNTHESIS OF IMMUCILLIN A ANALOGUE BEARING NATURAL ADENINE	125
5.2.2.1	CONFORMATIONAL ANALYSIS OF IMMUCILLIN A ANALOGUE.....	126
5.2.3	SYNTHESIS OF IMMUCILLIN ANALOGUE BEARING 9-DEAZAPURINE	127
5.3	CONCLUDING REMARKS	130
5.4	EXPERIMENTAL SECTION.....	131
5.5	BIBLIOGRAPHY	135
6	SYNTHESIS OF PROPARGYLATED NUCLEOSIDE ANALOGUES FOR VISUALIZATION OF VIRAL REPLICATION	140
6.1	INTRODUCTION.....	140
6.1.1	TRACKING VIRAL GENOME	140
6.1.1.1	VIRAL GENOME VISUALIZATION BY CLICK CHEMISTRY	141
6.1.1.2	PROPARGYLATED PURINE DEOXYNUCLEOSIDES FOR VISUALIZATION OF HIV-1 REPLICATION.....	142
6.2	RESULTS AND DISCUSSION.....	144
6.2.1	SYNTHESIS OF PROPARGYL-CONTAINING NUCLEOSIDES	144
6.2.1.1	SYNTHESIS OF PROPARGYLATED ADENOSINE AND GUANOSINE ANALOGUES	145
6.2.1.2	SYNTHESIS OF PROPARGYLATED INOSINE ANALOGUES	147
6.2.2	PRELIMINARY BIOLOGICAL ASSAYS.....	148
6.3	CONCLUDING REMARKS	149
6.4	EXPERIMENTAL SECTION.....	150
6.5	BIBLIOGRAPHY	160
	APPENDIX A	164

PREFACE

Over the years introduction of innovative approaches and technologies in drug discovery and development has enabled the identification of several compounds of pharmaceutical interest. Accordingly, several novel life-changing medicines have been introduced on the market improving the health-quality and increasing the life-expectancy worldwide. For example, medications are transforming many cancers into treatable diseases or have dramatically improved the survival rate for people affected by human immunodeficiency virus (HIV), as well as are offering new options for patients affected by rare diseases.

Organic chemistry and asymmetric synthesis play a key role in the drug discovery process particularly in its early stages. On one hand, synthetic chemistry enables the preparation of bioactive naturally occurring compounds. On the other hand, starting from promising drug candidates, change in stereochemistry, geometry, functional groups or new chemical bond formation allow the synthesis of analogues with improved pharmacological properties and/or lower toxicity. As an example, from the discovery of penicillin in 1930s, identification of novel synthetic methods gave access to the preparation of analogue fused β -lactams opening the way for the antibiotic drug discovery. Analogously, innovative synthetic methodologies have been used for the preparation of targeted successful drugs for the treatment of chronic hepatitis C infections (HCV).

In this PhD thesis, synthetic chemistry has been used as tool for the preparation of novel molecules endowed with therapeutic potential, in different medical contexts, with focus on rare and infectious diseases. Stereoselective synthetic methodologies have been herein exploited to obtain compounds with selected features that would improve pharmacological activity and biological selectivity for the target pathogens or host enzymes. On the bases of the targeted disease for which compounds have been conceived, this thesis consists of three main sections.

The *first section* is focused on Cystic Fibrosis (CF), a rare genetic disorder characterized by chronic infection and inflammation of the airways. Herein, the stereoselective synthesis of the unnatural *N*-alkyl-L-deoxyimosugars has been considered for their application as anti-inflammatory agents in CF.

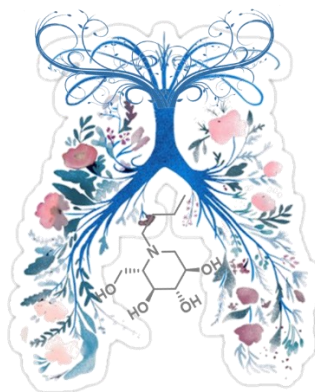
In the *second section*, the synthesis of novel candidates for the treatment of bacterial infections has been reported with the aim to identify alternative therapeutics to face with the serious and global threat of antibacterial resistance. To this purpose, *N*-alkyl D- and L-deoxyimosugars and their cholesteryl-bearing derivatives were considered for their application as inhibitor of bacterial growth. On the other hand, a novel synthetic route aimed to the preparation of the corticosteroid drug Deflazacort has been explored for it repurposing as antibacterial agent.

In the *last section*, the attention has been focused on synthesis of nucleoside analogues for their use in viral diseases. Sugar modified nucleosides have been synthesized as potential tools to selectively target viral polymerases, acting as antiviral agents while purine modified nucleosides bearing a propargyl residue have been conceived for *in vivo* viral life cycle visualization.

In all cases preliminary biological evaluation has also been provided with *in vitro* and in some cases, *in vivo* studies, to demonstrate the value of our efforts for the identification of valid drug candidates.

CYSTIC FIBROSIS

*N-Alkyl-Deoxyiminosugars as Anti-Inflammatory Agents
for Application in Cystic Fibrosis*



1 *N*-ALKYL-DEOXYIMINOSUGARS AS ANTI-INFLAMMATORY AGENTS FOR APPLICATION IN CYSTIC FIBROSIS

1.1 INTRODUCTION

1.1.1 CYSTIC FIBROSIS

Cystic Fibrosis (CF) is an autosomal recessive inherited disease mainly affecting respiratory, digestive and reproductive systems.¹ It is the most common life-limiting rare disease among Caucasians and affects about 70000 individuals worldwide.² CF is caused by mutations in the CF transmembrane conductance regulator (CFTR) gene encoding for a cAMP-activated chloride channel, expressed at the apical membrane of most of the surface epithelial cells in tissues of the airways, intestine, pancreas, kidney, sweat gland and male reproductive tract. In addition to chloride transport, CFTR protein is known to have additional functions including bicarbonate secretion and inhibition of epithelial sodium channel (ENaC) playing a key role in hydrating airway secretions.³⁻⁵ In the lung, defective CFTR causes depletion of the airway surface liquid, increasing mucus viscosity and impairing mucociliary clearance. Consequently, a cascade of pathological events takes place characterized by chronic inflammation and bacterial lung infections that contribute to perpetuate the inflammation. This vicious cycle of airway obstruction, infection and inflammation leads to progressive and irreversible lung damage that represents the primary cause of mortality in CF patients.⁵

CFTR mutations can be divided into six classes according to their effects on protein function⁶ (**FIGURE 1.1**). Class I mutations affect protein synthesis resulting in no protein production; class II mutations cause defective CFTR protein processing and trafficking to the plasma membrane (PM). This class includes the most common mutation, F508del, (carried out by about 90% of CF patients) characterized by protein misfolding and prolonged retention in the endoplasmic reticulum (ER) with subsequent degradation. Class III mutations are relatively rare and are characterized by altered gating and open probability of the channel while class IV mutations reduce chloride ions transported through the channel. Class V and VI mutations are characterized by reduced amount and low stability of CFTR protein at the cell surface respectively.

Notably, many CFTR mutations present more than one class defect; for example although F508del is predominantly a class II trafficking mutation, around 3% of protein is trafficked to the PM where it is not functional and has a gating defect (class III) and reduced stability at PM (class VI mutation).⁷

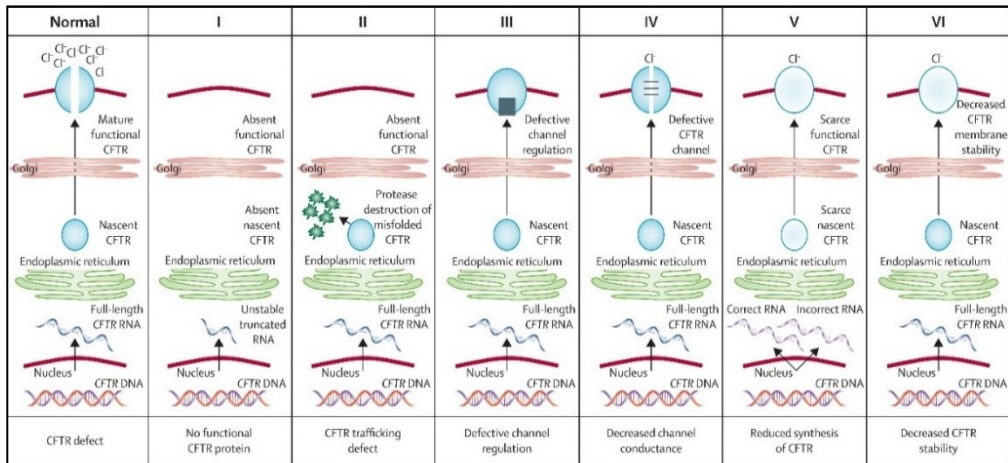


FIGURE 1.1. Classes of CFTR Mutations. The Figure is republished with the permission of Ref 6.

1.1.1.1 THERAPEUTIC APPROACHES FOR CYSTIC FIBROSIS TREATMENT

Over the years many efforts have been devoted to the development of therapeutic agents for the treatment of CF (FIGURE 1.2).⁸ Until 2012 therapies for CF patients were focused on the treatment of the clinical manifestations of the disease: airway obstruction, infection and inflammation. Although several antibiotic therapies are available, remarkable persistence of infections characterizes CF patients. Chronic lung infections, together with chronic inflammation (for which the only approved drug is ibuprofen) lead to permanent damage of airways and decline in pulmonary function.⁹

Recently, the identification of the so-called CFTR modulators has deeply changed the progression of the disease.¹⁰ CFTR modulators are small molecules able to enhance CFTR intracellular trafficking (*correctors*), CFTR ion channel function (*potentiators*) and to increase the amount of CFTR protein to the apical cell membrane or to improve the availability of CFTR for interaction with other modulators (*amplifiers*). Four CFTR modulator-based therapies are currently in clinical use and consist in the administration of: the recently approved TrikaftaTM (corrector/potentiator combination),¹¹ Kalydeco[®] (potentiator)¹², Orkambi[®] (corrector/potentiator combination)¹³ and Symdeko[®] (corrector/potentiator combination).¹⁴

Despite the advances in CFTR restoration, these therapies are not available for all CF patients as approximately 2000 CFTR variants have been reported and most of them are rare.⁷ In addition, CFTR modulators are not able to reverse lung damage, caused by chronic infection and inflammation.¹⁵

Accordingly, identification of novel therapies aimed to handle the basic molecular defect in CF, as well as to control the clinical consequences of CFTR dysfunctions, with particular focus

on excessive inflammation and dysregulation in innate immune response, remains an urgently need to ensure clinical benefits to all CF patients.¹⁶

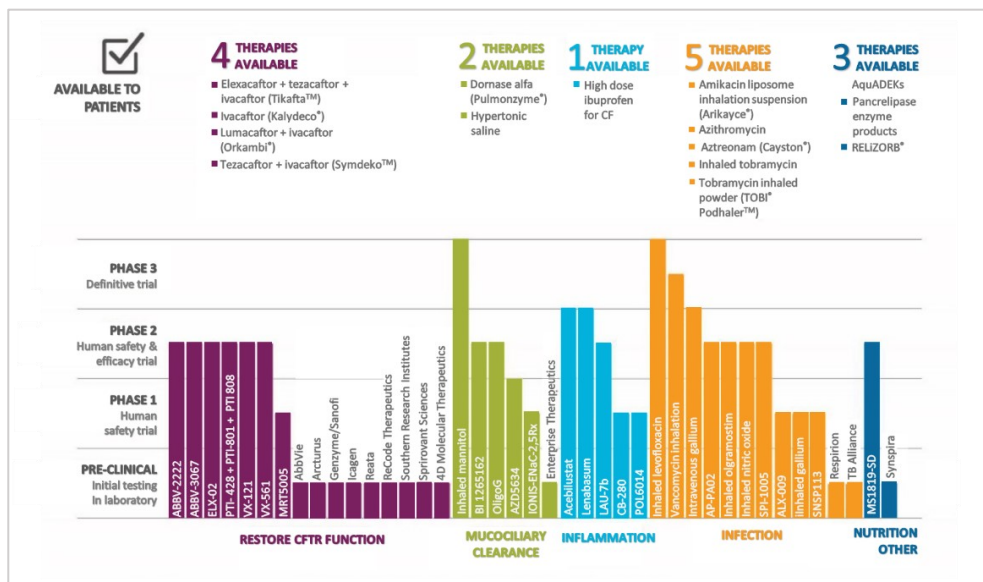


FIGURE 1.2. CF drug pipeline. The Figure is republished with the permission of Ref.8.

In this context, iminosugars have demonstrated an interesting potential whether in CFTR restoration or in the management of inflammation in CF lung disease.¹⁷

1.1.2 IMINOSUGARS: POWERFUL GLYCOMIMETICS

Iminosugars are natural or synthetic sugar analogues having an amino function in place of the endocyclic oxygen of the corresponding carbohydrates.¹⁸ The main skeletal framework of iminosugars may be recognized into several classes of compounds such as pyrrolidines, piperidines, indolizidines, pyrrolizidines and nortropans¹⁹ (FIGURE 1.3A).

The first natural iminosugar, Nojirimycin (NJ, FIGURE 1.3B) was discovered in Japan in 1966. Isolated from the cultured broth of the *Streptomyces* species, NJ exhibited interesting therapeutic potential as antibiotic agent. However, its chemical instability, due to the hemiaminal function, hampered the use of this molecule *in vivo*.²⁰ The 1-deoxy derivative of NJ, deoxynojirimycin (DNJ, FIGURE 1.3B), was originally prepared by catalytic hydrogenation of NJ with a platinum catalyst or by chemical reduction with sodium borohydride (NaBH₄) and was even later isolated from the root bark of mulberry trees.²¹ The remarkable inhibitory properties toward glycosidases exhibited by DNJ prompted to the search of novel related compounds with improved *in vivo* activity opening the way to the advent of this class of glycomimetics.

Iminosugars represent the most important class of glycomimetics discovered so far.¹⁸ Thanks to their simple structure strictly related to carbohydrates, iminosugars are endowed with an excellent drug profile. They are water soluble and therefore orally administrable. The entry of iminosugars into cells appears to work by passive, non-facilitated diffusion, or by flip-flop across the membrane.²² In addition, as most iminosugars lack the acetal function of carbohydrates, they are chemically and biologically stable to the main processes of the carbohydrates-transforming enzymes resulting in their unchanged excretion essentially in urine.¹⁹

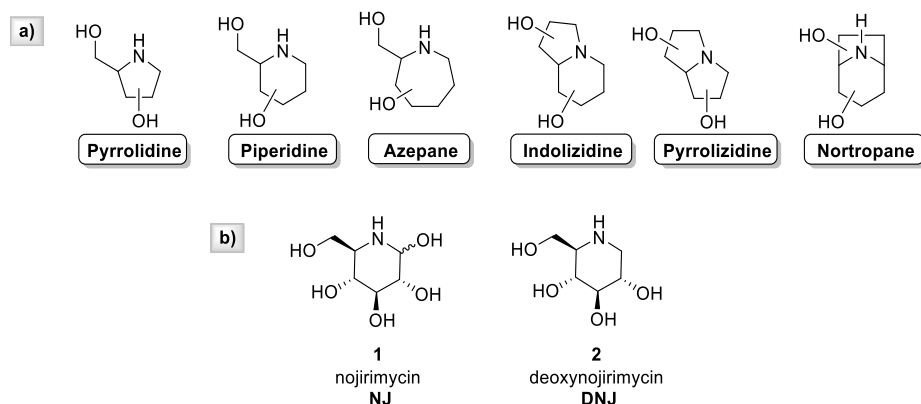


FIGURE 1.3. a) Iminosugar structural motif. b) NJ and DNJ.

Due to their close structural resemblance to the terminal sugar moiety in the natural substrates, iminosugars are able to interact with carbohydrate-processing enzymes such as glycosidases, glycosyltransferases or glycogen phosphorylases acting either as inhibitors or enhancers.^{18,21} Being these enzymes involved in several important biological processes, iminosugars have demonstrated an high pharmacological potential in several therapeutic fields including diabetes,²³ viral infections,²⁴ malignancies,²⁵ lysosomal storage disorders²⁶ and other genetic disease, including cystic fibrosis.¹⁷

The great aptitude of iminosugars to inhibit glycosidases and glycosyltransferases arises from the similarity between the iminosugar scaffold in its protonated form, which occurs under physiological conditions and the transition state (TS) involved in the reactions catalyzed by these enzymes (glycoside hydrolysis and glycosylation reactions respectively; **FIGURE 1.4**). In both cases, the TS is supposed to be quite close to a cation/oxocarbenium ion with a sp^2 character at the anomeric carbon and spatially oriented in a half-chair conformation.^{18,27}

However, it should be noted that most iminosugars (including NJ and DNJ) typically adopt a chair-like conformation instead of the half chair form (**FIGURE 1.5**) and therefore they should be considered as imperfect transition state analogues and can be defined as mimic in terms of charge.²⁸

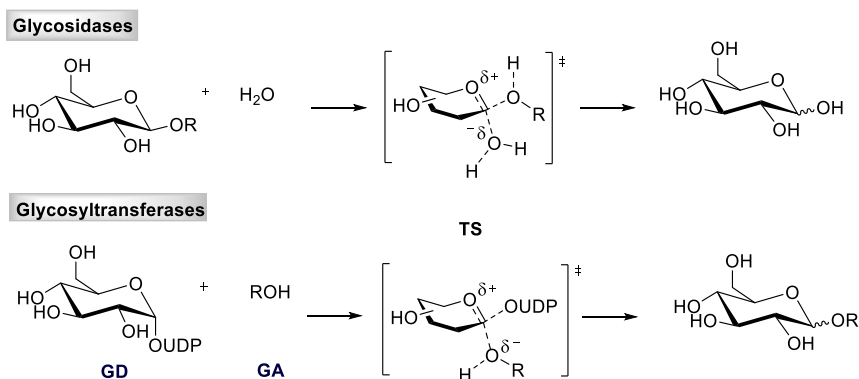


FIGURE 1.4. Action mechanism of glycosidases and glycosyltransferases.
GD = Glycosyl Donor; GA = Glycosyl Acceptor; TS = Transition State.

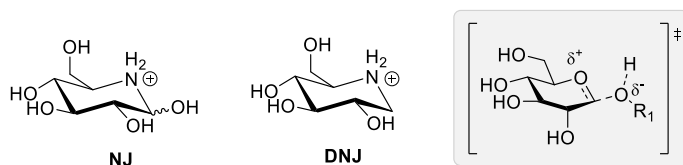


FIGURE 1.5. Comparison between protonated NJ and DNJ and the transition state of glycosidase hydrolysis.

1.1.2.1 PHARMACOLOGICAL APPLICATIONS OF IMINOSUGARS

The first therapeutic application of iminosugars has been in their use as antidiabetics. In this context, Glyset[®] (3, Miglitol, **FIGURE 1.6**) was the first iminosugar to reach the market, approved in 1996 for the treatment of non-insulin-dependent (type II) diabetes mellitus owing to its ability to inhibit intestinal α -1,4-glucosidases thus leading to a reduction in glucose absorption from the gut. However, closely related to its mechanism of action, Miglitol exhibited several side-effects, mainly at the level of digestive system. The second iminosugar to be marketed has been Zavesca[®] (4, Miglustat, also known as NBDNJ, **FIGURE 1.6**). NBDNJ is the *N*-butyl-DNJ derivative, licensed for the treatment of type I Gaucher's disease and Niemann–Pick type C disease, both of which are lysosomal storage disorders.^{19,26} Gaucher's disease is caused by a deficiency in glucocerebrosidase (GCCase) and Niemann–Pick type C disease is due to a deficiency in metabolism of cholesterol and other lipids. NBDNJ inhibits glucosylceramide synthase (GCS), enzyme catalyzing the first step of glycosphingolipid synthesis, decreasing the excessive cellular storage of glucosylceramide.²⁶ As for Miglitol, NBDNJ has been associated with gastrointestinal side effects. However, the successful presence of these compounds on the market inspired the research toward this class of compounds in order to identify novel iminosugars endowed with enhanced potency and higher specificity for the target enzymes.

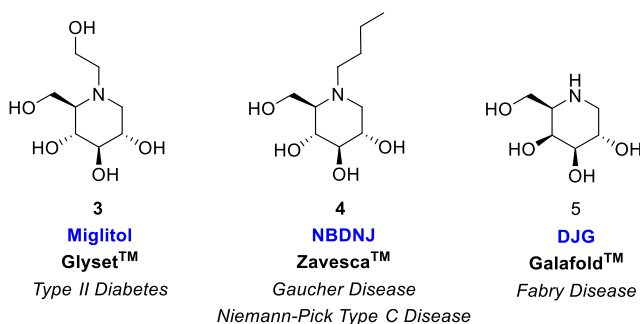


FIGURE 1.6. Marketed iminosugars.

Even though the most widespread pharmacological property of iminosugars concerns their ability to act as inhibitors of glycosidases and glycosyltransferases, over the last years, it has become clear that they can also act as active-site chaperones able to bind, reversibly and at subinhibitory concentrations, to lysosomal glycosidases and enhance the stability of the mutant enzymes, enabling correct processing and trafficking from endoplasmic reticulum to the lysosome. These findings opened the way for the use of iminosugars in the treatment of lysosomal storage disorders (LSDs, rare genetic diseases characterized by a deficiency of glycosidases involved in the catabolism of glycosphingolipids in the lysosome²⁹) leading to the approval in 2016 of Galafold[®] (**5**, deoxygalactonojirimycin, Migalastat, **FIGURE 1.6**) for the therapy of Fabry disease (FD).^{30,31} Indeed, Migalastat was able to restore the proper conformation of mutated alpha-galactosidase A (α -GalA), the enzyme responsible for the accumulation of globotriaosylceramide in the lysosomal compartment in FD patients.

In addition to the three marketed iminosugars described above, over the years other derivatives entered in clinical trials and have been evaluated for their use as drug candidates in different diseases.¹⁹ Therapeutic application of iminosugars in CF treatment is described in detail in the next paragraph.

1.1.2.2 IMINOSUGARS IN CYSTIC FIBROSIS

Due to the involvement of specific glycosidases in biological processes which are relevant in the pathogenesis of CF, over the last years iminosugars have been evaluated as drug candidates in CF whether as correctors of defective CFTR mutants (particularly of the most common F508del-CFTR) or as anti-inflammatory agents.¹⁷

○ **Iminosugars as CFTR correctors.** Among the bioactive iminosugars, NBDNJ has been identified as the first candidate showing ability to restore the trafficking and function of defective F508del-CFTR protein by inhibiting the trimming of endoplasmic reticulum (ER) glucosidases.³² Indeed, inhibition of ER-glucosidases I and II by NBDNJ is thought to prevent the interaction of misfolded F508del-CFTR with ER chaperone calnexin and hence its degradation by the ER-

quality control machinery, termed endoplasmic reticulum-associated degradation (ERAD). Despite the strong *in vitro* and preclinical evidences,^{33–35} the correction effect of NBDNJ was not confirmed in clinical trials.³⁶ Starting from the promising results obtained with NBDNJ, a variety of iminosugar derivatives have been evaluated for their capacity to rescue F508del-CFTR (FIGURE 1.7).

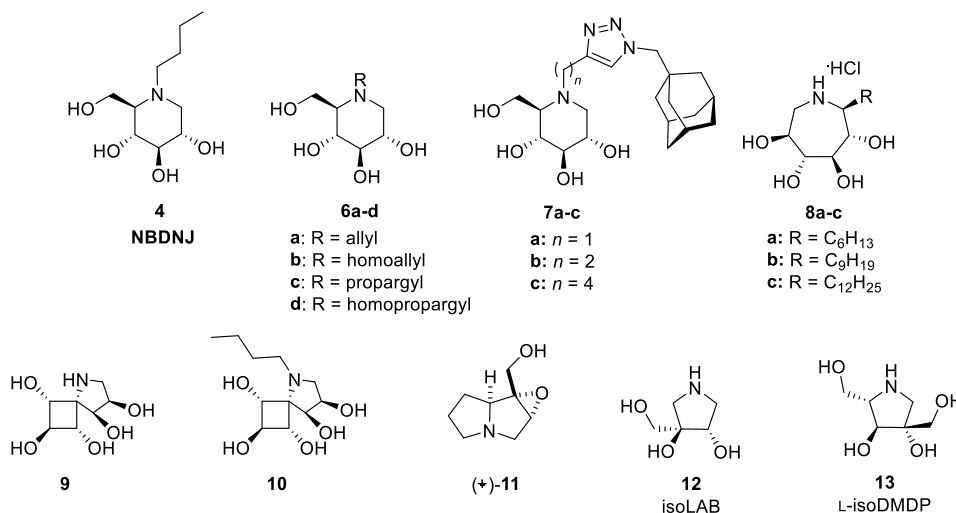


FIGURE 1.7. Iminosugars able to rescue defective F508del-CFTR.

Unsaturated and triazole-bearing derivatives^{37,38} **6** and **7**, azepanes³⁹ **8**, constrained NBDNJ analogues⁴⁰ **9** and **10**, carbon-branched pyrrolizidines⁴¹ **11** and pyrrolidines^{42,43} **12** and **13** have been considered and in some cases enhanced properties as correctors, compared to NBDNJ were observed, with pyrrolidine isoLAB (**12**) displaying the most promising pharmacological potential in F508del-CFTR rescue (FIGURE 1.7). Noteworthy, several of these iminosugars did not inhibit ER glucosidases suggesting that the mechanism underlying F508del-CFTR function rescue could be different compared to that initially proposed.¹⁷

○ **Iminosugars as anti-inflammatory agents.** Even more interesting results have been obtained when iminosugars were evaluated for symptomatic treatment of CF, *i.e.* when considered as anti-inflammatory agents in CF lung disease. In this context, recently Dehecchi *et al.* demonstrated that NBDNJ exerted a significant anti-inflammatory effect, both in human bronchial epithelial cells *in vitro*, and in murine models of lung inflammation *in vivo*, by reducing *P. aeruginosa* (the most predominant lung infection in CF) induced ceramide* production.^{44–46}

* Ceramide plays an important role in the infection by *P. aeruginosa* by reorganizing lipid rafts on cellular membranes into larger signaling platforms, which is a feature conducive to internalizing bacteria, inducing apoptosis and regulating the cytokine response.

These results were in line with evidences about the involvement of sphingolipid (SL) metabolism (whose ceramide represents the central hub) in the regulation of the inflammatory response in CF.⁴⁷⁻⁴⁹ Particularly, the anti-inflammatory effect exerted by NBDNJ has been associated to the inhibition of the non-lysosomal β -glucosidase 2 (GBA2-encoded NLGase), the enzyme involved in the metabolism of SLs by ceramide production at the plasma membrane level.⁵⁰ As matter of fact, not only NBDNJ but also the potent NLGase inhibitor, AMP-DNM (adamantanemethoxypentyl DNJ, **14**, **FIGURE 1.8**),⁵¹ as well as its triazole-bearing derivatives **7**, were able to reduce the *P. aeruginosa* stimulated IL-8 mRNA expression in CF bronchial cells^{50,52} providing further evidences on the potential of the enzymes involved in SL metabolism as novel targets for CF lung disease treatment. These findings opened new perspectives for the therapeutic use of iminosugars in CF as potential host-directed therapeutics being able to reduce the exacerbated inflammation that represents the most severe symptom observed in CF patients.

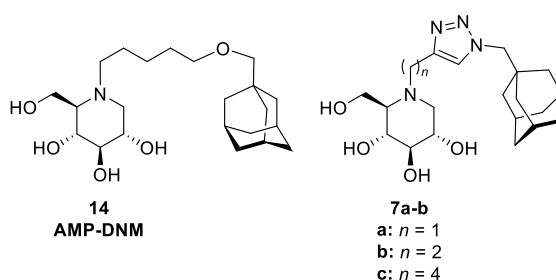


FIGURE 1.8. Iminosugars with anti-inflammatory activity.

1.1.2.3 IMPROVING ENZYMATIC SELECTIVITY OF IMINOSUGARS: ROLE OF THE LIPOPHILICITY AND OF CONFIGURATION

Despite the powerful therapeutic potential exhibited by iminosugars, the progression of these candidates to marketed drugs has been hampered by their limited *in vivo* selectivity. Indeed, iminosugars can be used for a plethora of therapeutic purposes, but their long-term use is always accompanied by a wide variety of side effects due to their activities against other cellular enzymes (abdominal bloating, flatulence, diarrhoea, transient tremor, weight loss, axonal and peripheral neuropathy).^{18,53}

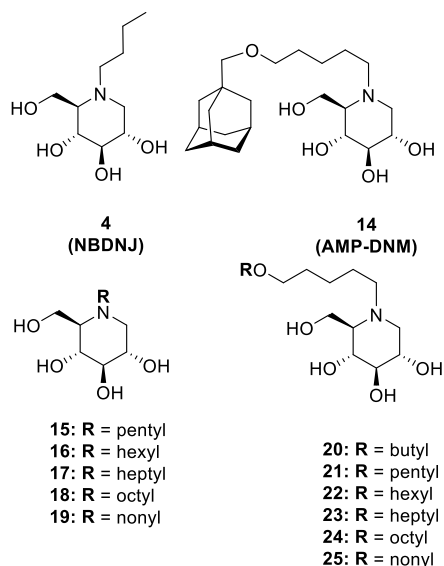
In order to overcome the drawbacks associated to the medical use of iminosugars, several structural modifications have been proposed over the years in order to balance biological activity and toxicity. In this context among the most important elements so far identified, both the role of lipophilicity and of the configuration of the iminosugars have been explored.

- **Role of Lipophilicity.** *N*-alkylation of iminosugars has been postulated to considerably enhance the selectivity for the target enzymes since lipophilic moieties can only be hosted by enzymes having lipophilic character. As an example, studies focused on the identification of

molecular features able to enhance the selective recognition of *N*-alkylated iminosugars by GCS (ceramide glucosyltransferase) in comparison with ER α -glucosidase I, revealed that the presence of an alkyl chain is obligatory for the transferase inhibition and there is a direct correlation between inhibition potency and chain length, probably due to the greater ceramide mimicry while the α -glucosidase inhibition is independent of the *N*-alkyl chain and changes in chain length.⁵⁴ In addition, increase of *N*-alkyl chain length has demonstrated to improve inhibitor properties toward GCS and GCase (lysosomal β -glucocerebrosidase, enzyme whose deficiency is responsible for Gaucher disease) but also results in more potent and selective NLGase inhibitors⁵⁵ (TABLE 1.1).

TABLE 1.1. IC₅₀ (μ M) of *N*-alkyl-D-iminosugars toward GCS, GCase and NLGase.
The table is adapted with the permission from Ref. 55.

Compound	GCS	GCase	NLGase
4	50	400	0.23
14	0.2	0.2	0.001
15	>20	500	0.4
16	>20	80	0.11
17	40	18.5	0.045
18	4	4	0.020
19	4	1.5	0.007
20	4	30	0.06
21	2	705	0.04
22	1	205	0.008
23	0.3	1.75	0.015
24	0.2	0.5	0.010
25	0.1	0.5	0.040



○ **Role of iminosugar chirality.** Over the years, the study of the pharmacological potential of iminosugars has been focused on the evaluation of those belonging to D-series whereas relatively little attention has been devoted to the corresponding L-enantiomers for their supposed lack of biological activity and for their limited availability from natural sources. However, in recent times, their importance has been completely reconsidered due to the interesting activity exhibited by these compounds in terms of potency and enzymatic selectivity.⁵⁶ Early reports about the biological activities of L-enantiomers concerned five-membered iminosugars. In this context, pyrrolidine analogues 1,4-dideoxy-1,4-imino-L-arabinitol (LAB), 2,5-Dideoxy-2,5-imino-L-mannitol (L-DMDP) and carbon-branched pyrrolidine iminosugar L-isoDMDP revealed a more

powerful and specific α -glucosidase inhibition than their naturally occurring D-antipodes (**FIGURE 1.9A**).^{43,57,58} Inspired by these findings, studies were devoted to the synthesis and biological evaluation of piperidine L-minosugars revealing an interesting pharmacological potential of this class of compounds. For example, L-DNJ and L-DGJ (**FIGURE 1.9B**) surprisingly demonstrated to be inhibitors of α -glucosidases and of α -galactosidase respectively (L-DNJ: $IC_{50} = 4.3 \mu\text{M}$; L-DGJ: $IC_{50} = 13 \mu\text{M}$) although less efficient than their D-enantiomers (D-DNJ: $IC_{50} = 0.03 \mu\text{M}$; D-DGJ: $IC_{50} = 0.003 \mu\text{M}$).⁵⁹

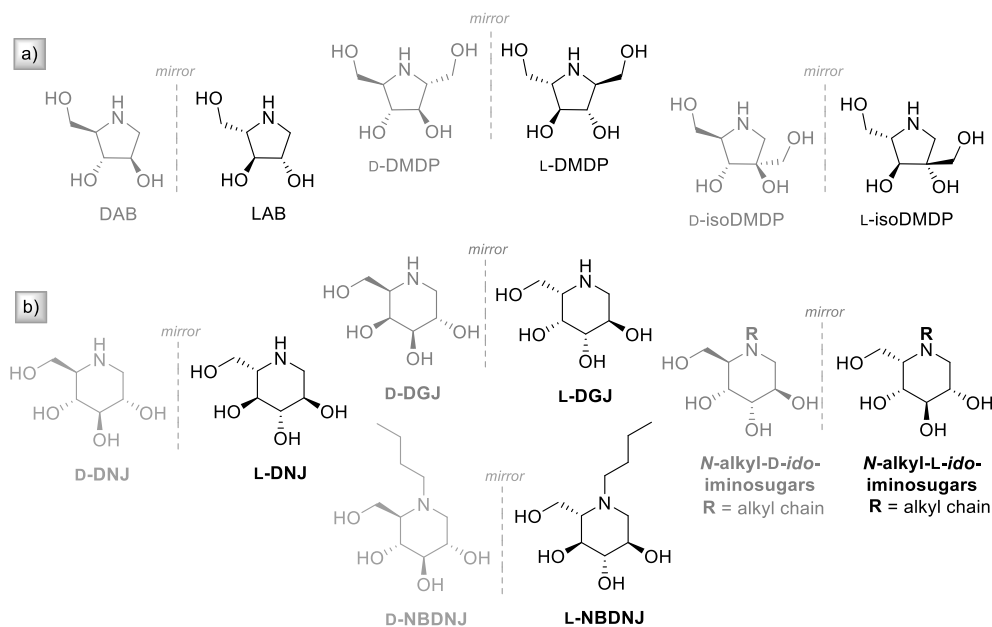


FIGURE 1.9. Pyrrolidine and piperidine L-minosugars.

The chirality of iminosugars demonstrated to play an important role on inhibitory properties also against NLGase as demonstrated for example by the remarkably high selectivity and potency of *N*-alkyl iminosugars with *L-ido* configuration compared with the activity of the corresponding *D-gluco* congeners.^{55,60} In more recent times very interesting results were obtained considering the enantiomer of the iminosugar drug D-NBDNJ, i.e L-NBDNJ (**FIGURE 1.9**), for application in Pompe disease (PD), the most common among LSDs. Due to its ability to improve the residual activity and lysosomal trafficking of mutated acid α -glucosidase (GAA) and to enhance the therapeutic efficacy of the recombinant human GAA (Myozyme, the only clinically approved therapy), D-NBDNJ represents one of the most promising candidates under development for the treatment of PD. In this context, D'Alonzo *et al.* demonstrated the ability of L-NBDNJ to increase the levels of Myozyme in fibroblasts from patients with PD, while not working as a glycosidase inhibitor, differently from its D-enantiomer.⁶¹

1.2 RESULTS AND DISCUSSION

Based on the considerations reported in the previous section, a topic of this PhD program was focused on the evaluation of the role of the iminosugar chirality in the anti-inflammatory treatment of CF lung disease. Particularly, the interesting anti-inflammatory effect exhibited by D-NBDNJ (**4**) in CF lung disease by inhibition of NLGase,⁵⁰ together with the promising pharmacological properties demonstrated by L-iminosugars and their *N*-alkyl derivatives,⁵⁶ prompted us to explore the anti-inflammatory potential of L-NBDNJ (*ent*-**4**) and the *N*-alkyl derivatives *ent*-**14,19,22,25** for therapeutic application in CF as anti-inflammatory agents (FIGURE 1.10). Target compounds were synthesized using a method relying on the use of the well-known polymer-supported triphenylphosphine/iodine (PS-TPP/I₂) reagent system to prepare reactive alkoxyalkyl iodides.⁶²

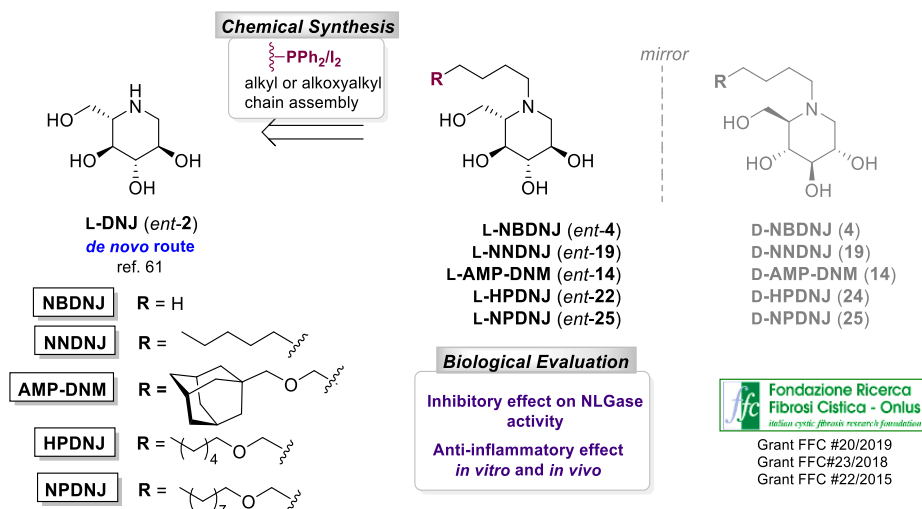


FIGURE 1.10. Synthesis of *N*-alkyl L-iminosugars and biological evaluation for application in CF.

N-alkyl L-deoxyiminosugars (*ent*-**4,14,19,22,25**) were evaluated *in vitro* for their inhibitory effect on NLGase and for their effect on the inflammatory response to *P. aeruginosa* (the most predominant lung infection in CF) either alone or in synergistic combination with their D-enantiomers. The anti-inflammatory effect of L-NBDNJ was also assessed in murine models of *P. aeruginosa* lung infection.

This work was founded by Italian Cystic Fibrosis Research Foundation grants number FFC #20/2015, FFC #23/2018 and FFC#20/2019.

1.2.1 SYNTHESIS OF *N*-ALKYL L-DEOXYIMINOSUGARS

A wide exploration of pharmacological potential of *N*-alkyl L-iminosugars has been often hampered by the difficult to synthesize the iminosugar core with high stereoselectivity. Indeed, to the best of our knowledge, the synthesis of *N*-alkyl L-DNJ derivatives has never been reported before. In this context, recently a *de novo* methodology aimed at the preparation of L-DNJ has been developed in our laboratory.⁶¹ This methodology, already used for the synthesis of unnatural carbohydrates and biomimetic agents,^{63–66} relied on the use of the synthetically available building block⁶⁷ **26** (FIGURE 1.12) whose coupling reaction with the L-enantiomer of Garner aldehyde (**27**) enabled to obtain the L-*gluco* configured iminosugar *ent*-**2**.⁶¹

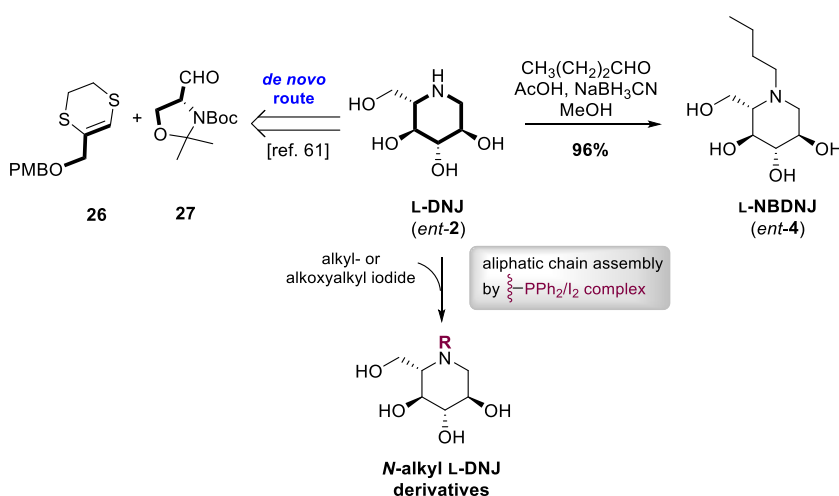


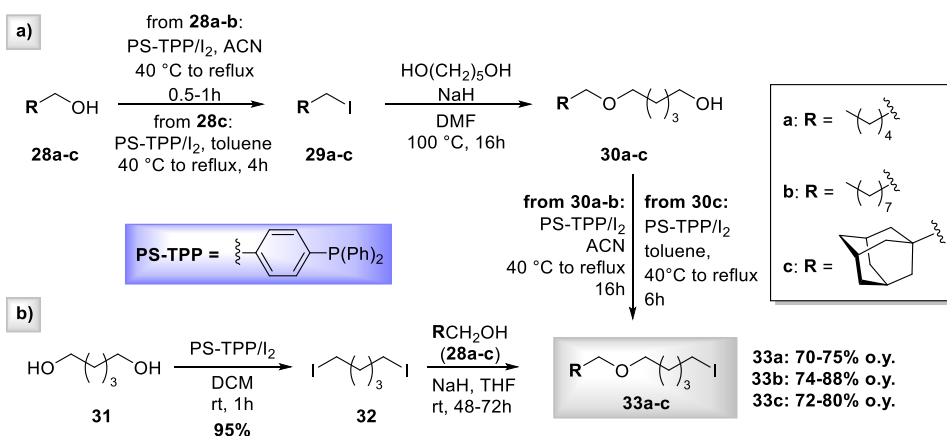
FIGURE 1.12. Synthetic route to *N*-alkyl L-DNJ derivatives.

Starting from the enantiomerically pure L-DNJ, herein our attention was focused on the obtainment of its *N*-alkylated derivatives. Particularly, while L-NBDNJ (*ent*-**4**), the non-superimposable mirror image of the iminosugar drug D-NBDNJ, was obtained by standard *N*-alkylation reaction conditions of *ent*-**2**,⁶¹ preparation of *ent*-(**14,19,22,25**) was performed by *N*-alkylation of L-DNJ with reactive alkyl and alkoxyalkyl iodides (FIGURE 1.12). The synthesis of these latter has been tuned up⁶² and relied on the use of the well-known PS-TPP/I₂ as iodination system, which has been long at the core of our synthetic studies aimed to a plethora of transformations, including the formation of glycosyl iodides,⁶⁸ the phosphorylation of nucleosides,⁶⁹ the acetalization of sugars⁷⁰ and steroids.⁷¹ The PS-TPP/I₂ reagent system, in this case, can be employed in the absence of the commonly used imidazole, thus enabling to devise a synthetic protocol with a sequence of steps not requiring extractive work-up and chromatographic purifications. Indeed, the only reaction by-product, i.e. the resin-bound phosphine oxide, can be easily filtered off and reduced to the original phosphine form by treatment with trichlorosilane.

In early studies, we devised a procedure based on two iodination reactions from alcohols **28a-c** (SCHEME 1.1a).

The first iodination enabled to convert alcohols **28a-c** into iodides **29a-c** by means of PS-TPP/I₂ in refluxing ACN for **28a** and **28b** or toluene for the lower reactive adamantanemethanol (**28c**). Iodides were then converted into the corresponding alcohols **30a-c** after coupling reaction with 1,5-pentandiol (NaH, DMF).

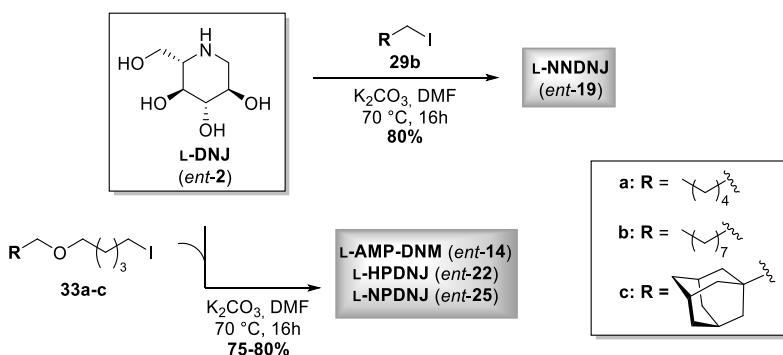
These latter were eventually converted into target iodides **33a-c** obtained with high conversion yields (70-88% o.y.) and without need of intermediate work-up steps of purifications.



SCHEME 1.1. Preparation of alkoxyalkyl iodides by PS-TPP/I₂ reagent system.

The procedure herein reported represents a faster and more convenient alternative procedure devoted to the synthesis of alkyl or alkoxyalkyl chains for the synthesis of *N*-alkylated iminosugars. An even more expeditious protocol was also explored (SCHEME 1.1b) and relied on the double iodination of 1,5-pentandiol (**31**) to provide after 1h at rt (DCM) 1,5-diiodopentane (**32**), followed by coupling reaction with alcohols **28a-c** (NaH, THF) to obtain iodides **33a-c** in satisfying yields (72-75%).

With iodides in hand, the eventual coupling reaction of iodide **29b** and alkoxyalkyl iodides **33a-c** with L-DNJ (*ent-2*) under standard conditions (K₂CO₃), smoothly provided *ent-19* (80% o.y.) and *ent*-(**14,22,25**) in satisfactory 75-80% (SCHEME 1.2).

SCHEME 1.2. Synthesis of *N*-alkyl L-DNJ derivatives.

1.2.2 BIOLOGICAL EVALUATION

The pharmacological potential of our *N*-alkyl L-imosugars as anti-inflammatory agents for CF treatment was evaluated by biological assays carried out by different research groups in the frame of three projects financed by Italian Cystic Fibrosis Research Foundation (FFC #20/2015, FFC #23/2018 and FFC#20/2019).

- **Effect of iminosugars on NLGase activity** (Prof. M. Aureli; University of Milan)

As the anti-inflammatory effect observed for NBDNJ was ascribed to NLGase inhibition, in first studies, the effect of the synthesized L-imosugars *ent*-(4,14,19,22,25) on NLGase activity was examined by *in vitro* assays in model SH-SY5Y cells, a human neuro- blastoma cell line having high activity of NLGase (TABLE 1.2).

Particularly, the inhibition effect of the corresponding D-imosugars 4,14,19,22,25 and of the racemic mixture *rac*-(4,14,19,22,25) was also considered in order to evaluate the effect of iminosugar chirality on NLGase inhibition.[†] As summarized in TABLE 1.2 L-imosugars *ent*-(4,14,19,22,25) acted as NLGase inhibitors (entries 2, 5, 8, 11 and 14) albeit to a lower extent (in the micromolar range) than those of D-imosugars. *Ent*-14 and *ent*-25 displayed the highest inhibitory activity among L-imosugars (IC₅₀ 65 nM and 137 nM, entries 8 and 14) in line with the role of the alkyl chain length regarding NLGase inhibition.⁵⁵

When the combined incubation of D- and L-imosugars *rac*-(4,14,19,22,25) was evaluated, no significant synergistic effect was found for *rac*-4, *rac*-19 and *rac*-22 (entries 3, 6 and 12), conversely *rac*-14 and *rac*-25 displayed a similar activity to that exerted by 14 and 25 when taken alone with a total inhibition of the NLGase activity.

[†] The use of racemic mixtures to evaluate their potential synergistic effect as NLGase inhibitors and as anti-inflammatory agents, arises from previously reported experimental evidences. As an example (Jenkinson, S.F. *Org. Lett.* **2011**, *13*, 4064-4067), D- and L-DGJ (DGJ: 1-deoxygalactonojirimycin) resulted singularly α -Galactosidase A inhibitors and, when co-administrated, synergistic pharmacological chaperones of the same enzyme.

TABLE 1.2 Effect of iminosugar chirality on glycohydrolase activity.
The table was reprinted from Ref. 62, with permission of Elsevier.

Entry	Compound	NLGase	
		IC ₅₀ (μM)	M.I. (%)
1	D-NBDNJ (4)	0.014	100
2	L-NBDNJ (ent-4)	7.7	100
3	rac-NBDNJ (rac-4)	0.260	100
4	D-NNDNJ (19)	0.003	100
5	L-NNDNJ (ent-19)	4.6	100
6	rac-NNDNJ (rac-19)	0.035	100
7	D-AMP-DNM (14)	0.003	100
8	L-AMP-DNM (ent-14)	0.065	10
9	rac-AMP-DNM (rac-14)	0.004	100
10	D-HPDNJ (22)	0.0004	100
11	L-HPDNJ (ent-22)	36.7	100
12	rac-HPDNJ (rac-22)	0.001	100
13	D-NPDNJ (25)	0.034	100
14	L-NPDNJ (ent-25)	0.137	10
15	rac-NPDNJ (rac-25)	0.044	100

The assays were performed on lysates of SH-SY5Y cells, using different concentrations of each compound (from 1 nM to 1 mM) in the presence of 750 mM CBE. IC₅₀: inhibitor concentration that produces 50% inhibition. M.I.: maximal inhibition.

- ***In vitro* anti-inflammatory effect** (Dr. M. Dehecchi; University of Verona)

A selection of *N*-alkylated iminosugar enantiomers were then evaluated for their effect on *P. aeruginosa* stimulated IL-8 mRNA expression in CF bronchial epithelial cells (**FIGURE 1.13a**). Both *ent-4* and *ent-14* reduced the IL-8 mRNA expression (up to a 20% and 29% reduction, respectively), with an effect comparable to that of the corresponding enantiomers. Conversely, *ent-19* exhibited a smaller effect (16% reduction) although it was greater than that of **19** (8% reduction). Interestingly, the combination of iminosugar enantiomers produced an even greater effect. These results suggest that the combination of D- and L-enantiomers could reduce the concentration of D-enantiomers, thus minimizing the side effects. The anti-inflammatory effect of racemic mixtures was also observed when tested in CF bronchial primary cells infected by *P. aeruginosa* (**FIGURE 1.13b**) and the greater effect was observed for *rac-4* and *rac-14*.

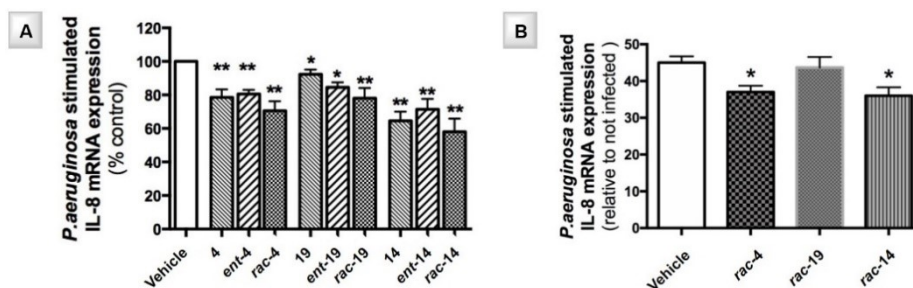


FIGURE 1.13. A) Effect of sugar chirality of iminosugars **4,14,19** and *ent-4, ent-14, ent-19* on the inflammatory response to *P. aeruginosa* in CF bronchial epithelial cells. CuFi-1 cells were treated with the compounds (0.1 μ M) for 1 h before *P. aeruginosa* infection. B) Effect of racemic mixtures on the inflammatory response to *P. aeruginosa* in CF primary cells (deriving from CF individuals). CF bronchial primary cells were treated with the racemic mixtures (0.01 μ M) for 1 h before *P. aeruginosa* infection. The figure was reprinted from Ref. 62, with permission of Elsevier.

Whether as single enantiomer or as racemic mixtures, *N*-alkylated iminosugars did not induce significant apoptosis in CF bronchial cells and did not significantly decrease cell viability in the same experimental model.

- ***In vivo* evaluation of anti-inflammatory effect** (Prof. Bragonzi, CFaCore, Milano)

The anti-inflammatory effect of L-NBDNJ (*ent-4*), as well as its inhibition potential against NLGase, were also assessed in C57Bl/6Ncr mice infected by *P. aeruginosa*. Indeed, as **4** was already studied *in vitro* and *in vivo* for its anti-inflammatory effect in CF⁴⁵ and being a marketed drug its pharmacokinetics and safety profile data are known, among all the synthesized compounds, *ent-4* was chosen for our preliminary studies aimed to explore the role of iminosugar chirality on the anti-inflammatory activity. As shown in **FIGURE 1.14a**, a reduction of recruitment of neutrophils in BAL (bronchoalveolar lavage) was observed for *ent-4* at a concentration as low as 10 mg/kg, i.e. 40-fold lower than that of **4** (for which an oral dose of 400 mg/Kg was effective in reducing strongly the neutrophils recruitment *in vivo*).⁴⁵ Very importantly, the decreased recruitment of neutrophils did not affect the host immune response as it did not increase the amount of bacteria recovered in the airways. Treatment with both **4** and *ent-4* was safe as shown by the weights of mice monitored during the experiment.

In addition, as shown in **FIGURE 1.14b** *ent-4* deeply inhibits NLGase suggesting, as previously observed for **4**, the involvement of NLGase inhibition in the inflammatory response to *P. aeruginosa* infection.

It is important to underline that the inability of L-NBDNJ to work as broad-spectrum glycosidase inhibitor⁶¹ point out its potential to act as drug able to control excessive inflammation without being accompanied by the side effects usually associated with the use of iminosugars as therapeutics.

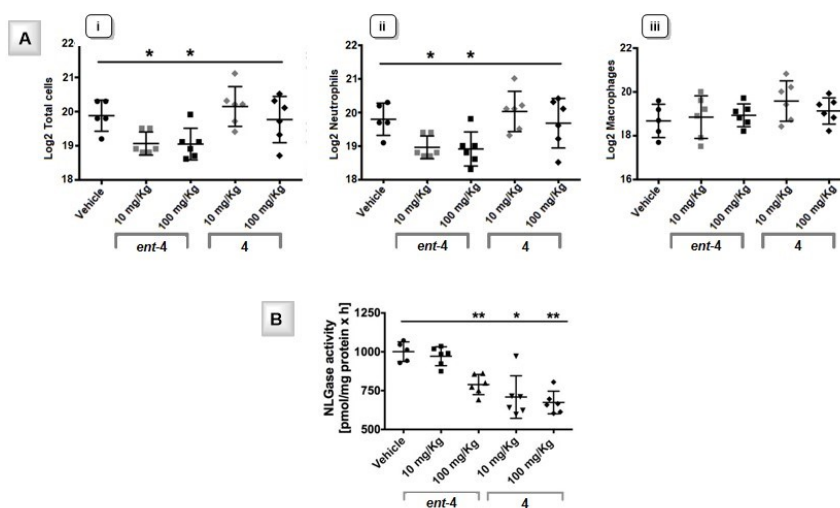


Figure 1.14. A) Effect of 4 and *ent-4* on cells recruited in BAL of C57Bl/6Ncr mice infected by *P. aeruginosa* (i, total cells; ii, neutrophils; iii, alveolar macrophages). B) NLGase activity in the lungs of mice infected by *P. aeruginosa*. The figure was reprinted from Ref. 62, with permission from Elsevier.

Lastly, other promising results have been collected in the frame of the recently concluded FFC project 20/2019 (data unpublished, manuscript in preparation) in which the anti-inflammatory effect of *ent-4* was evaluated in chronically infected mice. Again, a reduction of the amounts of neutrophils recruited in the BAL of infected mice was observed. Interestingly, a strong decrease of bacteria recovered in lung and BAL was also observed after treatment with *ent-4* and a dose-dependent increase of bacterial clearance was found. These data confirm the anti-inflammatory effect of this compound and suggest that it can prevent chronic infection leading us to explore its anti-bacterial potential as will be described in Chapter 2.

1.3 CONCLUDING REMARKS

A key topic of this PhD program was focused on the evaluation of the role of the chirality of *N*-alkyl iminosugars in the anti-inflammatory treatment of CF lung disease. Inspired by the powerful pharmacological potential of iminosugars and on the *in vitro* and *in vivo* anti-inflammatory effects exhibited by the iminosugar drug NBDNJ by inhibition of NLGase, herein, the anti-inflammatory potential of L-NBDNJ (*ent-4*) and its *N*-alkyl derivatives (*ent-14,19,22,25*) has been explored for therapeutic application in CF. Target glycomimetics were prepared by the shortest and most convenient approach reported to date, relying on the use of the well-known PS-TPP/I₂ reagent system to prepare reactive alkoxyalkyl iodides, acting as key intermediates. *N*-alkyl L-iminosugars herein synthesized were found to act as NLGase inhibitors, although less efficient than their D-enantiomers, and were found to significantly reduce the inflammatory response

induced by *P. aeruginosa in vitro* either alone or in synergistic combination with their D-enantiomers. When evaluated *in vivo*, a reduction of recruitment of neutrophils was observed for L-NBDNJ at a much lower dosage (40-fold) than that of D-NBDNJ and a strong inhibition of NLGase activity. These results combined with the inability of L-NBDNJ to act as inhibitor for most glycosidases, is expected to limit the onset of undesired effects, which are typically associated with the administration of its D-enantiomer and highlight strong evidence of the therapeutic potential of *N*-alkyl L-iminosugars as anti-inflammatory agents in CF.

In addition, last results on the ability of L-NBDNJ to significantly decrease bacteria recovered in lung and BAL of chronically infected mice, along with increase of bacterial clearance, suggests an antibacterial activity of this molecule inspiring us to explore the anti-infective potential of L-NBDNJ, as well as of the other *N*-alkyl L-iminosugars as will be described in next chapter.

1.4 EXPERIMENTAL SECTION

CHEMICAL SYNTHESIS: GENERAL METHODS

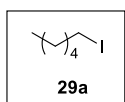
All chemicals and solvents were purchased with the highest degree of purity (Sigma-Aldrich, Alfa Aesar, VWR) and used without further purification. All moisture-sensitive reactions were performed under nitrogen atmosphere using oven-dried glassware. The reactions were monitored by TLC (precoated silica gel plate F254, Merck) and the products were detected by exposure to ultraviolet radiation, iodine vapor, chromic mixture and ninhydrin. Column chromatography: Merck Kieselgel 60 (70-230 mesh); flash chromatography: Merck Kieselgel 60 (230-400 mesh). The purity of the synthetic intermediates and the final compounds was determined by CHNS analysis and was $\geq 95\%$ in all cases. NMR spectra were recorded on NMR spectrometers operating at 400 MHz (Bruker DRX, Bruker AVANCE) or 500 MHz (Varian Inova), using CDCl₃ solutions unless otherwise specified. Coupling constant values (J) were reported in Hz. Chemical synthesis of L-DNJ (*ent-2*) was achieved as previously reported by a *de novo* route. Optical purity of this latter (deduced by optical rotation value)⁶¹ ensured the optical purity of the *N*-alkylated compounds herein synthesized.

SYNTHESIS OF ALKOXYALKYL IODIDES

Method A: *Step I:* To a stirred solution of alcohol **28** (1.0 equiv) in the appropriate anhydrous solvent (**28a** and **28b**: ACN; **28c**: toluene), polymer supported triphenylphosphine (PS-TPP; 100-200 mesh, extent of labeling: ~ 3 mmol/g triphenylphosphine loading) (2.0 equiv) was added. The mixture was warmed to 40 °C and I₂ (2.0 equiv) was added. The suspension was stirred to reflux temperature for the appropriate time (**28a**: 0.5 h; **28b**: 1 h; **28c**: 4 h), and then the mixture was cooled at rt, filtered and the solvent removed under reduced pressure at room temperature, affording iodide **29**. *Step II:* An appropriate amount of 1,5-pentandiol (**29a** and **29b**: 1.0 equiv; **7c**: 5.0 equiv) was dissolved in dry DMF (**29a** and **29b**: 1.0 mL; **29c**: 5.0 mL) and NaH (60% dispersion in mineral oil; **29a** and **29b**: 1.2 equiv; **29c**: 5.0 equiv) was added. The mixture was

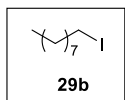
stirred for 30 min at room temperature. Then a solution of the crude iodide **29** in dry DMF (0.5 mL) was added dropwise. After 16h at 100 °C, the mixture was concentrated under reduced pressure to furnish **30**. For **30c**, the crude was washed repetitively with hexane in order to remove the excess of 1,5-pentandiol. *Step III*: PS-TPP (2.0 equiv) was added to a solution of alcohol **30** in the appropriate anhydrous solvent (**30a** and **30b**: ACN, 2.5 mL; **30c**: toluene, 5 mL). The mixture was warmed to 40 °C and I₂ was added (2.0 equiv). The suspension was stirred to reflux temperature for the appropriate time (**30a** and **30b**: 3 h; **30c**: 6 h), and then the mixture was filtered, and the filtrate evaporated under reduced pressure. Column chromatography of the crude residue (hexane/EtOAc) gave the pure alkoxyalkyl iodide **30**.

Method B: *Step I*: 1,5-pentandiol (1.0 equiv) was added dropwise to a solution of PS-TPP (100-200 mesh, extent of labeling: ~3 mmol/g triphenylphosphine loading) (4.0 equiv) and iodine (4.0 equiv) in anhydrous DCM. The reaction was stirred at room temperature for 1 h, then filtered, to remove triphenylphosphine oxide, and washed with saturated aq Na₂S₂O₃, brine and extracted with DCM. Organic layers were dried (Na₂SO₄) and evaporated under reduced pressure at room temperature to give the pure 1,5-diiodopentane (**32**) as a pale-yellow oil. *Step 2*: NaH (60% dispersion in mineral oil; 1.0 equiv) was added to a stirred solution of alcohol **28** (1.5 equiv) in dry THF (1.5 mL) at 0 °C. The reaction mixture was stirred at the same temperature for 2 h and then *Bis*-iodide **32** (0.70 mmol) was added. The mixture was warmed and after the appropriate time (**28a** and **28b**: 48 h; **28c**: 72 h) was diluted with DCM and washed with aq NH₄Cl and brine. The organic layer was dried with Na₂SO₄ and the solvent evaporated under reduced pressure. Chromatography of the crude residue over silica gel provided the pure iodides **33**.



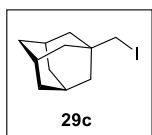
1-Iodohexane (29a): Method A, Step I (from 28a).

¹H and ¹³C NMR spectra were fully in agreement with those reported in the literature.⁷²



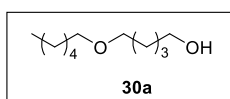
1-Iodononane (29b): Method A, Step I (from 28b).

¹H and ¹³C NMR spectra were fully in agreement with those reported in the literature.⁷²



Adamantanemethyl iodide (29c): Method A, Step I (from 28).

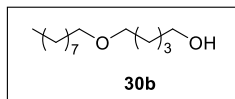
¹H NMR (500 MHz): δ 1.51 (d, *J* = 2.5, 6H), 1.64-1.67 (m, 3H), 1.72-1.75 (m, 3H), 1.99 (s, 3H), 3.20 (s, 2H). ¹³C NMR (125 MHz): δ 27.1, 28.8, 36.7, 42.2. Anal. calcd for C₁₁H₁₇I: C, 47.84; H, 6.20. Found: C, 47.77; H, 6.22.



5-Hexyloxy-1-pentanol (30a): Method A, Step II (from 29a).

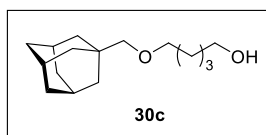
¹H NMR (400 MHz): δ 0.88 (t, *J* = 6.4, 3H), 1.25-1.35 (m, 6H), 1.41-1.47 (m, 2H), 1.52-1.64 (m, 6H), 3.40 (q, *J* = 6.7, 4H), 3.65 (t, *J* = 6.5, 2H). ¹³C NMR (100 MHz): δ 14.2, 22.7, 22.8, 26.0, 29.6, 29.9, 31.9,

32.7, 63.0, 70.9, 71.2. Anal. calcd for $C_{11}H_{24}O_2$: C, 70.16; H, 12.85; O, 16.99. Found: C, 70.06; H, 12.89.



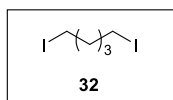
5-Nonyloxy-1-pentanol (30b): Method A, Step II (from **29b**).

1H NMR (400 MHz): δ 0.87 (t, $J = 6.6$, 3H), 1.21–1.36 (m, 12H), 1.38–1.46 (m, 2H), 1.51–1.65 (m, 6H), 3.39 (q, $J = 6.6$, 4H), 3.65 (t, $J = 6.5$ Hz, 2H). ^{13}C NMR (125 MHz): δ 14.2, 22.5, 22.7, 26.3, 29.3, 29.5, 29.6, 29.6, 29.8, 32.0, 32.6, 63.0, 70.8, 71.1. Anal. calcd for $C_{14}H_{30}O_2$: C, 72.99; H, 13.12; O, 13.89. Found: C, 73.10; H, 13.06.



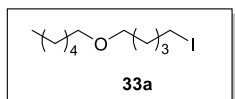
5-Adamantanemethoxypentanol (30c): Method A, Step II (from **29c**).

1H NMR (500 MHz): δ 1.39–1.45 (m, 2H), 1.52–1.53 (m, 6H), 1.56–1.61 (m, 4H), 1.63–1.72 (m, 6H), 1.95 (bs, 3H), 2.96 (s, 2H), 3.39 (t, $J = 6.5$, 2H), 3.66 (t, $J = 6.6$, 2H). ^{13}C NMR (125 MHz): δ 22.6, 28.5, 29.4, 32.7, 34.3, 37.4, 39.9, 63.1, 71.7, 82.1. Anal. calcd for $C_{16}H_{28}O_2$: C, 76.14; H, 11.18; O, 12.68. Found: C, 76.05; H, 11.22.



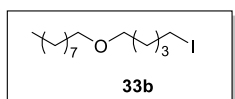
1,5-diiodopentane (32): Method B, Step I. Oil; 95% yield.

1H NMR (500 MHz): δ 1.49–1.55 (m, 2H), 1.82–1.88 (m, 4H), 3.19 (t, $J = 7.0$, 4H). ^{13}C NMR (100 MHz): δ : 6.3(2C), 31.1, 32.5(2C). Anal. calcd for $C_5H_{10}I_2$: C, 18.54; H, 3.11; I, 78.35. Found: C, 18.62; H, 3.12.



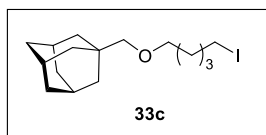
1-Iodo-5-hexyloxy-pentane (33a): Method A, Step III: 70% o.y. from **28a**; **Method B, Step II:** 75% o.y. from **32**.

1H NMR (400 MHz): δ 0.89 (t, $J = 6.7$, 3H), 1.25–1.37 (m, 5H), 1.42–1.50 (m, 2H), 1.52–1.63 (m, 5H), 1.82–1.89 (m, 2H), 3.19 (t, $J = 7.0$, 2H), 3.39 (t, $J = 5.0$, 2H), 3.41 (t, $J = 4.4$, 2H). ^{13}C NMR (100 MHz): δ 7.1, 14.2, 22.7, 26.0, 27.4, 28.8, 29.9, 31.9, 33.5, 70.6, 71.2. Anal. calcd for $C_{11}H_{23}IO$: C, 44.30; H, 7.77; I, 42.56; O, 5.37. Found: C, 44.22; H, 7.44.



1-Iodo-5-nonyloxy-pentane (33b): Method A, Step III: 88% o.y. from **28b**; **Method B, Step II:** 74% o.y. from **32**.

1H NMR (500 MHz): δ 0.88 (t, $J = 6.8$, 3H), 1.25–1.34 (m, 12H), 1.43–1.49 (m, 2H), 1.53–1.63 (m, 4H), 1.82–1.88 (m, $J = 7.1$, 2H), 3.19 (t, $J = 7.0$, 2H), 3.4 (q, $J = 6.4$, 4H). ^{13}C NMR (125 MHz): δ 7.3, 14.5, 23.1, 26.6, 27.7, 29.1, 29.7, 29.9, 30.0, 30.2, 32.3, 33.8, 70.9, 71.5. Anal. calcd for $C_{14}H_{29}IO$: C, 49.41; H, 8.59; I, 37.29; O, 4.70. Found: C, 49.50; H, 8.56.

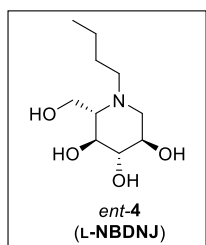


Iodo-5-adamantanemethoxyl-pentane (33c): Method A, Step III: 80% o.y. from **28c**; **Method B, Step II:** 80% o.y. from **32**.

1H NMR (500 MHz): δ 1.41–1.50 (m, 2H), 1.50–1.54 (m, 6H), 1.54–1.60 (m, 2H), 1.60–1.74 (m, 6H), 1.80–1.89 (m, 2H), 1.92–1.99 (m, 3H), 2.94 (s, 2H), 3.19 (t, $J = 7.1$, 2H), 3.37 (t, $J = 6.3$, 2H). ^{13}C NMR

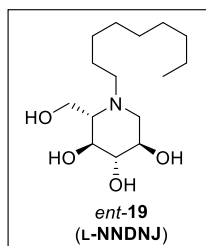
(125 MHz): δ 7.2, 27.4, 28.4, 28.5, 28.6, 28.7, 29.8, 31.4, 32.2, 33.5, 34.2, 37.4, 37.5, 39.9, 71.4, 82.1. Anal. calcd for C₁₆H₂₇IO: C, 53.04; H, 7.51; I, 35.03; O, 4.42. Found: C, 53.16; H, 7.54.

SYNTHESIS OF *N*-ALKYL L-DEOXYIMINOSUGARS

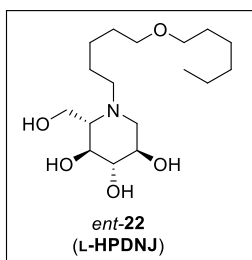


***N*-Butyl-L-deoxyiminosugar (*ent*-4).** Butanal (16.4 μ L, 0.18 mmol) was added to a stirring solution of L-DNJ (28 mg, 0.14 mmol) in an acetic acid/methanol (2 mL, 1:200 v/v) solution. After a few minutes, NaBH₃CN (8.8 mg, 0.14 mmol) was added. The resulting mixture was stirred at room temperature for 16 h; then the volatiles were removed under reduced pressure. Chromatography of the crude residue over silica gel (CHCl₃:MeOH = 9:1) yielded the pure *ent*-4 (30 mg, 96% yield) as a colorless oil. $[\alpha]_D +17.0$, c 0.27. ¹H NMR (400 MHz, D₂O): δ 0.92 (t, J = 7.3, 3H), 1.31 (sext, J = 7.3, 2H), 1.47-1.59 (m, 2H), 2.40-2.55 (m, 2H), 2.68-2.80 (m, 1H), 2.82-2.95 (m, 1H), 3.10-3.21 (m, 1H), 3.32 (t, J = 9.3, 1H), 3.45 (t, J = 9.5, 1H), 3.61 (ddd, J = 10.7, 9.3, 4.9, 1H), 3.89 (dd, J = 12.9, 2.5, 1H), 3.94 (dd, J = 12.9, 2.5, 1H). ¹³C NMR (100 MHz, CD₃OD): ppm 14.2, 21.4, 27.0, 53.7, 56.5, 57.7, 67.4, 69.6, 70.8, 79.6. Anal. calcd for C₁₀H₂₁NO₄: C, 54.77; H, 9.65; N, 6.39. Found: C, 54.77; H, 9.65; N, 6.39. HRMS: m/z [M + H]⁺, calcd: 220.1471; found: 220.1533.

General procedure for the synthesis of L-DNJ derivatives from iodides 33: A solution of iodide **29b**, **33a-c** (1.2 equiv) in anhydrous DMF (3.5 mL) was added dropwise to a solution of L-DNJ (1.0 equiv) and K₂CO₃ (3.0 equiv) in DMF (3.5 mL). The reaction was warmed to the appropriate temperature (**29b**: 70 °C; **33a-c**: 80 °C) and stirred for 16 h. Afterwards, the solvent was removed under reduced pressure. Chromatography of the crude residue over silica gel (*ent*-**14**,**19**,**22**: acetone/MeOH = 8:2; *ent*-**25**: acetone/MeOH = 9:1) afforded the DNJ derivatives *ent*-**14**,**19**,**22**,**25** as oil. The compound, dissolved in water, was further purified with Dowex® 1X8, 50-100 mesh, ion-exchange resin.

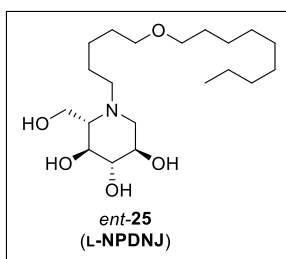


L-N-nonyl DNJ (*ent*-19): 80% yield; ¹H NMR (400 MHz, CD₃OD): δ 0.90 (t, J = 7.0, 3H), 1.22-1.38 (m, 12H), 1.45-1.57 (m, 2H), 2.18-2.20 (m, 1H), 2.24 (t, J = 10.9, 1H), 2.60-2.66 (m, 1H), 2.81-2.87 (m, 1H), 3.02 (dd, J = 4.8, 11.3, 1H), 3.15 (t, J = 9.1, 1H), 3.37 (t, J = 9.3, 1H), 3.49 (dt, J = 4.9, 5.3, 1H), 3.86 (bs, 2H). ¹³C NMR (100 MHz, CD₃OD), δ : 14.4, 23.7, 24.5, 27.9, 30.3(2C), 30.6, 33.0, 54.1, 55.5, 56.4, 67.4, 68.6, 69.7, 78.7. Anal. calcd for C₁₅H₃₁NO₄: C, 62.25; H, 10.80; N, 4.84; O, 22.11. Found: C, 62.40; H, 10.76; N, 4.81. LC-TOF MS: m/z [M + H]⁺, calcd: 290.23; found: 290.23.



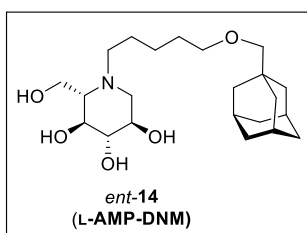
L-N-[5-(Hexoxy)pentyl]-DNJ (*ent*-22): 78% yield; ^1H NMR (500 MHz, CD_3OD): δ 0.93 (t, $J = 6.7$ Hz, 3H), 1.31-1.39 (m, 8H), 1.52-1.65 (m, 6H), 2.15-2.24 (m, 2H), 2.59-2.65 (m, 1H), 2.81-2.87 (m, 1H), 3.02 (dd, $J = 4.9, 11.2$, 1H), 3.15 (t, $J = 9.1$, 1H), 3.37 (dd, $J = 9.4, 12.0$, 1H), 3.45 (q, $J = 6.2$, 4H), 3.49 (dt, $J = 4.9, 10.3$, 1H), 3.86 (dd, $J = 2.7, 12.0$, 1H), 3.89 (dd, $J = 2.6, 12.0$, 1H). ^{13}C NMR (500 MHz, CD_3OD): δ 14.4, 23.7, 23.9, 24.5, 26.9, 30.1, 30.7, 32.8, 54.3, 54.9, 54.9, 67.4, 67.8, 68.8, 71.4, 72.1, 78.1. Anal. calcd for $\text{C}_{17}\text{H}_{35}\text{NO}_5$: C, 61.23; H, 10.58; N, 4.20; O, 23.99. Found: C, 61.13; H, 10.62; N, 4.21. LC-TOF MS: m/z $[\text{M} + \text{H}]^+$, calcd: 334.26; found: 334.25.

$\text{C}_{17}\text{H}_{35}\text{NO}_5$: C, 61.23; H, 10.58; N, 4.20; O, 23.99. Found: C, 61.13; H, 10.62; N, 4.21. LC-TOF MS: m/z $[\text{M} + \text{H}]^+$, calcd: 334.26; found: 334.25.



L-N-[5-(Nonyloxy)pentyl]DNJ (*ent*-25): 75% yield; ^1H NMR (500 MHz, CD_3OD): δ : 0.92 (t, $J = 6.6$ Hz, 3H), 1.29-1.41 (m, 14H), 1.51-1.64 (m, 6H), 2.13 (bd, $J = 9.5$, 1H), 2.19 (dd, $J = 6.7, 10.8$, 1H), 2.57-2.63 (m, 1H), 2.79-2.85 (m, 1H), 3.01 (dd, $J = 4.9, 11.2$, 1H), 3.14 (t, $J = 9.1$, 1H), 3.37 (t, $J = 9.0$, 1H), 3.44 (q, $J = 6.3$, 4H), 3.49 (dt, $J = 4.8$, 1H), 3.85 (dd, $J = 2.2, 11.9$, 1H), 3.89 (dd, $J = 1.9, 11.9$, 1H). ^{13}C NMR (100 MHz, CD_3OD), δ : 14.4, 23.7, 24.0, 24.5, 27.3, 30.2, 30.4, 30.6, 30.7, 30.8, 33.0, 54.3, 54.8, 54.9, 67.4, 67.8,

68.8, 71.4, 72.1, 78.2. Anal. calcd for $\text{C}_{20}\text{H}_{41}\text{NO}_5$: C, 63.96; H, 11.00; N, 3.73; O, 21.30. Found: C, 64.07; H, 10.96; N, 3.72. LC-TOF MS: m/z $[\text{M} + \text{H}]^+$, calcd: 376.31; found: 376.30.



L-N-Adamantanemethoxypentyl-DNJ (*ent*-14): 80% yield; ^1H NMR (500 MHz, CD_3OD): δ 1.31-1.40 (m, 2H), 1.50-1.64 (m, 10H), 1.69 (bd, $J = 11.9$, 3H), 1.76 (bd, $J = 12.0$, 3H), 1.95 (bs, 3H), 2.09-2.15 (m, 1H), 2.16-2.22 (m, 1H), 2.55-2.63 (m, 1H), 2.77-2.83 (m, 1H), 2.97 (s, 2H), 2.99 (dd, $J = 4.8, 11.3$, 1H), 3.13 (t, $J = 9.1$, 1H), 3.35 (t, $J = 8.9$, 1H), 3.39 (t, $J = 6.2$, 2H), 3.45-3.50 (m, 1H), 3.84 (dd, $J = 1.7, 12.0$, 1H), 3.87 (dd, $J = 2.3, 12.2$, 1H). ^{13}C NMR (100 MHz, CD_3OD), δ : 24.2,

24.7, 29.7, 30.2, 33.4, 38.3, 40.8, 55.1, 55.7, 67.4, 68.1, 69.2, 72.2, 72.6, 78.4, 83.1. Anal. calcd for $\text{C}_{22}\text{H}_{39}\text{NO}_5$: C, 66.47; H, 9.89; N, 3.52; O, 20.12. Found: C, 66.37; H, 9.92; N, 3.51. LC-TOF MS: m/z $[\text{M} + \text{H}]^+$, calcd: 398.29; found: 398.29.

1.5 BIBLIOGRAPHY

- (1) Fraser-Pitt, D.; O’Neil, D. Cystic Fibrosis – a Multiorgan Protein Misfolding Disease. *Futur. Sci. OA* **2015**, *1* (2), 10.4155/fso.15.57. <https://doi.org/10.4155/fso.15.57>.
- (2) Ratjen, F.; Bell, S. C.; Rowe, S. M.; Goss, C. H.; Quittner, A. L.; Bush, A. Cystic Fibrosis. *Nat. Rev. Dis. Prim.* **2015**, *1* (May), 15010. <https://doi.org/10.1038/nrdp.2015.10>.
- (3) Lubamba, B.; Dhooghe, B.; Noel, S.; Leal, T. Cystic Fibrosis: Insight into CFTR Pathophysiology and Pharmacotherapy. *Clin. Biochem.* **2012**, *45* (15), 1132–1144. <https://doi.org/10.1016/j.clinbiochem.2012.05.034>.
- (4) Elborn, J. S. Cystic Fibrosis. *Lancet* **2016**, *388* (10059), 2519–2531. [https://doi.org/10.1016/S0140-6736\(16\)00576-6](https://doi.org/10.1016/S0140-6736(16)00576-6).
- (5) Cutting, G. R. Cystic Fibrosis Genetics: From Molecular Understanding to Clinical Application. *Nat. Rev. Genet.* **2015**, *16* (1), 45–56. <https://doi.org/10.1038/nrg3849>.
- (6) Bell, S. C.; Mall, M. A.; Gutierrez, H.; Macek, M.; Madge, S.; Davies, J. C.; Burgel, P. R.; Tullis, E.; Castaños, C.; Castellani, C.; Byrnes, C. A.; Cathcart, F.; Chotirmall, S. H.; Cosgriff, R.; Eichler, I.; Fajac, I.; Goss, C. H.; Drevinek, P.; Farrell, P. M.; Gravelle, A. M.; Havermans, T.; Mayer-Hamblett, N.; Kashirskaya, N.; Kerem, E.; Mathew, J. L.; McKone, E. F.; Naehrlich, L.; Nasr, S. Z.; Oates, G. R.; O’Neill, C.; Pypops, U.; Raraigh, K. S.; Rowe, S. M.; Southern, K. W.; Sivam, S.; Stephenson, A. L.; Zampoli, M.; Ratjen, F. The Future of Cystic Fibrosis Care: A Global Perspective. *Lancet Respir. Med.* **2020**, *8* (1), 65–124. [https://doi.org/10.1016/S2213-2600\(19\)30337-6](https://doi.org/10.1016/S2213-2600(19)30337-6).
- (7) Dechecchi, M. C.; Tamanini, A.; Cabrini, G. Molecular Basis of Cystic Fibrosis: From Bench to Bedside. *Ann. Transl. Med.* **2018**, *6* (17), 334–334. <https://doi.org/10.21037/atm.2018.06.48>.
- (8) Mayer-Hamblett, N.; van Koningsbruggen-Rietschel, S.; Nichols, D. P.; VanDevanter, D. R.; Davies, J. C.; Lee, T.; Durmowicz, A. G.; Ratjen, F.; Konstan, M. W.; Pearson, K.; Bell, S. C.; Clancy, J. P.; Taylor-Cousar, J. L.; De Boeck, K.; Donaldson, S. H.; Downey, D. G.; Flume, P. A.; Drevinek, P.; Goss, C. H.; Fajac, I.; Magaret, A. S.; Quon, B. S.; Singleton, S. M.; VanDalfsen, J. M.; Retsch-Bogart, G. Z. Building Global Development Strategies for Cf Therapeutics during a Transitional Cfr Modulator Era. *J. Cyst. Fibros.* **2020**, *19* (5), 677–687. <https://doi.org/10.1016/j.jcf.2020.05.011>.
- (9) Cantin, A. M.; Hartl, D.; Konstan, M. W.; Chmiel, J. F. Inflammation in Cystic Fibrosis Lung Disease: Pathogenesis and Therapy. *J. Cyst. Fibros.* **2015**, *14* (4), 419–430. <https://doi.org/10.1016/j.jcf.2015.03.003>.
- (10) Pedemonte, N. Editorial: Special Issue on “Therapeutic Approaches for Cystic Fibrosis.” *Int. J. Mol. Sci.* **2020**, *21* (18), 6657. <https://doi.org/10.3390/ijms21186657>.
- (11) Heijerman, H. G. M.; McKone, E. F.; Downey, D. G.; Van Braeckel, E.; Rowe, S. M.; Tullis, E.; Mall, M. A.; Welter, J. J.; Ramsey, B. W.; McKee, C. M.; Marigowda, G.; Moskowitz, S. M.; Waltz, D.; Sosnay, P. R.; Simard, C.; Ahluwalia, N.; Xuan, F.; Zhang, Y.; Taylor-Cousar, J. L.; McCoy, K. S.; McCoy, K.; Donaldson, S.; Walker, S.; Chmiel, J.; Rubenstein, R.; Froh, D. K.; Neuringer, I.; Jain, M.; Moffett, K.; Taylor-Cousar, J. L.; Barnett, B.; Mueller, G.; Flume, P.; Livingston, F.; Mehdi, N.; Teneback, C.; Welter, J.; Jain, R.; Kissner, D.; Patel, K.; Calimano, F. J.; Johannes, J.; Daines, C.; Keens, T.; Scher, H.; Chittivelu, S.; Reddivalam, S.; Klingsberg, R. C.; Johnson, L. G.; Verhulst, S.; Macedo, P.; Downey, D.; Connett, G.; Nash, E.; Withers, N.; Lee, T.; Bakker, M.; Heijerman, H.; Vermeulen, F.; Van Braeckel, E.; Knoop, C.; De Wachter, E.; van der

- Meer, R.; Merkus, P.; Majoor, C. Efficacy and Safety of the Elexacaftor plus Tezacaftor plus Ivacaftor Combination Regimen in People with Cystic Fibrosis Homozygous for the F508del Mutation: A Double-Blind, Randomised, Phase 3 Trial. *Lancet* **2019**, *394* (10212), 1940–1948. [https://doi.org/10.1016/S0140-6736\(19\)32597-8](https://doi.org/10.1016/S0140-6736(19)32597-8).
- (12) Ramsey, B. W.; Davies, J.; McElvaney, N. G.; Tullis, E.; Bell, S. C.; Dřevínek, P.; Griese, M.; McKone, E. F.; Wainwright, C. E.; Konstan, M. W.; Moss, R.; Ratjen, F.; Sermet-Gaudelus, I.; Rowe, S. M.; Dong, Q.; Rodriguez, S.; Yen, K.; Ordoñez, C.; Elborn, J. S. A CFTR Potentiator in Patients with Cystic Fibrosis and the G551D Mutation. *N. Engl. J. Med.* **2011**, *365* (18), 1663–1672. <https://doi.org/10.1056/NEJMOA1105185>.
- (13) Wainwright, C. E.; Elborn, J. S.; Ramsey, B. W.; Marigowda, G.; Huang, X.; Cipolli, M.; Colombo, C.; Davies, J. C.; De Boeck, K.; Flume, P. A.; Konstan, M. W.; McColley, S. A.; McCoy, K.; McKone, E. F.; Munck, A.; Ratjen, F.; Rowe, S. M.; Waltz, D.; Boyle, M. P. Lumacaftor–Ivacaftor in Patients with Cystic Fibrosis Homozygous for Phe508del CFTR. *N. Engl. J. Med.* **2015**, *373* (3), 220–231. <https://doi.org/10.1056/NEJMOA1409547>.
- (14) Taylor-Cousar, J. L.; Munck, A.; McKone, E. F.; van der Ent, C. K.; Moeller, A.; Simard, C.; Wang, L. T.; Ingenito, E. P.; McKee, C.; Lu, Y.; Lekstrom-Himes, J.; Elborn, J. S. Tezacaftor–Ivacaftor in Patients with Cystic Fibrosis Homozygous for Phe508del. *N. Engl. J. Med.* **2017**, *377* (21), 2013–2023. <https://doi.org/10.1056/NEJMOA1709846>.
- (15) Roesch, E. A.; Nichols, D. P.; Chmiel, J. F. Inflammation in Cystic Fibrosis: An Update. *Pediatr. Pulmonol.* **2018**, *53* (June), S30–S50. <https://doi.org/10.1002/ppul.24129>.
- (16) Mitri, C.; Xu, Z.; Bardin, P.; Corvol, H.; Touqui, L.; Tabary, O. Novel Anti-Inflammatory Approaches for Cystic Fibrosis Lung Disease: Identification of Molecular Targets and Design of Innovative Therapies. *Front. Pharmacol.* **2020**, *11* (July), 1–25. <https://doi.org/10.3389/fphar.2020.01096>.
- (17) Esposito, A.; D’Alonzo, D.; De Fenza, M.; De Gregorio, E.; Tamanini, A.; Lippi, G.; Dececchi, M. C.; Guaragna, A. Synthesis and Therapeutic Applications of Iminosugars in Cystic Fibrosis. *Int. J. Mol. Sci.* **2020**, *21* (9), 3353. <https://doi.org/10.3390/ijms21093353>.
- (18) Compain, Philippe; Martin, O. *Iminosugars: From Synthesis to Therapeutic Applications*; Compain, P., Martin, O. R., Eds.; John Wiley & Sons, Ltd: Chichester, UK, 2007. <https://doi.org/10.1002/9780470517437>.
- (19) Nash, R. J.; Kato, A.; Yu, C. Y.; Fleet, G. W. Iminosugars as Therapeutic Agents: Recent Advances and Promising Trends. *Future Med. Chem.* **2011**, *3* (12), 1513–1521. <https://doi.org/10.4155/fmc.11.117>.
- (20) Inouye, S.; Tsuruoka, T.; Nida, T. The Structure of Nojirimycin, a Piperidinose Sugar Antibiotic. *J. Antibiot. (Tokyo)*. **1966**, *19* (6), 288–292. <https://doi.org/10.7164/antibiotics.19.288>.
- (21) Gao, K.; Zheng, C.; Wang, T.; Zhao, H.; Wang, J.; Wang, Z.; Zhai, X.; Jia, Z.; Chen, J.; Zhou, Y.; Wang, W. 1-Deoxynojirimycin: Occurrence, Extraction, Chemistry, Oral Pharmacokinetics, Biological Activities and In Silico Target Fishing. *Molecules* **2016**, *21* (11), 1600. <https://doi.org/10.3390/molecules21111600>.
- (22) Mellor, H. R.; Nolan, J.; Pickering, L.; Wormald, M. R.; Platt, F. M.; Dwek, R. A.; Fleet, G. W. J.; Butters, T. D. Preparation, Biochemical Characterization and Biological Properties of Radiolabelled N-Alkylated Deoxynojirimycins. *Biochem. J.* **2002**, *233*, 225–233.
- (23) Scott, L. J.; Spencer, C. M. Miglitol: A Review of Its Therapeutic Potential in Type 2

- Diabetes Mellitus. *Drugs*. Adis International Ltd October 2000, pp 521–549. <https://doi.org/10.2165/00003495-200059030-00012>.
- (24) Alonzi, D. S.; Scott, K. A.; Dwek, R. A.; Zitzmann, N. Iminosugar Antivirals: The Therapeutic Sweet Spot. *Biochem. Soc. Trans.* **2017**, *45* (2), 571–582. <https://doi.org/10.1042/BST20160182>.
- (25) Fiaux, H.; Popowycz, F.; Favre, S.; Schütz, C.; Vogel, P.; Gerber-Lemaire, S.; Juillerat-Jeanneret, L. Functionalized Pyrrolidines Inhibit α -Mannosidase Activity and Growth of Human Glioblastoma and Melanoma Cells. *J. Med. Chem.* **2005**, *48* (13), 4237–4246. <https://doi.org/10.1021/jm0409019>.
- (26) Hollak, C. E. M.; Hughes, D.; van Schaik, I. N.; Schwierin, B.; Bembi, B. Miglustat (Zavesca®) in Type 1 Gaucher Disease: 5-Year Results of a Post-Authorisation Safety Surveillance Programme. *Pharmacoepidemiol. Drug Saf.* **2009**, *18* (9), 770–777. <https://doi.org/10.1002/pds.1779>.
- (27) Stütz, A. E. *Iminosugars as Glycosidase Inhibitors*; Stütz, A. E., Ed.; Wiley, 1998. <https://doi.org/10.1002/3527601740>.
- (28) Lillelund, V. H.; Jensen, H. H.; Liang, X.; Bols, M. Recent Developments of Transition-State Analogue Glycosidase Inhibitors of Non-Natural Product Origin. *Chem. Rev.* **2002**, *102* (2), 515–553.
- (29) Platt, F. M.; d’Azzo, A.; Davidson, B. L.; Neufeld, E. F.; Tiffet, C. J. Lysosomal Storage Diseases. *Nat. Rev. Dis. Prim.* **2018**, *4* (1). <https://doi.org/10.1038/s41572-018-0025-4>.
- (30) Benjamin, E. R.; Della Valle, M. C.; Wu, X.; Katz, E.; Pruthi, F.; Bond, S.; Bronfin, B.; Williams, H.; Yu, J.; Bichet, D. G.; Germain, D. P.; Giugliani, R.; Hughes, D.; Schiffmann, R.; Wilcox, W. R.; Desnick, R. J.; Kirk, J.; Barth, J.; Barlow, C.; Valenzano, K. J.; Castelli, J.; Lockhart, D. J. The Validation of Pharmacogenetics for the Identification of Fabry Patients to Be Treated with Migalastat. *Genet. Med.* **2017**, *19* (4), 430–438. <https://doi.org/10.1038/gim.2016.122>.
- (31) Khanna, R.; Soska, R.; Lun, Y.; Feng, J.; Frascella, M.; Young, B.; Brignol, N.; Pellegrino, L.; Sitaraman, S. A.; Desnick, R. J.; Benjamin, E. R.; Lockhart, D. J.; Valenzano, K. J. The Pharmacological Chaperone 1-Deoxygalactonojirimycin Reduces Tissue Globotriaosylceramide Levels in a Mouse Model of Fabry Disease. *Mol. Ther.* **2010**, *18* (1), 23–33. <https://doi.org/10.1038/mt.2009.220>.
- (32) Norez, C.; Noel, S.; Wilke, M.; Bijvelds, M.; Jorna, H.; Melin, P.; Dejonge, H.; Becq, F. Rescue of Functional Δ F508-CFTR Channels in Cystic Fibrosis Epithelial Cells by the α -Glucosidase Inhibitor Miglustat. *FEBS Lett.* **2006**, *580* (8), 2081–2086. <https://doi.org/10.1016/j.febslet.2006.03.010>.
- (33) Antigny, F.; Norez, C.; Becq, F.; Vandebrouck, C. Calcium Homeostasis Is Abnormal in Cystic Fibrosis Airway Epithelial Cells but Is Normalized after Rescue of F508del-CFTR. *Cell Calcium* **2008**, *43* (2), 175–183. <https://doi.org/10.1016/j.ceca.2007.05.002>.
- (34) Norez, C.; Antigny, F.; Noel, S.; Vandebrouck, C.; Becq, F. A Cystic Fibrosis Respiratory Epithelial Cell Chronically Treated by Miglustat Acquires a Non-Cystic Fibrosis-like Phenotype. *Am. J. Respir. Cell Mol. Biol.* **2009**, *41* (2), 217–225. <https://doi.org/10.1165/rcmb.2008-0285OC>.
- (35) Lubamba, B.; Lebacqz, J.; Lebecque, P.; Vanbever, R.; Leonard, A.; Wallemacq, P.; Leal, T. Airway Delivery of Low-Dose Miglustat Normalizes Nasal Potential Difference in F508del Cystic Fibrosis Mice. *Am. J. Respir. Crit. Care Med.* **2009**, *179* (11), 1022–1028. <https://doi.org/10.1164/rccm.200901-0049OC>.
- (36) Leonard, A.; Lebecque, P.; Dingemans, J.; Leal, T. A Randomized Placebo-Controlled Trial of Miglustat in Cystic Fibrosis Based on Nasal Potential Difference. *J. Cyst. Fibros.* **2012**, *11* (3),

- 231–236. <https://doi.org/10.1016/j.jcf.2011.12.004>.
- (37) Cendret, V.; Legigan, T.; Mingot, A.; Thibaudeau, S.; Adachi, I.; Forcella, M.; Parenti, P.; Bertrand, J.; Becq, F.; Norez, C.; Désiré, J.; Kato, A.; Blériot, Y. Synthetic Deoxynojirimycin Derivatives Bearing a Thiolated, Fluorinated or Unsaturated N-Alkyl Chain: Identification of Potent α -Glucosidase and Trehalase Inhibitors as Well as F508del-CFTR Correctors. *Org. Biomol. Chem.* **2015**, *13* (43), 10734–10744. <https://doi.org/10.1039/c5ob01526j>.
- (38) Ardes-Guisot, N.; Alonzi, D. S.; Reinkensmeier, G.; Butters, T. D.; Norez, C.; Becq, F.; Shimada, Y.; Nakagawa, S.; Kato, A.; Blériot, Y.; Sollogoub, M.; Vauzeilles, B. Selection of the Biological Activity of DNJ Neoglycoconjugates through Click Length Variation of the Side Chain. *Org. Biomol. Chem.* **2011**, *9* (15), 5373–5388. <https://doi.org/10.1039/c1ob05119a>.
- (39) Désiré, J.; Mondon, M.; Fontelle, N.; Nakagawa, S.; Hirokami, Y.; Adachi, I.; Iwaki, R.; Fleet, G. W. J.; Alonzi, D. S.; Twigg, G.; Butters, T. D.; Bertrand, J.; Cendret, V.; Becq, F.; Norez, C.; Marrot, J.; Kato, A.; Blériot, Y. N- and C-Alkylation of Seven-Membered Iminosugars Generates Potent Glucocerebrosidase Inhibitors and F508del-CFTR Correctors. *Org. Biomol. Chem.* **2014**, *12* (44), 8977–8996. <https://doi.org/10.1039/C4OB00325J>.
- (40) Nocquet, P. A.; Hensienne, R.; Wencel-Delord, J.; Laigre, E.; Sidelarbi, K.; Becq, F.; Norez, C.; Hazelard, D.; Compain, P. Pushing the Limits of Catalytic C-H Amination in Polyoxygenated Cyclobutanes. *Org. Biomol. Chem.* **2016**, *14* (9), 2780–2796. <https://doi.org/10.1039/c5ob02602d>.
- (41) Dehoux, C.; Castellán, T.; Enel, M.; André-Barrès, C.; Mirval, S.; Becq, F.; Ballereau, S.; Génisson, Y. Transalpinecine and Analogues: First Total Synthesis, Stereochemical Revision and Biological Evaluation. *European J. Org. Chem.* **2019**, *2019* (8), 1830–1834. <https://doi.org/10.1002/ejoc.201900071>.
- (42) Best, D.; Jenkinson, S. F.; Saville, A. W.; Alonzi, D. S.; Wormald, M. R.; Butters, T. D.; Norez, C.; Becq, F.; Blériot, Y.; Adachi, I.; Kato, A.; Fleet, G. W. J. Cystic Fibrosis and Diabetes: IsoLAB and IsoDAB, Enantiomeric Carbon-Branched Pyrrolidine Iminosugars. *Tetrahedron Lett.* **2010**, *51* (32), 4170–4174. <https://doi.org/10.1016/j.tetlet.2010.05.131>.
- (43) Yu, C.-Y.; Asano, N.; Ikeda, K.; Wang, M.-X.; Butters, T. D.; Wormald, M. R.; Dwek, R. A.; Winters, A. L.; Nash, R. J.; Fleet, G. W. J. Looking Glass Inhibitors: L-DMDP, a More Potent and Specific Inhibitor of α -Glucosidases than the Enantiomeric Natural Product DMDP. *Chem. Commun.* **2004**, No. 17, 1936–1937. <https://doi.org/10.1039/B406035K>.
- (44) Dehecchi, M. C.; Nicolis, E.; Mazzi, P.; Cioffi, F.; Bezzerri, V.; Lampronti, I.; Huang, S.; Wiszniewski, L.; Gambari, R.; Scupoli, M. T.; Berton, G.; Cabrini, G. Modulators of Sphingolipid Metabolism Reduce Lung Inflammation. *Am. J. Respir. Cell Mol. Biol.* **2011**, *45* (4), 825–833. <https://doi.org/10.1165/rcmb.2010-0457OC>.
- (45) Dehecchi, M. C.; Nicolis, E.; Norez, C.; Bezzerri, V.; Borgatti, M.; Mancini, I.; Rizzotti, P.; Ribeiro, C. M. P.; Gambari, R.; Becq, F.; Cabrini, G. Anti-Inflammatory Effect of Miglustat in Bronchial Epithelial Cells. *J. Cyst. Fibros.* **2008**, *7* (6), 555–565. <https://doi.org/10.1016/j.jcf.2008.06.002>.
- (46) Dehecchi, M. C.; Nicolis, E.; Mazzi, P.; Paroni, M.; Cioffi, F.; Tamanini, A.; Bezzerri, V.; Tebon, M.; Lampronti, I.; Huang, S.; Wiszniewski, L.; Scupoli, M. T.; Bragonzi, A.; Gambari, R.; Berton, G.; Cabrini, G. Pharmacological Modulators of Sphingolipid Metabolism for the Treatment of Cystic Fibrosis Lung Inflammation. In *Cystic Fibrosis - Renewed Hopes Through Research*; InTech, 2012. <https://doi.org/10.5772/31050>.
- (47) Schiumarini, D.; Loberto, N.; Mancini, G.; Bassi, R.; Giussani, P.; Chiricozzi, E.; Samarani, M.;

- Munari, S.; Tamanini, A.; Cabrini, G.; Lippi, G.; Dececchi, M. C.; Sonnino, S.; Aureli, M. Evidence for the Involvement of Lipid Rafts and Plasma Membrane Sphingolipid Hydrolases in *Pseudomonas Aeruginosa* Infection of Cystic Fibrosis Bronchial Epithelial Cells. *Mediators Inflamm.* **2017**, No. 2, 1–16. <https://doi.org/10.1155/2017/1730245>.
- (48) Chiricozzi, E.; Loberto, N.; Schiumarini, D.; Samarani, M.; Mancini, G.; Tamanini, A.; Lippi, G.; Dececchi, M. C.; Bassi, R.; Giussani, P.; Aureli, M. Sphingolipids Role in the Regulation of Inflammatory Response: From Leukocyte Biology to Bacterial Infection. *J. Leukoc. Biol.* **2018**, *103* (3), 445–456. <https://doi.org/10.1002/JLB.3MR0717-269R>.
- (49) Aureli, M.; Schiumarini, D.; Loberto, N.; Bassi, R.; Tamanini, A.; Mancini, G.; Tironi, M.; Munari, S.; Cabrini, G.; Dececchi, M. C.; Sonnino, S. Unravelling the Role of Sphingolipids in Cystic Fibrosis Lung Disease. *Chem. Phys. Lipids* **2016**, *200*, 94–103. <https://doi.org/10.1016/j.chemphyslip.2016.08.002>.
- (50) Loberto, N.; Tebon, M.; Lampronti, I.; Marchetti, N.; Aureli, M.; Bassi, R.; Giri, M. G.; Bezzetti, V.; Lovato, V.; Cantù, C.; Munari, S.; Cheng, S. H.; Cavazzini, A.; Gambari, R.; Sonnino, S.; Cabrini, G.; Dececchi, M. C. GBA2-Encoded β -Glucosidase Activity Is Involved in the Inflammatory Response to *Pseudomonas Aeruginosa*. *PLoS One* **2014**, *9* (8), e104763. <https://doi.org/10.1371/journal.pone.0104763>.
- (51) Overkleeft, H. S.; Renkema, G. H.; Neele, J.; Vianello, P.; Hung, I. O.; Strijland, A.; Van Der Burg, A. M.; Koomen, G. J.; Pandit, U. K.; Aerts, J. M. F. G. Generation of Specific Deoxynojirimycin-Type Inhibitors of the Non- Lysosomal Glucosylceramidase. *J. Biol. Chem.* **1998**, *273* (41), 26522–26527. <https://doi.org/10.1074/jbc.273.41.26522>.
- (52) Munari, S.; Loberto, N.; Aureli, M.; Baron, A.; Guisot, N.; Bassi, R.; Tironi, M.; Giri, M. G.; Tamanini, A.; Lippi, G.; Cabrini, G.; Dececchi, M. C. Neoglycoconjugates Derived from Deoxynojirimycin as Possible Therapeutic Agents for Cystic Fibrosis Lung Disease , by Modulation of the Sphingolipid Metabolism. *JSM Genet Genomics* **2016**, *3*, 2–7.
- (53) Horne, G.; Wilson, F. X.; Tinsley, J.; Williams, D. H.; Storer, R. Iminosugars Past, Present and Future: Medicines for Tomorrow. *Drug Discov. Today* **2011**, *16* (3–4), 107–118. <https://doi.org/10.1016/j.drudis.2010.08.017>.
- (54) Butters, T. D.; Van Den Broek, L. A. G. M.; Fleet, G. W. J.; Krulle, T. M.; Wormald, M. R.; Dwek, R. A.; Platt, F. M. Molecular Requirements of Imino Sugars for the Selective Control of N-Linked Glycosylation and Glycosphingolipid Biosynthesis. *Tetrahedron Asymmetry* **2000**, *11* (1), 113–124. [https://doi.org/10.1016/S0957-4166\(99\)00468-1](https://doi.org/10.1016/S0957-4166(99)00468-1).
- (55) Ghisaidoobe, A.; Bikker, P.; De Bruijn, A. C. J.; Godschalk, F. D.; Rogaar, E.; Guijt, M. C.; Hagens, P.; Halma, J. M.; Van't Hart, S. M.; Luitjens, S. B.; Van Rixel, V. H. S.; Wijzenbroek, M.; Zweegers, T.; Donker-Koopman, W. E.; Strijland, A.; Boot, R.; Van Der Marel, G.; Overkleeft, H. S.; Aerts, J. M. F. G.; Van Den Berg, R. J. B. H. N. Identification of Potent and Selective Glucosylceramide Synthase Inhibitors from a Library of N-Alkylated Iminosugars. *ACS Med. Chem. Lett.* **2011**, *2* (2), 119–123. <https://doi.org/10.1021/ml100192b>.
- (56) D'Alonzo, D.; Guaragna, A.; Palumbo, G. Glycomimetics at the Mirror: Medicinal Chemistry of L-Iminosugars. *Curr. Med. Chem.* **2009**, *16* (4), 473–505. <https://doi.org/10.2174/092986709787315540>.
- (57) Fleet, G. W. J.; Nicholas, S. J.; Smith, P. W.; Evans, S. V.; Fellows, L. E.; Nash, R. J. Potent Competitive Inhibition of α -Galactosidase and α -Glucosidase Activity by 1,4-Dideoxy-1,4-Iminopentitols: Syntheses of 1,4-Dideoxy-1,4-Imino-d-Lyxitol and of Both Enantiomers of 1,4-

- Dideoxy-1,4-Iminoarabinitol. *Tetrahedron Lett.* **1985**, 26 (26), 3127–3130. [https://doi.org/10.1016/S0040-4039\(00\)98636-2](https://doi.org/10.1016/S0040-4039(00)98636-2).
- (58) Jenkinson, S. F.; Best, D.; Saville, A. W.; Mui, J.; Martínez, R. F.; Nakagawa, S.; Kunimatsu, T.; Alonzi, D. S.; Butters, T. D.; Norez, C.; Becq, F.; Blériot, Y.; Wilson, F. X.; Weymouth-Wilson, A. C.; Kato, A.; Fleet, G. W. J. C-Branched Iminosugars: α -Glucosidase Inhibition by Enantiomers of IsoDMDP, IsoDGDP, and IsoDAB-1 -IsoDMDP Compared to Miglitol and Miglustat. *J. Org. Chem.* **2013**, 78 (15), 7380–7397. <https://doi.org/10.1021/jo4005487>.
- (59) Kato, A.; Kato, N.; Kano, E.; Adachi, I.; Ikeda, K.; Yu, L.; Okamoto, T.; Banba, Y.; Ouchi, H.; Takahata, H.; Asano, N. Biological Properties of α - and β -1-Deoxyzasugars. *J. Med. Chem.* **2005**, 48 (6), 2036–2044. <https://doi.org/10.1021/jm0495881>.
- (60) Lahav, D.; Liu, B.; Van Den Berg, R. J. B. H. N.; Van Den Nieuwendijk, A. M. C. H.; Wennekes, T.; Ghisaidoobe, A. T.; Breen, I.; Ferraz, M. J.; Kuo, C. L.; Wu, L.; Geurink, P. P.; Ovaa, H.; Van Der Marel, G. A.; Van Der Stelt, M.; Boot, R. G.; Davies, G. J.; Aerts, J. M. F. G.; Overkleeft, H. S. A Fluorescence Polarization Activity-Based Protein Profiling Assay in the Discovery of Potent, Selective Inhibitors for Human Nonlysosomal Glucosylceramidase. *J. Am. Chem. Soc.* **2017**, 139 (40), 14192–14197. <https://doi.org/10.1021/jacs.7b07352>.
- (61) D'Alonzo, D.; De Fenza, M.; Porto, C.; Iacono, R.; Huebecker, M.; Cobucci-Ponzano, B.; Priestman, D. A.; Platt, F.; Parenti, G.; Moracci, M.; Palumbo, G.; Guaragna, A. *N*-Butyl-L-Deoxyojirimycin (L-NBDNJ): Synthesis of an Allosteric Enhancer of α -Glucosidase Activity for the Treatment of Pompe Disease. *J. Med. Chem.* **2017**, 60 (23), 9462–9469. <https://doi.org/10.1021/acs.jmedchem.7b00646>.
- (62) De Fenza, M.; D'Alonzo, D.; Esposito, A.; Munari, S.; Loberto, N.; Santangelo, A.; Lampronti, I.; Tamanini, A.; Rossi, A.; Ranucci, S.; De Fino, I.; Bragonzi, A.; Aureli, M.; Bassi, R.; Tironi, M.; Lippi, G.; Gambari, R.; Cabrini, G.; Palumbo, G.; Dececchi, M. C.; Guaragna, A. Exploring the Effect of Chirality on the Therapeutic Potential of *N*-Alkyl-Deoxyiminosugars: Anti-Inflammatory Response to *Pseudomonas Aeruginosa* Infections for Application in CF Lung Disease. *Eur. J. Med. Chem.* **2019**, 175, 63–71. <https://doi.org/10.1016/j.ejmech.2019.04.061>.
- (63) D'Alonzo, D.; Guaragna, A.; Palumbo, G. Recent Advances in Monosaccharide Synthesis: A Journey into L-Hexose World. *Curr. Org. Chem.* **2009**, 13 (1), 71–98. <https://doi.org/10.2174/138527209787193828>.
- (64) Guaragna, A.; Dalonzo, D.; Paoletta, C.; Napolitano, C.; Palumbo, G. Highly Stereoselective de Novo Synthesis of α -Hexoses. *J. Org. Chem.* **2010**, 75 (11), 3558–3568. <https://doi.org/10.1021/jo100077k>.
- (65) Guaragna, A.; Napolitano, C.; D'Alonzo, D.; Pedatella, S.; Palumbo, G. A Versatile Route to L-Hexoses: Synthesis of L-Mannose and L-Altrose. *Org. Lett.* **2006**, 8 (21), 4863–4866. <https://doi.org/10.1021/ol061916z>.
- (66) Paoletta, C.; D'Alonzo, D.; Palumbo, G.; Guaragna, A. Sulfur-Assisted Domino Access to Bicyclic Dihydrofurans: Case Study and Early Synthetic Applications. *Org. Biomol. Chem.* **2013**, 11 (45), 7825–7829. <https://doi.org/10.1039/c3ob41324a>.
- (67) Guaragna, A.; Pedatella, S.; Palumbo, G. 5,6-Dihydro-1,4-Dithiin-2-Yl [(4-Methoxybenzyl)Oxy]Methane. In *Encyclopedia of Reagents for Organic Synthesis*; John Wiley & Sons, Ltd: Chichester, UK, 2008. <https://doi.org/10.1002/047084289X.rm00831>.
- (68) Caputo, R.; Kunz, H.; Mastroianni, D.; Palumbo, G.; Pedatella, S.; Solla, F. Mild Synthesis of Protected α -D-Glycosyl Iodides. *European J. Org. Chem.* **1999**, 1999 (11), 3147–3150.

- [https://doi.org/10.1002/\(SICI\)1099-0690\(199911\)1999:11<3147::AID-EJOC3147>3.0.CO;2-I](https://doi.org/10.1002/(SICI)1099-0690(199911)1999:11<3147::AID-EJOC3147>3.0.CO;2-I)
- (69) Caputo, R.; Guaragna, A.; Pedatella, S.; Palumbo, G. Mild and Regiospecific Phosphorylation of Nucleosides. *Synlett* **1997**, *1997* (8), 917–918. <https://doi.org/10.1055/s-1997-950>.
- (70) Pedatella, S.; Guaragna, A.; D'Alonzo, D.; De Nisco, M.; Palumbo, G. Triphenylphosphine Polymer-Bound/Iodine Complex: A Suitable Reagent for the Preparation of O -Isopropylidene Sugar Derivatives. *Synthesis (Stuttg)*. **2006**, No. 2, 305–308. <https://doi.org/10.1055/s-2005-918521>.
- (71) Esposito, A.; De Gregorio, E.; De Fenza, M.; D'Alonzo, D.; Satawani, A.; Guaragna, A. Expedient Synthesis and Preliminary Antimicrobial Activity of Deflazacort and Its Precursors. *RSC Adv*. **2019**, *9* (37), 21519–21524. <https://doi.org/10.1039/C9RA03673C>.
- (72) Montoro, R.; Wirth, T. Direct Bromination and Iodination of Non-Activated Alkanes by Hypohalite Reagents. *Synthesis (Stuttg)*. **2005**, No. 9, 1473–1478. <https://doi.org/10.1055/s-2005-865322>

BACTERIAL INFECTIONS



*N-Alkyl-Deoxyiminosugars and their
Lipophilic Conjugates as novel
Antibacterial Agents*

*Synthesis and Antibacterial Activity of
Deflazacort and its Synthetic Precursors*

2 N-ALKYL-DEOXYIMINOSUGARS AND THEIR LIPOPHILIC CONJUGATES AS NOVEL ANTIBACTERIAL AGENTS

2.1 INTRODUCTION

2.1.1 ANTIMICROBIAL RESISTANCE: A GLOBAL THREAT

Antimicrobial resistance (AMR) is nowadays one of the major threats to human health. According to the *Review on Antimicrobial Resistance* issued in 2015, at least 700,000 people die each year for drug-resistant infections and AMR will cause 10 million death/year by 2050 surpassing the deaths caused by cancer.¹ The problem of AMR, is particularly urgent regarding antibiotic resistance in bacteria. Over several decades, bacteria causing common or severe infections have developed resistance to a new antibiotic, often within a few years after its introduction on the market.² As proof of this emergency, in 2017 the World Health Organization (WHO) published a list of the 12 bacteria that represent the greatest danger to human health because of their resistance to antibiotics (FIGURE 2.1).

Priority 1: critical
<i>Acinetobacter baumannii</i> , carbapenem resistant
<i>Pseudomonas aeruginosa</i> , carbapenem resistant
<i>Enterobacteriaceae</i> , carbapenem resistant, third generation cephalosporin resistant
Priority 2: high
<i>Enterococcus faecium</i> , vancomycin resistant
<i>Staphylococcus aureus</i> , methicillin resistant, vancomycin resistant
<i>Helicobacter pylori</i> , clarithromycin resistant
<i>Campylobacter spp.</i> , fluoroquinolone resistant
<i>Salmonella spp.</i> , fluoroquinolone resistant
<i>Neisseria gonorrhoeae</i> , third generation cephalosporin resistant
Priority 3: medium
<i>Streptococcus pneumoniae</i> , penicillin non-susceptible
<i>Haemophilus influenzae</i> , ampicillin resistant
<i>Shigella spp.</i> , fluoroquinolone resistant

FIGURE 2.1. WHO priority list for research and development of new antibiotics for antibiotic-resistant bacteria.

The WHO list classified the pathogens into three categories according to urgency of intervention (critical, high and medium priority). Notably, although its resistance to traditional

treatments has been growing in recent years, *Mycobacterium tuberculosis* was not inserted into this list because belonging to other dedicated programs.³ The category of critical pathogens include *A. baumannii*, *P. aeruginosa* and various *Enterobacteriaceae* (including *Klebsiella*, *E. coli*, *Serratia*, and *Proteus*). These bacteria can cause severe and often deadly infections, such as bloodstream infections and pneumonia, and have become resistant to a large number of antibiotics, including carbapenems and third generation cephalosporins (the best available antibiotics for treating multidrug resistant bacteria).

The second and third tiers in the list include other increasingly drug resistant bacteria that cause more common diseases. Particularly, the high-priority group included vancomycin-resistant *E. faecium*, methicillin-resistant and vancomycin-resistant *S. aureus*, clarithromycin-resistant *H. pylori*, fluoroquinolone-resistant *Campylobacter spp* and *Salmonella spp*, and fluoroquinolone-resistant and third-generation cephalosporin-resistant *N. gonorrhoeae*. Penicillin-non-susceptible *S. pneumoniae*; ampicillin-resistant *H. influenza* and fluoroquinolone-resistant *Shigella spp*. instead belong to the category with lower priority.⁴

The major aim of this list is funding and coordinating the global efforts to the research and development of alternative drugs active against these resistant bacteria.³

2.1.2 ANTIBIOTIC RESISTANT PATHOGENS

There are more than 15 classes of antibiotics whose targets are involved in essential physiological or metabolic functions of the bacterial cell. β -lactams (as for example penicillins, cephalosporins) and glycopeptides (Vancomycin) target cell wall synthesis by inhibition of peptidoglycan synthesis; tetracyclines (Minocycline), cationic peptides (Colistin) and lipopeptides (Daptomycin) affected cell membrane, aminoglycosides (Gentamicin, Streptomycin) and macrolides (Erythromycin, Azithromycin) inhibit the protein synthesis, fluoroquinolones (Ciprofloxacin) and rifamycins (Rifampin) affected DNA and RNA synthesis, while sulfonamides (Sulfamethoxazole) competitively inhibit folic acid synthesis (**FIGURE 2.2**).⁵

All these classes of antibiotics have developed a mechanism of resistance that often appears shortly after the introduction of a new antimicrobial agent.⁶ For example, sulfonamide-resistant *S. pyogenes* emerged in military hospitals in the 1930s with a mechanism of resistance still operating currently.⁷ Penicillin-resistant *S. aureus* emerged very soon after the introduction of penicillin in the 1940s⁸ and similarly, methicillin-resistant strains of *S. aureus* was reported soon after the introduction of Methicillin, the semisynthetic penicillinase-resistant penicillin, while in 2002 clinical isolates of Vancomycin resistant *S. aureus* were found.⁹ Resistance to multiple drugs instead was first detected in enteric bacteria such as *E. coli*, *Shigella* and *Salmonella* in the late 1950s to early 1960s.¹⁰

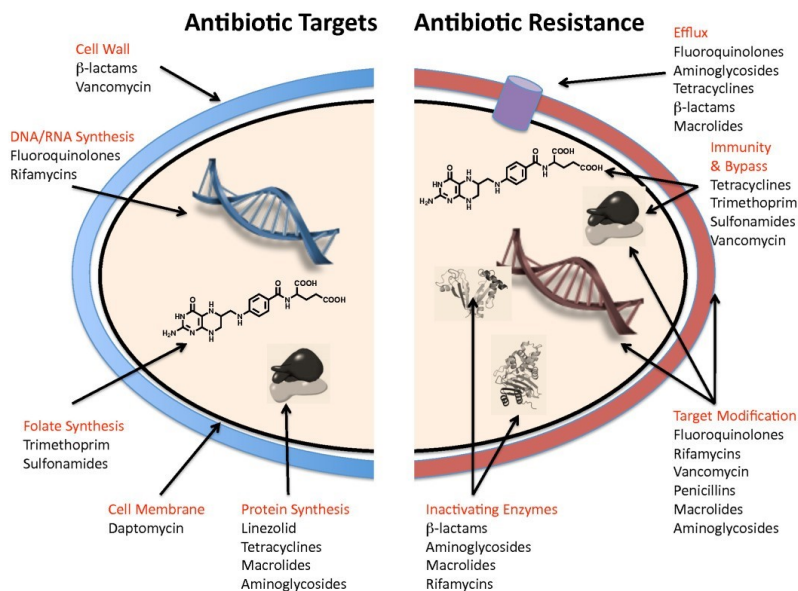


FIGURE 2.2. Antibiotic targets and mechanisms of resistance.
The figure was reproduced from Ref. 5.

The molecular mechanisms beyond the resistance to antibiotics have been studied extensively. Resistance process occurs via gene level mutations and can arise as the result of altered molecular targets, efflux of antibiotics from within the cell, blockade of antibiotic entry into the cell, and chemical modification or destruction of the compounds (**FIGURE 2.2**). In many cases, a single antibiotic or class is impacted by more than one, or even all, of these mechanisms. Furthermore, these mechanisms can be acquired by a single organism resulting in combinatorial resistance (multidrug resistant bacteria).¹¹

As mentioned above, resistance to antibiotics emerges soon after the introduction of a new antibiotic; indeed, as result of the selective pressure induced by antimicrobial drugs, bacteria start a process of selection that eventually will makes the antibiotic useless. In addition, the often improper or excessive use of antibiotics greatly contributed to the development of drug-resistant bacterial pathogens. Up to 1970s resistance to antibiotics was kept under control as there was a continuous identification of novel drugs. However, in the last few decades, research and development in antibiotic field was very limited, essentially for economic and regulatory issues and no new class of antibiotics has been discovered.¹²

Based on these considerations, it appears indispensable that great efforts have to be devoted to the search for novel antibiotic classes, as well as for alternative strategies to treat bacterial infections in order to face with this serious and global threat.

2.1.3 IMINOSUGARS AS ANTIBACTERIAL AND ANTIBIOFILM AGENTS

Iminosugars have been identified as therapeutic candidates against a broad range of diseases including malignancies, viral infections and genetic disorders (Chapter 1).^{13–15} On the contrary, only rarely they have been considered for their antibacterial activity. The first isolated iminosugar, nojirimycin (NJ), exhibited antibacterial activity against *Xanthomonas oryzae*, *Shigella flexneri* and *Mycobacterium smegmatis* ATCC 607¹⁶ (FIGURE 2.3). To the best of our knowledge, no data are reported about the mechanism beyond these antibiotic properties; however, these findings inspired to further explore this class of molecules leading to the isolation, as well as to the synthesis of NJ derivatives enabling to identify the other therapeutic properties associated to these powerful glycomimetics. Differently from NJ, its 1-deoxy derivative, DNJ, did not affect bacterial growth but it was found to inhibit biofilm formation in *Streptococcus mutans*.^{17,18}

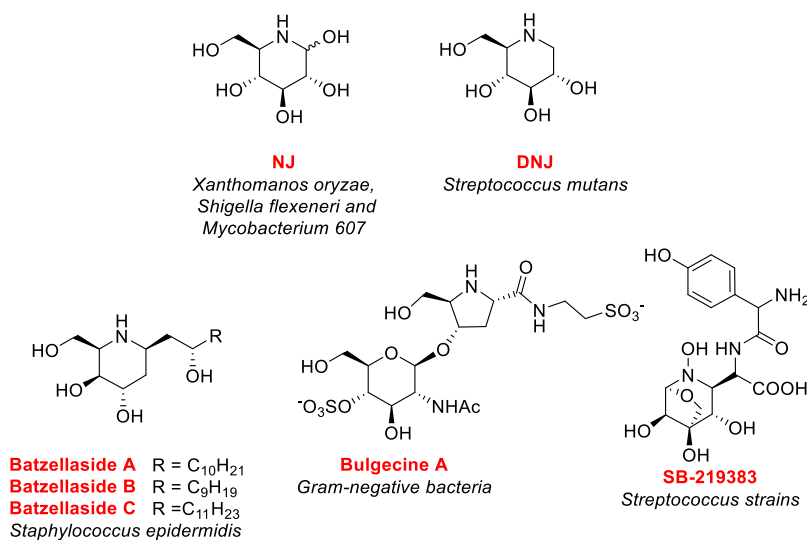


FIGURE 2.3. Iminosugars showing antibacterial and antibiofilm activity.

Other modified iminosugars such as Batzellaside A-C, isolated from a Madagascar *Batzella* sponge,¹⁹ and Bulgecin A held interesting properties against *Staphylococcus epidermidis* and Gram-negative bacteria respectively, while the antimicrobial activity against *Staphylococcus aureus* was highlighted for SB-219383 by inhibition bacterial tyrosyl tRNA synthetase¹⁶ (FIGURE 2.3). Eventually, selected piperidine and indolizidine iminosugars were found to inhibit the early biofilm formation of *Pseudomonas aeruginosa*.²⁰

These data, together with our findings about the potential antimicrobial activity of L-NBDNJ reported in Chapter 1, prompted us to explore the antibacterial activity of D- and L-DNJ and its *N*-alkyl derivatives in order to evaluate the role of both the chirality and of the lipophilicity on the eventual anti-infective activity of these molecules.

2.2 RESULTS AND DISCUSSION

Our recent results about the ability of L-NBDNJ (*ent-4*, **FIGURE 2.4**) to significantly decrease bacteria recovered in lung and BAL of *P. aeruginosa* chronically infected mice along with increase of bacterial clearance (see Chapter 1), suggest a potential antibacterial activity of this compound. Intrigued by these findings and by the data about the ability of some iminosugar derivatives to affect bacterial growth, herein we evaluated the potential of *N*-alkyl deoxyiminosugars to act as antibacterial agents.²¹ Particularly we evaluated the inhibition of *S. aureus* ATCC 29213 growth by DNJ (**2**) and its *N*-alkyl derivatives (**4,14,19,22,25**), in both their enantiomeric forms, in order to explore the eventual role of chirality and of lipophilicity on the antibacterial activity.

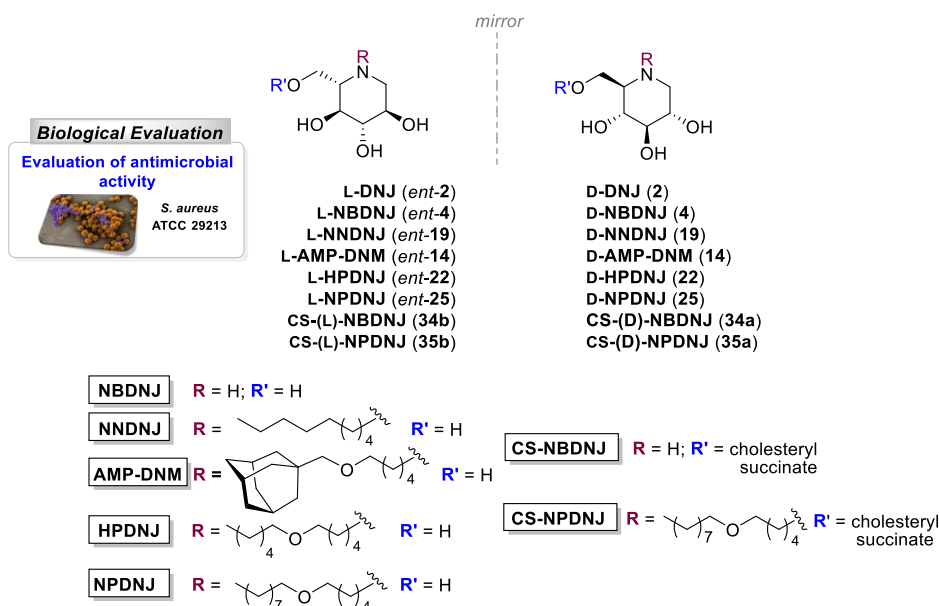


FIGURE 2.4. D- and L-DNJ and its *N*-alkyl derivatives as antimicrobial agents against *S. aureus*.

Cholesterol-bearing iminosugars **34** and **35** (**FIGURE 2.4**), were also considered in order to widen the library of *N*-alkyl deoxyiminosugars with more lipophilic derivatives. Indeed, iminosugar conjugates **34** and **35** were conceived to enhance the lipophilicity of iminosugars with the idea that conjugation of iminosugars with lipophilic moieties (even at different positions than the amino group) through a cleavable linker would positively contribute to iminosugar delivery and release within the bacterial cell.

From a synthetic standpoint, while the preparation of *N*-alkyl D- and L-deoxyiminosugars was described in the previous chapter, herein, the synthetic route aimed to obtain iminosugar conjugates **34** and **35** was studied.²² The established TPP/I₂ activating system was used for the

conjugation of the iminosugars with the cholesterol moiety. All the iminosugars were screened against *S. aureus* ATCC 29213 as preliminary evaluation of the antibacterial potential of these molecules.

2.2.1 SYNTHESIS OF LIPOPHILIC CONJUGATES OF *N*-ALKYL IMINOSUGARS

With the aim to widen the library of *N*-alkyl deoxyiminosugars and obtain more lipophilic derivatives, herein the conjugation of iminosugars with a cholesterol unit was considered through a short succinic bis-ester, taken as model linker^{23,24} (FIGURE 2.5). Cholesterol was chosen as lipophilic moiety for both the antimicrobial properties exhibited by cholesterol-containing molecules^{25,26} and its drug delivery properties,²⁷ while NBDNJ (2) and NPDNJ (25), in both their enantiomeric forms, were selected as model iminosugars for early synthetic efforts.

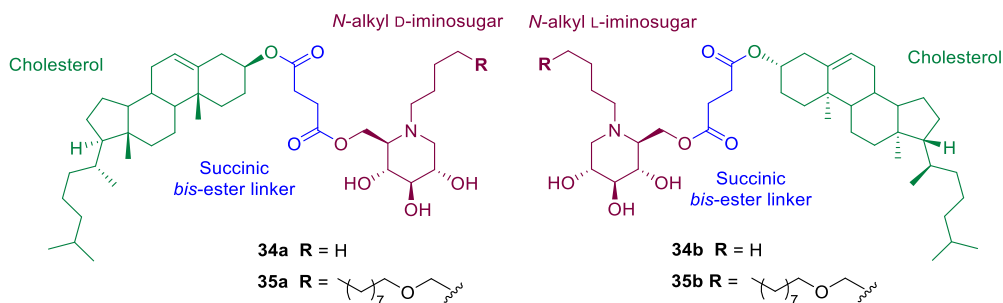


FIGURE 2.5. Structural motif of iminosugar conjugates **34** and **35**.

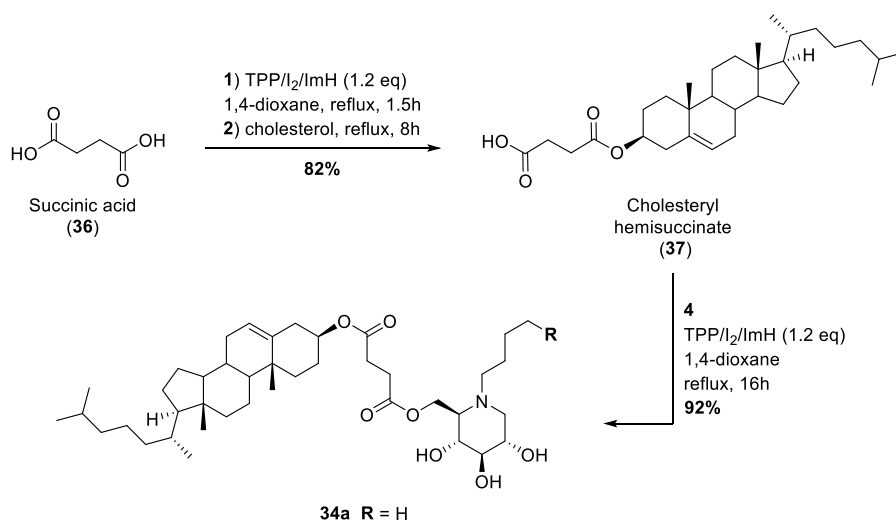
Our early efforts were devoted to study an expeditious procedure able to activate the carboxylic moieties of succinic acid (**36**), while leaving the remaining functionalities of cholesterol and iminosugar unreacted in order to afford iminosugar conjugates **34** and **35** in a one-pot procedure. To this end, we explored the use of the triphenyl phosphine (TPP), molecular iodine (I_2) and imidazole (ImH) system as activating agent.^{28–31}

With the aim to tune the reaction conditions of the single transformation, a stepwise procedure was at first explored (SCHEME 2.1). Coupling reaction of succinic acid (**36**) with cholesterol was initially considered. Succinic acid (**36**) was first treated with the pre-formed TPP/ I_2 /ImH complex in refluxing dioxane for 1.5 h. Then, upon cholesterol addition, the reaction mixture was left while stirring under reflux for 8 h, yielding cholesteryl hemisuccinate (**37**) in 82% (SCHEME 2.1a).

Noteworthy, several solvents were tested and dioxane has been identified as the most suitable solvent considering the best solubility of all reagents in view of the one-pot procedure. The reaction gave roughly the same results when cholesterol was reacted, using a previously described procedure³² with succinic anhydride and triethylamine in hot toluene (60°C) for 8 h.

With cholesteryl hemisuccinate in hand, the subsequent coupling reaction with unprotected iminosugars was studied. Treatment of **37** with pre-mixed TPP/ I_2 /ImH (1.2 eq) under previously

described conditions (refluxing dioxane, 1.5 h) led to the corresponding acyl iodide, as suggested by the formation of a low polarity UV-visible³³ spot in the TLC analysis of the reaction mixture, which was a hint of covalent iodine incorporation by the starting material. Subsequent addition of D-NBDNJ (as model substrate) afforded, after 16 h in refluxing dioxane, cholesterol-imosugar conjugate **34a** in a good 92% yield (SCHEME 2.1), while more established coupling conditions were found as not efficient in this case. As an example, the reaction of hemisuccinate **37** and D-NBDNJ (**4**) with 2-(1H-benzotriazole-1-yl)-1,1,3,3-tetramethylaminium tetrafluoroborate (TBTU) and DIPEA, which has already demonstrated to succeed in the esterification of similar substrates,³⁴ furnished conjugate **34a** only in moderate 49% yield.



SCHEME 2.1 Stepwise route to iminosugar conjugates **34a** TPP/I₂/ImH reagent system.

The occurred conjugation at the C6-OH function of D-NBDNJ, was confirmed by NMR analysis. As shown in FIGURE 2.6, the shift of diastereotopic methylene protons of the iminosugar moiety in DMSO-*d*₆ was observed (**4**: H-6a, 3.54 ppm, H-6b, 3.72 ppm; **34a**: H-6a, 4.02 ppm, H-6b, 4.37 ppm), while all the other protons were unchanged, suggesting the formation of the desired ester bond.

The success of the stepwise approach enables us to repeat the reaction using a one-pot procedure²² (SCHEME 2.2). In this case, we chose to replace TPP with its recyclable polymer supported-variant (PS-TPP), to simplify the work-up procedure and increase the synthetic potential of the procedure on a higher scale.³¹

The same conditions were also effective when L-NBDNJ was used as iminosugar, leading to conjugate **34b** in 95% yield. Similarly, the reaction with D- and L-NPDNJ provided the corresponding conjugates **35a** and **35b** in 90% and 93% yields, respectively.

Not unexpected, ¹H NMR analysis of diastereomeric couples **34a-34b** and **35a-35b** indicated that the corresponding signals have wholly superimposable chemical shifts and multiplicities, presumably owing to the lack of interactions between the chiral centers of cholesterol and those of iminosugar enantiomers.

2.2.2 BIOLOGICAL EVALUATION

Biological assays aimed to evaluate the effect of synthesized iminosugars on the growth of *S. aureus* ATCC 29213 were carried out by Prof. Eliana De Gregorio (University of Napoli Federico II, Dept. of Molecular Medicine and Medical Biotechnology). *S. aureus* ATCC 29213 was chosen as pathogen for preliminary evaluation as it is responsible for a wide range of hospital-associated infections and because of its ability to develop multi-resistance to antibiotics. Minimum inhibitory concentration (MIC) and minimum bactericidal concentration (MBC) were determined by a broth microdilution assay and are reported in **TABLE 2.1**. DNJ and its butylated derivative NBDNJ were inactive against *S. aureus* 29213 regardless of the configuration of the iminosugars (**TABLE 2.1**, entries 1-4) while D- and L-NNDNJ, as well as D- and L-HPDNJ showed very low antimicrobial activity at the MIC value of 1000 µg/mL (entries 5-8). More interesting results were obtained for the iminosugars bearing longer alkyl chains, NPDNJ and AMP-DNM. D-NPDNJ (entry 9) and D- and L-AMP-DNM (entries 11 and 12) showed a modest antimicrobial activity, with MIC values ranging from 256 to 512 µg/mL while L-NPDNJ (entry 10) exhibited better activity (albeit to a lower extent than the marketed drug gentamicin) with a MIC value of 128 µg/mL a MBC value of 256 µg/mL.²¹

In contrast with our previous results about the involvement of the iminosugar chirality on the biological activity,^{31,35} in this case the antibacterial activity was not influenced by the configuration of the iminosugar core. Indeed, even for NPDNJ, only a slight preference for the L-enantiomer was observed. Conversely, our results highlighted the role of lipophilicity in the antimicrobial potential of *N*-alkyl deoxyiminosugars. A hypothesis to explain this behavior could be the improved internalization within the bacterial cell with the increase of lipophilicity.

Consequently, the lipophilic conjugates **34** and **35** were expected to be the most active candidates. However, for these compounds, the assays were strongly hampered by the very limited solubility of the conjugates in the bacterial culture broth, which always precipitated even after pre-solubilization in DMSO.²² Future studies will be aimed to overcome these limitations, by searching alternative solutions that will exploit the amphiphilic character of the glycomimetic agents.

TABLE 2.1. MIC ($\mu\text{g/mL}$) and MBC ($\mu\text{g/mL}$) values of D- and L-DNJ and their *N*-alkyl derivatives against *S. aureus* ATCC 29213.

<i>Entry</i>	<i>Compound</i>	MIC	MBC
1	D-DNJ (2)	>1000	>1000
2	L-DNJ (<i>ent-2</i>)	>1000	>1000
3	D-NBDNJ (4)	>1000	>1000
4	L-NBDNJ (<i>ent-4</i>)	>1000	>1000
5	D-NNDNJ (19)	1000	>1000
6	L-NNDNJ (<i>ent-19</i>)	1000	>1000
7	D-HPDNJ (22)	1000	>1000
8	L-HPDNJ (22)	1000	>1000
9	D-NPDNJ (25)	256	1000
10	L-NPDNJ (<i>ent-25</i>)	128	256
11	D-AMP-DNM (14)	256	>1000
12	L-AMP-DNM (<i>ent-14</i>)	512	>1000
13	CS-(D)-NBDNJ (34a)	ND	ND
14	CS-(L)-NBDNJ (34b)	ND	ND
15	CS-(D)-NPDNJ (35a)	ND	ND
16	CS-(L)-NPDNJ (35b)	ND	ND
17	Gentamicin	1	2

MIC: minimum inhibitory concentration; MBC: minimum bactericidal concentration; ND: not determined

With L-NPDNJ being the most effective growth inhibitor, further experiments were performed for a deeper evaluation of its antimicrobial potential.²¹ When evaluated for its activity against a panel of *S. aureus* clinical isolates showing different antibiotic resistance profiles, the observed MIC and MBC values were identical to those obtained against the reference *S. aureus* ATCC 29213 strain. In order to evaluate the ability of L-NPDNJ to potentiate or restore the antibacterial activity of currently available antibiotics against *S. aureus*, the iminosugar was evaluated in combinations with gentamicin and oxacillin against the antimicrobial-resistant 717 isolate of *S. aureus*. In both cases, an additive effect was observed as highlighted by the lowered MIC values of both antibiotics (**TABLE 2.2**) revealing the ability of L-NPDNJ to restore the efficacy of oxacillin against methicillin-resistant *S. aureus* strains, while improving the antimicrobial activity of gentamicin.

TABLE 2.2. Additive effect of L-NPDNJ with antibiotics against *S. aureus* 717 isolate.

Bacterial strain	Combination	MIC ^a (µg/ml)	MIC ^b (µg/ml)	FIC index
<i>S. aureus</i> 1013-717	L-NPDNJ /oxacillin	128/128	64/1	0.5078
	L-NPDNJ /gentamicin	128/256	64/8	0.5312

MIC^a: MIC of L-NPDNJ (blue) or antibiotics (green) alone; MIC^b: MIC of L-NPDNJ in combination with antibiotic (blue) and of antibiotic (green) in combination with L-NPDNJ ; FIC index: fractional inhibitory concentration index.

Antibiofilm activity of L-NPDNJ against *S. aureus* ATCC 29213 was also evaluated with the aim to further explore its antimicrobial potential. Indeed, the ability of *S. aureus* strains to develop biofilms (communities of bacterial cells, attached to each other and/or to surfaces, embedded in a self-produced matrix of extracellular polymeric substances) on biotic and abiotic surfaces deeply contributes to worsen its pathogenicity enabling resistance to clearance mechanisms and promoting chronic disease.³⁶ As shown in FIGURE 2.6, a dose-dependent reduction of biofilm formation of *S. aureus* was observed at sub-inhibitory concentrations of L-NPDNJ (reduction of 98%, 60% and 45% at 64, 32 and 16 µg/mL). Notably, the inhibitory effect on biofilm formation was not related to growth inhibition as planktonic growth was not affected by these concentrations (sub-MIC values).

The effect of L-NPDNJ on *S. aureus* virulence factors was eventually evaluated revealing its ability to inhibit the expression of virulence and regulator genes suggesting the potential of this molecule to exert anti-virulence activity.²¹

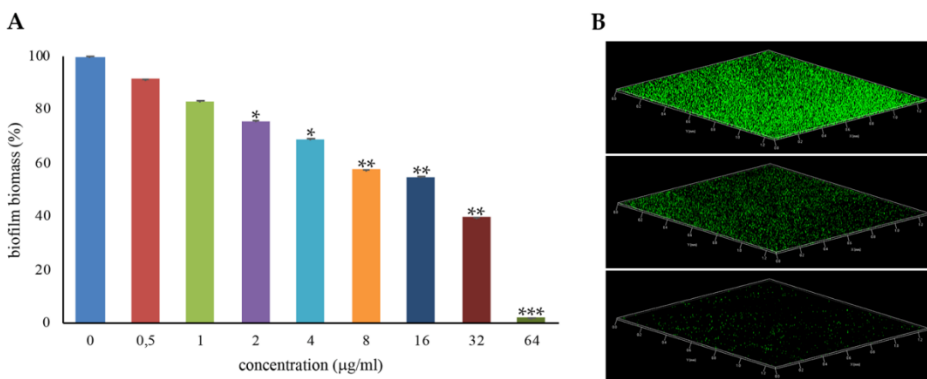


FIGURE 2.6. Inhibition of *S. aureus* ATCC 29213 biofilm formation with L-NPDNJ. A) Biofilm was quantified after crystal-violet staining. Values are presented as means ±SDs. Asterisks indicate statistically significant differences between treated and untreated biofilms (*p < 0.05 and **p < 0.01, ***p < 0.001, respectively). B) Confocal laser scanning microscopy (CLSM) analysis of the biofilm formed in the absence (upper panel) or presence of L-NPDNJ at the concentrations of 32 µg/mL (middle panel) and 64 µg/mL (inferior panel).

Further studies will be necessary to establish the molecular mechanism responsible for the effect of L-NPDNJ on *S. aureus* planktonic growth and biofilm formation, as well as to explore the antibacterial potential of these compounds against other bacterial pathogens.

Based on these interesting findings regarding the antimicrobial properties of L-NPDNJ, a novel FFC project (#13/2020) aimed at the evaluation of the antimicrobial potential of L-iminosugars in CF has been recently granted and is currently ongoing.

2.3 CONCLUDING REMARKS

Inspired by our findings about the ability of L-NBDNJ (*ent-4*) to increase bacterial clearance in murine models of *P. aeruginosa* acute and chronic infections (see Chapter 1), herein the antibacterial potential of *N*-alkyl deoxyiminosugars has been evaluated. On one hand, DNJ (**2**) and its *N*-alkyl derivatives (**4,14,19,22,25**) in both their entantiomeric forms were considered in order to explore the eventual role of chirality on the antibacterial activity. On the other hand, cholesterol-bearing iminosugars **34** and **35** were also synthesized through a one-pot procedure to study the role of lipophilicity on the eventual antibacterial properties of iminosugars. *S. aureus* ATCC 29213 was considered as bacterial pathogen for preliminary biological evaluation, leading to the identification of L-NPDNJ (*ent-25*) as the most interesting candidate being able to affect growth, biofilm formation and virulence factor expression of *S. aureus*. Overall, our data revealed that, while the antibacterial activity was not influenced by the configuration of the iminosugar core, lipophilicity of iminosugars contributed to the antibacterial effect, even if the *in vitro* evaluation of the most lipophilic derivatives **34** and **35** was hampered by solubility problems. Therefore further studies will be devoted to alternative strategies for their *in vitro* evaluation, eventually exploiting the amphiphilic character of these glycomimetic agents. The results herein reported open new perspectives on the therapeutic use of L-iminosugars. Indeed, if D-iminosugars only rarely have been considered as antibacterial agents, to the best of our knowledge there are no reports about the ability of their L-enantiomers to affect bacterial growth, as well as biofilm formation. In addition, these data hold a relevance in the frame of our studies on the therapeutic application of L-iminosugars in Cystic Fibrosis (CF). Indeed, the antibacterial and antibiofilm properties exhibited by L-NPDNJ associated with our findings about the *in vitro* and *in vivo* anti-inflammatory activity exerted by L-iminosugars point out the potential of these glycomimetics to act as dual drugs in CF treatment as both anti-inflammatory and antibacterial agents.

2.4 EXPERIMENTAL SECTION

CHEMICAL SYNTHESIS: GENERAL METHODS

All commercially available reagents and solvents were purchased at the highest degree of purity from commercial sources and used without purification. TLC analysis was carried out on precoated silica gel plate F254 (Merck), and products were visualized under UV radiation or by exposure to iodine vapor and chromic mixture. Column chromatography was performed with silica gel (70–230 mesh, Merck Kiesegel 60). CHNS analysis was performed to assess the purity of compounds and was $\geq 95\%$ in all cases. NMR spectra were recorded on a Bruker AVANCE 400 MHz. Coupling constant values (J) were reported in Hz.

PROCEDURE FOR THE SYNTHESIS OF 34-35 THROUGH A STEPWISE ROUTE

Step 1: formation of cholesteryl hemisuccinate 37.

I₂ (1.2 eq) and imidazole (2.4 eq) were added to a stirred solution of TPP (1.2 eq) in anhydrous 1,4-dioxane at rt. After 10 min, succinic acid (1.0 eq) was added to the slight yellow suspension and the pH of the solution was led to neutrality with addition of imidazole. The resulting colorless solution was warmed to reflux temperature and stirred for 1.5 h. Then cholesterol (1.0 eq) was added and the mixture was stirred at the same temperature for 8 h. The mixture was then cooled at rt, washed with brine and extracted with DCM. Organic layers were dried (Na₂SO₄) and evaporated under reduced pressure. Column chromatography of the crude residue over silica gel (hexane/EtOAc = 6:4) afforded the conjugate **37** (82% yield). ¹H and ¹³C NMR spectra were fully in agreement with those reported in literature.³²

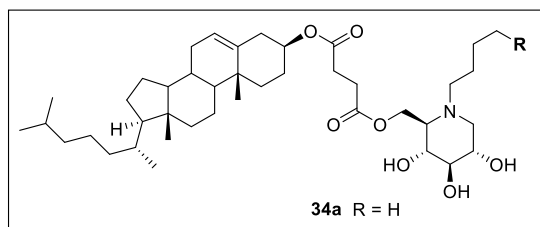
Step2: formation of iminosugar conjugate 34a

I₂ (1.2 eq) and imidazole (2.4 eq) were added to a stirred solution of TPP (1.2 eq) in anhydrous 1,4-dioxane at rt. After 10 min, hemisuccinate **37** (1.0 eq) was added to the slight yellow suspension and the pH of the solution was led to neutrality with addition of imidazole. The resulting colorless solution was warmed to reflux temperature and stirred for 1.5 h. D-NBDNJ (1.0 eq) was then added and the mixture was stirred at the same temperature for 8 h. The mixture was cooled at rt, diluted with DCM and the organic layers were washed with brine, dried (Na₂SO₄) and concentrated under reduced pressure. Chromatography of the crude residue over silica gel (DCM/MeOH = 96:4) afforded the conjugate **34a** (92% yield) as a white solid. Chemical characterization for **34a** is reported below at the end of the one-pot procedure.

GENERAL PROCEDURE FOR THE SYNTHESIS OF 34-35 THROUGH A ONE-POT ROUTE

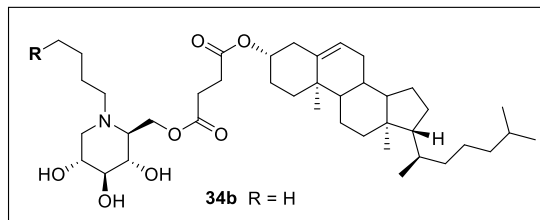
I₂ (2.4 eq) and imidazole (4.8 eq) were added to a stirred solution of polymer supported triphenylphosphine (PS-TPP; 100-200 mesh, extent of labeling: ~3 mmol/g triphenylphosphine loading) (2.4 eq) in anhydrous 1,4-dioxane at rt. After 10 min, succinic acid (1.0 eq) was added to the slight yellow suspension and the pH of the solution was led to neutrality with addition of imidazole. The resulting colorless solution was warmed to reflux temperature and stirred for

1.5 h. Then cholesterol (1.0 eq) was added and the mixture was stirred at the same temperature for 8 h. The appropriate iminosugar **4** (or **25**) and *ent*-**4** (or *ent*-**25**) (1.0 eq) was then added and the mixture was stirred for 16 h at the reflux temperature. The mixture was then cooled at rt, filtered (DCM) to remove triphenylphosphine oxide, washed with brine and extracted with DCM. Organic layers were dried (Na₂SO₄) and evaporated under reduced pressure affording the desired NBDNJ derivatives **34a** and **34b** (**34a**: 96% o.y.; **34b**: 95% o.y) and the NPDNJ derivatives **35a** and **35b** (**35a**: 94% o.y.; **35b**: 93% o.y).



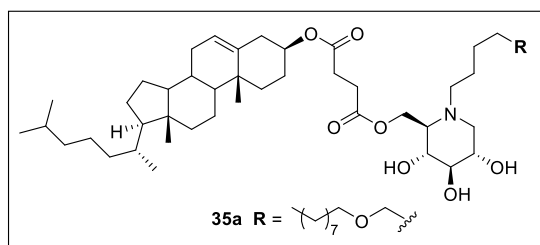
34a: ¹H NMR (400 MHz, DMSO-d₆): δ 0.66 (s, 3H), 0.83-0.94 (m, 13H), 0.98 (s, 3H), 0.98-1.44 (m, 18H), 1.45-1.61 (m, 5H), 1.73-1.87 (m, 3H), 1.88-2.01 (m, 3H), 2.16 (ddd, *J* = 1.6, 4.3, 9.1, 1H), 2.26 (td, *J* = 7.7, 1H), 2.25-2.36 (m, 1H), 2.53 (s, 4H), 2.54-2.65 (m, 1H), 2.81 (dd, *J* = 4.8, 11.1,

1H), 2.92 (t, *J* = 9.1, 1H), 3.01 (d, *J* = 5.3, 9.1, 1H), 3.17-3.26 (m, 1H), 4.05 (dd, *J* = 4.3, 12.0, 1H), 4.39 (dd, *J* = 1.6, 12.0, 1H), 4.40-4.49 (m, 1H), 4.72 (d, *J* = 4.6, 1H), 4.81 (bs, 1H), 4.89 (d, *J* = 5.3, 1H), 5.35 (d, *J* = 3.7, 1H). ¹³C NMR (100 MHz, DMSO-d₆): δ 12.1, 14.4, 19.0, 19.4, 20.5, 21.0, 22.9, 23.1, 23.5, 24.2, 26.8, 27.8, 28.2, 29.2, 31.8; 35.6, 36.1, 36.5, 36.9, 38.1, 42.3, 49.9, 52.2, 56.0, 56.6, 57.2, 62.8, 64.3, 69.8, 70.9, 73.9, 79.4, 122.6, 139.9, 171.7, 172.3. Anal. calcd for C₄₁H₆₉NO₇: C, 71.58; H, 10.11; N, 2.04; O, 16.28. Found: C, 71.67; H, 10.07; N, 2.04.



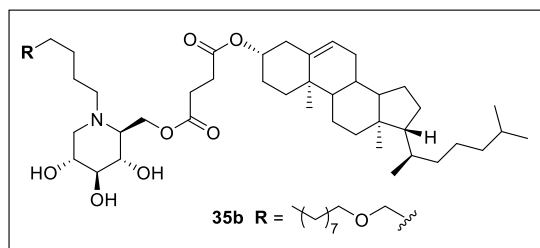
34b: ¹H NMR (400 MHz, DMSO-d₆): δ 0.65 (s, 3H), 0.83-0.95 (m, 13H), 0.98 (s, 3H), 0.98-1.45 (m, 18H), 1.45-1.62 (m, 5H), 1.71-1.87 (m, 3H), 1.88-2.02 (m, 3H), 2.15 (d, *J* = 8.8, 1H), 2.21-2.35 (m, 2H), 2.46 (s, 4H), 2.54-2.65 (m, 1H), 2.81 (dd, *J* = 4.7, 11.0, 1H), 2.92 (t, *J* = 8.8, 1H), 3.00

(t, *J* = 8.8, 1H), 3.16-3.27 (m, 1H), 4.04 (dd, *J* = 3.5, 12.0, 1H), 4.39 (d, *J* = 12.0, 1H), 4.42-4.52 (m, 1H), 4.65-4.94 (m, 3H), 5.34 (d, *J* = 3.5, 1H). ¹³C NMR data for compound **34b** were fully in line with those reported above for the corresponding diastereoisomer **34a**. Anal. calcd for C₄₁H₆₉NO₇: C, 71.58; H, 10.11; N, 2.04; O, 16.28. Found: C, 71.52; H, 10.14; N, 2.04.



35a: ¹H NMR (400 MHz, CD₃OD): δ 0.74 (s, 3H), 0.87-0.99 (m, 12H), 1.01-1.10 (m, 5H), 1.11-1.25 (m, 6H), 1.26-1.46 (m, 19H), 1.48-1.70 (m, 12H), 1.82-2.11 (m, 5H), 2.18 (t, *J* = 11.0, 1H), 2.28-2.39 (m, 3H), 2.44-2.54 (m, 1H), 2.59-2.67 (m, 4H), 2.70-2.80 (m, 1H), 3.03 (dd, *J* = 4.9, 11.0,

1H), 3.15 (t, $J = 9.0$, 1H), 3.25-3.33 (m, 1H), 3.40-3.45 (m, 4H), 3.46-3.54 (m, 1H), 4.29 (dd, $J = 3.5$, 12.3, 1H), 4.51 (dd, $J = 1.8$, 12.3, 1H), 5.41 (d, $J = 4.5$, 1H). ^{13}C NMR (100 MHz, CD_3OD); δ 12.3, 14.5, 19.2, 19.7, 22.2, 22.9, 23.2, 23.8, 24.9, 25.2, 25.3, 27.3, 28.8, 29.1, 29.3, 29.9, 30.3, 30.7, 30.8, 33.0; 33.2, 37.1, 37.4, 37.8, 38.3, 39.2, 40.7, 41.1, 43.5, 51.6, 53.8, 57.6, 57.7, 58.1, 62.6, 65.4, 70.8, 71.9, 72.0, 72.1, 75.7, 80.4, 123.7, 141.0, 173.4, 174.1. Anal. calcd for $\text{C}_{51}\text{H}_{89}\text{NO}_8$: C, 72.55; H, 10.63; N, 1.66; O, 15.16. Found: C, 72.65; H, 10.59; N, 1.66.



35b: ^1H NMR (400 MHz, CD_3OD): δ 0.75 (s, 3H), 0.87-1.00 (m, 12H), 1.01-1.10 (m, 5H), 1.11-1.25 (m, 6H), 1.26-1.47 (m, 19H), 1.48-1.70 (m, 12H), 1.83-2.10 (m, 5H), 2.18 (t, $J = 10.9$, 1H), 2.28-2.39 (m, 3H), 2.44-2.54 (m, 1H), 2.57-2.70 (m, 4H), 2.70-2.81 (m, 1H), 3.03 (dd, $J = 4.8$, 11.3, 1H), 3.15 (t, $J = 9.0$, 1H), 3.25-3.33 (m,

1H), 3.40-3.54 (m, 5H), 4.29 (dd, $J = 3.4$, 12.4, 1H), 4.52 (dd, $J = 1.8$, 12.4, 1H), 5.41 (d, $J = 5.0$, 1H). ^{13}C NMR data for compound **35b** were fully in line with those reported above for the corresponding diastereoisomer **35a**. Anal. calcd for $\text{C}_{51}\text{H}_{89}\text{NO}_8$: C, 72.55; H, 10.63; N, 1.66; O, 15.16. Found: C, 72.64; H, 10.60; N, 1.66.

2.5 BIBLIOGRAPHY

- (1) Neill, J. O.'. Antimicrobial Resistance: Tackling a Crisis for the Health and Wealth of Nations The Review on Antimicrobial Resistance Chaired. **2014**, No. December.
- (2) Zaman, S. Bin; Hussain, M. A.; Nye, R.; Mehta, V.; Mamun, K. T.; Hossain, N. A Review on Antibiotic Resistance: Alarm Bells Are Ringing. *Cureus* **2017**, *9* (6). <https://doi.org/10.7759/cureus.1403>.
- (3) Tacconelli, E.; Carrara, E.; Savoldi, A.; Harbarth, S.; Mendelson, M.; Monnet, D. L.; Pulcini, C.; Kahlmeter, G.; Kluytmans, J.; Carmeli, Y.; Ouellette, M.; Outtersson, K.; Patel, J.; Cavalieri, M.; Cox, E. M.; Houchens, C. R.; Grayson, M. L.; Hansen, P.; Singh, N.; Theuretzbacher, U.; Magrini, N.; Aboderin, A. O.; Al-Abri, S. S.; Awang Jalil, N.; Benzonana, N.; Bhattacharya, S.; Brink, A. J.; Burkert, F. R.; Cars, O.; Cornaglia, G.; Dyar, O. J.; Friedrich, A. W.; Gales, A. C. *et al.* Discovery, Research, and Development of New Antibiotics: The WHO Priority List of Antibiotic-Resistant Bacteria and Tuberculosis. *Lancet Infect. Dis.* **2018**, *18* (3), 318–327. [https://doi.org/10.1016/S1473-3099\(17\)30753-3](https://doi.org/10.1016/S1473-3099(17)30753-3).
- (4) Tagliabue, A.; Rappuoli, R. Changing Priorities in Vaccinology: Antibiotic Resistance Moving to the Top. *Front. Immunol.* **2018**, *9* (MAY), 1–9. <https://doi.org/10.3389/fimmu.2018.01068>.
- (5) Wright, G. D. Antibiotic Resistance: Where Does It Come from and What Can We Do about It? *BMC Biol.* **2010**, *8* (1), 123. <https://doi.org/10.1186/1741-7007-8-123>.
- (6) Levy, S. B.; Marshall, B. Antibacterial Resistance Worldwide: Causes, Challenges and Responses. *Nat. Med.* **2004**, *10* (S12), S122–S129. <https://doi.org/10.1038/nm1145>.
- (7) Chopra, R.; Alderborn, G.; Podczeck, F.; Newton, J. M. The Influence of Pellet Shape and Surface

- Properties on the Drug Release from Uncoated and Coated Pellets. *Int. J. Pharm.* **2002**, *239* (1–2), 171–178. [https://doi.org/10.1016/S0378-5173\(02\)00104-7](https://doi.org/10.1016/S0378-5173(02)00104-7).
- (8) Barber, M.; Rozwadowska-Dowzenko, M. Infection by Penicillin-Resistant Staphylococci. *Lancet* **1948**, *252* (6530), 641–644. [https://doi.org/10.1016/S0140-6736\(48\)92166-7](https://doi.org/10.1016/S0140-6736(48)92166-7).
- (9) Appelbaum, P. C. The Emergence of Vancomycin-Intermediate and Vancomycin-Resistant Staphylococcus Aureus. *Clin. Microbiol. Infect.* **2006**, *12*, 16–23. <https://doi.org/10.1111/j.1469-0691.2006.01344.x>.
- (10) Levy, S. B. Antibiotic Resistance: Consequences of Inaction. *Clin. Infect. Dis.* **2001**, *33* (s3), S124–S129. <https://doi.org/10.1086/321837>.
- (11) Morar, M.; Wright, G. D. The Genomic Enzymology of Antibiotic Resistance. *Annu. Rev. Genet.* **2010**, *44* (1), 25–51. <https://doi.org/10.1146/annurev-genet-102209-163517>.
- (12) Bartlett, J. G.; Gilbert, D. N.; Spellberg, B. Seven Ways to Preserve the Miracle of Antibiotics. *Clin. Infect. Dis.* **2013**, *56* (10), 1445–1450. <https://doi.org/10.1093/cid/cit070>.
- (13) Compain, Philippe; Martin, O. *Iminosugars: From Synthesis to Therapeutic Applications*; Compain, P., Martin, O. R., Eds.; John Wiley & Sons, Ltd: Chichester, UK, 2007. <https://doi.org/10.1002/9780470517437>.
- (14) Winchester, B. G. Iminosugars: From Botanical Curiosities to Licensed Drugs. *Tetrahedron Asymmetry* **2009**, *20* (6–8), 645–651. <https://doi.org/10.1016/j.tetasy.2009.02.048>.
- (15) Nash, R. J.; Kato, A.; Yu, C. Y.; Fleet, G. W. Iminosugars as Therapeutic Agents: Recent Advances and Promising Trends. *Future Med. Chem.* **2011**, *3* (12), 1513–1521. <https://doi.org/10.4155/fmc.11.117>.
- (16) Greimel, P.; Spreitz, J.; Stutz, A.; Wrodnigg, T. Iminosugars and Relatives as Antiviral and Potential Anti-Infective Agents. *Curr. Top. Med. Chem.* **2005**, *3* (5), 513–523. <https://doi.org/10.2174/1568026033452456>.
- (17) Islam, B.; Khan, S. N.; Haque, I.; Alam, M.; Mushfiq, M.; Khan, A. U. Novel Anti-Adherence Activity of Mulberry Leaves: Inhibition of Streptococcus Mutans Biofilm by 1-Deoxynojirimycin Isolated from Morus Alba. *J. Antimicrob. Chemother.* **2008**, *62* (4), 751–757. <https://doi.org/10.1093/jac/dkn253>.
- (18) Hasan, S.; Singh, K.; Danisuddin, M.; Verma, P. K.; Khan, A. U. Inhibition of Major Virulence Pathways of Streptococcus Mutans by Quercitrin and Deoxynojirimycin: A Synergistic Approach of Infection Control. *PLoS One* **2014**, *9* (3), 1–12. <https://doi.org/10.1371/journal.pone.0091736>.
- (19) Segraves, N. L.; Crews, P. A Madagascar Sponge Batzella Sp. as a Source of Alkylated Iminosugars. *J. Nat. Prod.* **2005**, *68* (1), 118–121. <https://doi.org/10.1021/np049763g>.
- (20) Strus, M.; Mikołajczyk, D.; Machul, A.; Heczko, P. B.; Chronowska, A.; Stochel, G.; Gallienne, E.; Nicolas, C.; Martin, O. R.; Kyzioł, A. Effects of the Selected Iminosugar Derivatives on Pseudomonas Aeruginosa Biofilm Formation. *Microb. Drug Resist.* **2016**, *22* (8), 638–645. <https://doi.org/10.1089/mdr.2015.0231>.
- (21) De Gregorio, E.; Esposito, A.; Vollaro, A.; De Fenza, M.; D’Alonzo, D.; Migliaccio, A.; Iula, V. D.; Zarrilli, R.; Guaragna, A. N-Nonyloxypentyl-1-Deoxynojirimycin Inhibits Growth, Biofilm Formation and Virulence Factors Expression of Staphylococcus Aureus. *Antibiotics* **2020**, *9* (6), 362. <https://doi.org/10.3390/antibiotics9060362>.
- (22) Esposito, A.; D’Alonzo, D.; D’Errico, S.; De Gregorio, E.; Guaragna, A. Toward the Identification of Novel Antimicrobial Agents: One-Pot Synthesis of Lipophilic Conjugates of N-Alkyl d- and l-Iminosugars. *Mar. Drugs* **2020**, *18* (11), 572. <https://doi.org/10.3390/md18110572>.

- (23) Rautio, J.; Meanwell, N. A.; Di, L.; Hageman, M. J. The Expanding Role of Prodrugs in Contemporary Drug Design and Development. *Nat. Rev. Drug Discov.* **2018**, *17* (8), 559–587. <https://doi.org/10.1038/nrd.2018.46>.
- (24) Wichitnithad, W.; Nimmannit, U.; Wacharasindhu, S.; Rojsitthisak, P. Synthesis, Characterization and Biological Evaluation of Succinate Prodrugs of Curcuminoids for Colon Cancer Treatment. *Molecules* **2011**, *16* (2), 1888–1900. <https://doi.org/10.3390/molecules16021888>.
- (25) Aly, M. R. E. S.; Saad, H. A.; Mohamed, M. A. M. Click Reaction Based Synthesis, Antimicrobial, and Cytotoxic Activities of New 1,2,3-Triazoles. *Bioorg. Med. Chem. Lett.* **2015**, *25* (14), 2824–2830. <https://doi.org/10.1016/j.bmcl.2015.04.096>.
- (26) Aly, M. R. E. S.; Saad, H. A.; Abdel-Hafez, S. H. Synthesis, Antimicrobial and Cytotoxicity Evaluation of New Cholesterol Congeners. *Beilstein J. Org. Chem.* **2015**, *11*, 1922–1932. <https://doi.org/10.3762/bjoc.11.208>.
- (27) Albuquerque, H.; Santos, C.; Silva, A. Cholesterol-Based Compounds: Recent Advances in Synthesis and Applications. *Molecules* **2018**, *24* (1), 116. <https://doi.org/10.3390/molecules24010116>.
- (28) Guaragna, A.; De Nisco, M.; Pedatella, S.; Pinto, V.; Palumbo, G. An Expedient Procedure for the Synthesis of Isotopically Labelled Fatty Acids: Preparation of 2,2-D₂-Nonadecanoic Acid. *J. Label. Compd. Radiopharm.* **2006**, *49* (8), 675–682. <https://doi.org/10.1002/jlcr.1094>.
- (29) Guaragna, A.; Amoresano, A.; Pinto, V.; Monti, G.; Mastrobuoni, G.; Marino, G.; Palumbo, G. Synthesis and Proteomic Activity Evaluation of a New Isotope-Coded Affinity Tagging (ICAT) Reagent. *Bioconjug. Chem.* **2008**, *19* (5), 1095–1104. <https://doi.org/10.1021/bc800010b>.
- (30) Pedatella, S.; Guaragna, A.; D'Alonzo, D.; De Nisco, M.; Palumbo, G. Triphenylphosphine Polymer-Bound/Iodine Complex: A Suitable Reagent for the Preparation of O-Isopropylidene Sugar Derivatives. *Synthesis (Stuttg.)* **2006**, No. 2, 305–308. <https://doi.org/10.1055/s-2005-918521>.
- (31) De Fenza, M.; D'Alonzo, D.; Esposito, A.; Munari, S.; Loberto, N.; Santangelo, A.; Lampronti, I.; Tamanini, A.; Rossi, A.; Ranucci, S.; De Fino, I.; Bragonzi, A.; Aureli, M.; Bassi, R.; Tironi, M.; Lippi, G.; Gambari, R.; Cabrini, G.; Palumbo, G.; Dececchi, M. C.; Guaragna, A. Exploring the Effect of Chirality on the Therapeutic Potential of N-Alkyl-Deoxyiminosugars: Anti-Inflammatory Response to *Pseudomonas Aeruginosa* Infections for Application in CF Lung Disease. *Eur. J. Med. Chem.* **2019**, *175*, 63–71. <https://doi.org/10.1016/j.ejmech.2019.04.061>.
- (32) Klumphu, P.; Lipshutz, B. H. “Nok”: A Phytosterol-Based Amphiphile Enabling Transition-Metal-Catalyzed Couplings in Water at Room Temperature. *J. Org. Chem.* **2014**, *79* (3), 888–900. <https://doi.org/10.1021/jo401744b>.
- (33) Kimura, K.; Nagakura, S. $N \rightarrow \Sigma^*$ Absorption Spectra of Saturated Organic Compounds Containing Bromine and Iodine. *Spectrochim. Acta* **1961**, *17* (2), 166–183. [https://doi.org/10.1016/0371-1951\(61\)80062-3](https://doi.org/10.1016/0371-1951(61)80062-3).
- (34) Twibanire, J. K.; Grindley, T. B. Efficient and Controllably Selective Preparation of Esters Using Uronium-Based Coupling Agents. *Org. Lett.* **2011**, *13* (12), 2988–2991. <https://doi.org/10.1021/ol201005s>.
- (35) D'Alonzo, D.; De Fenza, M.; Porto, C.; Iacono, R.; Huebecker, M.; Cobucci-Ponzano, B.; Priestman, D. A.; Platt, F.; Parenti, G.; Moracci, M.; Palumbo, G.; Guaragna, A. N-Butyl-l-Deoxyojirimycin (L-NBDNJ): Synthesis of an Allosteric Enhancer of α -Glucosidase Activity for the Treatment of Pompe Disease. *J. Med. Chem.* **2017**, *60* (23), 9462–9469.

- (36) <https://doi.org/10.1021/acs.jmedchem.7b00646>.
Otto, M. Staphylococcal Infections: Mechanisms of Biofilm Maturation and Detachment as Critical Determinants of Pathogenicity. *Annu. Rev. Med.* **2013**, *64* (1), 175–188.
<https://doi.org/10.1146/annurev-med-042711-140023>.

3 SYNTHESIS AND ANTIBACTERIAL ACTIVITY OF DEFLAZACORT AND ITS SYNTHETIC PRECURSORS

3.1 INTRODUCTION

3.1.1 PHARMACOLOGICAL PROPERTIES OF NATURAL AND SYNTHETIC CORTICOSTEROIDS

Corticosteroids (also known as steroids) are among the most widely used drugs in clinical practice because of their anti-inflammatory and immunosuppressive properties.^{1,2} They are used in almost all areas of medicine: as replacement therapy in adrenal insufficiency (at physiologic doses), as well as in supraphysiologic doses for the treatment of various dermatologic, ophthalmologic, rheumatologic, pulmonary, hematologic and gastrointestinal disorders.³

The basic chemical structure of corticosteroids consists of a skeleton of 21 carbon atoms⁴ and they are basically classified on the basis of their preferential biological activity, depending on their involvement in the regulation of carbohydrate metabolism *i.e.* glucocorticoids, or in the balancing of fluids and electrolytes *i.e.* mineralocorticoids.⁵ Cortisol (also known as hydrocortisone) is the main glucocorticoid, produced by adrenal cortex, while aldosterone is the main mineralocorticoid (**FIGURE 3.1a**). Notably, this classification is not a strict rule as corticosteroids belonging to one group can also exhibit biological activity typical of the other group.⁶

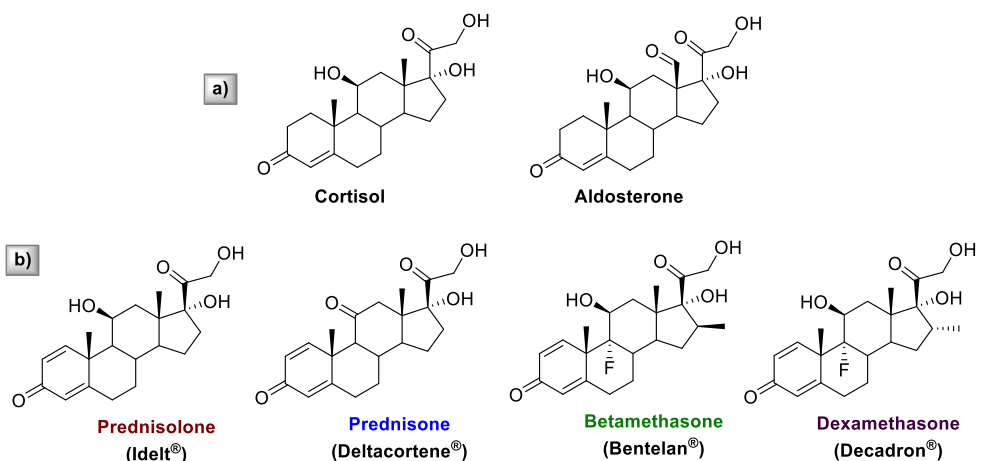


FIGURE 3.1. a) Chemical structure of cortisol and aldosterone; b) Some of the currently marketed synthetic corticosteroids.

The immunosuppressive and anti-inflammatory properties of corticosteroids rely on their interaction with specific cytosolic receptors leading to alteration of gene transcription in both

anti-inflammatory leukocytes and in structural cells such as epithelium.⁷ Particularly, corticosteroids act either upregulating or downregulating the transcription of inflammatory genes to affect the production of pro-inflammatory cytokine and chemokine, cell adhesion molecules and other key enzymes involved into the host inflammatory response.^{8,9}

Since the early stages of the scientific research on corticosteroids, their clinical use, especially when used in high doses and for long periods, was associated to several adverse effects including osteoporosis and fractures; adrenal suppression (AS); hyperglycemia and diabetes; cardiovascular disease (CVD) and dyslipidemia, psychiatric disturbances and immunosuppression.² Therefore, in the 1950-60s great attention was devoted to the identification of novel compounds endowed with a higher anti-inflammatory potency and a lower incidence of side effects than natural steroids,¹ leading to the synthesis of the currently used prednisolone, betamethasone or dexamethasone (FIGURE 3.1b).

3.1.2 DEFLAZACORT: A POWERFUL GLUCOCORTICOID

The search for novel anti-inflammatory drugs characterized by high efficacy associated to good tolerability and low adverse effects led to the identification of Deflazacort (DFZ, **38**; FIGURE 3.2), the oxazoline derivative of prednisolone. Indeed, DFZ is endowed with a lower interference with carbohydrate and phosphocalcium metabolism compared with previous-generation corticosteroids and it is therefore able to produce less serious metabolic events.⁶

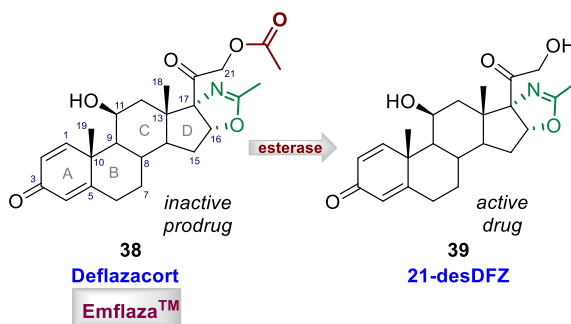


FIGURE 3.2. Deflazacort (**38**) and its active metabolite 21-desDFZ (**39**).

After oral administration, DFZ is rapidly converted into the active metabolite, 21-desacetyldeflazacort (**39**; FIGURE 3.2), by cellular esterases.¹⁰ To exert its pharmacological effect, DFZ acts as corticosteroid hormone receptor agonist, exploiting the high binding affinity for tissue glucocorticoid receptors.¹¹ DFZ was first marketed in 1980s and since early 1990s it has been used frequently as a therapeutic alternative for several disorders including rheumatoid arthritis, sensorineural hearing loss and ureterolithiasis.⁶ As proof of its good tolerability, recently, DFZ was approved^{12,13} by the FDA (trade name: Emflaza) as therapy for children suffered from Duchenne Muscular Dystrophy (DMD), a genetic disorder that affects 1/3600

infants worldwide. However, the precise mechanism by which DFZ exerts its therapeutic effect in patients with DMD is still unknown.¹⁴

3.1.2.1 SYNTHETIC APPROACHES TO DEFLAZACORT

Due to the excellent biological properties of DFZ and its therapeutic potential for the treatment of a broad range of diseases, to date there are several procedures aimed to its preparation. However, in all cases synthesis of DFZ involves several and laborious reaction steps with low yields and high costs. As an example, one of the main routes used for pilot-scale production of DFZ is reported in **FIGURE 3.3**. The synthesis starts from 3 β -acetoxy-5 α -pregn-16-ene-11,20-dione a derivative of 17 α -hydroxyprogesterone (a steroid hormone released from adrenal glands) and consists overall of 13 steps of reaction with the ultimate aim to insert the oxazoline ring at C16-C17 position and the acetylated 21-hydroxyl function.¹⁵ Herein, the β -oriented methyl group at C18 position enables the introduction at first of the α -configured epoxy function and then of the vicinal azido-alcohol function by acid-catalyzed epoxide ring opening.

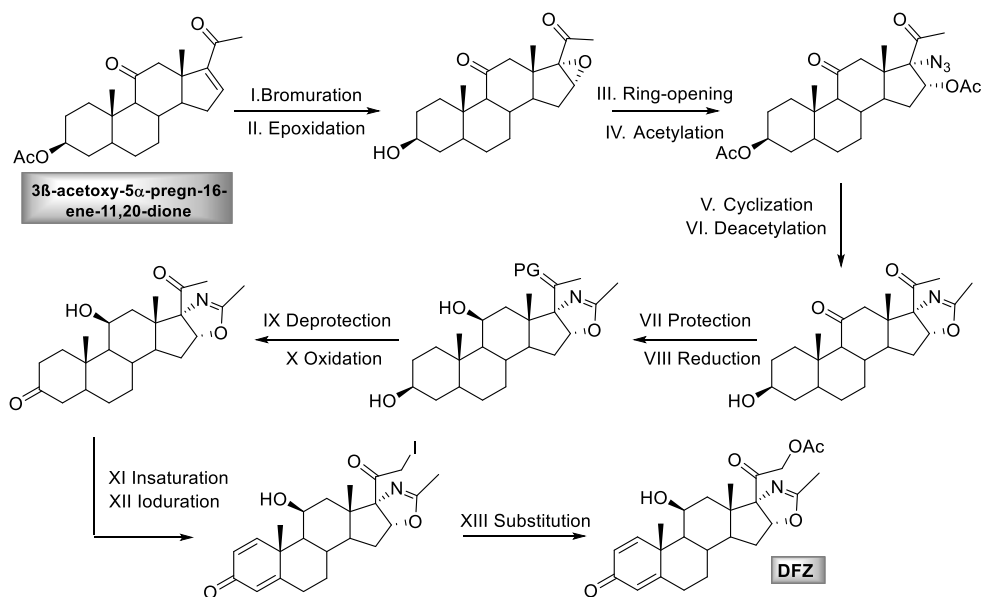


FIGURE 3.3. Synthetic route to Deflazacort.

3.1.2.1 ANTIBACTERIAL ACTIVITY OF CORTICOSTEROIDS

Even though the anti-inflammatory and immunosuppressive activity of DFZ is well-known, to the best of our knowledge, there are no reports to about its direct action on bacterial infections. However, there are several examples of corticosteroids exhibiting an interesting activity as antibacterial agents as for example cationic steroids Squalamine¹⁶ and Ceragenine CSA-13¹⁷ (FIGURE 3.4). Isolated from tissues of the dogfish shark *Squalus acanthias*, Squalamine showed potent bactericidal activity against both Gram-negative and Gram-positive bacteria inspiring the synthesis of its analogues.¹⁸ Analogously, Ceragenine CSA-13, conceived as mimic of endogenous antimicrobial peptides, exhibited broad-spectrum activity against multidrug-resistant bacteria.¹⁹ Being both Squalamine and CSA-13 cationic steroids, their antibacterial activity is ascribed to their amphiphilic properties that enable bacterial membrane disruption. Even more interesting, Fusidic acid is an antibiotic isolated from the fungus *Fusidium coccineum*, in 1960 currently marketed (trade name Fucidin™) for the treatment of infections caused by methicillin resistant *Staphylococcus aureus* strains by inhibition of synthesis of bacterial protein by binding with elongation factor G (EF-G).²⁰

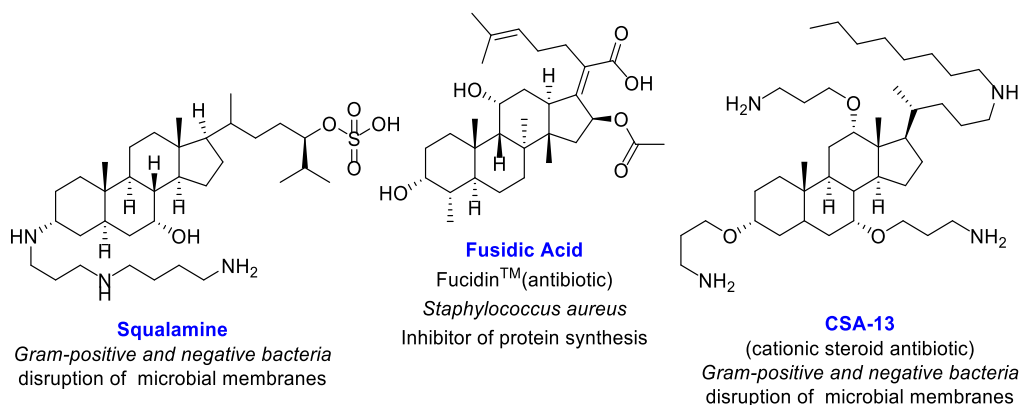


FIGURE 3.4. Examples of corticosteroids showing antibacterial activity.

These findings about the potential of corticosteroids to concomitantly act as antibacterial agents inspired us to explore the antimicrobial properties of Deflazacort, in order to evaluate whether the excellent biological properties of this well-known anti-inflammatory drug can be exploited also for the treatment of bacterial infections.

3.2 RESULTS AND DISCUSSION

Inspired by the clinical relevance of the corticosteroid drug Deflazacort (DFZ) and driven by the growing need for the development of novel alternative candidates active against bacterial pathogens, a novel synthetic route aimed to the preparation of DFZ has been herein explored and the potential of this molecule as antibacterial and antibiofilm agent has been evaluated (FIGURE 3.5). Indeed, even though the anti-inflammatory and immunosuppressive activity of DFZ is well-known, to the best of our knowledge, there are no reports about its direct action on bacterial infections.

In order to develop a shorter and more convenient route to DFZ as alternative to the existing methods, 9-bromotriene acetate **40** was considered as building block for our strategy.²¹ On one hand, the use of **40** allowed us to have the proper functionalization at C21 position, as required by the DFZ structure, avoiding the installation of the acetylated 21-hydroxyl function in a late stage of the synthesis, as commonly reported for preparation of oxazoline-containing steroids. On the other hand, double bond functionalization at C16-C17 position of **40** gave access to the epoxide **41**, key intermediate to insert the methyl-oxazoline ring after a stereo- and regioselective epoxide-opening providing a straightforward access to Deflazacort.

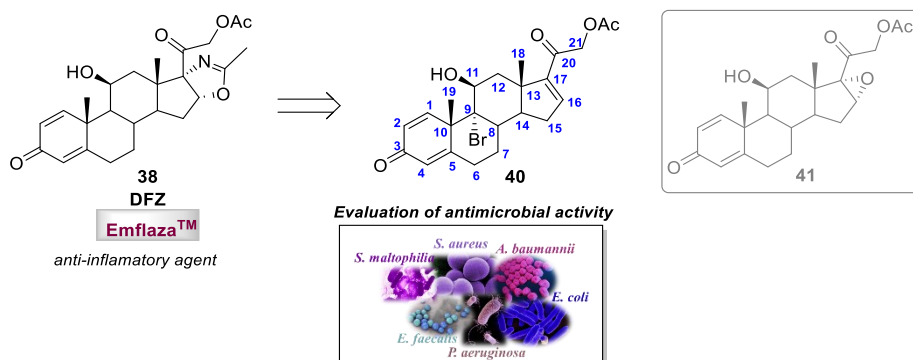


FIGURE 3.5. Synthesis and antimicrobial evaluation of Deflazacort and its precursors.

Deflazacort and its synthetic precursors were evaluated for their antibacterial activity against a panel of Gram-negative and Gram-positive pathogens responsible for drug-resistant infections including *S. aureus*, *E. faecalis*, *A. baumannii*, *P. aeruginosa*, *E. coli*, *S. maltophilia*.^{22–24}

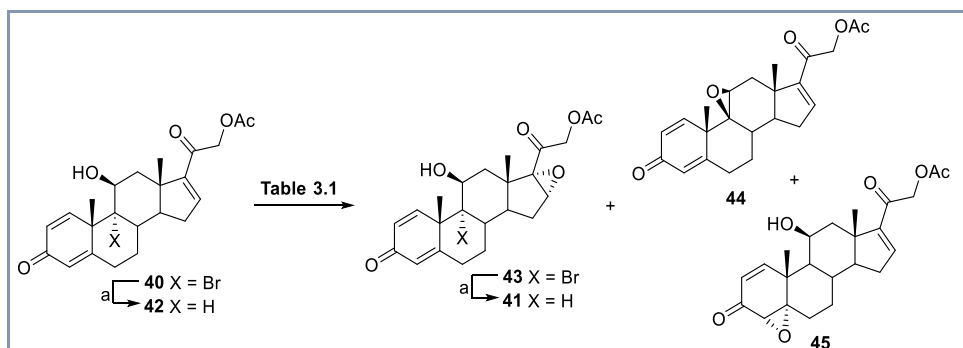
3.2.1 SYNTHETIC APPROACH TO DEFLAZACORT

Our synthesis started from 9-bromotriene acetate **40** readily obtained from the commercially available tetraene acetate²⁵ (3TR), an industrial key intermediate already used for the synthesis of currently marketed bioactive glucocorticoid drugs.²⁶ Starting from **40**, double bond epoxidation at C16-C17 position was studied to obtain the key epoxide **41** as suitable intermediate

for insertion of the oxazoline ring. The epoxidation reaction was attempted on both **40** and its debrominated derivative **42**, in turn obtained by treatment of **40** with Bu_3SnH and AIBN in refluxing THF (93% yield) (TABLE 3.1).

Nearly neutral or acidic conditions were tested, since alkaline double bond epoxidation was hampered by the presence of the acetyl group at C21 position. The use of *in situ* generated TFDO (Oxone/ NaHCO_3 /aq Na_2EDTA) (entries 2 and 5, TABLE 3.1) demonstrated to be unsuited, as it led to the formation of undesired epoxides **44** and **45** (from **40** and **42**, respectively). Similarly, bicarbonate-catalyzed epoxidation of **40** with aqueous hydrogen peroxide²⁷ led to the formation of undesired epoxide **44** as the main product (59%) (entry 3, TABLE 3.1) while under the same conditions, the reaction from olefin **42** led to the recovery of totally unreacted starting material (entry 6).

TABLE 3.1. Epoxidation of derivatives **40** and **42**.



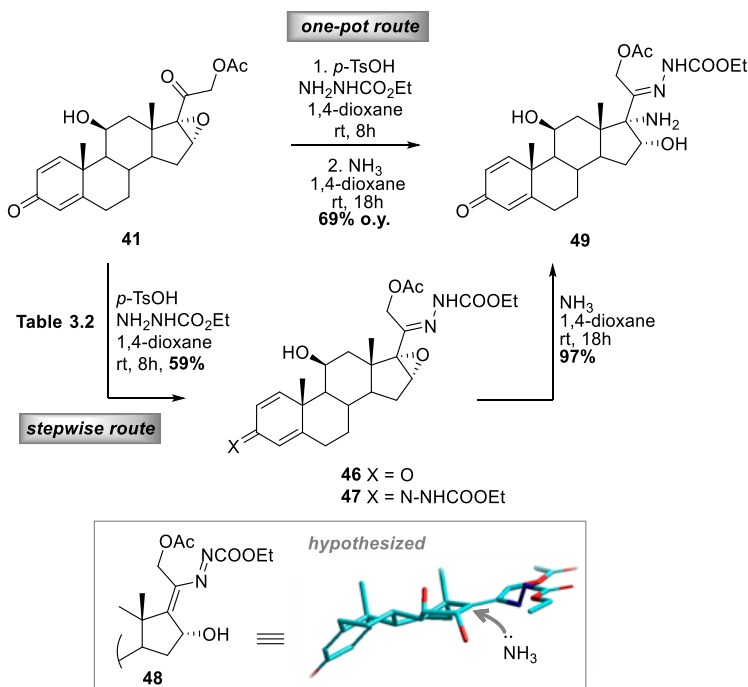
Entry	Compd	Reacting system	Solvent	T [°C]	t [h]	Yield [%]
1	40	MCPBA	DCM	Δ	16	43 : 47
2	40	Oxone/ NaHCO_3 / aq Na_2EDTA	$\text{CF}_3\text{COCH}_3/\text{ACN}$	rt	18	44 : 51
3	40	$\text{H}_2\text{O}_2/\text{NH}_4\text{HCO}_3$	$\text{ACN}/\text{H}_2\text{O}$	rt	16	44 : 59
4	42	MCPBA	DCM	Δ	16	41 : 40
5	42	Oxone/ NaHCO_3 / aq Na_2EDTA	$\text{CF}_3\text{COCH}_3/\text{ACN}$	rt	18	45 : 55
6	42	$\text{H}_2\text{O}_2/\text{NH}_4\text{HCO}_3$	$\text{ACN}/\text{H}_2\text{O}$	rt	18	//
7	40	Phtalic anhydride/ H_2O_2	DCM	Δ	24	43 : 82

^a Bu_3SnH , AIBN, THF, reflux, 30°, 93-98%

Installation of the epoxy function at the desired C16-C17 position was achieved by treatment of **40** or **42** with *m*CPBA in refluxing DCM (entries 1 and 4, TABLE 3.1), obtaining in both cases the desired α -epoxides **43** and **41** in 47% and 40% yield, respectively. In both cases the

introduction of the epoxy function with the desired α -configuration was driven by the presence of the β -oriented methyl group at C18 position. Even better results were obtained with the in situ generated monopero-phthalic acid (phthalic anhydride/H₂O₂)²⁸ (entry 7) leading to the desired epoxide **43** in satisfying 82% yield whose debromination (AIBN/Bu₃SnH) provided the epoxide **41**.

With epoxide **41** in hand, conversion of the latter into *cis*-17-amino-16-hydroxy derivative **49** was accomplished either by a stepwise route (path a, SCHEME 3.1) or by a one-pot procedure (path b, SCHEME 3.1), exploiting the formation of the corresponding carboethoxy hydrazone **46**. Indeed, the data about the ability of hydrazone group-containing oxidosteroids to efficiently drive the regio- and stereoselective ring opening of neighbouring three-membered heterocycles,²⁹ prompted us to consider hydrazone **46** as intermediate to selectively introduce a vicinal amino-alcohol function in C16 and C17 positions with the desired *cis*-configuration. Different reaction conditions were explored for the conversion of ketone **41** into hydrazone **46** varying both the reaction solvent and the activating agent in presence of ethyl carbazate (TABLE 3.2). In almost all cases, unsatisfactory results were obtained (entries 1-3), since only limited conversions were achieved, while the recovery of unreacted starting material was mainly found.



SCHEME 3.1. Regio- and stereoselective ring opening of epoxide **41**.

When the reaction was carried out with Py·HCl in pyridine (entry 4), the desired hydrazone **46** was isolated albeit in low yield (30%, entry 4) due to the formation of hydrazone **47** with both C20 and C3 carbonyl functions protected. The C20 monoprotected derivative **46** was instead easily obtained in good yield (59%), using ethyl carbazate and *p*-toluenesulfonic acid in anhydrous 1,4 dioxane (entry 5). The epoxide ring opening from hydrazone **46** was then carried out by treatment of **46** with NH₃ in dioxane affording the desired *cis*-17-amino-16-hydroxy derivative **49** in 97% yield (SCHEME 3.1, stepwise route). Similar results in terms of reaction times and yields were obtained through a one-pot procedure (SCHEME 3.1, one-pot route). The stereochemical outcome of the reaction herein observed was assumed to rely on the formation, under basic conditions, of intermediate **48** (SCHEME 3.1). Indeed, differently from the well-known acid-catalyzed epoxide ring opening, carried out on similar steroid derivatives, it is reasonable to hypothesize that NH₃ deprotonates hydrazone **46**, enabling epoxide ring opening to give **48** (PM3; HyperChem™, rel 8.0.3).

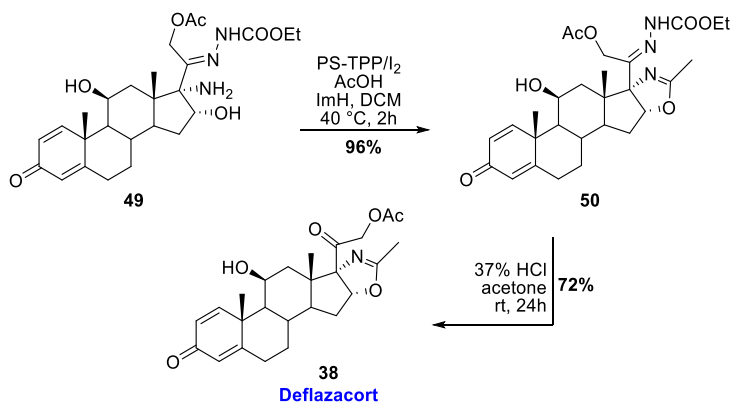
TABLE 3.2. Experimental conditions for the conversion of ketone **41** into carboethoxy hydrazone **46**

Entry	Activating agent	Solvent	t(h)	Yield (%)
1	AcOH	1,4-dioxane	18	12
2	H ₂ SO ₄	DMF	16	20
3	CSA	toluene	16	16
4	Py·HCl	pyridine	24	30
5	<i>p</i> -TsOH	1,4-dioxane	8	59

The latter then undergoes nucleophilic attack by ammonia from the less hindered side of D ring, leading to amino-alcohol **49**. Oxazoline ring formation was then performed using the polymer supported triphenylphosphine/iodine/imidazole (PS-TPP/I₂/ImH) system as activating agent³⁰⁻³² (SCHEME 3.2). The occurred formation of the oxazoline ring confirms the introduction of the amino-alcohol function in **49** with a *cis* configuration. Treatment of acetic acid (AcOH) with 2.0 equivalents of the previously mixed PS-TPP/I₂ followed by the addition of **49** and imidazole to the reaction mixture provided, already after 2h in refluxing DCM, the desired **50** in high yield (96%) and purity.

It should be noted that a two-fold amount of PS-TPP/I₂ was added to enable activation of acetic acid at first, and then the hydroxyl group activation, while the addition of ImH to the reaction

medium ensures neutral/mild alkaline environment, by trapping protons released during the course of the reaction, and promotes the amide proton abstraction, thus allowing oxazoline ring closure. Lastly, removal of C20 hydrazone function (HCl/acetone) on **50** smoothly provided the pure Deflazacort (**38**) in 72% yield.



SCHEME 3.2. Oxazoline ring formation and access to Deflazacort.

3.2.2 BIOLOGICAL EVALUATION

Biological assays aimed at the evaluation of the antibacterial potential of DFZ and its synthetic precursors were performed by Prof. Eliana De Gregorio (University of Napoli Federico II, Department of Molecular Medicine and Medical Biotechnology).

In early studies,^{21,22} compounds **38**, **41**, **46**, **49**, **50** were screened against a panel of Gram-positive and Gram-negative pathogens responsible for drug-resistant infections and thus classified as critical and high priority pathogens³³ including *Staphylococcus aureus*, *Enterococcus* spp., *Acinetobacter baumannii*, *Pseudomonas aeruginosa*, *Klebsiella pneumoniae*, *Escherichia coli* and *Enterobacter* spp. Minimum inhibitory concentration (MIC) and minimum bactericidal concentration (MBC) were determined by a broth microdilution assay and are reported in TABLE 3.3. Deflazacort, as well as its synthetic precursor **49**, were inactive as growth inhibitors for all the pathogens considered even at high experimental concentrations (entries 3 and 5). Compounds **46** (entry 2) and **50** (entry 4) showed only a weak antimicrobial activity against *E. faecalis* and *S. aureus* and only the compound **46** showed a weak antimicrobial activity against *P. aeruginosa*. On the contrary, epoxide **41** (entry 1) showed interesting potential as growth inhibitor with MIC values of 4 µg/mL against *E. faecalis*, 16 µg/mL against *S. aureus* and *A. baumannii* and 128 µg/mL against both *E. coli* and *P. aeruginosa*. Interestingly, compound **41** also works as bactericidal agents, having minimum bactericidal concentration (MBC) values equal to the MIC values. All compounds did not exert any appreciable inhibition of the other Gram-negative bacteria considered, *K. pneumoniae* and *E. aerogenes*, up to the concentrations of 1000 µg/mL.

Table 3.3. MIC ($\mu\text{g/mL}$) and MBC ($\mu\text{g/mL}$) values of DFZ and its precursors against a panel of Gram-negative and Gram-positive pathogens.

Entry	Compound	Bacteria											
		<i>S. aureus</i> ATCC 29213		<i>A. baumannii</i> ATCC 17978		<i>E. faecalis</i> 29212		<i>P. aeruginosa</i> ATCC 27859		<i>E. coli</i> ATCC 25922			
		MIC	MBC	MIC	MBC	MIC	MBC	MIC	MBC	MIC	MBC		
1	41	16	16	16	16	4	16	128	1000	128	128		
2	46	375	>1000	>1000	>1000	187	>1000	750	>1000	>1000	>1000		
3	49	>1000	>1000	>1000	>1000	>1000	>1000	>1000	>1000	>1000	>1000		
4	50	750	>1000	>1000	>1000	375	>1000	>1000	>1000	>1000	>1000		
5	DFZ	>1000	>1000	>1000	>1000	>1000	>1000	>1000	>1000	>1000	>1000		
6	51	256	512	512	512	128	256	1000	1000	1000	1000		
7	52	1000	1000	1000	1000	1000	1000	1000	1000	1000	1000		
8	53	>1000	>1000	>1000	>1000	>1000	>1000	>1000	>1000	>1000	>1000		
9	Methicillin	2.5	ND	ND	ND	ND	ND	ND	ND	ND	ND		
10	Gentamicin	0.5	ND	1.5	ND	ND	ND	ND	ND	ND	ND		
11	Ampicillin	ND	ND	>0.032	ND	ND	ND	ND	ND	ND	ND		
12	Amikacin	ND	ND	4	ND	ND	ND	ND	ND	ND	ND		
13	Vancomycin	1	ND	ND	ND	ND	ND	ND	ND	ND	ND		

MIC: minimum inhibitory concentration; MBC: minimum bactericidal concentration; MIC experiments were carried out in triplicates and repeated three times and was determined by broth microdilution assay as previously described.³⁴
 ND: Not Determined.

With the aim to identify which functionalities could be responsible for the antimicrobial activity of **41** we also evaluated the biological potential of derivatives **51**, **52** and **53**, that share common residues with **41** (FIGURE 3.6). Compound **51**, in which the epoxy function at C16-C17 positions was replaced by a double bond (FIGURE 3.6), exhibited antibacterial activity against *S. aureus*, *A. baumannii* and *E. faecalis* strains but at much higher concentration than **41**. In contrast compound **52**, in which the hydroxyl function at C10 position is absent, worked only at concentration of 1 mg/mL while compound **53**, in which the acetyl group at 21 hydroxyl function is missing, was inactive as growth inhibitor. These data clearly suggest that the epoxy function on C16-C17 positions of the steroidal scaffold, the C10 hydroxyl group and the acetyl residue are all crucial for the antimicrobial activity exhibited by **41**. Cytotoxicity of **41** was assessed *in vitro* using hemolytic assay³⁵ measuring its hemolytic activity against horse RBCs at final concentrations ranging from 1 to 512 $\mu\text{g/mL}$. Epoxide **41** showed no hemolytic activity at concentrations up to 128 $\mu\text{g/mL}$, whereas was 62,8% and 78,6% at 256 $\mu\text{g/mL}$ and 512 $\mu\text{g/mL}$, respectively.

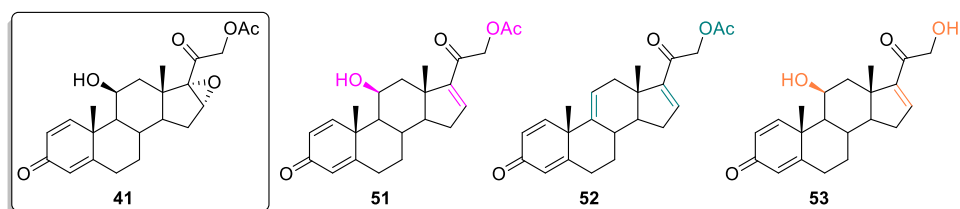


FIGURE 3.6. Steroid derivatives evaluated for their antibacterial potential for comparison with epoxide **41**.

With epoxide **41** being the most effective microbial growth inhibitor, further experiments were performed²²⁻²⁴ for a deeper evaluation of its antimicrobial potential as described below.

- **Antibacterial and antibiofilm activity of epoxide 41 against *S. aureus* strain**

In-depth studies on the antimicrobial potential of **41** were focused on its activity against *S. aureus*, pathogen responsible for several infections and able to acquire resistance to many available antibiotic drug classes.³⁶ In order to evaluate the ability of **41** to potentiate or restore the antibacterial activity of conventional antibiotics against drug-resistant strains, it was tested in combination with gentamicin and oxacillin against MRSA (methicillin-resistant *S. aureus*) 00717, an isolate resistant to the selected antibiotics. The MIC value for **41** against *S. aureus* 00717 was 16 $\mu\text{g/mL}$ while for gentamicin and oxacillin the MIC values were 256 $\mu\text{g/mL}$ and 128 $\mu\text{g/mL}$, respectively. As highlighted by checkerboard dilution test[‡] (TABLE 3.4) epoxide **41**

[‡] The checkerboard dilution test is widely used to determine the effect of antibiotic combinations in comparison with the activity of compounds taken alone. The effects of drug combination are expressed with fractional inhibitory concentration (FIC) index values that indicate the combination of drugs producing the greatest change from the individual antibiotic's MIC.

exhibited an additive effect being able to reduce the MICs of gentamicin (from 256 to 16 $\mu\text{g}/\text{mL}$) and oxacillin (from 128 to 2 $\mu\text{g}/\text{mL}$).

The effect of **41** on *S. aureus* virulence factors was also evaluated revealing its ability to inhibit the expression of virulence and regulator genes including enterotoxins, autolysin and hemolysin suggesting the potential of this molecule to exert anti-virulence activity.²²

TABLE 3.4. Additive effect of **41** with antibiotics against *S. aureus* 00717.

Bacterial strain	Combination	MIC ^a ($\mu\text{g}/\text{mL}$)	MIC ^b ($\mu\text{g}/\text{mL}$)	FIC index
<i>S. aureus</i> 00717	41 /gentamicin	16/256	8/16	0.5625
	41 /oxacillin	16/128	8/2	0.5156

^a MIC of **41** (blue) or antibiotics (green) alone; ^b MIC of **41** in combination with antibiotics (blue) and of antibiotics in combination with **41** (green). FIC index: fractional inhibitory concentration index.

The antibiofilm activity against *S. aureus* of epoxide **41** was also studied. Indeed, *S. aureus* is the major Gram-positive bacteria able to develop biofilms on a wide range of surface leading to chronic antibiotic-resistant infections. The effect of **41** was evaluated on both biofilm formation and eradication of preformed biofilm by *S. aureus*. A dose-dependent reduction of biofilm development was observed as highlighted by both crystal violet staining assay (FIGURE 3.7A) and confocal laser scanning (FIGURE 3.7B) with complete inhibition at 8 $\mu\text{g}/\text{mL}$.

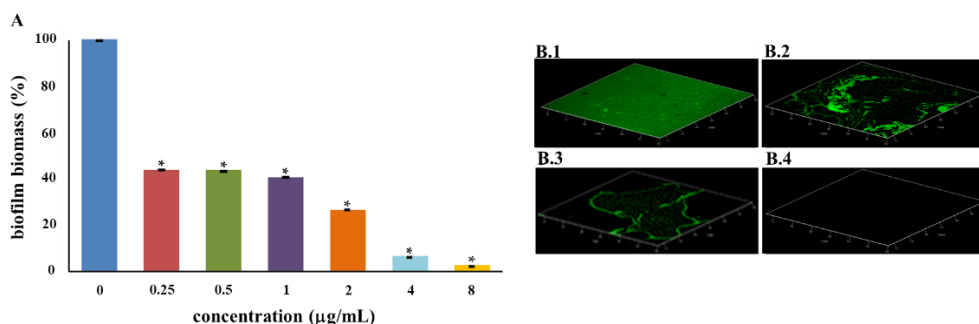


FIGURE 3.7. Inhibitory effect of **41** on *S. aureus* biofilm formation. (A) Biofilm quantification by crystal-violet staining. (B) Confocal laser scanning microscopy analysis of the biofilm formed by *S. aureus* absence (B.1) or presence of **41**, at the concentrations of 2 $\mu\text{g}/\text{mL}$ (B.2), 4 $\mu\text{g}/\text{mL}$ (B.3), and 8 $\mu\text{g}/\text{mL}$ (B.4).

Similarly, epoxide **41** was found to be able to reduce preformed (24 h old) *S. aureus* biofilm with 95% eradication at 64 $\mu\text{g}/\text{mL}$ (FIGURE 3.8). Preliminary transcriptional studies revealed that the eradication of *S. aureus* established biofilm can be ascribed to the downregulation of the expression of several biofilm- and toxin-related genes.²⁴

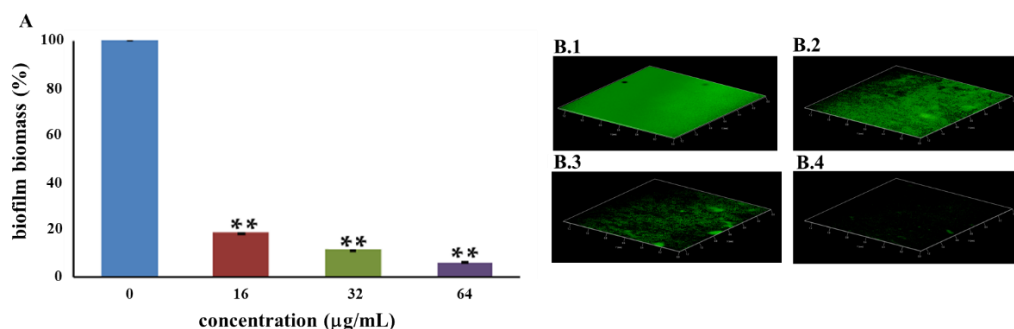


FIGURE 3.8. Eradicating effect of **41** on *S. aureus* preformed biofilm. (A) Biofilm biomass quantification by crystal violet-staining. (B) Confocal laser scanning microscopy analysis of preformed *S. aureus* biofilm without treatment (B.1) or treated with **41** at 16 µg/mL (B.2), 32 µg/mL (B.3), and 64 µg/mL (B.4) for 24h.

• **Antibacterial and antibiofilm activity of epoxide 41 against *S. maltophilia* strain**

Subsequent studies were focused on the activity of DFZ and its synthetic precursors against the Gram-negative bacterium *Stenotrophomonas maltophilia*, an emerging nosocomial opportunistic pathogen that causes life-threatening infections in immunocompromised patients.^{37,38} Therapeutic treatment of *S. maltophilia* infections is often hampered by intrinsic or acquired resistance to antibiotics and therefore development of novel alternative antimicrobial agents represents an urgent need. As shown in TABLE 3.4, epoxide **41** exhibited a weak effect on bacterial growth (256 µg/mL) while the other derivatives were inactive against *S. maltophilia* K279a cells.

Table 3.4. MIC (µg/mL) and MBC (µg/mL) values of DFZ and its precursors against *S. maltophilia* K279a

entry	Compound	<i>S. maltophilia</i> K279a	
		MIC	MBC
1	41	256	512
2	46	750	>1000
3	49	>1000	>1000
4	50	512	>1
5	DFZ	>1000	>1000
6	51	>1000	>1000
7	52	1000	>1000
8	53	>1000	>1000
9	STX	1	1

STX: Trimethoprim-sulfamethoxazole; MIC: minimum inhibitory concentration; MBC: minimum bactericidal concentration; MIC experiments were carried out in triplicates and was determined by broth microdilution assay as previously described.³⁴

Effect of epoxide **41** was then evaluated in combination with gentamicin and amikacin, two marketed antibiotics belonging to the class of aminoglycosides. Broth microdilution checkerboard assay revealed a synergistic effect with both compounds as shown by the reduction of MIC by eightfold and fourfold for gentamicin and amikacin respectively (TABLE 3.5) highlighting an interesting therapeutic potential of **41** for its use against multidrug-resistant strains.

TABLE 3.5. Synergistic effect of **41** with antibiotics against *S. maltophilia* K279a.

Bacterial strain	Combination	MIC ^a ($\mu\text{g/ml}$)	MIC ^b ($\mu\text{g/ml}$)	FIC index
<i>S. maltophilia</i> K279a	41 /gentamicin	256/16	64/4	0.5
	41 /amikacin	256/16	64/2	0.375

^aMIC of **41** (blue) or antibiotics (green) alone; ^bMIC of **41** in combination with antibiotics (blue) or of antibiotics in combination with **41** (green). FIC index: fractional inhibitory concentration index.

The ability of **41** to inhibit *S. maltophilia* K279a biofilm formation was then evaluated and a dose-dependent reduction was found with complete inhibition at 64 $\mu\text{g/ml}$ as shown in FIGURE 3.9.

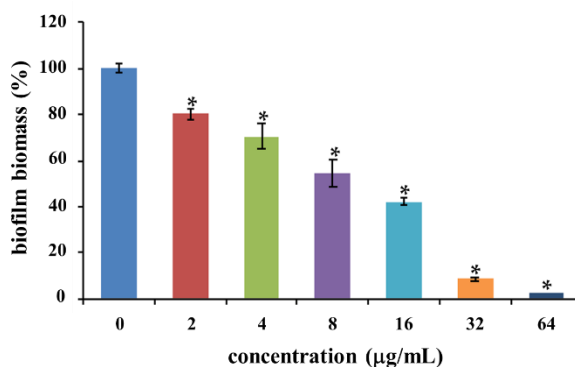


FIGURE 3.9. *S. malophilis* K279a biofilm formation following treatment with the **41**. Cells were incubated for 24 h in the presence of sub-inhibitory concentrations of **41**. Biofilms were quantified after crystal-violet staining. Values are presented as mean \pm SD. *P < 0.05.

3.3 CONCLUDING REMARKS

In search for novel candidates active against bacterial infections, herein the therapeutic potential of Deflazacort, an oxazoline-containing corticosteroid, as antibacterial agent has been explored. The excellent biological properties of DFZ (it is currently marketed for anti-inflammatory and immunosuppressive activity and has demonstrated high efficacy associated to a good tolerability) led us to develop a novel procedure for its preparation and to evaluate its activity, as well as of some of its synthetic precursors against both Gram-positive and Gram-negative bacteria responsible for drug-resistant infections including *S. aureus*, *E. faecalis*, *A. baumannii*, *P. aeruginosa*, *E. coli*, *S. maltophilia*. Our route relied on the use of 9-bromotriene acetate **40** whose synthetic manipulation gave a straightforward access to DFZ in only five reaction steps. When evaluated as growth inhibitor, DFZ was inactive against all the bacteria considered. Conversely, one of its synthetic precursors, epoxide **41**, showed interesting antibacterial activity against *E. faecalis*, *S. aureus*, *A. baumannii*, *E. coli*, *P. aeruginosa* and *S. maltophilia*.

In depth studies were then performed to evaluate the antimicrobial and antibiofilm activity of **41** against *S. aureus* and *S. maltophilia*. On one hand **41** demonstrated to be able to inhibit biofilm formation, as well as to eradicate preformed biofilms. On the other, this compound showed antibacterial activity against *S. maltophilia* in combination with gentamicin or amikacin and inhibits biofilm formation.

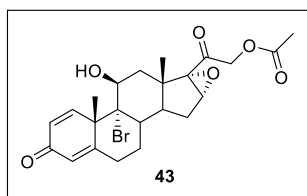
Our data overall demonstrate the high potential of compound **41** as antibacterial and antibiofilm agent especially regarding for its activity against drug-resistant pathogens. Further studies will be necessary to establish the molecular mechanism responsible for the effect of **41** on planktonic growth and biofilm formation and eradication, as well as to explore the antibacterial potential of these molecules against other bacterial pathogens.

3.4 EXPERIMENTAL SECTION

CHEMICAL SYNTHESIS: GENERAL METHODS

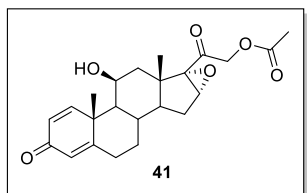
All chemicals and solvents were purchased with the highest degree of purity (Sigma- Aldrich, Alfa Aesar, VWR) and used without further purification. 9-Bromotriene acetate **40** was provided by Symbiotec Pharmalab PVT. All moisture-sensitive reactions were performed under nitrogen atmosphere using oven-dried glassware. The reactions were monitored by TLC (precoated silica gel plate F254, Merck) and the products were detected by exposure to ultraviolet radiation, iodine vapor, and chromic mixture. Column chromatography: Merck Kieselgel 60 (70–230 mesh); flash chromatography: Merck Kieselgel 60 (230–400 mesh). The purity of the synthetic intermediates and the final compound was determined by CHNS analysis and was $\geq 95\%$ in all cases. NMR spectra were recorded on NMR spectrometers operating at 400 MHz (Bruker AVANCE) or 500 MHz (Varian Inova), using CDCl₃ solutions unless otherwise specified. Coupling constant values (J) were reported in Hz.

SYNTHESIS OF DEFLAZACORT (DFZ)



1,4-Pregnadiene-9-bromo-11 β -hydroxy-16 α ,17 α -epoxy-3,20-dione (43). **METHOD A.** To a stirred solution of 9-bromotriene acetate **40** (1.0 g, 2.16 mmol) in anhydrous DCM (30 mL), *m*-CPBA (0.75 g, 4.32 mmol) was added at room temperature. The mixture was warmed to reflux and stirred for 16 h. Then, aq. NaHCO₃ was added and the mixture was extracted with DCM;

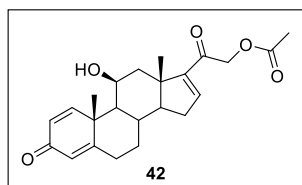
the organic layer was dried (Na₂SO₄) and the solvent evaporated under reduced pressure. The solid residue was recrystallized from AcOEt to give the final compound **43** (0.49 g, 47% yield) as a white solid. **METHOD B.** Phthalic anhydride (0.13 g, 0.86 mmol) was added in one portion to a stirred solution of **40** in DCM (2.0 mL) at room temperature. After few minutes, phthalic anhydride was completely dissolved to give a yellow clear solution. At the same temperature 50% aq H₂O₂ was then added dropwise in 2 h and the mixture was then heated to reflux temperature. Formation of a white precipitate was observed and after 24 h, water and solid NaHCO₃ were added to the cooled reaction mixture until pH 7, and then the mixture was extracted with a CHCl₃/MeOH (9/1) mixture. The organic layers were combined, dried with Na₂SO₄ and concentrated under reduced pressure to give a yellow solid. AcOEt was added to the crude residue. The resulted precipitate was decanted, and the orange mother liquors removed. This operation was repeated until a white powder was obtained. All the mother liquors previously obtained were combined and concentrated. The resulting precipitate was decanted, separated from the mother liquors and repeatedly washed with ethyl acetate until to obtain epoxide derivative **43** as a white powder (85 mg, 82%yield). ¹H NMR (400 MHz): δ 1.41 (s, 3H), 1.48-1.55 (m, 1H), 1.70 (s, 3H), 1.71-1.82 (m, 2H), 1.94-2.05 (m, 3H), 2.15 (s, 3H), 2.16-2.25 (m, 1H), 2.36-2.49 (m, 2H), 2.55-2.68 (m, 1H), 3.85 (s, 1H), 4.59 (d, *J* = 13.4, 1H), 4.67 (d, *J* = 13.4, 1H), 4.76 (bs, 1H), 6.07 (bs, 1H), 6.32 (d, *J* = 10.1, 1H), 7.21 (d, *J* = 10.1, 1H). ¹³C NMR (100 MHz): 18.3, 20.4, 24.9, 27.0, 28.3, 30.4, 33.5, 37.3, 39.3, 42.1, 50.2, 61.1, 65.7, 70.5, 75.9, 85.3, 125.1, 129.3, 152.3, 165.5, 170.4, 186.2, 198.9. Anal. calcd for C₂₃H₂₇BrO₆: C, 57.63; H, 5.68; Br, 16.67. Found: C, 57.75; H, 5.66; Br, 16.62.



1,4-Pregnadiene-11 β -hydroxy-16 α ,17 α -epoxy-3,20-dione (41). To a boiling and stirring suspension of epoxide **43** (0.50 g, 1.04 mmol) in anhydrous THF (13.0 mL), a solution of Bu₃SnH (0.36 mL, 1.25 mmol) and AIBN (catalytic amount, 33.3 mg, 0.21 mmol) in THF (10 mL) was added dropwise under nitrogen atmosphere. The reaction mixture was stirred for 30 minutes at

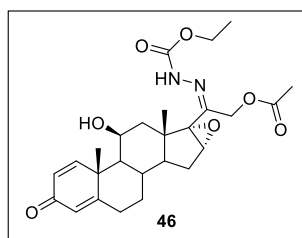
reflux temperature. The crude residue was then concentrated under reduced pressure and recrystallized from AcOEt to give the final compound **41** (0.41 g, 98% yield); white solid. ¹H NMR (400 MHz): δ 1.02-1.14 (m, 2H), 1.39 (s, 3H), 1.46 (s, 3H), 1.46-1.51 (m, 2H), 1.62-1.70 (m, 1H), 1.97-2.02 (m, 3H), 2.15 (s, 3H), 2.15-2.19 (m, 1H), 2.29-2.38 (m, 1H), 2.51-2.62 (m, 1H), 3.82 (s, 1H), 4.42 (bs, 1H), 4.57 (d, *J* = 13.4, 1H), 4.66 (d, *J* = 13.4, 1H), 6.00 (bs, 1H), 6.26

(dd, $J=1.8, 10.1$, 1H), 7.21 (d, $J=10.1$, 1H). ^{13}C NMR (100 MHz): 17.4, 20.5, 21.3, 27.8, 28.3, 29.5, 31.9, 33.4, 41.0, 42.0, 44.2, 45.1, 56.2, 61.4, 65.8, 69.9, 122.6, 128.0, 156.1, 169.6, 170.4, 186.6, 190.0. Anal. calcd for $\text{C}_{23}\text{H}_{28}\text{O}_6$: C, 68.98; H, 7.05. Found: C, 69.05; H, 7.03.



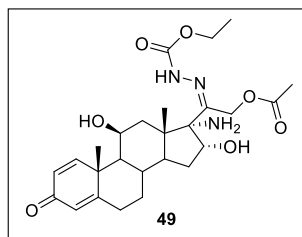
1,4,17-Pregnatriene-11 β -hydroxy-3,20-dione (42).

Compound **42** was obtained in 93% yield from **40** using the same conditions reported above for preparation of **41**. Data for **42**: white solid, ^1H NMR (500 MHz): δ 1.06-1.21 (m, 1H), 1.26 (s, 3H), 1.32-1.38 (m, 1H), 1.49 (s, 3H), 1.59-1.63 (m, 2H), 2.06-2.12 (m, 1H), 2.17 (s, 3H), 2.18-2.30 (m, 2H), 2.33-2.43 (m, 2H), 2.45-2.51 (m, 1H), 2.55-2.67 (m, 1H), 4.40 (bs, 1H), 4.85 (d, $J=16.1$, 1H), 5.01 (d, $J=16.1$, 1H), 6.01 (bs, 1H), 6.27 (d, $J=10.1$, 1H), 6.73 (bs, 1H), 7.31 (d, $J=10.1$, 1H). ^{13}C NMR (100 MHz): 18.4, 20.5, 21.2, 30.1, 31.8, 32.8, 33.6, 44.2, 44.6, 46.1, 56.1, 56.4, 65.5, 70.2, 122.5, 128.0, 143.5, 152.2, 156.1, 169.4, 170.2, 186.6, 190.5. Anal. calcd for $\text{C}_{23}\text{H}_{28}\text{O}_5$: C, 71.85; H, 7.34. Found: C, 71.80; H, 7.35



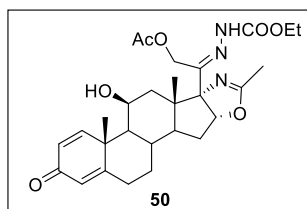
20-Carboethoxyhydrazone of 1,4-pregnadiene-11 β -hydroxy-16 α ,17 α -epoxy-3-one (46).

To a stirring suspension of **41** (0.50 g, 1.25 mmol) in anhydrous 1,4-dioxane (24 mL), ethyl carbazate (0.26 g, 2.5 mmol) and *p*-toluenesulfonic acid (0.24 g, 1.25 mmol) were sequentially added at room temperature under argon atmosphere. The resulting mixture was stirred at the same temperature for 8 h. Then aq NaHCO_3 was added and the mixture was extracted with EtOAc; the organic layer was dried (Na_2SO_4) and the solvent evaporated under reduced pressure. The solid residue was recrystallized from Et₂O to give the final compound **46** (0.36 g, 59% yield) as a white solid. ^1H NMR (500 MHz): δ 1.01-1.12 (m, 2H), 1.15-1.27 (m, 2H), 1.31 (s, 3H), 1.33 (t, $J=7.1$, 3H), 1.40-1.44 (m, 1H), 1.47 (s, 3H), 1.68 (dd, $J=3.1, 14.2$, 1H), 1.96-2.04 (m, 2H), 2.13 (s, 3H), 2.15-2.18 (m, 1H), 2.32 (dd, $J=3.0, 12.7$, 1H), 2.50-2.61 (m, 2H), 3.67 (s, 1H), 4.22-4.29 (m, 2H), 4.31 (d, $J=13.1$, 1H), 4.40 (bs, 1H), 4.56 (d, $J=13.1$, 1H), 6.00 (bs, 1H), 6.25 (d, $J=10.1$, 1H), 7.29 (d, $J=10.1$, 1H). ^{13}C NMR (125 MHz): 14.6, 18.2, 20.6, 21.2, 27.2, 29.9, 31.9, 33.5, 41.4, 41.7, 44.2, 45.9, 55.0, 56.2, 59.6, 62.1, 69.8, 70.2, 122.5, 127.8, 142.5, 153.6, 156.2, 169.7, 171.2, 186.6. Anal. calcd for $\text{C}_{26}\text{H}_{34}\text{N}_2\text{O}_7$: C, 64.18; H, 7.04; N 5.76. Found: C, 64.29; H, 7.02; N 5.75.



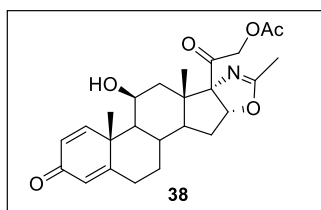
20-Carboethoxyhydrazone of 1,4-pregnadiene-16 α -amino-11 β ,17 α -diol-3-one (49). METHOD A. Epoxide **46** (0.30 g, 0.62 mmol) was dissolved in anhydrous 1,4-dioxane (15 mL) under nitrogen atmosphere at rt. Anhydrous ammonia was then gently bubbled into the solution for 3 minutes and the reaction was stirred at the same temperature for 18 h. Nitrogen was then bubbled in the reaction mixture until the ammonia was eliminated from the

solution (pH = 7). The mixture was diluted with DCM and the organic layers were washed with brine, dried (Na_2SO_4) and concentrated under reduced pressure. The solid residue was recrystallized from Et_2O to give the final compound **49** (0.30 g, 97 % yield) as a white solid. **METHOD B (one-pot procedure)**. To a stirred suspension of **41** (0.50 g, 1.25 mmol) in anhydrous 1,4-dioxane (24 mL), ethyl carbazate (0.26 g, 2.5 mmol) and *p*-toluenesulfonic acid (0.24 g, 1.25 mmol) were sequentially added at room temperature under argon atmosphere. The resulting mixture was stirred at the same temperature for 8 h and then anhydrous ammonia was gently bubbled into the solution for 3 minutes. The reaction mixture was stirred at room temperature for 18h. The mixture was diluted with DCM and the organic layers were washed with brine, dried (Na_2SO_4) and concentrated under reduced pressure. The solid residue was recrystallized from Et_2O to give the final compound **49** (0.43 g, 69% overall yield). ^1H NMR (400 MHz, acetone- d_6): δ 1.04-1.16 (m, 5H), 1.21-1.41 (m, 4H), 1.51 (s, 3H), 1.52-1.57 (m, 1H), 1.78-1.99 (m, 4H), 2.03-2.17 (m, 7H), 2.35 (dd, $J = 3.4, 13.4$, 1H), 2.62 (td, $J = 4.9, 13.4$, 1H), 3.81 (bs, 1H), 4.17 (q, $J = 7.1$, 2H), 4.47 (bs, 1H), 4.76 (d, $J = 13.0$, 1H), 4.90 (d, $J = 13.0$, 1H), 5.16 (dd, $J = 3.0, 9.2$, 1H), 5.92 (bs, 1H), 6.14 (dd, $J = 1.6, 10.1$, 1H), 7.33 (d, $J = 10.1$, 1H). ^{13}C NMR (100 MHz, acetone- d_6): 14.0, 18.2, 19.9, 20.8, 29.7, 30.9, 31.6, 33.9, 40.9, 44.0, 46.4, 48.9, 55.6, 58.2, 60.8, 69.4, 81.2, 83.7, 121.8, 127.3, 149.4, 153.6, 155.9, 170.1, 170.3, 185.1. Anal. calcd for $\text{C}_{26}\text{H}_{37}\text{N}_3\text{O}_7$: C, 62.01; H, 7.41; N 8.34. Found: C, 62.08; H, 7.38; N 8.36.



20-Carboethoxyhydrazone of 1,4-pregnadiene-11 β -hydroxy-16 α ,17 α -oxazole-3-one (50). I_2 (0.30 g, 1.19 mmol) was added to a stirred solution of polymer supported triphenylphosphine (PS-TPP; 100-200 mesh, extent of labeling: ~ 3 mmol/g triphenylphosphine loading) (0.40 g, 1.19 mmol) in anhydrous DCM (20 mL) at rt. Then glacial acetic acid (35 μL , 0.59 mmol) was added and the solution was stirred at room temperature for

20'. Afterwards, **49** (0.30 g, 0.59 mmol) and imidazole (0.16 g, 2.38 mmol) were sequentially added and the solution was warmed to 40 $^\circ\text{C}$ and stirred for 2 h. The mixture was then filtered and the solvent removed under reduced pressure. The solid residue was recrystallized from Et_2O to give the final compound **50** (0.29 g, 96% yield) as a white solid. ^1H NMR (500 MHz, acetone- d_6): δ 1.04 (dd, $J = 3.7, 11.4$, 1H), 1.07 (s, 1H), 1.09-1.18 (m, 1H), 1.27 (t, $J = 7.1$, 1H), 1.29-1.36 (m, 3H), 1.51 (s, 3H), 1.74 (dd, $J = 5.7, 13.6$, 1H), 1.81 (dd, $J = 7.6, 13.6$, 1H), 1.85-1.90 (m, 4H), 2.12 (s, 3H), 2.18-2.25 (m, 1H), 2.35 (dd, $J = 3.4, 13.5$, 1H), 2.65 (td, $J = 5.7, 13.5$, 1H), 3.83 (bs, 1H), 4.17 (q, $J = 7.1$, 2H), 4.47 (bs, 1H), 4.73 (d, $J = 13.0$, 1H), 4.92 (d, $J = 13.0$, 1H), 5.66 (d, $J = 5.7$, 1H), 5.92 (bs, 1H), 6.14 (dd, $J = 1.8, 10.1$, 1H), 7.31 (d, $J = 10.1$, 1H), 9.37 (bs, 1H). ^{13}C NMR (125 MHz, acetone- d_6): 13.2, 14.0, 19.1, 19.9, 20.8, 29.7, 30.6, 31.5, 33.9, 41.7, 43.9, 47.0, 50.4, 55.5, 57.5, 60.9, 69.1, 83.7, 91.6, 121.9, 127.4, 145.9, 153.4, 155.7, 165.1, 169.5, 170.2, 185.0. Anal. calcd for $\text{C}_{28}\text{H}_{37}\text{N}_3\text{O}_7$: C, 63.74; H, 7.07; N 7.96. Found: C, 63.81; H, 7.02; N 7.99.



Deflazacort (38). To a stirred solution of **50** (0.30 g, 0.57 mmol) in acetone (8 mL), HCl 37% solution (0.09 mL, 1.14 mmol) was added and the solution was stirred at rt for 24h. Then aq. NaHCO₃ was added and the mixture was extracted with DCM; the combined organic layers were washed with brine, dried (Na₂SO₄) and the solvent was evaporated under reduced pressure. Chromatography of the crude residue over silica gel

(hexane:acetone = 7:3) gave the pure DFZ (**38**) (0.18 g, 72% yield) as a white solid. ¹H NMR (400 MHz, CD₃OD): δ 1.01 (dd, *J* = 3.6, 11.3, 1H), 1.02 (s, 3H), 1.06-1.25 (m, 2H), 1.49 (s, 3H), 1.75 (dd, *J* = 5.9, 13.8, 1H), 1.79-1.85 (m, 1H), 1.89 (dd, *J* = 3.9, 14.2, 1H), 1.97 (s, 3H), 2.01 (dd, *J* = 2.7, 13.8, 1H), 2.06-2.12 (m, 1H), 2.13 (s, 3H), 2.20 (dd, *J* = 4.1, 11.6, 1H), 2.37 (ddd, *J* = 1.8, 4.6, 13.4, 1H), 2.65 (td, *J* = 5.7, 13.4, 1H), 4.41 (dd, *J* = 3.2, 6.3, 1H), 4.93 (s, 2H), 5.30 (d, *J* = 5.5, 1H), 6.00 (bs, 1H), 6.25 (dd, *J* = 1.9, 10.1, 1H), 7.45 (d, *J* = 10.1, 1H). ¹³C NMR (125 MHz, CD₃OD): 12.5, 17.2, 18.9, 20.1, 30.4, 31.6, 33.9, 34.0, 40.9, 44.5, 50.4, 55.5, 67.0, 69.0, 84.8, 94.2, 121.2, 126.5, 158.3, 168.0, 170.6, 172.8, 187.5, 200.9. Anal. calcd for C₂₅H₃₁NO₆: C, 68.01; H, 7.08; N 3.17. Found: C, 68.09; H, 7.06; N 3.15.

3.5 BIBLIOGRAPHY

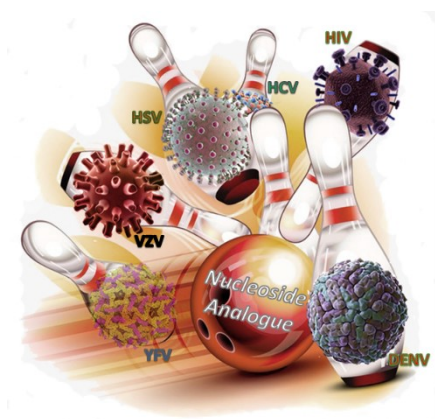
- (1) Buttgereit, F.; Burmester, G.; Lipworth, B. Optimised Glucocorticoid Therapy: The Sharpening of an Old Spear. *Lancet* **2005**, *365* (9461), 801–803. [https://doi.org/10.1016/S0140-6736\(05\)71005-9](https://doi.org/10.1016/S0140-6736(05)71005-9).
- (2) Hoes, J. N.; Jacobs, J. W. G.; Buttgereit, F.; Bijlsma, J. W. J. Current View of Glucocorticoid Co-Therapy with DMARDs in Rheumatoid Arthritis. *Nat. Rev. Rheumatol.* **2010**, *6* (12), 693–702. <https://doi.org/10.1038/nrrheum.2010.179>.
- (3) Liu, D.; Ahmet, A.; Ward, L.; Krishnamoorthy, P.; Mandelcorn, E. D.; Leigh, R.; Brown, J. P.; Cohen, A.; Kim, H. A Practical Guide to the Monitoring and Management of the Complications of Systemic Corticosteroid Therapy. *Allergy, Asthma Clin. Immunol.* **2013**, *9* (1), 30. <https://doi.org/10.1186/1710-1492-9-30>.
- (4) Swartz, S. L.; Dluhy, R. G. Corticosteroids. *Drugs* **1978**, *16* (3), 238–255. <https://doi.org/10.2165/00003495-197816030-00006>.
- (5) Samuel, S.; Nguyen, T.; Choi, H. A. Pharmacologic Characteristics of Corticosteroids. *J. Neurocritical Care* **2017**, *10* (2), 53–59. <https://doi.org/10.18700/jnc.170035>.
- (6) Parente, L. Deflazacort: Therapeutic Index, Relative Potency and Equivalent Doses versus Other Corticosteroids. *BMC Pharmacol. Toxicol.* **2017**, *18* (1), 1–8. <https://doi.org/10.1186/s40360-016-0111-8>.
- (7) Coutinho, A. E.; Chapman, K. E. The Anti-Inflammatory and Immunosuppressive Effects of Glucocorticoids, Recent Developments and Mechanistic Insights. *Mol. Cell. Endocrinol.* **2011**, *335* (1), 2–13. <https://doi.org/10.1016/j.mce.2010.04.005>.
- (8) Smoak, K. A.; Cidlowski, J. A. Mechanisms of Glucocorticoid Receptor Signaling during Inflammation. *Mech. Ageing Dev.* **2004**, *125* (10–11), 697–706.

- <https://doi.org/10.1016/j.mad.2004.06.010>.
- (9) Stellato, C. Post-Transcriptional and Nongenomic Effects of Glucocorticoids. *Proc. Am. Thorac. Soc.* **2004**, *1* (3), 255–263. <https://doi.org/10.1513/pats.200402-015MS>.
 - (10) Assandri A, Buniva G, Martinelli E, Perazzi A, Z. L. Pharmacokinetics and Metabolism of Deflazacort in the Rat, Dog, Monkey and Man. *Adv Exp Med Biol* **1984**, *171*, 9–23.
 - (11) Markham, A.; Bryson, H. M. Deflazacort. *Drugs* **1995**, *50* (2), 317–333. <https://doi.org/10.2165/00003495-199550020-00008>.
 - (12) McKeage, K.; Lyseng-Williamson, K. A. Deflazacort in Duchenne Muscular Dystrophy: A Profile of Its Use in the USA. *Drugs Ther. Perspect.* **2018**, *34* (1), 16–22. <https://doi.org/10.1007/s40267-017-0466-y>.
 - (13) Griggs, R. C.; Miller, J. P.; Greenberg, C. R.; Fehlings, D. L.; Pestronk, A.; Mendell, J. R.; Moxley, R. T.; King, W.; Kissel, J. T.; Cwik, V.; Vanasse, M.; Florence, J. M.; Pandya, S.; Dubow, J. S.; Meyer, J. M. Efficacy and Safety of Deflazacort vs Prednisone and Placebo for Duchenne Muscular Dystrophy. *Neurology* **2016**, *87* (20), 2123–2131. <https://doi.org/10.1212/WNL.0000000000003217>.
 - (14) Verhaart, I. E. C.; Aartsma-Rus, A. Therapeutic Developments for Duchenne Muscular Dystrophy. *Nat. Rev. Neurol.* **2019**, *15* (7), 373–386. <https://doi.org/10.1038/s41582-019-0203-3>.
 - (15) Nathansohn, G.; Winters, G.; Testa, E. Steroids Possessing Nitrogen Atoms. III. Synthesis of New Highly Active Corticoids. [17 α ,16 α ,- d]Oxazolino Steroids. *J. Med. Chem.* **1967**, *10* (5), 799–802. <https://doi.org/10.1021/jm00317a009>.
 - (16) Moore, K. S.; Wehrli, S.; Roder, H.; Rogers, M.; Forrest, J. N.; McCrimmon, D.; Zasloff, M. Squalamine: An Aminosterol Antibiotic from the Shark. *Proc. Natl. Acad. Sci.* **1993**, *90* (4), 1354–1358. <https://doi.org/10.1073/pnas.90.4.1354>.
 - (17) Bergstrom, B. E.; Abdelkhalik, A.; Younis, W.; Hammac, G. K.; Townsend, W. M.; Seleem, M. N.; Chin, J. N.; Rybak, M. J.; Cheung, C. M.; Savage, P. B. Antibacterial Activity and Safety of Commercial Veterinary Cationic Steroid Antibiotics and Neutral Superoxidized Water. *PLoS One* **2007**, *51* (3), 1–13. <https://doi.org/10.1371/journal.pone.0193217>.
 - (18) Savage, P. Antibacterial Properties of Cationic Steroid Antibiotics. *FEMS Microbiol. Lett.* **2002**, *217* (1), 1–7. [https://doi.org/10.1016/S0378-1097\(02\)01036-4](https://doi.org/10.1016/S0378-1097(02)01036-4).
 - (19) Chin, J. N.; Rybak, M. J.; Cheung, C. M.; Savage, P. B. Antimicrobial Activities of Ceragenins against Clinical Isolates of Resistant Staphylococcus Aureus. *Antimicrob. Agents Chemother.* **2007**, *51* (4), 1268–1273. <https://doi.org/10.1128/AAC.01325-06>.
 - (20) Curbete, M. M.; Salgado, H. R. N. A Critical Review of the Properties of Fusidic Acid and Analytical Methods for Its Determination. *Crit. Rev. Anal. Chem.* **2016**, *46* (4), 352–360. <https://doi.org/10.1080/10408347.2015.1084225>.
 - (21) Esposito, A.; De Gregorio, E.; De Fenza, M.; D’Alonzo, D.; Satawani, A.; Guaragna, A. Expeditious Synthesis and Preliminary Antimicrobial Activity of Deflazacort and Its Precursors. *RSC Adv.* **2019**, *9* (37), 21519–21524. <https://doi.org/10.1039/C9RA03673C>.
 - (22) Vollaro, A.; Esposito, A.; Antonaki, E.; Iula, V. D.; Alonzo, D. D.; Guaragna, A.; Gregorio, E. De. Steroid Derivatives as Potential Antimicrobial Agents against Staphylococcus Aureus Planktonic Cells. *Microorganisms* **2020**, 1–14.
 - (23) Esposito, A.; Vollaro, A.; Esposito, E. P.; D’Alonzo, D.; Guaragna, A.; Zarrilli, R.; De Gregorio, E. Antibacterial and Antivirulence Activity of Glucocorticoid PYED-1 against Stenotrophomonas Maltophilia. *Antibiotics* **2020**, *9* (3), 105. <https://doi.org/10.3390/antibiotics9030105>.

- (24) Vollaro, A.; Esposito, A.; Esposito, E. P.; Zarrilli, R.; Guaragna, A.; De Gregorio, E. Pyed-1 Inhibits Biofilm Formation and Disrupts the Preformed Biofilm of *Staphylococcus Aureus*. *Antibiotics* **2020**, *9* (5), 1–11. <https://doi.org/10.3390/antibiotics9050240>.
- (25) Jia, P.; Wu, X.; Yu, Y.; Zhang, G. An Efficient One-Pot Synthesis of 5, 9-Cyclo-1, 11-Oxido-Pregn-16-Ene-3, 20-Dione from 9-Bromide-11-Hydroxypregna-1, 4, 16-Trien-3, 20-Dione by Two Annulation Reactions. *Steroids* **2009**, *74* (2), 229–232. <https://doi.org/10.1016/j.steroids.2008.10.018>.
- (26) Jouve, R.; They, V.; Ducki, S.; Helfenbein, J.; Thiery, J.-C.; Job, A.; Picard, E.; Mallet, C.; Ripoche, I.; Bennis, K. Optimization of the Synthesis of a Key Intermediate for the Preparation of Glucocorticoids. *Steroids* **2018**, *137*, 14–21. <https://doi.org/10.1016/j.steroids.2018.06.007>.
- (27) Yao, H.; Richardson, D. E. Epoxidation of Alkenes with Bicarbonate-Activated Hydrogen Peroxide [3]. *J. Am. Chem. Soc.* **2000**, *122* (13), 3220–3221. <https://doi.org/10.1021/ja993935s>.
- (28) Swern, D. Epoxidation and Hydroxylation of Ethylenic Compounds with Organic Peracids. In *Organic Reactions*; John Wiley & Sons, Inc.: Hoboken, NJ, USA, 2011; pp 378–434. <https://doi.org/10.1002/0471264180.or007.07>.
- (29) Kamernitskii, A. V.; Turuta, A. M. Use of 20-Hydrazones as Protecting Groups in the Synthesis of 16,17-Heterocyclic Steroids. *Pharm. Chem. J.* **1992**, *26* (6), 526–536. <https://doi.org/10.1007/BF00773081>.
- (30) De Fenza, M.; D’Alonzo, D.; Esposito, A.; Munari, S.; Loberto, N.; Santangelo, A.; Lampronti, I.; Tamanini, A.; Rossi, A.; Ranucci, S.; De Fino, I.; Bragonzi, A.; Aureli, M.; Bassi, R.; Tironi, M.; Lippi, G.; Gambari, R.; Cabrini, G.; Palumbo, G.; Dececchi, M. C.; Guaragna, A. Exploring the Effect of Chirality on the Therapeutic Potential of N-Alkyl-Deoxyiminosugars: Anti-Inflammatory Response to *Pseudomonas Aeruginosa* Infections for Application in CF Lung Disease. *Eur. J. Med. Chem.* **2019**, *175*, 63–71. <https://doi.org/10.1016/j.ejmech.2019.04.061>.
- (31) Caputo, R.; Cecere, G.; Guaragna, A.; Palumbo, G.; Pedatella, S. β -Amino- α -Hydroxy Esters by Asymmetric Hydroxylation of α -Amino Acid Esters. *European J. Org. Chem.* **2002**, *17*, 3050–3054. [https://doi.org/10.1002/1099-0690\(200209\)2002:17<3050::AID-EJOC3050>3.0.CO;2-1](https://doi.org/10.1002/1099-0690(200209)2002:17<3050::AID-EJOC3050>3.0.CO;2-1).
- (32) Pedatella, S.; Guaragna, A.; D’Alonzo, D.; De Nisco, M.; Palumbo, G. Triphenylphosphine Polymer-Bound/Iodine Complex: A Suitable Reagent for the Preparation of O-Isopropylidene Sugar Derivatives. *Synthesis (Stuttg.)* **2006**, No. 2, 305–308. <https://doi.org/10.1055/s-2005-918521>.
- (33) Tacconelli, E.; Carrara, E.; Savoldi, A.; Harbarth, S.; Mendelson, M.; Monnet, D. L.; Pulcini, C.; Kahlmeter, G.; Kluytmans, J.; Carmeli, Y.; Ouellette, M.; Outtersson, K.; Patel, J.; Cavalieri, M.; Cox, E. M.; Houchens, C. R.; Grayson, M. L.; Hansen, P.; Singh, N.; Theuretzbacher, U.; Magrini, N.; Aboderin, A. O.; Al-Abri, S. S.; Awang Jalil, N.; Benzonana, N.; Bhattacharya, S.; Brink, A. J.; Burkert, F. R.; Cars, O.; Cornaglia, G.; Dyar, O. J.; Friedrich, A. W.; Gales, A. C.; Gandra, S.; Giske, C. G.; Goff, D. A.; Goossens, H.; Gottlieb, T.; Guzman Blanco, M.; Hryniewicz, W.; Kattula, D.; Jinks, T.; Kanj, S. S.; Kerr, L.; Kieny, M. P.; Kim, Y. S.; Kozlov, R. S.; Labarca, J.; Laxminarayan, R.; Leder, K.; Leibovici, L.; Levy-Hara, G.; Littman, J.; Malhotra-Kumar, S.; Manchanda, V.; Moja, L.; Ndoye, B.; Pan, A.; Paterson, D. L.; Paul, M.; Qiu, H.; Ramon-Pardo, P.; Rodríguez-Baño, J.; Sanguinetti, M.; Sengupta, S.; Sharland, M.; Si-Mehand, M.; Silver, L. L.; Song, W.; Steinbakk, M.; Thomsen, J.; Thwaites, G. E.; van der Meer, J. W.; Van Kinh, N.; Vega, S.; Villegas, M. V.; Wechsler-Fördös, A.; Wertheim, H. F. L.; Wesangula, E.; Woodford, N.;

- Yilmaz, F. O.; Zorzet, A. Discovery, Research, and Development of New Antibiotics: The WHO Priority List of Antibiotic-Resistant Bacteria and Tuberculosis. *Lancet Infect. Dis.* **2018**, *18* (3), 318–327. [https://doi.org/10.1016/S1473-3099\(17\)30753-3](https://doi.org/10.1016/S1473-3099(17)30753-3).
- (34) Pane, K.; Cafaro, V.; Avitabile, A.; Torres, M. D. T.; Vollaro, A.; De Gregorio, E.; Catania, M. R.; Di Maro, A.; Bosso, A.; Gallo, G.; Zanfardino, A.; Varcamonti, M.; Pizzo, E.; Di Donato, A.; Lu, T. K.; de la Fuente-Nunez, C.; Notomista, E. Identification of Novel Cryptic Multifunctional Antimicrobial Peptides from the Human Stomach Enabled by a Computational–Experimental Platform. *ACS Synth. Biol.* **2018**, *7* (9), 2105–2115. <https://doi.org/10.1021/acssynbio.8b00084>.
- (35) Ebbensgaard, A.; Mordhorst, H.; Overgaard, M. T.; Aarestrup, F. M.; Hansen, E. B. Dissection of the Antimicrobial and Hemolytic Activity of Cap18: Generation of Cap18 Derivatives with Enhanced Specificity. *PLoS One* **2018**, *13* (5), e0197742. <https://doi.org/10.1371/journal.pone.0197742>.
- (36) Vestergaard, M.; Frees, D.; Ingmer, H. Antibiotic Resistance and the MRSA Problem. *Microbiol. Spectr.* **2019**, *7* (2). <https://doi.org/10.1128/microbiolspec.GPP3-0057-2018>.
- (37) Brooke, J. S. *Stenotrophomonas Maltophilia*: An Emerging Global Opportunistic Pathogen. *Clin. Microbiol. Rev.* **2012**, *25* (1), 2–41. <https://doi.org/10.1128/CMR.00019-11>.
- (38) Jeon, Y. D.; Jeong, W. Y.; Kim, M. H.; Jung, I. Y.; Ahn, M. Y.; Ann, H. W.; Ahn, J. Y.; Han, S. H.; Choi, J. Y.; Song, Y. G.; Kim, J. M.; Ku, N. S. Risk Factors for Mortality in Patients with *Stenotrophomonas Maltophilia* Bacteremia. *Medicine (Baltimore)*. **2016**, *95* (31), e4375. <https://doi.org/10.1097/MD.0000000000004375>.

VIRAL DISEASES



Synthesis of Cyclohexenyl Nucleosides and their ProTide Derivatives as novel Antiviral Agents

Synthesis of Piperidine-based Nucleosides: mimicking the Bioactive Conformation of Immucillin-A

Synthesis of Propargylated Nucleoside Analogues for Visualization of Viral Replication

4 SYNTHESIS OF CYCLOHEXENYL NUCLEOSIDES AND THEIR PROTIDE DERIVATIVES AS NOVEL ANTIVIRAL AGENTS

4.1 INTRODUCTION

Despite the remarkable advancements achieved in antiviral drug discovery with about 90 antiviral drugs formally approved over the past 5 decades,¹ viral diseases still represent a serious threat in the public health. On one hand, hepatitis B (HBV), C (HCV) and the human immunodeficiency virus (HIV), for which antiviral therapies are available, even today cause millions of deaths every year.² On the other hand, an increasing number of emerging or reemerging viral pathogens for which no licensed treatments or vaccines exist, such as Dengue, Zika, Ebola, Chikungunya, West Nile, Yellow fever viruses or the newly emerged coronavirus SARS-CoV-2 responsible for the ongoing COVID-19 pandemic, continue to affect the global health.^{3,4} Therefore, development of novel effective antiviral agents able to inhibit old and new pathogens by preventing their spread worldwide represents a compelling and challenging need.

The aim of antiviral therapy is to achieve substantial and prolonged suppression of viral replication by interfering with the viral life cycle in one of its key events, including viral attachment, fusion/endocytosis, viral DNA/RNA synthesis, viral polyprotein cleavage and viral release from the cells.⁵ In this context, the most successful strategy consists in targeting well-conserved viral proteins mainly by the use of polymerases or protease inhibitors that have been demonstrated to be very effective in the treatment of viral diseases representing the dominant classes of antiviral drugs currently marketed.^{1,3,6-8} Among them, nucleoside analogues (NAs) hold a privileged position and have become cornerstones of treatment of viral infections.⁹⁻¹¹

4.1.1 NUCLEOSIDE ANALOGUES AS ANTIVIRAL AGENTS

NAs are synthetic, chemically modified compounds devised to mimic the structure of the corresponding natural counterparts in order to exploit their cellular metabolism. Because of their structural relationship with natural nucleosides, these biomimetic agents are able to inhibit the replication processes of a wide variety of viral infections by interfering with the corresponding viral life cycles at transcriptional level, and by blocking the information flow enclosed in virus genome.¹² The metabolic pathway of NAs is the same of that exploited by endogenous ones. Once inside the cell, in order to gain pharmacological activity, antiviral NAs require serial phosphorylation, *via* the mono- and the diphosphate intermediates, to the triphosphorylated form. While some viruses (as for example HIV) exploit host kinases to this end, others (among them, herpes viruses) encode their own nucleoside-phosphorylating enzymes especially for the first phosphorylation step. Triphosphate NAs compete with natural nucleotides acting as intracellular enzyme inhibitors, as well as they can be incorporated into newly synthesized viral DNA or RNA

inducing termination of chain elongation (many NAs either are missing or are blocked at the 3'-OH group, resulting in failure of chain elongation of the nascent DNA/RNA, **FIGURE 4.1**),¹³ accumulation of mutations in viral progeny (lethal mutagenesis), or inducing cell apoptosis.^{5,12}

Over the last decades, the effectiveness of NAs as antiviral agents was established with their approval for the treatment of infections caused by human immunodeficiency virus (HIV), hepatitis B and C viruses (HBV and HCV) and human herpes viruses (HHV).⁸ Despite the high efficacy of the currently approved drugs, the development of novel NAs remains a field of study of great interest and several NAs are under preclinical and clinical evaluation. Indeed, there is a growing interest to obtain pharmacological agents endowed with improved properties, including greater selectivity for molecular targets to balance therapeutic efficacy and toxicity, as well as a higher barrier to antiviral resistance.¹²

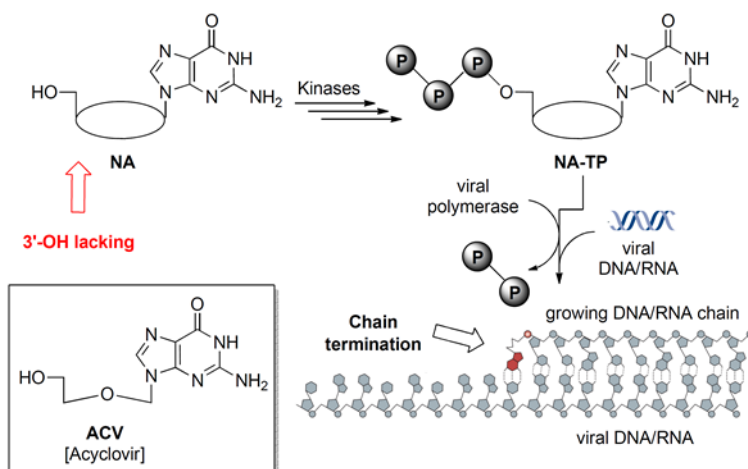


FIGURE 4.1. Anti-HSV drug Acyclovir as example of NA acting as chain terminator.

4.1.2. SUGAR-MODIFIED NUCLEOSIDES

One of the most successful strategies for developing NAs able to act as efficient bioisosters of natural nucleosides is represented by modifications of the sugar moiety.^{11,14}

The changes on the natural furanose unit typically include: elimination of 2' and 3' hydroxyl groups, as in the case of HIV agent Stavudine, change of the configuration of the sugar core (Telbivudine), exchange of substituents, as for example introduction of fluorine atoms (Gemcitabine), replacement of the furanose ring by an acyclic (Ganciclovir), carbocyclic (Abacavir) or heterocyclic ring (Lamivudine) (**FIGURE 4.2**). However, in all these modifications the hydroxymethyl group is preserved being important for biological activity.

Among the sugar-modified NAs mentioned above, carbocyclic nucleosides have received considerable attention over the last years.^{14,15}

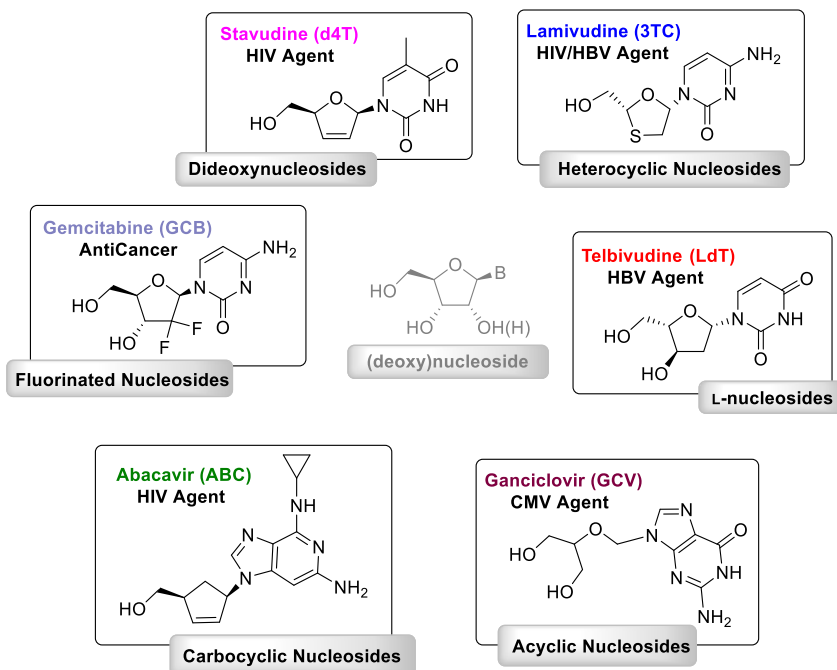


FIGURE 4.2. Sugar-modified nucleosides.

4.1.2.1 CARBOCYCLIC NUCLEOSIDES

The replacement of the oxygen atom of natural nucleosides with a methylene unit makes the carbocyclic nucleosides (also referred as carbanucleosides) an interesting class of biomimetic agents with potent biological activity.^{16,17} Because of the absence of the *N*-glycosidic bond, the resulting molecules possess high chemical and metabolic stability (they are very resistant to phosphorylases and hydrolases).^{18,19} However, the expected similarity in bond lengths and bond angles of tetrahydrofuran and cyclopentane rings, still allows the recognition of these analogues by target enzymes (i.e. kinases and polymerases) acting as their substrates or inhibitors. Furthermore, the increasing lipophilicity, as known, has a crucial role in to improve the pharmacokinetic and pharmacodynamic properties of the corresponding compounds.²⁰

Therapeutic potential of carbanucleosides was highlighted for the first time in 1966 when the natural occurring carbocyclic nucleosides Aristeomycin and Neplanocin A (FIGURE 4.3) revealed antibiotic and antitumor activity.¹⁴

Since then the research on this class of NAs has been subject of intense efforts and other synthetic nucleosides with important therapeutic application were discovered as demonstrated by the anti-HIV drug Abacavir (ABC) or by Entecavir (ETV), a guanosine analogue, approved by FDA in 2005 for oral treatment of HBV (FIGURE 4.3).

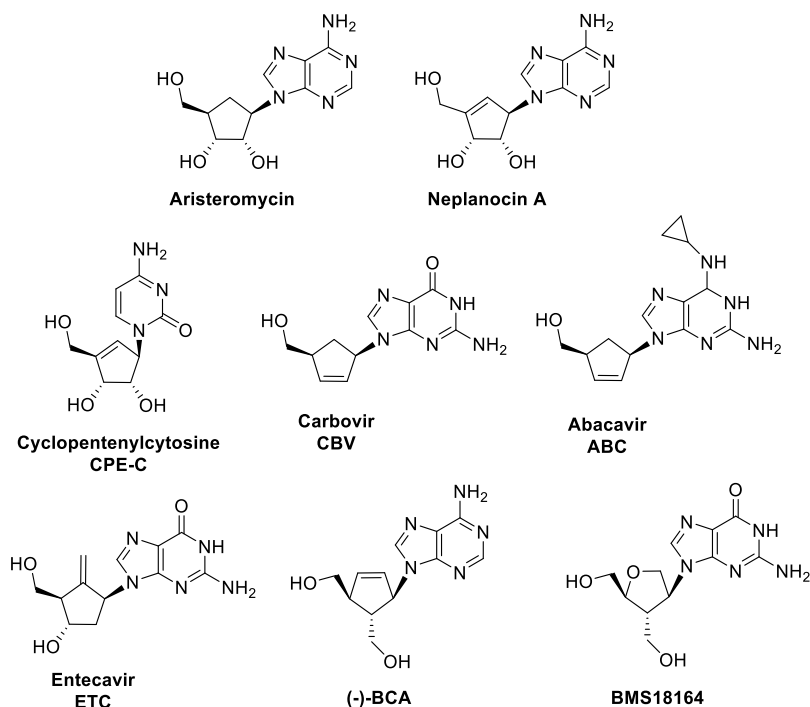


FIGURE 4.3. Chemical structures of carbanucleosides displaying anti-infective and antitumor activity.

4.1.2.2 BRIEF OVERVIEW ON THE SYNTHETIC APPROACHES FOR THE SYNTHESIS OF CARBOCYCLIC NUCLEOSIDES

Due to the biological relevance of carbanucleosides, over the years great attention has been devoted to the development of synthetic methodologies aimed at their preparation. As shown in **FIGURE 4.4**, carbanucleosides can be prepared mainly by two approaches: *linear* synthesis or *convergent* insertion of the nucleobase on a functionalized carbocyclic ring.^{18,21}

- 1) *Linear synthesis*: the nucleobase is literally constructed on the carbocyclic pseudo sugar moiety properly functionalized with exocyclic amino group, which becomes the N9 of a purine or the N1 of a pyrimidine.
- 2) *Convergent synthesis*: the direct coupling of the nucleobase with the carbocyclic pseudo sugar can be accomplished by several methods.²¹ Among the most common methods, the Mitsunobu conditions are largely used; the reaction leads to the substitution of alcohols with acidic nucleophiles in the presence of diethyl azodicarboxylate (DEAD) and triphenylphosphine (**SCHEME 4.1a**). As known, the reaction occurs reversing the configuration of the carbon atom directly involved in the substitution.

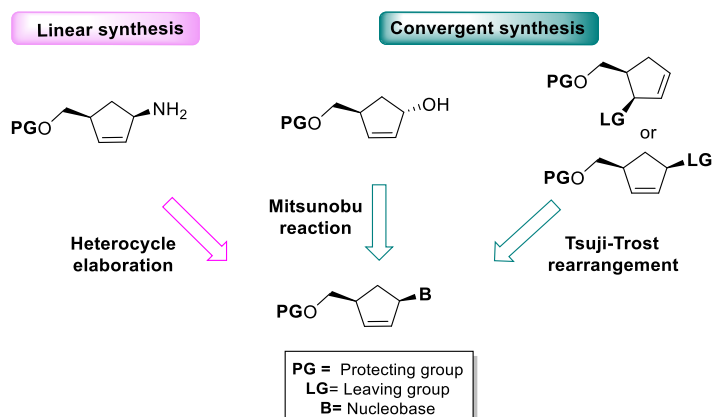
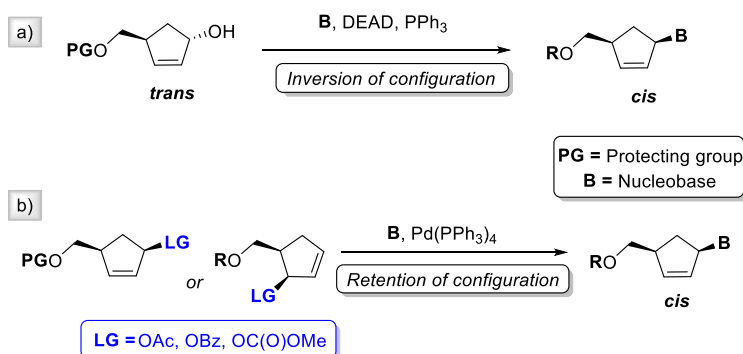


FIGURE 4.4. Main synthetic approaches to prepare carbanucleosides.

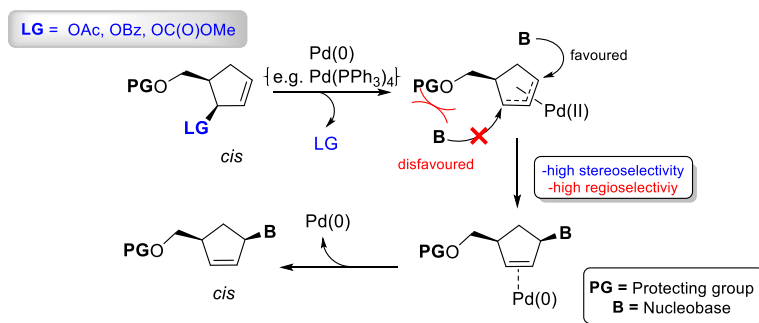
Another strategy for the convergent synthesis of carbocyclic nucleosides is the palladium catalysed substitution of allylic esters or carbonates^{22–25} (also known as Tsuji–Trost reaction, **SCHEME 4.1b**). Over the years, Tsuji–Trost reaction has become one of the most popular method to introduce nucleobases on carbocyclic structures to prepare bioactive carbocyclic nucleosides^{19,26,27} (including the anti-HIV drug Abacavir).



SCHEME 4.1. Synthesis of *cis*-carbanucleosides by (a) Mitsunobu reaction and (b) Tsuji–Trost reaction.

The efficiency of this method relies on its high selectivity in terms of stereo- and regioselectivity. As widely reported for cyclopentenyl substrates¹⁸ (**SCHEME 4.2**), the reaction relies on the treatment of allylic esters or carbonates with a bulky Pd(0) catalyst [such as tetrakis-triphenylphosphine palladium, Pd(PPh₃)₄] to generate an intermediate η^3 -allyl palladium(II) complex by ionization of the leaving group. The complex then undergoes nucleophilic attack by a nucleobase to the less hindered carbon atom, to give access to the corresponding S_N2' product, still in the form of an unstable η^2 -allyl complex; final decomplexation releases the corresponding

cyclopentenyl nucleoside. Since the process involves a double inversion of configuration, both in the formation of the η^3 -complex and in the subsequent substitution stage, the reaction overall proceeds with retention of configuration, providing *cis* nucleosides from *cis* esters/carbonates while their *trans*-isomers lead to the formation of *trans*-products.^{21,28}



SCHEME 4.2. Reaction mechanism of Tsuji–Trost reaction.

4.1.2.3 CYCLOHEXENYL NUCLEOSIDES

Even though cyclopentenyl nucleosides have demonstrated to be the most successful among carbanucleosides, as exemplified by the approved drug Abacavir (ABC) or by Entecavir (ETV) (FIGURE 4.3), the replacement of the five-membered ring with a cyclohexene moiety led to NAs endowed with interesting antiviral properties. The interesting pharmacological potential of cyclohexenyl nucleosides is due to the ability by cyclohexenyl ring to act as an efficient bioisostere of the natural furanose unit.²⁹ Indeed, a cyclohexene ring mainly exists in two half-chair forms (³H₂ and ²H₃), closely mimicking the ³T₂ and ²T₃ sugar ring puckers of natural counterparts (*North* and *South* conformation). Moreover, the energy jump required for the conformational change ³H₂ ⇌ ²H₃ is even lower³⁰ (ΔG ~ 10 kJ/mol) than that involving the ²T₃ ⇌ ³T₂ interconversion (ΔG ~ 20 kJ/mol; FIGURE 4.5). This feature of the cyclohexenyl ring results in a great potential of these systems in terms of biological activity. Indeed, it was established that the two enzymes involved into the biochemical path leading to NA incorporation into a nucleic acid, *i.e.* kinases and polymerases (viral or cellular) recognized natural nucleosides and their analogues in a specific conformation. Particularly, while the first seems to prefer a nucleoside in a *S* conformation, the second requires a nucleotide in a *N* form.³¹ Accordingly, being able to resemble both the *N* and *S* sugar ring puckers of natural nucleoside, cyclohexenyl nucleosides may act as suitable substrates for both kinases and polymerases.

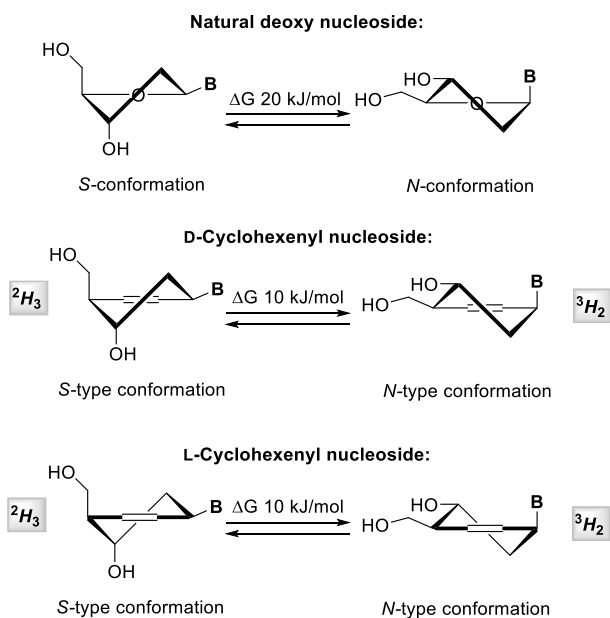
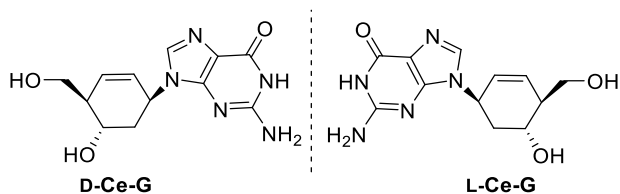


FIGURE 4.5. Conformational equilibria of furanosyl and cyclohexenyl nucleosides.

Cyclohexenyl nucleosides were evaluated against a broad range of human infections: in particular, both D- and L-enantiomers of cyclohexenyl-guanine exhibited potent and selective antiviral activity against HSV-1 and 2, VZV and CMV, comparable to that of the well-known antiviral drugs acyclovir and ganciclovir³⁰ (**FIGURE 4.6**). These results highlighted the great potential of carbocyclic NAs bearing six-membered moiety to act as antiviral agents inspiring further studies in search of other derivatives endowed with even higher therapeutic activity.



Virus	Activity (IC ₅₀ , µg/mL)			
	D-Ce-G	L-Ce-G	Acyclovir	Ganciclovir
HSV-1	0.002 - 0.004	0.003 - 0.004	0.003 - 0.07	0.001 - 0.01
HSV-2	0.05 - 0.07	0.007 - 0.1	0.02	0.002 - 0.001
VZV	0.41 - 2.8	1.2 - 6.8	0.8 - 28	ND
CMV	0.8 - 0.6	1.7 - 1.5	ND	0.8 - 0.6

FIGURE 4.6. D- and L-cyclohexenyl guanine as anti-HHV agents.

4.1.3 FROM NUCLEOSIDE ANALOGUES TO THEIR PRODRUGS: THE PROTIDE APPROACH

As described above, in order to exert their pharmacological activity, NAs require intracellular phosphorylation by viral/cellular kinase via three consecutive phosphorylations with the first one being usually the rate-limiting step.³² The low or inefficient *in vivo* phosphorylation of NAs, that can occur when the virus either does not express a specific kinase or develop resistance toward the compound by enzyme mutations while the human cell fails to secure phosphorylation, often has limited the therapeutic potential of many NAs.³³ To overcome this issue and improve therapeutic properties, nucleosides with a phosphate group already present in the structure have been designed. Even though nucleoside 5'-monophosphates bypass the slow first phosphorylation step, their direct administration results in low cellular permeability and poor *in vivo* stability, and therefore, numerous prodrug technologies have been developed.³⁴ The rationale behind the design of such agents is to achieve temporary masking of the free phosphoric group until absorption and delivery of NAs, allowing the *in vivo* release of the active drug only once at the target site.³² Once inside the cell, NA monophosphates undergo a demasking step to release their monophosphates derivatives, which are subsequently further phosphorylated to generate the active triphosphate species (FIGURE 4.7).

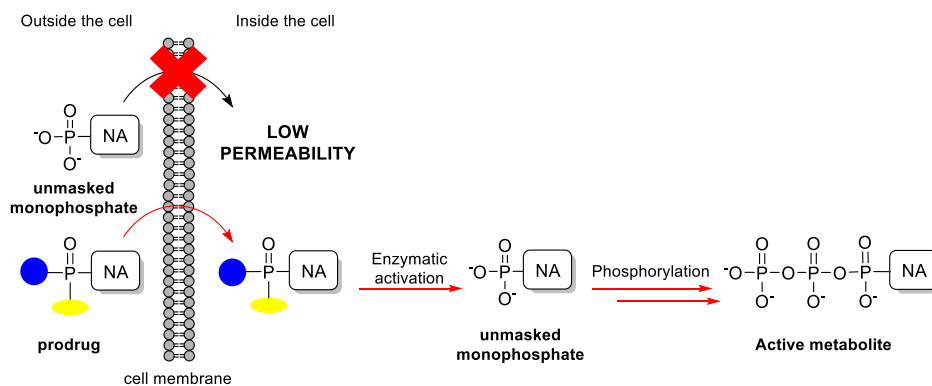


FIGURE 4.7. Mechanism of action of nucleoside monophosphate prodrugs.

Among the prodrug approaches, the most successful one is the ProTide technology, pioneered by McGuigan³⁵ almost 25 years ago, which has proved to be a powerful tool in the discovery of efficacious nucleoside monophosphate prodrug therapeutics against HIV, HBV, HCV and Ebola virus.³³

A ProTide (PROdrug + nucleoTIDE) (FIGURE 4.8) is a nucleoside aryl phosphate or phosphonate masked with an amino acid ester moiety linked via P-N bond. Phenyl and 1-naphthyl are commonly used as aryl components while L-alanine was proven to be the preferred amino acid being featured in all the ProTides entered into the clinic.³⁶

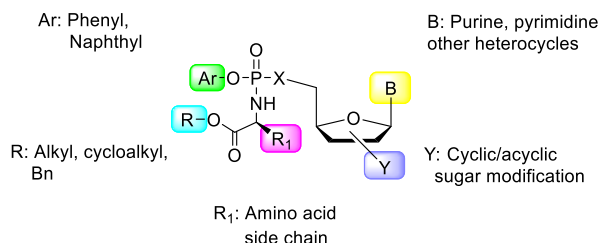


FIGURE 4.8 General structure of ProTide scaffold.

Nowadays, ProTide technology is recognized as a prodrug strategy with proven capacity to generate new drug candidates for nucleoside-based antiviral therapies. This approach not only has produced nucleosides endowed with enhanced activity compared with the parent ones, but often has generated potent compounds otherwise inactive in their nucleoside form, essentially due to the failure of the first step in the phosphorylation process.^{37,38} The effectiveness of ProTide technology was confirmed by discovery of agents that are currently in clinical use as the FDA approved Sofosbuvir (Sovaldi[®], FIGURE 4.9) marketed for the treatment of HCV³⁹ and the anti-HIV and anti-HBV drug Tenofovir Alafenamide⁴⁰ (TAF, Vemlidy[®], FIGURE 4.9).

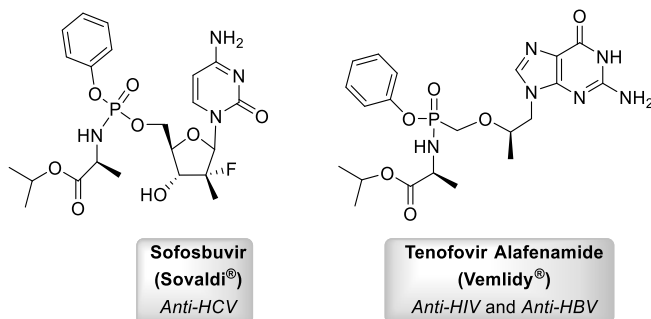


FIGURE 4.9. Chemical structures of two FDA-approved antiviral ProTides.

Once inside the cell, ProTides require to be processed in order to release the nucleoside monophosphate. The activation pathway of the ProTides of NAs containing different amino acids and ester moieties has been investigated for a long time. The metabolic conversion process is believed to be mediated by two-step enzymatic process, which eventually release the active monophosphate form of the parent nucleoside.³³ The first step (FIGURE 4.10) involves the cleavage of the amino acid ester by intracellular esterase (with Cathepsin A, identified as the major esterase acting at this step) leading to intermediate A. Under physiological pH (<7.4), the unmasked and negatively charged carboxyl group give a nucleophilic attack on the phosphate group, leading to the loss of the aryl motif and the formation of a highly unstable five-membered ring (metabolite B, FIGURE 4.10). Metabolite B formation is followed by a rapid nucleophilic attack by a water molecule on the phosphate (option 1, FIGURE 4.10) or on the carbon of the

carbonyl group of the amino acid (option 2, **FIGURE 4.10**) to open up the ring and to generate the phosphoramidate metabolite (metabolite C, **FIGURE 4.10**). The final step in the metabolism of the ProTides is the cleavage of the P–N bond by a second enzyme known as phosphoramidase-type enzyme (Histidine Triad Nucleotide Binding Protein, HINT1). This step leads to the release of the nucleoside monophosphate that will be further phosphorylated to its di- and triphosphate forms to exert its pharmacological effect by competing with natural nucleosides.

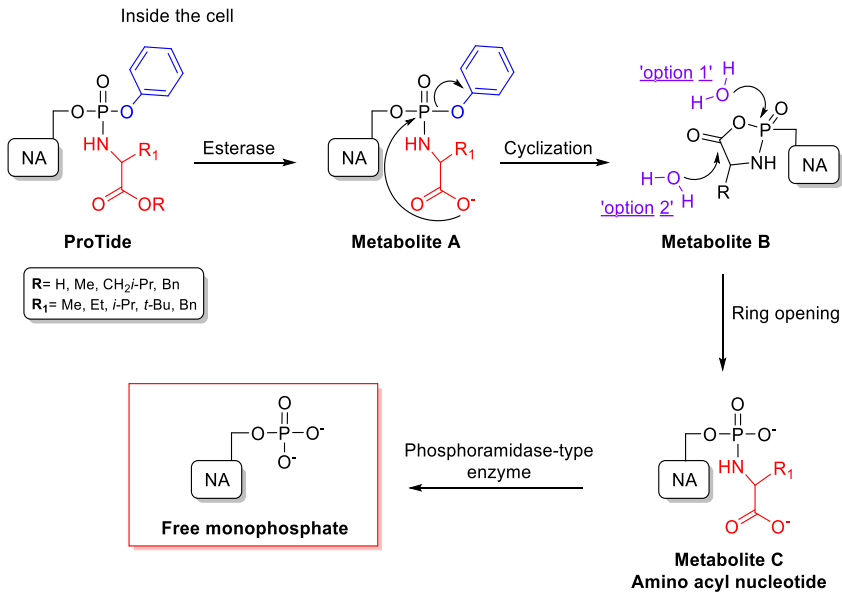


FIGURE 4.10. Postulated mechanism of phosphoramidate activation.

4.2 RESULTS AND DISCUSSION

Based on the promising biological potential exhibited by D- and L-cyclohexenyl nucleosides, a synthetic route aimed at the preparation of novel cyclohexenyl nucleosides in both their enantiomeric forms (D- and L-CeNAs, **FIGURE 4.11a**) was herein explored.⁴¹ Pharmacological potential of these compounds is due to the capacity of the cyclohexenyl ring to act as a conformational bioisostere of natural deoxyribose.^{29,42} Indeed, the flexible nature of cyclohexenyl nucleosides, rapidly fluctuating between the low energy 2H_3 and 3H_2 conformations, enables a close resemblance with the bioactive sugar ring puckers (2T_3 and 3T_2) of natural nucleosides (**FIGURE 4.11a**) and thus resulting suitable substrates either for kinases and polymerases. In addition, compared with the previously reported examples of cyclohexenyl NAs,^{30,43} the lack of *sec*-OH group at C5' position highlights potential therapeutic application of these nucleosides as chain terminators.^{13,14}

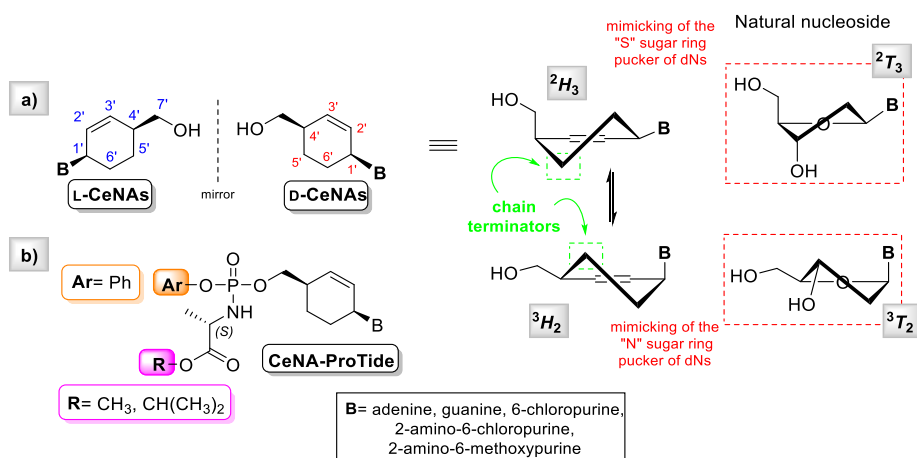


FIGURE 4.11. a) CeNAs as conformational mimetics of natural nucleosides.
b) Application of ProTide Technology to CeNAs.

Different CeNA derivatives bearing pyrimidine nucleobases were herein synthesized (**FIGURE 4.11a**) along with early examples of their corresponding ProTides (**FIGURE 4.11b**) with the aim to explore the potential of this technology applied to our nucleosides in terms of biological activity.

Access to CeNAs, in both their enantiomeric forms, was devised through a highly regio- and stereoselective approach starting from the inexpensive cyclohexanone **54** and exploiting the Tsuji-Trost reaction of carbonate **55** for the insertion of nucleobase on the cyclohexenyl moiety (**FIGURE 4.12**).

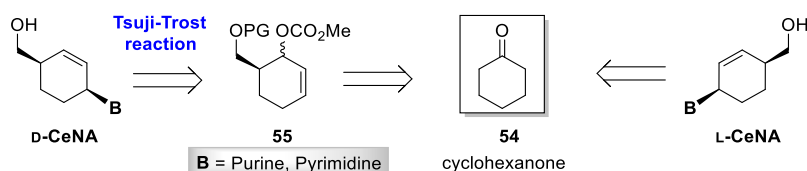


FIGURE 4.12. Synthesis of D- and L-CeNAs

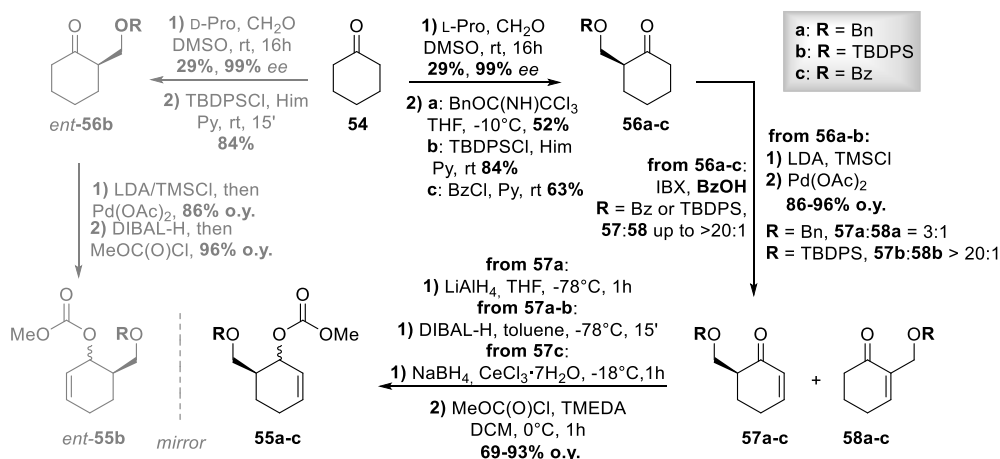
Contrarily to the widely accepted mechanism (see paragraph 4.1.2.2), an unprecedented stereoconvergent reaction outcome was herein observed, leading us to further explore this unexpected behavior by DFT studies.

Preliminary biological evaluation of synthesized nucleosides was also provided in order to assess their antiviral properties against DNA and RNA viruses.

4.2.1 SYNTHESIS OF D- AND L-CYCLOHEXENYL NUCLEOSIDES

4.2.1.1 ENANTIOSELECTIVE SYNTHESIS OF THE CYCLOHEXENYL MOIETY

The synthesis of cyclohexenyl moiety started with the organocatalyzed hydroxymethylation of commercial cyclohexanone (SCHEME 4.2), enabling the introduction of the first chiral centre which will determine the steric series of the target cyclohexenyl nucleoside. L-Proline (10%) was employed to catalyze aldol condensation between **54** and formaldehyde, leading to, after protection of the resulting alcohol (**56a**: BnOC(NH)CCl₃/TfOH; **56b**: TBDPSCI/imidazole; **56c**: BzCl/Py), ketone **56** with the appropriate *S* configuration at the C2 stereocentre (required for the synthesis of D-CeNAs).⁴⁴ Access to α,β -unsaturated carbonyl compounds **57a-c** was accomplished, at first, by Saegusa dehydrogenation of ketones **56a-b** [LDA/TMSCl, then Pd(OAc)₂] (SCHEME 4.3).


 SCHEME 4.3. Synthesis of carbonates **55a-c** and *ent*-**55a-c**.

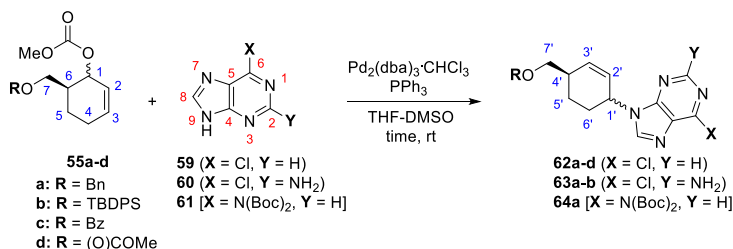
Parallel to the two-steps dehydrogenation protocol, the direct conversion of ketones **56a-c** into cyclohexenones **57a-c** with 2-iodoxybenzoic acid (IBX)⁴⁵ was also explored. In this case, we found that, while the reaction provided a mixture of unsaturated ketones **57** and **58** (e.g. **57a:58a** up to 3:1), the addition of 1 eq benzoic acid (BzOH) significantly improved the reaction regioselectivity toward the desired **57** (e.g., **57c:58c** > 20:1; 69% yield).⁴¹

Optically active cyclohexenones **57a-c** were then converted into corresponding carbonates **55a-c**, which represented the suitable starting materials for the subsequent Tsuji-Trost reaction. Carbonyl group reduction of benzyl ether **57a** using LiAlH₄ as the reducing agent followed by protection of the resulting allylic alcohol [MeOC(O)Cl/TMEDA] yielded *trans*-**55a** as the main product (86%; *cis:trans* = 1:10). Conversely, reduction with DIBAL-H (from **57a-b**) or NaBH₄/CeCl₃ (from **57c**) and subsequent protection gave a 1:1 mixture of *cis*- and *trans*-**55a-c** (69-93%). The same synthetic path described in SCHEME 4.3, using D-Proline as chiral catalyst in the first step of the synthesis, allowed the preparation of carbonates *ent*-**55b**.

4.2.1.2 NUCLEOSIDE SYNTHESIS: TSUJI-TROST REACTION

Nucleoside synthesis was then approached exploiting the well-known Tsuji-Trost reaction (TABLE 4.1). As described in the previous section for cyclopentenyl substrates, this reaction relies on the use of allylic esters or carbonates, which are treated with a bulky Pd(0) catalyst [such as tetrakis-triphenylphosphine palladium, Pd(PPh₃)₄].^{18,26,27,46} As the stereoselectivity of reaction, in presence of soft nucleophiles, is known to occur with a net retention of configuration, among the two carbonates *cis*- and *trans*-**55**, only the *cis* isomer was at first considered of synthetic utility for our aims. Treatment of *cis*-**55a** with 6-chloropurine (**59**), Pd₂(dba)₃CHCl₃ (0.1 eq) and PPh₃ (1.0 eq) in a 1:1 THF/DMSO mixture provided, after 1h at rt, the expected nucleoside *cis*-**62a** (entry 1), whose relative configuration was assessed by ¹H NMR analysis (*J*_{1'-6'a} = 2 Hz; *J*_{1'-6'b} = 4 Hz), along with its N7 regioisomer²⁸ (N9:N7 = 2:1). Surprisingly, when the same reaction was carried out starting from *trans*-**55a**, the formation of *cis*-**62a** was again observed (entry 2), while only traces of the corresponding *trans* nucleoside were detected⁴⁷ (*cis:trans* > 10:1). Same results, in terms of stereochemical outcome, were obtained with different nucleobases *i.e.* 2-amino-6-chloropurine (**60**, entries 7 and 8) or with N6-*bis*-Boc-adenine (**61**, entry 10). As expected, in the latter case a much higher stereo- and regioselectivity was found (*cis:trans* > 20:1; N9:N7 = 95:5). When the inseparable mixture of TBDPS ethers *cis/trans*-**55b** was used as the starting material, a similar stereochemical outcome for the reaction was again observed, providing *cis*- nucleosides (entries 3 and 9) as the sole N9 stereoisomers, albeit with different conversion rates (from *trans*-**55b**: 20h; from *cis*-**55b**: 1h). In presence of ester and carbonate groups on C7 position (**55c** and **55d**), the same reactivity profile was observed for *cis* isomer (entries 4 and 6) while *trans*- isomers were recovered unreacted from the reaction mixture. In this case, a complete conversion to *cis* nucleoside could be observed only when a stoichiometric amount of Pd₂(dba)₃ was added (entry 5).

Table 4.1. Pd-catalyzed allylic substitution reaction of carbonates *cis*- and *trans*-**55a-d**.
The table was reproduced with the permission from Ref 41.



Entry	Carbonate	Nucleobase	Nucleoside	t(h)	Yield ^a (%)	<i>cis:trans</i>	N9:N7
1	<i>cis</i> - 55a	59	62a	1	90 (60) ^b	>20:1	2:1
2	<i>trans</i> - 55a	59	62a	1	83 (66) ^b	>10:1	4:1
3	<i>cis/trans</i> - 55b	59	62b	20	76 (65) ^b	>20:1	6:1
4	<i>cis</i> - 55c	59	62c	1	69 (55) ^b	>20:1	4:1
5	<i>trans</i> - 55c ^c	59	62c	2	76 (57) ^b	>10:1	3:1
6	<i>cis/trans</i> - 55d ^c	59	62d	2	82 (68) ^b	>20:1	5:1
7	<i>cis</i> - 55a	60	63a	1	97 (73) ^b	>20:1	3:1
8	<i>trans</i> - 55a	60	63a	1	98 (70) ^b	>10:1	2.5:1
9	<i>cis/trans</i> - 55b	60	63b	20	83 (69) ^b	>20:1	5:1
10	<i>trans</i> - 55a	61	64a	1	78 ^b	>20:1	>95:5

General reaction conditions (unless otherwise stated): nucleobase, 1.0 eq; Pd₂(dba)₃, 0.1 eq (corresponding to 0.2 eq of Pd(0) active catalyst); PPh₃, 1.0 eq.

[a] Sum of regioisomeric N9 and N7 nucleosides. [b] Sum of *cis* and *trans* N9 nucleosides.

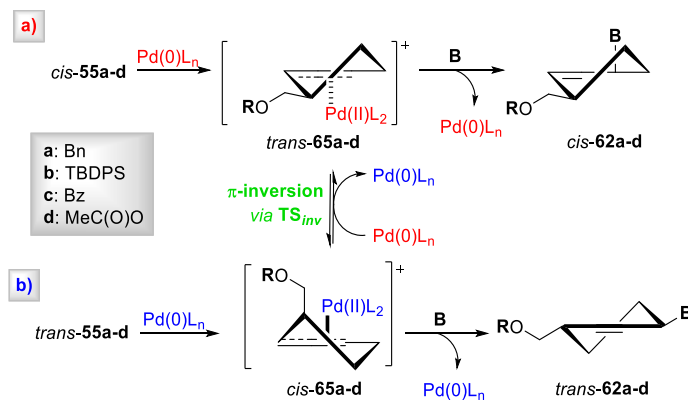
[c] Reaction performed with 0.5 eq of Pd₂(dba)₃, corresponding to 1 eq of Pd(0) active catalyst.

The data herein reported revealed an unexpected stereoconvergent outcome of the Tsuji-Trost reaction.⁴ Indeed, to the best of our knowledge, this unusual behaviour was only observed for sterically hindered substrates⁴⁸ and therefore a reconsideration of the reaction mechanism was needed to explain our data.

As widely reported,^{22,23,25} the treatment of *cis*-**55** with Pd(PPh₃)₄ is expected to provide the (η^3 -cyclohexenyl)palladium(II) complex *trans*-**65** (SCHEME 4.4a), leading to *cis*-**62** after nucleobase attack. To explain the stereoconvergent outcome herein observed, we hypothesize that, even though *trans*-**55** could be similarly converted into the η^3 -complex *cis*-**65**, the latter, rather than

⁴ In a few cases, loss of stereospecificity under specific reaction conditions has been observed on both cyclic and acyclic compounds, see: B.M. Trost, T.R. Verhoeven, *J. Am. Chem. Soc.* **1980**, *14*, 4730-4743.

giving nucleoside *trans*-62, was isomerized to *trans*-65 by the well-known Pd-catalyzed π -inversion,^{46,49} thus providing nucleoside *cis*-62 (SCHEME 4.4b).



Scheme 4.4. Stereoconvergent Tsuji-Trost reaction of *cis*- and *trans*-55: a mechanistic hypothesis. The figure was reproduced with the permission from Ref. 41.

The origin of the reaction stereoselectivity was explored by DFT calculations (studies performed by Prof. G. Talarico, Dept. of Chemical Sciences, University of Napoli) using the Bn-containing carbonate **55a** as model substrate. The calculated free energy profile for the Pd-catalyzed reaction of *cis*- and *trans*-55a is shown in **FIGURE 4.13**.

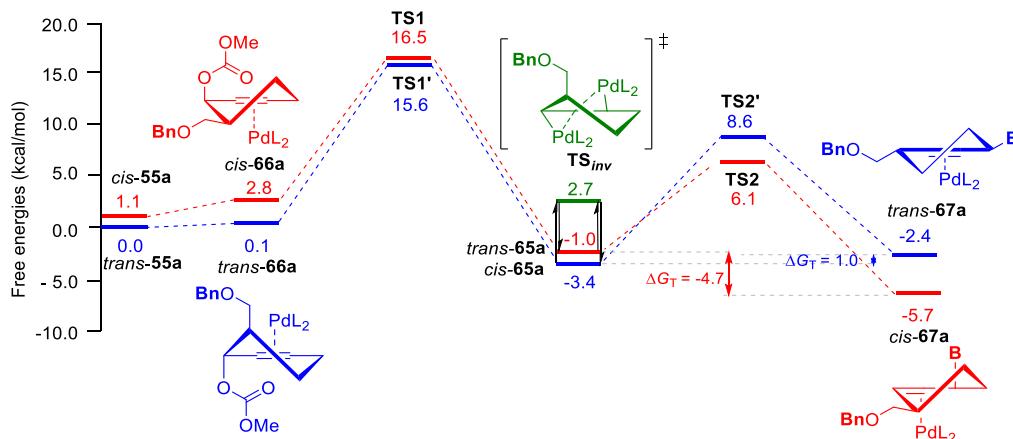


FIGURE 4.13. Free energies for the Tsuji-Trost reaction of *cis*- and *trans*-55a.

The figure was reproduced with the permission from Ref 41.

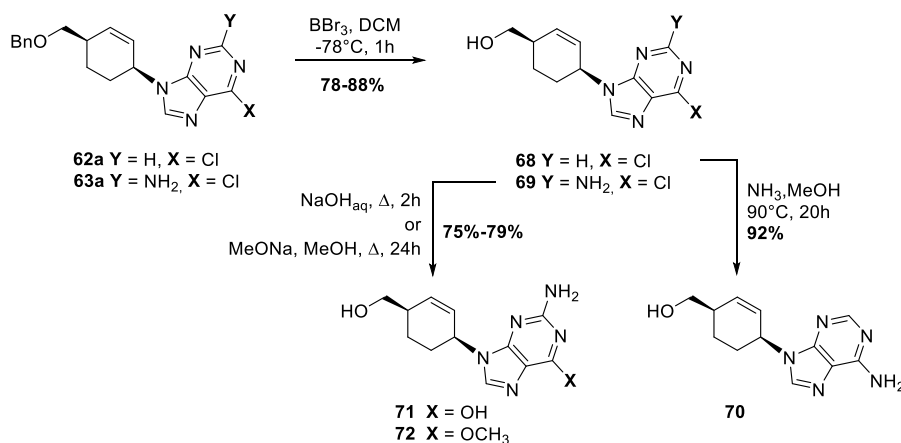
As shown in the calculated free energy profile of the Pd-catalyzed reaction of *cis*- and *trans*-55a (**FIGURE 4.13**), the formation of η^3 complexes *cis*- and *trans*-65 was found to represent, in both cases, the rate-limiting step. In addition, the conversion of *cis*-65 into its *trans*-isomer by the

Pd-catalyzed π -inversion required a low activation energy (6.1 kcal/mol; via TS_{inv}). Based on this fast equilibrium, the conversion of *cis*- and *trans*-**55a** into *cis*-**67a** appears to be favored by both kinetic and thermodynamic factors. On one hand, the $\text{S}_{\text{N}}2'$ substitution of *trans*-**65a** leading to *cis*-**67a** (via TS_2) is associated to an activation energy of 7.1 kcal/mol, whereas a higher value (12.0 kcal/mol) is necessary to convert *cis*-**65a** into *trans*-**67a** (via TS_2'). On the other hand, the formation of *cis*-**67a** was favored by the thermodynamics ($\Delta G_{\text{T}} = -4.7$ kcal/mol), which is against the transformation *cis*-**65a** \rightarrow *trans*-**67a** ($\Delta G_{\text{T}} = +1.0$ kcal/mol).

The results of **TABLE 4.1** also suggest that, the nature of the protective group at C7 position influence the reactivity of *trans*-**55** in the Tsuji-Trost reaction. In the presence of ether groups (e.g. in **55a-b**), the relative reaction rates of *trans* isomers depend on the steric hindrance of the protective group (the bulkier TBDPS group affecting the reactivity of *trans*-**55b**, compared to the faster reaction with Bn-protected *trans*-**55a**). Conversely, the peculiar reactivity of *trans*-**55c-d** bearing carbonyl-containing protective groups suggest the occurrence of other than steric effects. In this case, a plausible hypothesis involves catalyst sequestration by the reaction product that would remove the catalyst from the reaction medium, thereby requiring the use of stoichiometric amounts (1.0 eq) of $\text{Pd}(\text{PPh}_3)_4$ to bring the reaction to completion.

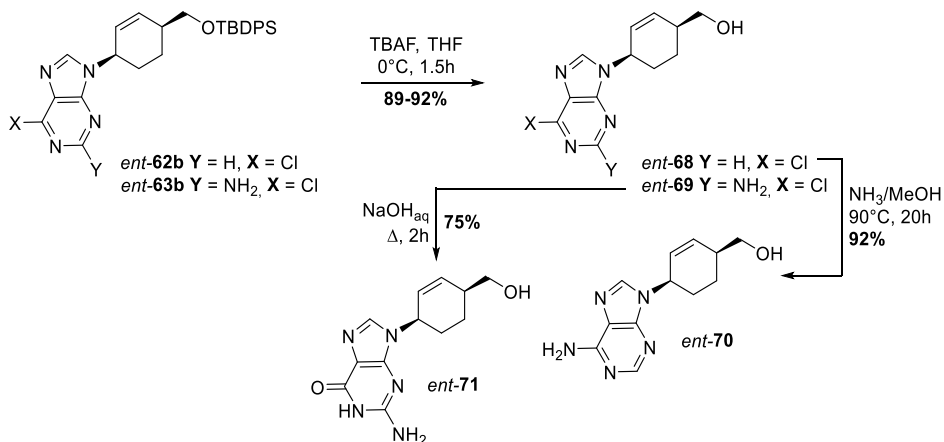
With the protected nucleosides **62a-63a** in hand, synthesis of the corresponding D-nucleoside analogues **70-72** was eventually accomplished in a straightforward way (**SCHEME 4.5**). De-*O*-benzylation was at first considered: while use of BCl_3 was ineffective, treatment of **62a** and **63a** with BBr_3 provided **68** and **69** (78 and 88% yield).

Displacement of chlorine atom of **68** with a free amino group (NH_3/MeOH) or with a methoxy group (MeONa/MeOH) led to nucleosides **70** (92% yield) and **72** (79% yield) respectively, while alkaline hydrolysis (NaOH) of **69** provided nucleoside **71** in 75% yield.



SCHEME 4.5. Synthesis of cyclohexenyl nucleosides **70-72**.

A similar reaction path (SCHEME 4.6), conducted on *ent*-62b and *ent*-63b, led to the corresponding enantiomeric nucleosides *ent*-70 and *ent*-71.



SCHEME 4.6. Synthesis of cyclohexenyl nucleosides 70-71.

4.2.2 SYNTHESIS OF CYCLOHEXENYL NUCLEOSIDE PROTIDES

ProTide technology was then applied to the synthesized cyclohexenyl nucleosides, in order to obtain the corresponding aryloxy phosphoramidates and to evaluate its effect on the biological properties. Indeed, as reported in the previous section, this technology is recognized as a prodrug strategy with proven capacity to generate effective drug candidates for nucleoside-based antiviral therapies, being able to enhance activity of parent nucleosides or to generate potent compounds otherwise inactive in their nucleoside form.³⁴

ProTide approach is aimed to the intracellular delivery of NA monophosphate by masking negative charges of phosphate group by an aryloxy group and an amino acid alkyl ester moiety, in order to overcome limitations and key resistance mechanism, usually associated with NAs, as poor cellular uptake and/or poor conversion to 5'-monophosphate form.³⁵ In this context, the accurate choice of the amino acid function and aryloxy group represented an important issue. Indeed, efficiency of this technology in intracellular delivery of monophosphate nucleoside is closely related to individual components of the phosphoramidate core.³³ Particularly, while aryloxy group is correlated with lipophilicity and consequently to cellular uptake of the prodrug,⁵⁰ on the other hand, amino acid moiety is crucial for its metabolic activation. In this context, phenyl group represents the mostly used aryl motif, although naphthyl group has been also employed, while L-alanine was found to be the preferred amino acid. In addition, earlier works on this topic⁵⁰ indicated that the rate of ester hydrolysis is an influencing factor in the biological activity of the ProTide and that it is closely related to the structure of the ester moiety itself: small esters like methyl, ethyl, isopropyl are processed by esterase faster than those bearing bulky esters.³³

Based on these data and on the structures of ProTides that have reached the clinic,^{36,37} phenol and L-alanine methyl and isopropyl ester were herein chosen, as aryloxy and amino acid groups respectively, to prepare early examples of CeNA ProTides considering nucleosides **69**, **71**, **72** for preliminary studies (FIGURE 4.14).

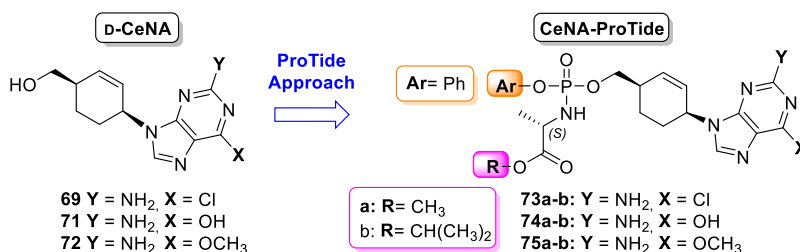
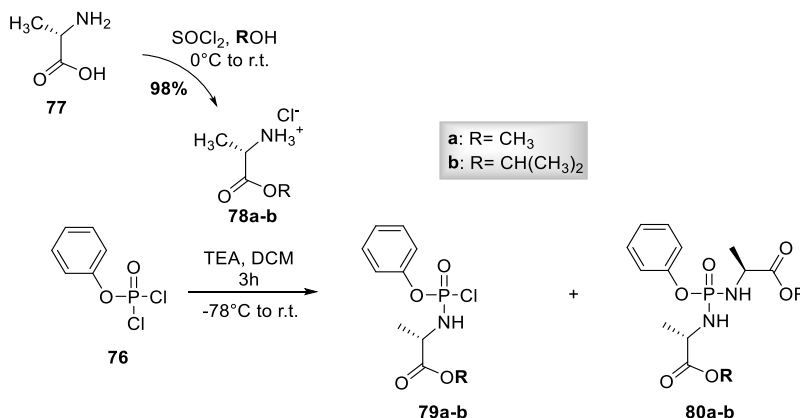


FIGURE 4.14 Aryloxy and amino acid ester motif chosen for CeNA ProTides.

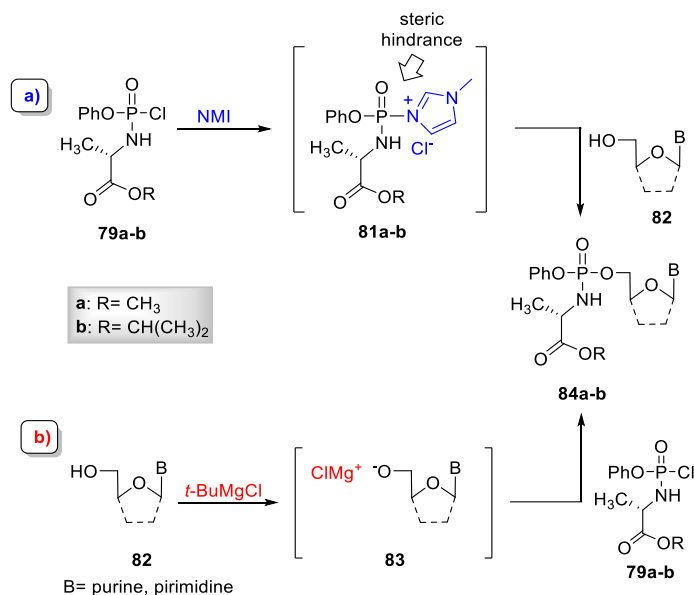
Access to CeNA ProTides was herein performed by the most common synthetic strategy used for the preparation of aryloxy phosphoramidates, consisting in the coupling reaction of the nucleoside with a phosphorochloridate reagent in presence of a suitable base.^{32,34}

As depicted in SCHEME 4.7, preparation of phosphorylating agent (**79a-b**) involved the use of the commercially available phenyl dichlorophosphate (**76**) and of the appropriate L-alanine alkyl ester HCl salt (**78a-b**), in turn prepared through esterification of L-alanine (**77**) by treatment with thionyl chloride in presence of the corresponding alcohol. Condensation reaction of L-alanine alkyl esters (**78a-b**) with commercially available phenyl dichlorophosphate **76** was accomplished in presence of TEA, at -78 °C, leading to the phosphorochloridate reagents **79a-b**, obtained as a pair of diastereoisomers at the phosphorus center, along with undesired bis-functionalized products **80a-b** whose formation was due to the dielectrophilic nature of **76**.



SCHEME 4.7 Preparation of phosphorochloridate reagent.

With phosphorochloridate **79a-b** in hand, synthesis of phosphoramidates was eventually performed by reaction with nucleosides in presence of a suitable base. To this purpose, *N*-methylimidazole (NMI) and the Grignard reagent, *tert*-butyl magnesium chloride (*t*-BuMgCl), are usually employed (SCHEME 4.8). The choice of the base is substrate-dependent³⁴ and is closely related to the presence of other free hydroxyl groups on sugar moiety that could couple to phosphorochloridate reagent. As exemplified in SCHEME 4.8, coupling reaction mediated by NMI enables the selective phosphorylation of the primary hydroxyl group at 5'-position of the nucleoside **82**, thanks to the steric hindrance of the imidazolium intermediate **81** (SCHEME 4.8a). On the other hand, if the nucleoside has only one hydroxyl group, the base of choice is *t*-BuMgCl which gives higher yields compared to NMI. In presence of the Grignard reagent, abstraction of 5' proton on the nucleoside gives the corresponding magnesium alkoxide **83**, which is phosphorylated by reaction with phosphorylating agent **79a-b** (SCHEME 4.8b). This last is a chemoselective method by Uchiyama,⁵¹ based on *O*-selective phosphorylation of nucleoside also in presence of free amino function on the nucleobase. The use of *t*-BuMgCl generates an equilibrium mixture of the magnesium alkoxide and amide: predominance of *O*- and *N*-phosphorylation is based on the equilibrium concentration of nucleoside anions as magnesium salts. Since the magnesium alkoxides are more reactive than the magnesium amides, selective *O*-phosphorylation occurs selectively to give the desired aryloxy phosphoramidates.

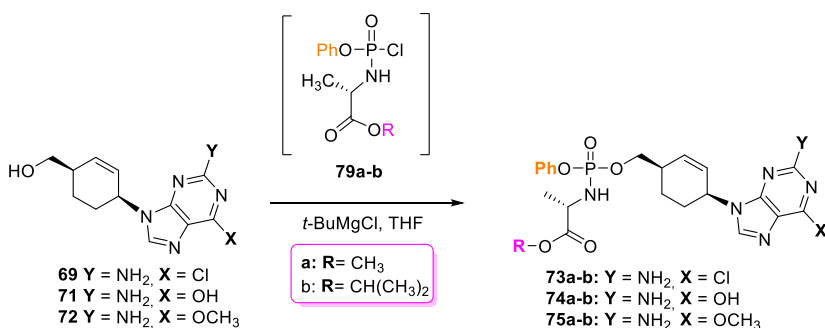


SCHEME 4.8. Approaches to generate phosphoramidate nucleoside prodrugs.

Accordingly, CeNAs **69**, **71**, **72** were treated with phosphorochloridate **79a** in presence of *t*-BuMgCl, in THF at rt, affording the corresponding aryloxy phosphoramidate **73a-75a** (TABLE

4.2, entries 1, 3 and 5) in satisfactory yields (61-68%). Similarly, treatment of nucleosides **69**, **71**, **72** with phosphorochloridate **79b** yielded ProTides **73-75b** in 59-71% (entries 2, 4 and 6). Notably, all CeNAs showed similar behaviour toward phosphorylation reaction exception made for guanosine analogue **71** for which prolonged reaction times were required for the low solubility of the nucleoside in the reaction solvent (entries 3 and 4).

TABLE 4.2 CeNA ProTides synthesis.



Entry	CeNA	Phosphorochloridate reagent	ProTide	Yield (%)	Time (h)
1	69	79a	73a	62	24
2	69	79b	73b	71	24
3	71	79a	74a	61	72
4	71	79b	74b	68	72
5	72	79a	75a	68	24
6	72	79b	75b	59	24

Being our phosphorochloridate reagents **79a-b** a couple of diastereoisomers, ProTides **73-75a-b** were also obtained as a pair of diastereoisomers (dr~1:1), as clearly highlighted by ¹H NMR and ³¹P NMR data (see experimental section).⁵² The slight differences in chemical behaviour of the two diastereoisomers hampered their chromatographic separation. However, as it is not always predictable whether or which of the two stereoisomers may be the active one and as the removal of phosphate group is the first step that happens once inside the cell, in early biological screening CeNA ProTides will be evaluated as a pair of diastereoisomers.

4.2.3 BIOLOGICAL EVALUATION OF CYCLOHEXYNYL NUCLEOSIDES

D- and L-cyclohexenyl nucleosides were subjected to an antiviral screening at Rega Institute for Medical Research (KU Leuven, Belgium, by Prof. Graciela Andrei and Prof. Robert Snoeck) with

the aim to study their potential towards various *Human Herpes Viruses* (HHVs). First results were obtained for adenosine and guanosine analogues **70** and **71** and their synthetic precursors **68** and **69** (TABLE 4.3). The corresponding L-enantiomers *ent*-(**67-71**) were also considered, while for **72**, as well as for ProTides **72-75**, biological assays are currently ongoing. All experiments were performed using HEL cells; the well-known anti-HHV drugs Cidofovir (CDV), Acyclovir (ACV) and Brivudin (BVDU) were used as reference compounds. In all cases, the antiviral potential was measured calculating the concentration required to reduce the virus-induced cytopathogenicity (HSV), plaque formation (VZV, CMV) or cell growth by 50% (EC₅₀).

TABLE 4.3. Anti-HHV activity of **68-71** and *ent*-**68-71** in HEL cell cultures.

Entry	Compd ^b	Activity (EC ₅₀ , μM) ^a						
		HSV-1 (KOS)	HSV-2 (G)	HSV/KOS ACVr	CMV (AD-169)	CMV (Davis)	VZV (TK ⁺)	VZV (TK ⁻)
1	68	>100	>100	>100	47.71	50.51	>100	>100
2	<i>ent</i> - 68	>100	>100	>100	>100	>100	>100	>100
3	69	>100	>100	>100	>100	>100	20	76.47
4	<i>ent</i> - 69	>100	>100	>100	>100	>100	>100	>100
5	70	>100	>100	>100	>20	13.37	100	>100
6	<i>ent</i> - 70	>100	>100	>100	>20	34.20	13.37	72.48
7	71 ^c	1.38	1.38	1.16	1.22	0.15	1.91	3.82
8	<i>ent</i> - 71	>100	>100	>100	>100	>100	>100	>100
9	BVDU	0.05	30.2	12.01	ND	ND	0.005	9.72
10	ACV	0.32	0.1	>90	ND	ND	1.57	32.8
11	CDV	1.07	1.07	0.81	0.34	0.91	ND	ND

[a] effective concentration required to reduce virus plaque formation by 50%

[b] in all cases MCC₅₀ values (effective concentration required to cause a microscopically detectable alteration of normal cell morphology) were >100 μM.

[c] in this case CC₅₀ value (cytotoxic concentration required to reduce cell growth by 50%) was >70 μM.

As shown in TABLE 4.3, synthetic precursors of guanosine and adenosine analogue, **68** and **69** showed a weak selective activity against *Varicella-zoster virus* (VZV) and *Cytomegalovirus* (CMV) respectively (entries 1 and 3) while the corresponding enantiomers *ent*-**68** and *ent*-**69** exhibited no inhibitory activity against the viral strains considered (entries 2 and 4). When adenosine analogue was considered, a selective activity of **70** was observed against CMV Davis strain (entry 5), while its enantiomer *ent*-**70** inhibited the replication of CMV Davis strain and

VZV (entry 6). However, for both **70** and *ent-70* the observed EC₅₀ values were always far higher than those reported by the reference drugs.

More interesting antiviral properties were observed for guanosine analogue. While *ent-71* was inactive against all the viral strains considered (entry 8), conversely, most EC₅₀ values related to **71** were comparable or only slightly higher than those of the reference drugs acyclovir (ACV), cidofovir (CDV) and brivudin (BVDU) (entry 7). Remarkably, antiviral activity of **71** was retained when evaluated in TK⁻ strains (mutated strains lacking viral kinase). In these cases, its antiviral properties were far superior than those of anti-HHV agents ACV and BVDU. Unfortunately, further antiviral assays performed to confirm the interesting antiviral activity showed by **71** did not provide the same positive results; in-depth studies are currently ongoing in order to understand these different results and to assess the effective antiviral activity of the compound.

For some nucleosides (**69-70** and *ent-69-70*), a preliminary evaluation of the antiviral potential against RNA viruses was also provided. As shown in TABLE 4.4 no activity was observed against the RNA viruses considered, exception made for the nucleoside **69** that exhibited a very interesting selective activity against Coxackie virus B4 with an EC₅₀ value of 8.9 μM.

TABLE 4.4 Antiviral activity of **69-70** and *ent-69-70* in Vero cell cultures.

Entry	Compd ^b	Activity (EC ₅₀ , μM) ^a					
		Para-influenza virus 3	Reovirus-1	Sindbis Virus	Coxackie Virus B4	Punta Toro virus	Yellow fever virus
1	69	>100	>100	>100	8.9	>100	>100
2	<i>ent-69</i>	>100	>100	>100	>100	>100	>100
3	70	>100	>100	>100	>100	>100	>100
4	<i>ent-70</i>	>100	>100	>100	>100	>100	>100
5	Ribavirin	112	>250	>250	>2500	112	>250
6	Mycophenolic acid	0.4	2.3	15	>100	4.0	2.3

[a] effective concentration required to reduce virus plaque formation by 50%

[b] in all cases MCC₅₀ values (effective concentration required to cause a microscopically detectable alteration of normal cell morphology) were >100 μM.

Despite the unclear data about the antiviral activity of **71**, overall, the biological assays revealed a potential of this class of molecules as antiviral agents. Indeed, on one hand the retained activity against mutated strains lacking viral kinase (TK⁻) suggests the ability of these compounds (not only the guanosine analogue **71** but also **69** and *ent-70*) to be recognized by cellular kinases highlighting their potential application in the treatment of those viral infections not holding their

own viral kinases, such as HIV. On the other, the antiviral activity of nucleoside **69** against Coxsackie virus B4 suggests a potential efficacy of these molecules against RNA viruses. However, further studies have to be performed to clearly assess the antiviral properties of these molecules including biological evaluation of the corresponding ProTide derivatives, whose results could reveal if the weak or no activity observed in most of the cases can be ascribed to a low or inefficient phosphorylation.

4.3 CONCLUDING REMARKS

A high regio- and stereoselective route leading to enantiomerically pure D- and L-cyclohexenyl nucleosides (CeNAs) has been herein finely tuned. The antiviral potential of these compounds relies on the high conformational flexibility of the pseudosaccharide units, enabling a close mimicry of the bioactive conformations (*N* and *S*) of natural D-nucleosides. In addition, the absence of any secondary hydroxyl function (which would resemble the OH group at the C3' position of natural nucleosides) justifies their use as chain terminators. The corresponding ProTide derivatives of some nucleosides were also synthesized with the aim to explore the potential of this successful technology applied to our nucleosides in terms of biological activity. From a synthetic standpoint, during the preparation of our CeNAs some notable findings regarding the Pd(0)-catalyzed reaction (Tsuji-Trost reaction) of cyclic allylic carbonates have been reported. Herein, an un-precedented example of stereoconvergent Tsuji-Trost reaction has been documented, enabling the preparation *cis*-configured cyclohexenyl nucleosides with high selectivity (*cis:trans* up to >20:1), regardless of the relative configuration of the starting materials. These results hold a synthetic relevance as no stereoselective processes for the synthesis of the substrates of the Tsuji-Trost reaction are required and suggest a reconsideration of the reaction mechanism. DFT calculations confirmed the experimental data and revealed the origin of the stereoconvergent reaction, pointing out the involvement of both kinetic and thermodynamic factors. We are currently working to widen the synthetic potential of the reaction beyond cyclohexene-based substrates to define scope and limitations of this methodology in asymmetric catalysis and more generally to demonstrate the importance of these results in the synthesis of bioactive molecules.

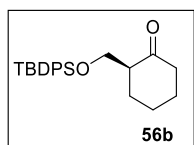
A preliminary screening aimed to study the capacity of CeNAs to interfere with the life cycles of various DNA and RNA viruses has been carried out at the Rega Institute for Medical Research. Despite some unclear results, overall, the biological assays revealed a promising potential of this class of molecules as antiviral agents leading us to a deeper evaluation of the antiviral properties of these compounds both as nucleosides and as their corresponding ProTide form.

4.4 EXPERIMENTAL SECTION

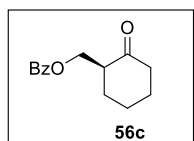
CHEMICAL SYNTHESIS: GENERAL METHODS

All moisture-sensitive reactions were performed under nitrogen atmosphere using oven-dried glassware. Solvents were dried over standard drying agents and freshly distilled prior to use. Reactions were monitored by TLC (precoated silica gel plate F254, Merck) and the products were detected by exposure to ultraviolet radiation, iodine vapor and chromic mixture. Column chromatography: Merck Kieselgel 60 (70-230 mesh); flash chromatography: Merck Kieselgel 60 (230-400 mesh). Optical rotations were measured at 25 ± 2 °C in the stated solvent. Combustion analyses were performed using a CHNS analyser. NMR spectra were recorded on NMR spectrometers operating at 400 MHz (Bruker DRX, Bruker AVANCE) or 500 MHz (Varian Inova equipped with a VnmrJ 4.0 software) using CDCl₃ solutions unless otherwise specified. Coupling constant values (*J*) were reported in Hz.

SYNTHESIS OF CYCLOHEXENYL NUCLEOSIDES

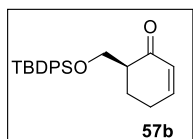


Silyl ether 56b. To a stirred solution of 2-(*S*)-hydroxymethyl cyclohexanone⁴⁴ (0.15 g, 1.17 mmol) in anhydrous pyridine (3 mL), TBDPSCI (0.36 mL, 1.40 mmol) and imidazole (95 mg, 1.40 mmol) were added. After stirring for 15' at rt, the reaction mixture was diluted with CH₂Cl₂ and washed with brine until neutral. The organic layer was dried with Na₂SO₄ and the solvent evaporated under reduced pressure. Chromatography of the crude residue over silica gel (hexane:EtOAc = 9.6:0.4) gave the pure (2*S*)-[(silyloxy)methyl]-cyclohexanone (**56b**) (0.36 g, 84% yield) as an oil. $[\alpha]^{25}_{\text{D}} -17.6$ (*c* 0.57, CHCl₃).⁵³ ¹H NMR (500 MHz): δ 1.04 (s, 9H), 1.42-1.52 (m, 1H), 1.61-1.72 (m, 2H), 1.85-1.93 (m, 1H), 1.99-2.08 (m, 1H), 2.23-2.40 (m, 3H), 2.49-2.58 (m, 1H), 3.67 (dd, *J* = 7.8, 10.5, 1H), 4.00 (dd, *J* = 4.6, 10.5, 1H), 7.32-7.45 (m, 6H), 7.66 (d, *J* = 7.7, 4H). ¹³C NMR (100 MHz): ppm 24.6, 26.5, 26.8, 27.6, 30.9, 42.1, 52.8, 63.0, 127.7, 129.6, 133.6, 134.8, 135.5, 211.9. Anal. calcd for C₂₃H₃₀O₂Si: C 75.36, H 8.25, O 8.73. Found: C 75.27, H 8.28, O 8.76.



Benzoyl ester 56c. To a stirred solution of 2-(*S*)-hydroxymethyl cyclohexane-1-one (0.24 g, 1.87 mmol) in anhydrous pyridine (2 mL), BzCl (0.43 mL, 3.74 mmol) was added at rt. After 16h, the mixture was extracted with EtOAc and washed with brine. The organic layers were dried (Na₂SO₄) and the solvent evaporated under reduced pressure. Chromatography of the crude residue over silica gel (hexane:EtOAc = 9:1) gave the pure **56c** (0.27 g, 63% yield) as an oil. ¹H NMR (500 MHz): δ 1.51-1.59 (m, 1H), 1.66-1.78 (m, 2H), 1.90-1.98 (m, 1H), 2.08-2.16 (m, 1H), 2.26- 2.39 (m, 2H), 2.43-2.48 (m, 1H), 2.82 (dddd, *J* = 1.1, 5.7, 6.7, 8.0, 1H), 4.32 (dd, *J* = 6.7, 11.3, 1H), 4.65 (dd, *J* = 5.7, 11.3, 1H), 7.43 (t, *J* = 7.7, 2H), 7.55 (t, *J* = 7.4, 1H), 8.02 (d, *J* = 7.4, 2H). ¹³C NMR (125 MHz): ppm 24.7, 27.6, 31.1, 42.1, 49.6, 63.8, 128.3, 129.3, 130.1, 132.9, 166.5, 210.4. Anal. calcd for C₁₄H₁₆O₃: C 72.39, H 6.94. Found: C 72.30, H 6.97.

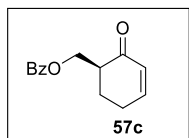
Two-steps dehydrogenation: general procedure. *n*-BuLi (2.5 M in hexane, 0.40 mL, 1.00 mmol) was added to a solution of freshly distilled DIPA (0.16 mL, 1.14 mmol) in anhydrous THF (2 mL), stirred at -78°C under nitrogen atmosphere. After 20', a solution of protected cyclohexan-1-one (0.95 mmol) in anhydrous THF (1.6 mL) was added dropwise to the mixture. After 1h, TMSCl [2.2 mL, previously distilled and deacidified with a solution of freshly dried triethylamine (TEA) in anhydrous THF] was added and the resulting mixture was stirred for 1h at -78°C . After control TLC indicated complete conversion of the starting ketone into the corresponding trimethylsilyl enol ether, the solvent was evaporated under reduced pressure and the mixture filtered on a celite pad, washing with pentane (10.5 mL). To a stirring solution of the crude trimethylsilyl enol ether in anhydrous CH_3CN (14 mL), $\text{Pd}(\text{OAc})_2$ (0.21 g, 0.95 mmol) was added at rt and the reaction was stirred at the same temperature for 16h. The mixture was then filtered on a celite pad, washing with CH_2Cl_2 . The filtrate was washed with brine. The organic layer was dried (Na_2SO_4) and evaporated under reduced pressure. Chromatography of the crude residue over silica gel gave the protected hydroxymethylcyclohexenone **57**.



Cyclohexenone 57b. The crude residue deriving from the two-steps dehydrogenation procedure was purified by chromatography over silica gel (hexane: Et_2O = 95:5), to provide the pure **57b** (86% o.y. from **56b**) as an oil. $[\alpha]_D^{25} +20.3$ (*c* 0.57, CHCl_3). ^1H NMR (500 MHz): δ 1.04 (s, 9H), 1.94-2.04 (m, 1H), 2.26-2.32 (m, 1H) 2.37-2.45 (m, 2H), 2.49-2.56 (m, 1H), 3.88 (dd, J = 7.2, 10.2, 1H), 3.99 (dd, J = 4.2, 10.2, 1H), 5.99 (dt, J = 2.2, 10.1, 1H), 6.96 (dddd, J = 1.2, 3.1, 4.9, 10.1, 1H), 7.35-7.44 (m, 6H), 7.65 (dd, J = 1.8, 8.0, 2H), 7.68 (dd, J = 1.5, 7.6, 2H). ^{13}C NMR (100 MHz): ppm 19.3, 25.2, 25.6, 26.9, 48.9, 62.8, 127.7, 129.6, 129.9, 133.5, 135.6, 135.7, 150.3, 199.4. Anal. calcd for $\text{C}_{23}\text{H}_{28}\text{O}_2\text{Si}$: C 75.78, H 7.74, O 8.78. Found: C 75.70, H 7.76, O 8.81.

IBX-Mediated dehydrogenation: general procedure.

To a solution of ketone **56** (1.07 mmol) in DMSO (9.3 mL), benzoic acid (0.13 g, 1.07 mmol) and IBX (0.59 g, 2.09 mmol) were added. The solution was heated to $60-65^{\circ}\text{C}$ and the reaction was monitored by TLC until complete consumption of starting material was observed. The reaction mixture was cooled to room temperature and diluted with Et_2O . The organic layer was washed with NaHCO_3 and brine. The organic layer was then dried with Na_2SO_4 and the solvent evaporated under reduced pressure. Chromatography of the crude residue over silica gel provided the corresponding protected hydroxymethyl cyclohexenone.



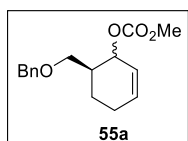
Cyclohexenone 57c. The crude residue deriving from the IBX-mediated dehydrogenation procedure was purified by chromatography over silica gel (hexane: Et_2O = 8:2) to give the pure **57c** (69% o. y. starting from (**56c**) as an oil. ^1H NMR (400 MHz): δ 1.93-2.04 (m, 1H), 2.21-2.30 (m, 1H), 2.44-2.52 (m, 2H), 2.79-2.85 (m, 1H), 4.54 (dd, J = 6.6, 11.2, 1H), 4.71 (dd, J = 4.4, 11.2, 1H), 6.08 (dt, J = 2.0, 10.1, 1H), 7.00-7.04 (m, 1H), 7.43 (t, J = 7.5, 2H), 7.56 (t, J = 7.5, 1H), 8.02 (d, J = 7.5, 2H). ^{13}C NMR (125 MHz): ppm 25.5, 26.1, 46.2, 63.7, 128.3, 129.5, 129.6,

130.1, 132.9, 150.5, 166.6, 198.4. Anal. calcd for $C_{14}H_{14}O_3$: C 73.03, H 6.13. Found: C 73.12, H 6.11.

Reduction-protection of ketones **57**: general procedure.

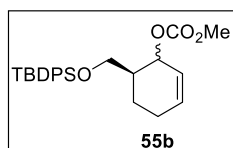
Reduction step: *Method A.* $LiAlH_4$ (7 mg, 0.18 mmol) was added to a cooled ($-78^\circ C$) solution of ketone **57** (0.74 mmol) in anhydrous THF (3.6 mL) under nitrogen atmosphere. After 1h, the mixture was warmed to $0^\circ C$ and diluted with EtOAc and H_2O . After 15 min, the solution was washed with aq. NH_4Cl and extracted with EtOAc. The organic layer was dried over Na_2SO_4 and concentrated under reduced pressure. *Method B.* To a stirred solution of **57a-b** (0.74 mmol) in anhydrous toluene (8 mL), DIBAL-H (1.5 M in toluene, 0.59 mL, 0.89 mmol) was added at $-78^\circ C$. After 15', the reaction mixture was warmed to $0^\circ C$, methanol and sodium potassium tartrate were added and the resulting mixture was extracted with EtOAc and washed with brine. The organic layer was dried (Na_2SO_4) and the solvent evaporated under reduced pressure. *Method C.* $CeCl_3 \cdot 7H_2O$ (0.83 g, 2.2 mmol) was added to a cooled ($-78^\circ C$) mixture of **57c** (0.74 mmol) in MeOH (3.5 mL). After 15', $NaBH_4$ (41 mg, 1.1 mmol) was added and the reaction mixture was stirred for 1h at $-18^\circ C$. The mixture was warmed to $0^\circ C$ and then diluted with EtOAc and the organic layer was washed with brine, dried over Na_2SO_4 and concentrated under reduced pressure.

Protection step: To a solution of the crude allylic alcohol (0.74 mmol) in anhydrous CH_2Cl_2 (14 mL), stirred at $0^\circ C$ under nitrogen atmosphere, TMEDA (0.11 ml, 0.74 mmol) and $ClCO_2Me$ (0.11 mL, 1.48 mmol) were added. The reaction was stirred for 1h at the same temperature; afterwards aq. NH_4Cl was added and the resulting mixture was extracted with CH_2Cl_2 and washed with brine. The organic layers were dried (Na_2SO_4) and concentrated under reduced pressure.



Carbonate 55a. The crude *cis/trans* mixture deriving from the reduction (*Method A* or *B*)/protection procedure of **57a** was purified by chromatography over silica gel (hexane:EtOAc = 95:5) to give the two stereoisomers *cis*- and *trans*-**55a** (*Method A*: 86% o.y., [d.r. (*cis:trans*) = 1:10]; *Method B*: 92% o.y., [d.r. (*cis:trans*) = 1:1]). Data for *trans*-**55a**:

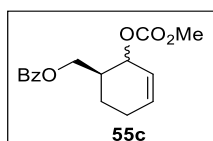
1H NMR (500 MHz): δ 1.49-1.57 (m, 1H), 1.84-1.90 (m, 1H), 1.96-2.06 (m, 3H), 3.43 (dd, $J = 6.5, 9.3$, 1H), 3.51 (dd, $J = 4.9, 9.3$, 1H), 3.75 (s, 3H), 4.47 (d, $J = 12.0$, 1H), 4.53 (d, $J = 12.0$, 1H), 5.15 (dt, $J = 2.0, 7.8$, 1H), 5.68 (dq, $J = 2.0, 10.1$, 1H), 5.89 (bd, $J = 10.1$, 1H), 7.28-7.36 (m, 5H). ^{13}C NMR (100 MHz): ppm 23.3, 23.9, 38.8, 54.6, 70.9, 73.1, 74.4, 125.4, 127.5, 127.6, 128.3, 132.0, 138.4, 155.6. Anal. calcd for $C_{16}H_{20}O_4$: C 69.45, H 7.29. Found: C 69.55, H 7.28. Data for *cis*-**55a**: 1H NMR (500 MHz): δ 1.60-1.69 (m, 2H), 2.00-2.22 (m, 3H), 3.41 (dd, $J = 6.8, 9.1$, 1H), 3.56 (dd, $J = 7.8, 9.1$, 1H), 3.74 (s, 3H), 4.48 (d, $J = 12.1$, 1H), 4.51 (d, $J = 12.1$, 1H), 5.18 (bt, $J = 4.0$, 1H), 5.92 (bd, $J = 9.9$, 1H), 6.01 (bd, $J = 9.9$, 1H), 7.28-7.36 (m, 5H). ^{13}C NMR (125 MHz): ppm 20.3, 25.1, 38.1, 54.5, 70.8, 73.2, 74.4, 124.2, 127.6, 128.5, 131.9, 134.3, 138.4, 155.4. Anal. calcd for $C_{16}H_{20}O_4$: C 69.55, H 7.30. Found: C 69.65, H 7.28.



Carbonate 55b. The compound **55b** (93% o.y.) was obtained as an inseparable 1:1 mixture of *cis* and *trans* stereoisomers from the reduction (*Method B*)/protection procedure without further purification.

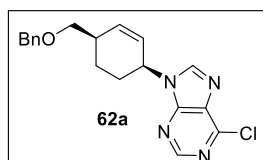
^1H NMR (500 MHz): δ 1.03 (s, 4.5H), 1.05 (s, 4.5H), 1.44-1.56 (m, 1H), 1.65-1.76 (m, 0.5H), 1.85-2.16 (m, 3.5H), 3.56 (dd, $J = 6.4, 9.9, 0.5\text{H}$),

3.64 (dd, $J = 4.3, 10.2, 0.5\text{H}$), 3.67 (dd, $J = 5.1, 10.2, 0.5\text{H}$), 3.72-3.78 (m, 3.5H), 5.23 (dt, $J = 2.0, 7.9, 0.5\text{H}$), 5.28 (bt, $J = 3.8, 0.5\text{H}$), 5.69 (dq, $J = 2.4, 10.1, 0.5\text{H}$), 5.88 (bd, $J = 10.1, 0.5\text{H}$), 5.97-6.03 (m, 1H), 7.31-7.43 (m, 6H), 7.58-7.67 (m, 4H). ^{13}C NMR (125 MHz): δ 19.2, 19.3, 19.7, 23.2, 24.1, 25.2, 26.7, 26.8, 40.3, 40.7, 54.5, 54.6, 63.8, 64.1, 70.2, 73.9, 124.1, 125.5, 127.5, 129.5, 131.8, 133.6, 133.8, 134.2, 135.5, 135.6, 155.4, 155.6. Anal. calcd for $\text{C}_{25}\text{H}_{32}\text{O}_4\text{Si}$: C 70.72, H 7.60, O 15.07. Found: C 70.67, H 7.63, O 15.12.



Carbonate 55c. The crude residue deriving from the reduction (*Method C*)/protection procedure was purified by silica gel chromatography (hexane:Et₂O = 96:4) to give the two stereoisomers *cis*- and *trans*-**55c** (69% o.y., [d.r. (*cis:trans*) = 1:1]). Data for *trans*-**55c**: ^1H NMR (500 MHz):

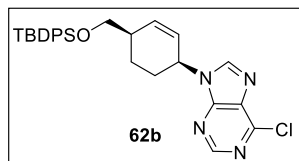
δ 1.63-1.75 (m, 2H), 1.92-2.01 (m, 1H), 2.12-2.19 (m, 1H), 2.24-2.32 (m, 1H), 3.74 (s, 3H), 4.32 (dd, $J = 5.6, 11.1, 1\text{H}$), 4.37 (dd, $J = 5.3, 11.1, 1\text{H}$), 5.24 (dt, $J = 1.6, 7.8, 1\text{H}$), 5.73 (dq, $J = 2.2, 10.1, 1\text{H}$), 5.96 (bd, $J = 10.1, 1\text{H}$), 7.45 (t, $J = 7.4, 2\text{H}$), 7.57 (t, $J = 7.4, 1\text{H}$), 8.05 (d, $J = 7.4, 2\text{H}$). ^{13}C NMR (100 MHz, DMSO-*d*₆): ppm 23.2, 23.9, 38.0, 55.0, 65.8, 74.3, 125.5, 129.3, 129.7, 130.1, 132.4, 133.8, 155.5, 166.1. Data for *cis*-**55c**: ^1H NMR (500 MHz): δ 1.66-1.75 (m, 2H), 2.08-2.17 (m, 1H), 2.21-2.32 (m, 2H), 3.74 (s, 3H), 4.33 (dd, $J = 8.4, 11.0, 1\text{H}$), 4.39 (dd, $J = 6.5, 11.0, 1\text{H}$), 5.27 (bt, $J = 4.0, 1\text{H}$), 5.95 (ddd, $J = 2.3, 4.0, 9.9, 1\text{H}$), 6.01 (ddd, $J = 2.4, 4.7, 9.9, 1\text{H}$), 7.45 (t, $J = 7.4, 2\text{H}$), 7.56 (t, $J = 7.4, 1\text{H}$), 8.04 (d, $J = 7.4, 2\text{H}$). ^{13}C NMR (100 MHz, CDCl₃): δ 20.1, 24.9, 37.2, 54.7, 65.0, 70.2, 123.7, 128.4, 129.6, 130.1, 132.9, 134.1, 155.5, 166.5. Anal. calcd for $\text{C}_{16}\text{H}_{18}\text{O}_5$: C 66.20, H 6.25. Found: C 66.09, H 6.27.



Nucleoside 62a. To a solution of 6-chloropurine **59** (56 mg, 0.36 mmol) in anhydrous DMSO (2.3 mL) stirred at rt under nitrogen atmosphere, Pd₂(dba)₃·CHCl₃ (37 mg, 36 μmol) and PPh₃ (94 mg, 0.36 mmol) were sequentially added. A solution of *trans*-**55a** (0.10 g, 0.36 mmol) in anhydrous THF (2.3 mL) was added dropwise and

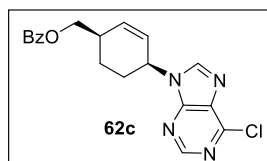
reaction mixture was further stirred for 1h. The resulting mixture was then washed with brine and extracted with EtOAc. The organic layers were dried (Na₂SO₄) and concentrated. Chromatography of the crude residue over silica gel (hexane:EtOAc = 7:3) gave nucleoside **62a** (84 mg, 66% yield; d.r. (*cis:trans*) > 10:1, r.r. (N9:N7) = 4:1).⁴⁷ Under the same conditions, after 1h, *cis*-**55a** gave nucleoside **62a** (60 % yield; d.r. (*cis:trans*) > 20:1, r.r. (N9:N7) = 2:1). ^1H NMR (400 MHz): δ 1.44-1.56 (m, 1H), 1.76-1.86 (m, 1H), 2.05-2.14 (m, 2H), 2.52-2.60 (m, 1H), 3.47 (dd, $J = 5.5, 9.0, 1\text{H}$), 3.54 (dd, $J = 5.9, 9.0, 1\text{H}$), 4.55 (d, $J = 12.5, 1\text{H}$), 4.58 (d, $J = 12.5, 1\text{H}$), 5.33 (bdd, $J = 2.0, 4.0, 1\text{H}$), 5.92 (ddd, $J = 2.4, 3.7, 10.0, 1\text{H}$), 6.27 (dt, $J = 1.8, 10.0, 1\text{H}$), 7.28-7.40 (m, 5H), 8.27 (bs, 1H), 8.75 (s, 1H). ^{13}C NMR (125 MHz): ppm 20.9, 27.8, 35.9, 49.4, 72.8,

73.3, 123.7, 127.6, 127.7, 128.4, 132.1, 137.4, 138.0, 144.8, 150.9, 151.3, 151.6. Anal. calcd for C₁₉H₁₉ClN₄O: C 64.31, H 5.40, Cl 9.99, N 15.79. Found: C 64.42, H 5.38, Cl 9.96, N 15.74.



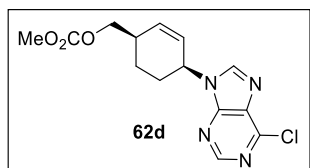
Nucleoside 62b. To a solution of 6-chloropurine **59** (35 mg, 0.23 mmol) in anhydrous DMSO (1.6 mL) stirred at rt under nitrogen atmosphere, Pd₂(dba)₃·CHCl₃ (31 mg, 30 μmol) and PPh₃ (60 mg, 0.23 mmol) were sequentially added. A solution of **55b** (0.10 g, 0.23 mmol, mixture of *cis*- and *trans*-isomers) in anhydrous THF

(1.6 mL) was added dropwise and reaction mixture was further stirred for 20h. The resulting mixture was then washed with brine and extracted with EtOAc. The organic layers were dried (Na₂SO₄) and concentrated. Chromatography of the crude residue over silica gel (hexane:EtOAc = 7:3) gave nucleoside **62b** (75 mg, 65% yield; d.r. (*cis:trans*) > 20:1, r.r. (N9:N7) = 6:1). ¹H NMR (500 MHz): δ 1.09 (s, 9H), 1.39-1.49 (m, 1H), 1.75, 1.83 (m, 1H), 1.99-2.12 (m, 2H), 2.44-2.52 (m, 1H), 3.65 (dd, *J* = 6.1, 9.9, 1H), 3.69 (dd, *J* = 6.4, 9.9, 1H), 5.28-5.33 (m, 1H), 5.89 (dq, *J* = 2.5, 10.1, 1H), 6.30 (dt, *J* = 1.9, 10.1, 1H), 7.38-7.46 (m, 6H), 7.64-7.69 (m, 4H), 8.11 (s, 1H), 8.75 (s, 1H). ¹³C NMR (125 MHz): ppm 19.4, 21.0, 27.1, 28.0, 38.2, 49.9, 66.9, 123.8, 127.9, 130.0, 132.3, 133.4, 135.7, 137.5, 144.6, 151.1, 151.5, 151.8. Anal. calcd for C₂₈H₃₁ClN₄OSi: C 66.84, H 6.21, Cl 7.05, N 11.14, O 3.18. Found: C 66.74, H 6.23, Cl 7.07, N 11.17, O 3.17.

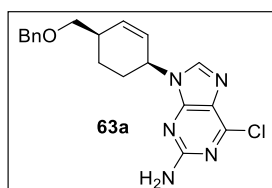


Nucleoside 62c. To a solution of 6-chloropurine **59** (42 mg, 0.27 mmol) in anhydrous DMSO (1.8 mL) stirred at rt under nitrogen atmosphere, Pd₂(dba)₃·CHCl₃ (28 mg, 27 μmol) and PPh₃ (71 mg, 0.27 mmol) were sequentially added. A solution of *cis*-**55c** (80 mg, 0.27 mmol) in anhydrous THF (1.8 mL) was added dropwise and the

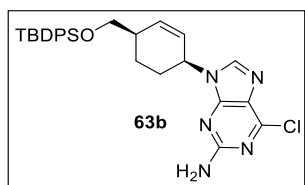
reaction mixture was further stirred for 0.5h. The resulting mixture was then washed with brine and extracted with EtOAc. The organic layers were dried (Na₂SO₄) and concentrated. Chromatography of the crude residue over silica gel (hexane:EtOAc = 4:6) gave nucleoside **62c** (55 mg, 55% yield; d.r. (*cis:trans*) > 20:1, r.r. (N9:N7) = 4:1). Under the same conditions reported for *cis*-**55c**, *trans*-**55c** (80 mg, 0.27 mmol) was recovered unreacted from the reaction mixture while its treatment with 0.5 eq of Pd₂(dba)₃·CHCl₃ (0.14 g, 0.13 mmol, corresponding to a 1 eq of active Pd catalyst) gave after 2h the nucleoside **62c** (57 mg, 57% yield; d.r. (*cis:trans*) > 10:1, r.r. (N9:N7) = 3:1). ¹H NMR (500 MHz): δ 1.51-1.61 (m, 1H), 1.91-1.98 (m, 1H), 2.14-2.22 (m, 2H), 2.75-2.82 (m, 1H), 4.36 (dd, *J* = 6.0, 11.0, 1H), 4.45 (dd, *J* = 6.7, 10.7, 1H), 5.33-5.39 (m, 1H), 6.01 (ddd, *J* = 2.6, 3.5, 10.0, 1H), 6.33 (dt, *J* = 2.1, 10.0, 1H), 7.48 (t, *J* = 7.7, 2H), 7.60 (t, *J* = 7.7, 1H), 8.05 (d, *J* = 7.7, 2H), 8.16 (s, 1H), 8.76 (s, 1H). ¹³C NMR (125 MHz): ppm 21.3, 27.9, 35.4, 49.7, 67.1, 125.1, 128.7, 129.7, 129.9, 132.3, 133.5, 135.9, 144.3, 151.3, 151.5, 151.9, 166.7. Anal. calcd for C₁₉H₁₇ClN₄O₂: C 61.88, H 4.65, Cl 9.61, N 15.19. Found: C 61.79, H 4.66, Cl 9.64, N 15.21.



Nucleoside 62d. To a solution of 6-chloropurine **59** (21 mg, 0.14 mmol) in anhydrous DMSO (0.9 mL) stirred at rt under nitrogen atmosphere, Pd₂(dba)₃ CHCl₃ (14 mg, 14 μmol) and PPh₃ (36 mg, 0.14 mmol) were sequentially added. A solution of **55d** (34 mg, 0.14 mmol, mixture of *cis*- and *trans*-isomers) in anhydrous THF (0.9 mL) was added dropwise and reaction mixture was further stirred for 1h. The resulting mixture was then washed with brine and extracted with EtOAc. The organic layers were dried (Na₂SO₄) and concentrated. Chromatography of the crude residue over silica gel (hexane:EtOAc = 4:6) gave nucleoside **62d** (31 mg, 68% yield; d.r. (*cis*:*trans*) > 20:1, r.r. (N9:N7) = 5:1) along with the unreacted *trans*-**55d**. On the other hand, treatment of *trans*-**55d** with a stoichiometric amount of Pd₂(dba)₃ CHCl₃ (64 mg, 61 μmol) gave after 2h the nucleoside **62d** (26 mg, 67% yield; d.r. (*cis*:*trans*) > 20:1, r.r. (N9:N7) = 5:1). ¹H NMR (400 MHz): δ 1.46-1.57 (m, 1H), 1.81-1.89 (m, 1H), 2.08-2.15 (m, 2H), 2.62-2.68 (m, 1H), 3.82 (s, 3H), 4.17 (dd, *J* = 5.1, 10.7 Hz, 1H), 4.26 (dd, *J* = 5.9, 10.7, 1H), 5.31-5.34 (m, 1H), 5.98 (ddd, *J* = 2.4, 4.0, 10.0, 1H), 6.29 (dt, *J* = 2.1, 10.0, 1H), 8.21 (s, 1H), 8.75 (s, 1H). ¹³C NMR (100 MHz): ppm 20.7, 27.6, 34.9, 49.3, 55.0, 69.9, 125.1, 132.1, 135.5, 144.5, 151.1, 151.3, 151.8, 155.8. Anal. calcd for C₁₄H₁₅ClN₄O₃: C 52.10, H 4.68, Cl 10.98, N 17.36. Found: C 52.21, H 4.67, Cl 10.94, N 17.30.

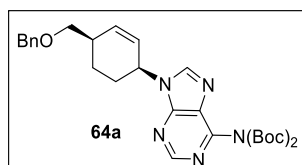


Nucleoside 63a. To a solution of 2-amino-6-chloropurine **60** (61 mg, 0.36 mmol) in anhydrous DMSO (2.4 mL) stirred at rt under nitrogen atmosphere, Pd₂(dba)₃ CHCl₃ (37 mg, 36 μmol) and PPh₃ (94 mg, 0.36 mmol) were sequentially added. A solution of *trans*-**55a** (0.10 g, 0.36 mmol) in anhydrous THF (2.4 mL) was added dropwise and reaction mixture was further stirred for 1h. The resulting mixture was then washed with brine and extracted with EtOAc. The organic layers were dried (Na₂SO₄) and concentrated. Chromatography of the crude residue over silica gel (hexane:EtOAc = 1:1) gave nucleoside **63a** (93 mg, 70% yield; d.r. (*cis*:*trans*) > 10:1, r.r. (N9:N7) = 2.5:1). Under the same conditions reported above, after 1h, *cis*-**55a** (0.10 mg, 0.36 mmol) gave nucleoside **63a** (97 mg, 73 % yield; d.r. (*cis*:*trans*) > 20:1, r.r. (N9:N7) = 3:1). ¹H NMR (400 MHz): δ 1.46-1.55 (m, 1H), 1.75-1.82 (m, 1H), 1.97-2.05 (m, 2H), 2.53 (m, 1H), 3.45 (dd, *J* = 5.8, 9.0, 1H), 3.50 (dd, *J* = 6.4, 9.0, 1H), 4.55 (d, *J* = 12.4, 1H), 4.57 (d, *J* = 12.4, 1H), 5.05 (bs, 3H), 5.86 (ddd, *J* = 2.0, 3.5, 10.0, 1H), 6.20 (bd, *J* = 10.0, 1H), 7.28-7.39 (m, 5H), 7.87 (s, 1H). ¹³C NMR (100 MHz): ppm 21.1, 27.7, 40.0, 48.9, 73.0, 73.3, 124.2, 125.8, 127.6, 127.7, 128.4, 136.6, 138.1, 141.8, 151.2, 153.3, 158.9. Anal. calcd for C₁₉H₂₀ClN₅O: C 61.70, H 5.45, Cl 9.58, N 18.94. Found: C 61.82, H 5.43, Cl 9.55, N 18.88.

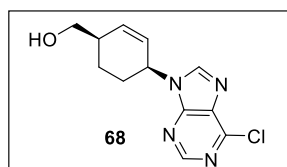


Nucleoside 63b. To a solution of 2-amino-6-chloropurine **60** (24 mg, 0.14 mmol) in anhydrous DMSO (2 mL) stirred at rt under nitrogen atmosphere, Pd₂(dba)₃ CHCl₃ (19 mg, 18 μmol) and PPh₃ (37 mg, 0.14 mmol) were sequentially added. A solution of **55b** (60 mg, 0.14 mmol, mixture of *cis*- and *trans*-isomers) in

anhydrous THF (2 mL) was added dropwise and reaction mixture was further stirred for 18h. The resulting mixture was then washed with brine and extracted with EtOAc. The organic layers were dried (Na₂SO₄) and concentrated. Chromatography of the crude residue over silica gel (hexane:EtOAc = 7:3) gave nucleoside **63b** (50 mg, 69% yield; d.r. (cis:trans) > 20:1, r.r. (N9:N7) = 5:1). [α]²⁵_D +66.7 (*c* 0.32, CHCl₃). ¹H NMR (400 MHz): δ 1.08 (s, 9H), 1.38-1.49 (m, 1H), 1.71-1.79 (m, 1H), 1.93-2.01 (m, 2H), 2.43-2.49 (m, 1H), 3.64 (dd, *J* = 6.3, 9.9, 1H), 3.68 (dd, *J* = 6.6, 9.9, 1H), 5.02-5.06 (m, 1H), 5.82 (dq, *J* = 2.3, 10.1, 1H), 6.22 (dt, *J* = 1.9, 10.1, 1H), 7.37-7.46 (m, 6H), 7.66-7.68 (m, 4H), 7.75 (s, 1H). ¹³C NMR (100 MHz): ppm 19.8, 20.9, 26.9, 27.6, 38.0, 49.2, 66.8, 124.2, 125.7, 127.8, 129.8, 133.4, 135.6, 136.6, 141.5, 151.2, 153.2, 158.9. Anal. calcd for C₂₈H₃₂ClN₅OSi: C 64.91, H 6.23, Cl 6.84, N 13.52, O 3.09. Found: C 64.80, H 6.25, Cl 6.85, N 13.57, O 3.10, Si 5.53.

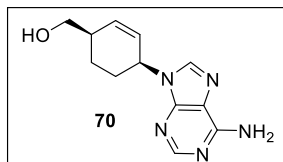


Nucleoside 64a. To a solution of *N*6-*bis*-Boc-adenine **61** (84 mg, 0.25 mmol) in anhydrous DMSO (1.7 mL) stirred at rt under nitrogen atmosphere, Pd₂(dba)₃ CHCl₃ (26 mg, 25 μ mol) and PPh₃ (66 mg, 0.25 mmol) were sequentially added. A solution of *trans*-**55a** (70 mg, 0.25 mmol) in anhydrous THF (1.7 mL) was added dropwise and reaction mixture was further stirred for 1h. The resulting mixture was then washed with brine and extracted with EtOAc. The organic layers were dried (Na₂SO₄) and concentrated. Chromatography of the crude residue over silica gel (hexane:EtOAc = 7:3) gave nucleoside **64a** (104 mg, 78% yield; d.r. (cis:trans) > 20:1, r.r. (N9:N7) = 95:5). ¹H NMR (400 MHz): δ 1.40-1.55 (m, 19H), 1.76-1.85 (m, 1H), 2.05-2.12 (m, 2H), 2.50-2.61 (bs, 1H), 3.47 (dd, *J* = 5.7, 9.0, 1H), 3.53 (dd, *J* = 6.0, 9.0, 1H), 4.54 (d, *J* = 12.6, 1H), 4.57 (d, *J* = 12.6, 1H), 5.32 (bs, 1H), 5.91 (ddd, *J* = 2.3, 3.7, 9.9, 1H), 6.25 (bd, *J* = 9.9, 1H), 7.27-7.39 (m, 5H), 8.18 (s, 1H), 8.86 (s, 1H). ¹³C NMR (125 MHz): ppm 21.1, 27.9, 36.1, 49.3, 73.1, 73.4, 83.9, 124.3, 127.6, 127.8, 128.5, 128.6, 129.4, 137.0, 138.3, 144.4, 150.3, 150.8, 151.9, 153.0. Anal. calcd for C₂₉H₃₇N₅O: C 65.03, H 6.96, N 13.07. Found: C 65.15, H 6.94, N 13.02.



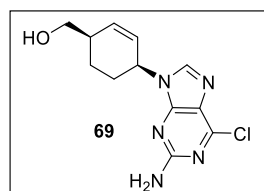
Nucleoside 68. To a solution of **62a** (23 mg, 0.06 mmol) in anhydrous CH₂Cl₂ (1.3 mL) stirred at -78°C under nitrogen atmosphere, BBr₃ (1 M solution in CH₂Cl₂, 0.16 mL, 0.16 mmol) was added at -78°C. After 1h at the same temperature, the mixture was quenched via addition of CH₂Cl₂ (1 mL), MeOH (1 mL) and Ag₂CO₃ (0.5 g) and stirred for 1h, slowly warming the mixture to 0°C. The solution was then filtered on a celite pad washing with a mixture of CH₂Cl₂: MeOH = 8:2. The filtrate was evaporated under reduced pressure. Chromatography of the crude residue over silica gel (CH₂Cl₂:CH₃OH = 98:2) provided the pure **68** (15 mg, 88% yield). [α]²⁵_D +6.0 (*c* 0.12, CH₃OH). ¹H NMR (500 MHz, CD₃OD): δ 1.48-1.59 (m, 1H), 1.78-1.85 (m, 1H), 2.07-2.20 (m, 2H), 2.37-2.46 (m, 1H), 3.62 (dd, *J* = 5.3, 10.7, 1H), 3.69 (dd, *J* = 6.0, 10.7, 1H), 5.34-5.40 (m, 1H), 6.00 (ddd, *J* = 2.4, 4.0, 10.1, 1H), 6.28 (dt, *J* = 1.8, 10.1, 1H), 8.56 (s, 1H), 8.74 (s, 1H). ¹³C NMR (100 MHz, CD₃OD): ppm 21.7, 28.5, 39.4, 51.6, 65.8, 125.3, 132.8, 138.1, 146.9,

147.3, 151.2, 152.8. Anal. calcd for $C_{12}H_{13}ClN_4O$: C 54.45, H 4.95, Cl 13.39, N 21.17. Found: C 54.30, H 4.97, Cl 13.44, N 21.23.



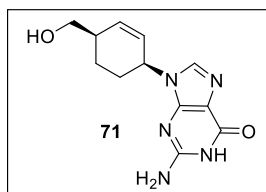
Adenine Nucleoside 70. Nucleoside **68** (20 mg, 0.07 mmol) was treated with a solution of ammonia in MeOH (7 M, 2.4 mL) and heated in a steel bomb for 20h at 90°C. After cooling, the solvent was removed under reduced pressure. Chromatography of the crude residue over silica gel (CH_2Cl_2 :MeOH = 85:15) gave the pure **70** (17 mg, 92% yield). $[\alpha]^{25}_D$ -3.5 (*c* 0.10, CH_3OH). 1H NMR (400

MHz, CD_3OD): δ 1.44-1.55 (m, 1H), 1.73-1.83 (m, 1H), 2.03-2.11 (m, 2H), 2.35-2.44 (m, 1H), 3.60 (dd, *J* = 5.5, 10.8, 1H), 3.66 (dd, *J* = 6.0, 10.8, 1H), 5.16-5.23 (m, 1H), 5.95 (ddd, *J* = 2.4, 4.0, 10.0, 1H), 6.23 (dt, *J* = 1.7, 10.0, 1H), 8.12 (s, 1H), 8.23 (s, 1H). ^{13}C NMR (500 MHz, CD_3OD): ppm 21.7, 28.9, 39.4, 50.6, 65.9, 125.7, 128.05, 134.9, 137.6, 141.8, 153.6, 157.4. Anal. calcd for $C_{12}H_{15}N_5O$: C 58.76, H 6.16, N 28.55. Found C 58.66, H 6.18, N 28.62.



2-amino-6-chloropurine Nucleoside 69. To a solution of **63a** (80 mg, 0.22 mmol) in anhydrous dichloromethane (5.0 mL) stirred at -78°C under nitrogen atmosphere, BBr_3 (1 M solution in CH_2Cl_2 , 0.55 mL, 0.55 mmol) was added at -78°C. After 1h at the same temperature, the mixture was quenched via addition of CH_2Cl_2 (1.5 mL), MeOH (1.5 mL) and Ag_2CO_3 (0.88 g) and stirred for 1h, slowly

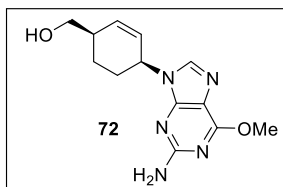
warming the mixture to 0°C. The solution was then filtered on a celite pad washing with a mixture of CH_2Cl_2 : MeOH = 8:2. The filtrate was evaporated under reduced pressure. Chromatography of the crude residue over silica gel (CH_2Cl_2 : CH_3OH = 95:5) provided the pure **69** (48 mg, 78% yield). $[\alpha]^{25}_D$ +74.9 (*c* 0.65, CH_3OH). 1H NMR (400 MHz, CD_3OD): δ 1.51 (dddd, *J* = 3.9, 8.7, 10.8, 15.4, 1H), 1.73-1.82 (m, 1H), 1.97-2.13 (m, 2H), 2.33-2.43 (m, 1H), 3.60 (dd, *J* = 5.5, 10.8, 1H), 3.66 (dd, *J* = 6.0, 10.8, 1H), 5.09-5.14 (m, 1H), 5.94 (dddd, *J* = 0.5, 2.4, 3.6, 10.1, 1H), 6.22 (dt, *J* = 1.9, 10.1, 1H), 8.06 (s, 1H). ^{13}C NMR (100 MHz, CD_3OD): ppm 21.8, 28.4, 39.4, 50.5, 65.9, 125.3, 125.7, 137.6, 143.4, 151.5.8, 154.8, 161.5. Anal. calcd for $C_{12}H_{14}ClN_5O$: C 51.53, H 5.04, Cl 12.67, N 25.04. Found: C 51.36, H 5.06, Cl 12.752, N 25.12.



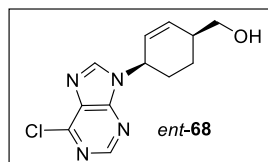
Guanine Nucleoside 71. Nucleoside **69** (45 mg, 0.16 mmol) was refluxed for 2h in a 0.5 N aq NaOH solution (2.9 mL). Then the reaction mixture was cooled to 0 °C, and 0.5 N HCl was carefully added until neutrality. The solvent was removed under reduced pressure and the crude residue was purified by chromatography over silica gel ($CHCl_3$ /MeOH = 8:2), affording the pure **71** (31 mg, 75%

yield). $[\alpha]^{25}_D$ +28.0 (*c* 0.13, DMSO). 1H NMR (500 MHz, DMSO-*d*₆): δ 1.34-1.144 (m, 1H), 1.57-1.69 (m, 1H), 1.79-1.91 (m, 2H), 2.19-2.29 (m, 1H), 3.39-3.50 (m, 1H), 4.71 (t, *J* = 4.71, 1H), 4.80-4.86 (m, 1H), 5.82 (d, *J* = 10.0, 1H), 6.07 (d, *J* = 10.1, 1H), 6.49 (bs, 2H), 7.55 (s, 1H). ^{13}C NMR (100 MHz, CD_3OD): ppm 21.8, 28.8, 39.4, 50.1, 66.0, 117.9, 126.0, 137.0, 138.5, 152.6,

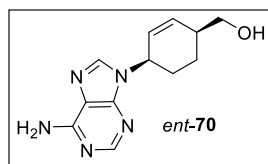
155.2, 159.5. Anal. calcd for $C_{12}H_{15}N_5O_2$: C 55.16, H 5.79, N 26.80. Found: C 55.04, H 5.81, N 26.86.



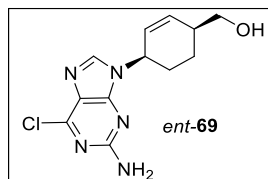
Nucleoside 72. To a solution of **69** (0.07 g, 0.25 mmol) in dry MeOH (3 mL) sodium methoxide was added (0.11 g, 2.0 mmol) under argon atmosphere. The reaction mixture was heated at reflux and stirred overnight. After 24 h, the solution was quenched with an aq NH_4Cl and the solvent was evaporated under reduced pressure. Chromatography of the crude residue over silica gel ($CH_2Cl_2/MeOH=95:5$) gave the pure **71** (54 mg, 79% yield) as a white solid. 1H NMR (400 MHz, CD_3OD): δ 1.44-1.54 (m, 1H, H-5'a), 1.72-1.79 (m, 1H, H-5'b), 1.99-2.04 (m, 2H, H-6'), 2.34-2.38 (m, 1H, H-4'), 3.58 (dd, $J_{7'a,4'}=5.5$ Hz, $J_{7'a,7'b}=10.7$ Hz, 1H, H-7'a), 3.64 (dd, $J_{7'b,4'}=4.6$, $J_{7'b,7'a}=10.7$, 1H, H-7'b), 4.05 (s, 3H, CH_3), 5.04-5.06 (m, 1H, H-1'), 5.91 (ddd, $J_{2',4'}=2.4$, $J_{2',1'}=4.1$, $J_{2',3'}=10.0$, 1H, H-2'), 6.19 (dt, $J_{3',1'}=J_{3',4'}=2.2$, $J_{3',2'}=10.0$, 1H, H-3'), 7.80 (s, 1H, H8). ^{13}C NMR (400 MHz, CD_3OD): δ 20.3, 27.3, 38.0, 48.7, 52.7, 64.6, 114.2, 124.6, 135.8, 138.5, 153.0, 160.3, 161.3.



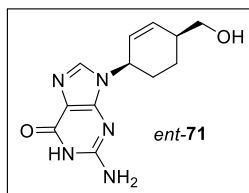
Nucleoside ent-68. To a solution of *ent-62b* (70 mg, 0.14 mmol) in THF (4.4 mL), tetrabutylammonium fluoride (1M solution in THF, 0.14 mL, 0.14 mmol) was added at $0^\circ C$. The reaction mixture was stirred at the same temperature for 1.5h; afterwards the solvent was removed under reduced pressure. Chromatography of the crude residue on silica gel (hexane:EtOAc = 2:8) gave the pure *ent-68* (33 mg, 89% yield). NMR data for compound *ent-68* were fully in line with those reported above for the corresponding enantiomer (**68**).



Nucleoside ent-70. Nucleoside *ent-68* (20 mg, 0.07 mmol) was treated with a solution of ammonia in MeOH (7 M, 2.4 mL) and heated in a steel bomb for 20h at $90^\circ C$. After cooling, the solvent was removed under reduced pressure. Chromatography of the crude residue over silica gel ($CH_2Cl_2:MeOH=85:15$) gave the pure *ent-70* (17 mg, 92% yield). NMR data of *ent-70* were fully in line with those reported above for the corresponding enantiomer (**70**).

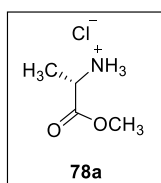


Nucleoside ent-69. To a solution of *ent-63b* (50 mg, 96 μ mol) in THF (2.6 mL), tetrabutylammonium fluoride (1 M solution in THF, 96 μ L, 96 μ mol) was added at $0^\circ C$. The reaction mixture was stirred at the same temperature for 1.5h; afterwards the solvent was removed under reduced pressure. Chromatography of the crude residue on silica gel ($CHCl_3/MeOH=95:5$) gave the pure *ent-69* (25 mg, 92% yield). NMR data of *ent-69* were fully in line with those reported above for the corresponding enantiomer (**69**).

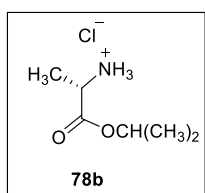


Nucleoside *ent*-71. Under the same conditions reported for the synthesis of **71**, its enantiomer *ent*-71 was obtained starting from 2-amino-6-chloropurine nucleosides *ent*-69. NMR data for compound *ent*-71 were fully in line with those reported above for the corresponding enantiomer (**71**).

SYNTHESIS OF CE₂NA PROTIDES



L-alanine methyl ester hydrochloride (78a). Thionyl chloride (3 mL, 34.3 mmol) was added dropwise to anhydrous MeOH (10 mL, 0.25 mol) at 0°C under argon atmosphere. The solution was stirred for 30 min at the same temperature; afterwards the reaction mixture was slowly warmed to room temperature and L-alanine **77** (0.70 g, 7.86 mmol) was added. After 3h, the complete consumption of starting material was observed by TLC and the solvent was evaporated under reduced pressure. The crude was recrystallized from Et₂O to give the pure compound **78a** (1.0 g, 98% yield) as white crystals. ¹H NMR (400 MHz, CD₃OD): δ 1.53 (d, *J*_{CH₃,CH} = 7.2 Hz, 3H, CHCH₃), 3.84 (s, 3H, COOCH₃), 4.10 (q, *J*_{CH,CH₃} = 7.2 Hz, 1H, CHCH₃).

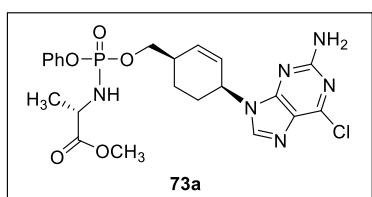


L-alanine isopropyl ester hydrochloride (78b). Thionyl chloride (0.3 mL, 3.38 mmol) was added dropwise to anhydrous *i*PrOH (8 mL, 0.10 mol) at 0°C under argon atmosphere. The solution was stirred for 30 min at the same temperature; afterwards the reaction mixture was slowly warmed to room temperature and L-alanine **77** (0.20 g, 2.25 mmol) was added. The solution was stirred to reflux temperature for 24h. The crude residue was recrystallized from Et₂O to give the pure compound **78b** (0.37 g, 98% yield) as white crystals. ¹H NMR (400 MHz): δ 1.27 (d, *J*_{(CH₃)₂,CH} = 4.1 Hz, 3H, CH(CH₃)₂), 1.29 (d, *J*_{(CH₃)₂,CH} = 4.1 Hz, 3H, CH(CH₃)₂), 1.70 (d, *J*_{CH₃,CH} = 7.2 Hz, 3H, CHCH₃), 2.05 (bs, 2H, NH₂), 4.14 (q, *J*_{CH,CH₃} = 7.1 Hz, 1H, CHCH₃), 5.09 (sept, *J*_{CH,(CH₃)₂} = 6.2 Hz, 1H, CH(CH₃)₂).

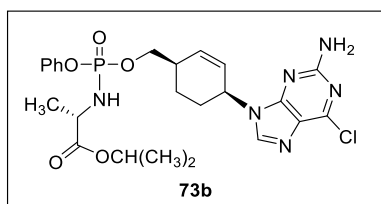
Preparation of Phosphorochloridate Reagents (79a-b). General Procedure. Phenyl dichlorophosphate **76** (1.37 mmol) was added dropwise to a solution of the appropriate amino acid ester hydrochloride salt **78a-b** (1.37 mmol) in anhydrous CH₂Cl₂ (6 mL) under argon atmosphere. The reaction mixture was then cooled at -78°C and anhydrous TEA (2.75 mmol) was added dropwise. The solution was slowly warmed to room temperature and stirred for 3 hours. Afterwards the solvent was removed under reduced pressure on a rotary evaporator protected from moisture by a calcium chloride trap; the crude residue was resuspended in dry Et₂O and filtered under argon. The filtrate was evaporated under reduced pressure to give the crude phosphorochloridates **79a-b** used in the next reaction without further purification.

Synthesis of CeNA phosphoramidates (ProTides) (73-75). General Procedure.

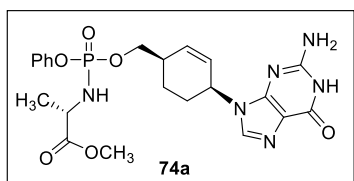
To a suspension of nucleoside **67**, **69**, **70** (0.07 mmol, previously dried by coevaporation with dry toluene) in anhydrous THF (0.4 ml), *t*-BuMgCl (0.07 mmol, 1.7 M solution in THF) was added dropwise under argon atmosphere. The resulting suspension was stirred for 10 min and then a solution of the appropriate phosphorochloridate **79a-b** in dry THF (0.21 mmol) was added dropwise. *t*-BuMgCl was added until pH 9 and the reaction mixture was stirred at room temperature for 24-72 h. The mixture was quenched with TEA until neutrality; the solvent was removed under reduced pressure and the resulting crude was coevaporated with CHCl₃.



Phosphoramidate 73a. Chromatography of the crude residue over silica gel (CH₂Cl₂/MeOH= 95:5) gave the pure **73a** (22 mg, 62%) as a colorless oil. ¹H NMR (400 MHz, acetone-*d*₆): δ 1.28-1.36 (m, 3H, CHCH₃), 1.54-1.64 (m, 1H, H-5'a), 1.78-1.85 (m, 1H, H-5'b), 2.08-2.19 (m, 2H, 2xH-6'), 2.60 (bs, 1H, H-4'), 3.66 (s, 3H, COOCH₃), 3.96-4.07 (m, 1H, CHNH), 4.13-4.25 (m, 2H, 2xH-7'), 4.86-4.85 (m, 1H, NH), 5.05 (bs, 1H, H-1'), 5.93-5.95 (m, 1H, H-2'), 6.13-6.15 (m, 1H, H-3'), 6.24 (bs, 2H, NH₂), 7.14-7.38 (m, 5H, OPh), 7.92, 7.96 (2s, 1H, H8). ³¹P NMR (400 MHz): δ 2.38, 2.73.

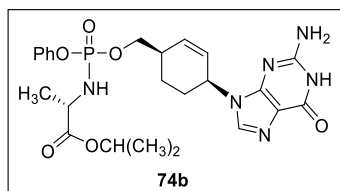


Phosphoramidate 73b. Chromatography of the crude residue over silica gel (CH₂Cl₂/MeOH= 97:3) gave the pure **73b** (28 mg, 71%) as a colourless oil. ¹H NMR (500 MHz): δ 1.20-1.24 (m, 6H, CH(CH₃)₂), 1.37 (d, *J*_{CH,CH₃}=7.0, 3H, CHCH₃), 1.43-1.53 (m, 1H, H-5'a), 1.75-1.82 (m, 1H, H-5'b), 2.08-2.19 (m, 2H, 2xH-6'), 2.56-2.63 (m, 1H, H-4'), 3.91-4.05 (m, 1H, CHNH), 4.08-4.20 (m, 2H, 2xH-7'), 4.97-5.03 (m, 1H, CH(CH₃)₂), 5.20 (d, *J* = 5.3, 1H, H-1'), 5.84-5.89 (m, 1H, H-2'), 6.12 (d, *J*_{3,2} = 10.5 Hz, 1H, H-3'), 7.13-7.35 (m, 5H, OPh), 7.76, 7.80 (2s, 1H, H8). ¹³C (400 MHz): δ 21.0, 21.6, 21.7, 27.0, 29.7, 35.8, 49.1, 49.3, 50.3, 50.4, 69.2, 69.3, 120.0, 120.1, 120.2, 125.0, 125.6, 125.8, 129.6, 129.7, 134.1, 134.2, 141.5, 150.7, 151.2, 153.3, 160.0, 172.9, 173.0. ³¹P NMR (400 MHz): δ 2.58, 2.73.



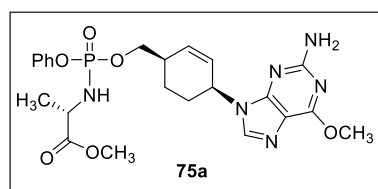
Phosphoramidate 74a. The reaction mixture was quenched with NaHCO₃ until pH 7, extracted with EtOAc/MeOH (9:1) and washed with brine. The organic layer was dried with Na₂SO₄ and the solvent evaporated under reduced pressure to obtain the crude product as an oil. Chromatography of the crude residue over silica gel (CH₂Cl₂/MeOH= 9:1) gave the pure compound **73b** (21 mg, 61%) as a colourless oil. ¹H NMR (500 MHz, CD₃OD): δ 1.29-1.38 (m, 3H, CHCH₃), 1.51-1.62 (m, 1H, H-5'b), 1.73-1.52 (m, 1H, H-5'a), 1.99-2.05 (m, 2H, 2xH-

6'), 2.55-2.59 (m, 1H, H-4'), 3.67 (s, 1.5H, COOCH₃), 3.69 (s, 1.5H, COOCH₃), 3.97 (q, $J_{\text{CH,CH}_3}$ = 7.74 Hz, 1H, CHNH), 4.09-4.23 (m, 2H, 2xH-7'), 5.00 (bs, 1H, H-1'), 5.89-5.94 (m, 1H, H-2'), 6.09-6.15 (m, 1H, H-3'), 7.16-7.40 (m, 5H, OPh), 7.75 (s, 0.5H, H-8), 7.63 (s, 0.5H, H-8). ¹³C (400 MHz, CD₃OD): δ 13.1, 18.1, 20.4, 21.1, 22.3, 27.0, 29.0, 29.3, 31.7, 36.0, 37.5, 39.8, 50.1, 50.3, 51.3, 69.2, 116.6, 120.0, 124.7, 126.0, 129.4, 133.6, 135.0, 137.0, 151.1, 154.0, 158.0, 174.0. ³¹P (400 MHz, CD₃OD): δ 4.06, 3.60.



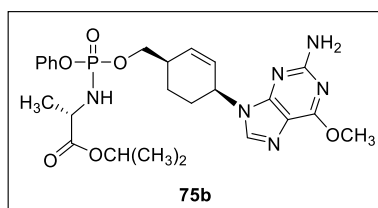
Phosphoramidate 74b. Chromatography of the crude residue over silica gel (CHCl₃/MeOH = 8:2) gave the pure **74b**. (25 mg, 68%) as a colourless oil. ¹H NMR (500 MHz, CD₃OD): δ 1.19-1.24 (m, 6H, CH(CH₃)₂), 1.68 (t, $J_{\text{CH}_3,\text{CH}}$ = 6.9 Hz, 3H, CHCH₃), 1.50-1.58 (m, 1H, H-5'a), 1.73-1.83 (m, 1H, H-5'b), 1.75-1.81 (m, 2H, 2xH-6'), 2.58 (bs, 1H, H-4'), 3.86-3.94 (m,

1H, CHNH), 4.09-4.22 (m, 2H, 2xH-7'), 4.94-5.00 (m, 1H, H-1', CH(CH₃)₂), 5.88-5.93 (m, 1H, H-2'), 6.08-6.14 (m, 1H, H-3'), 7.17-7.38 (m, 5H, OPh), 7.64 (s, 0.5H, H-8), 7.71 (s, 0.5H, H-8). ¹³C (400 MHz, CD₃OD): δ 19.0, 20.3, 20.4, 20.5, 20.6, 27.0, 29.3, 35.8, 48.6, 48.8, 50.2, 50.4, 68.7, 69.0, 116.7, 119.9, 120.0, 120.1, 124.7, 125.7, 126.0, 129.3, 129.4, 133.5, 133.7, 137.0, 150.8, 150.9, 151.2, 153.7, 158.1, 173.0, 173.3. ³¹P NMR (400 MHz, CD₃OD): δ 3.67, 4.09.



Phosphoramidate 75a. Chromatography of the crude residue over silica gel (CH₂Cl₂/MeOH = 95:5) gave the pure **75a** (24 mg, 68%) as a colourless oil. ¹H NMR (500 MHz, acetone-*d*₆): δ 1.29-1.36 (m, 3H, CHCH₃), 1.54-1.63 (m, 1H, H-5'b), 1.74-1.52 (m, 1H, H-5'a), 1.94-2.01 (m, 1H, 2xH-6'), 2.54-2.64 (m, 1H, H-4'), 3.66 (s, 3H,

COOCH₃), 3.97 (s, 3H, CH₃), 3.99-4.05 (m, 1H, CHNH), 4.12-4.23 (m, 2H, 2xH-7'), 4.86-4.85 (m, 1H, NH), 4.99-5.03 (m, 1H, H-1'), 5.84 (bs, 2H, NH₂), 5.89-5.84 (m, 1H, H-2'), 6.10-6.14 (m, 1H, H-3'), 7.26-7.38 (m, 5H, OPh), 7.69 (s, 0.5H, H-8), 7.73 (s, 0.5H, H-8). ¹³C (400 MHz, CD₃OD): δ 18.9, 19.0, 20.3, 20.4, 26.9, 29.0, 29.3, 25.9, 39.0, 50.0, 50.2, 51.3, 52.8, 69.1, 114.2, 119.9, 120.0, 120.1, 124.6, 125.7, 125.8, 129.3, 133.7, 133.8, 138.5, 150.9, 153.0, 160.3, 161.3, 174.0, 174.2. ³¹P NMR (400 MHz, CD₃OD): δ 3.59, 4.07.



Phosphoramidate 75b. Chromatography of the crude residue over silica gel (CH₂Cl₂/MeOH = 97:3) gave the pure **75b** (22 mg, 59%) as a colourless oil. ¹H NMR (500 MHz, CD₃OD): δ 1.20-1.24 (m, 6H, CH(CH₃)₂), 1.68 (d, $J_{\text{CH,CH}_3}$ = 6.9 Hz, 3H, CHCH₃), 1.48-1.57 (m, 1H, H-5'a), 1.73-1.83 (m, 1H, H-5'b), 1.75-1.81 (m, 2H, 2xH-6'), 2.56-2.63 (m, 1H, H-4'), 4.05 (s, 3H, CH₃), 3.09-4.14 (m,

1H, CHNH), 4.15-4.22 (m, 2H, 2xH-7'), 4.93-5.00 (m, 1H, CH(CH₃)₂), 5.02-5.09 (m, 1H, H-1'), 5.90-5.96 (m, 1H, H-2'), 6.10-6.14 (m, 1H, H-3'), 7.17-7.38 (m, 5H, OPh), 7.75 (s, 0.5H, H-8),

7.82 (s, 0.5H, H-8). ¹³C (400 MHz, CD₃OD): δ 17.0, 17.3, 19.0, 20.3, 20.5, 20.6, 23.9, 26.9, 29.3, 36.0, 50.3, 52.8, 69.0, 114.2, 120.0, 120.1, 120.3, 124.7, 125.6, 125.8, 128.7, 129.1, 129.4, 133.9, 138.5, 150.9, 153.0, 160.3, 161.3. ³¹P NMR (400 MHz, CD₃OD): δ 3.66, 4.08.

4.5 BIBLIOGRAPHY

- (1) De Clercq, E.; Li, G. Approved Antiviral Drugs over the Past 50 Years. *Clin. Microbiol. Rev.* **2016**, *29* (3), 695–747. <https://doi.org/10.1128/CMR.00102-15>.
- (2) Leoni, M. C.; Ustianowski, A.; Farooq, H.; Arends, J. E. HIV, HCV and HBV: A Review of Parallels and Differences. *Infect. Dis. Ther.* **2018**, *7* (4), 407–419. <https://doi.org/10.1007/s40121-018-0210-5>.
- (3) Ji, X.; Li, Z. Medicinal Chemistry Strategies toward Host Targeting Antiviral Agents. *Med. Res. Rev.* **2020**, *40* (5), 1519–1557. <https://doi.org/10.1002/med.21664>.
- (4) Hu, B.; Guo, H.; Zhou, P.; Shi, Z. L. Characteristics of SARS-CoV-2 and COVID-19. *Nat. Rev. Microbiol.* **2020**, No. December. <https://doi.org/10.1038/s41579-020-00459-7>.
- (5) De Clercq, E. Strategies in the Design of Antiviral Drugs. *Nat. Rev. Drug Discov.* **2002**, *1* (1), 13–25. <https://doi.org/10.1038/nrd703>.
- (6) Debing, Y.; Neyts, J.; Delang, L. The Future of Antivirals. *Curr. Opin. Infect. Dis.* **2015**, *28* (6), 596–602. <https://doi.org/10.1097/QCO.0000000000000212>.
- (7) Bekerman, E.; Einav, S. Combating Emerging Viral Threats. *Science (80-.)*. **2015**, *348* (6232), 282–283. <https://doi.org/10.1126/science.aaa3778>.
- (8) Martinez, J. P.; Sasse, F.; Brönstrup, M.; Diez, J.; Meyerhans, A. Antiviral Drug Discovery: Broad-Spectrum Drugs from Nature. *Nat. Prod. Rep.* **2015**, *32* (1), 29–48. <https://doi.org/10.1039/c4np00085d>.
- (9) de Clercq, E. Milestones in the Discovery of Antiviral Agents: Nucleosides and Nucleotides. *Acta Pharm. Sin. B* **2012**, *2* (6), 535–548. <https://doi.org/10.1016/j.apsb.2012.10.001>.
- (10) De Clercq, E. A 40-Year Journey in Search of Selective Antiviral Chemotherapy*. *Annu. Rev. Pharmacol. Toxicol.* **2011**, *51* (1), 1–24. <https://doi.org/10.1146/annurev-pharmtox-010510-100228>.
- (11) Yates, M. K.; Seley-Radtke, K. L. The Evolution of Antiviral Nucleoside Analogues: A Review for Chemists and Non-Chemists. Part II: Complex Modifications to the Nucleoside Scaffold. *Antiviral Res.* **2019**, *162* (October 2018), 5–21. <https://doi.org/10.1016/j.antiviral.2018.11.016>.
- (12) Jordheim, L. P.; Durantel, D.; Zoulim, F.; Dumontet, C. Advances in the Development of Nucleoside and Nucleotide Analogues for Cancer and Viral Diseases. *Nat. Rev. Drug Discov.* **2013**, *12* (6), 447–464. <https://doi.org/10.1038/nrd4010>.
- (13) De Clercq, E.; Neyts, J. Antiviral Agents Acting as DNA or RNA Chain Terminators. *Handb. Exp. Pharmacol.* **2009**, *189*, 53–84. https://doi.org/10.1007/978-3-540-79086-0_3.
- (14) Seley-Radtke, K. L.; Yates, M. K. The Evolution of Nucleoside Analogue Antivirals: A Review for Chemists and Non-Chemists. Part I: Early Structural Modifications to the Nucleoside Scaffold. *Antiviral Res.* **2018**, *154* (March), 66–86. <https://doi.org/10.1016/j.antiviral.2018.04.004>.
- (15) Temburnikar, K.; Seley-Radtke, K. L. Recent Advances in Synthetic Approaches for Medicinal Chemistry of C-Nucleosides. *Beilstein J. Org. Chem.* **2018**, *14*, 772–785. <https://doi.org/10.3762/bjoc.14.65>.

- (16) Merino, P. *Chemical Synthesis of Nucleoside Analogues*; 2013. <https://doi.org/10.1002/9781118498088>.
- (17) Mieczkowski, A.; Agrofoglio, L. A. Synthesis and Biological Activity of Selected Carbocyclic Nucleosides. In *Modified Nucleosides*; Wiley-VCH Verlag GmbH & Co. KGaA: Weinheim, Germany; pp 393–424. <https://doi.org/10.1002/9783527623112.ch15>.
- (18) Boutureira, O.; Isabel Matheu, M.; Díaz, Y.; Castellón, S. Advances in the Enantioselective Synthesis of Carbocyclic Nucleosides. *Chem. Soc. Rev.* **2013**, *42* (12), 5056–5072. <https://doi.org/10.1039/c3cs00003f>.
- (19) Bessières, M.; Chevrier, F.; Roy, V.; Agrofoglio, L. A. Recent Progress for the Synthesis of Selected Carbocyclic Nucleosides. *Future Med. Chem.* **2015**, *7* (13), 1809–1828. <https://doi.org/10.4155/fmc.15.105>.
- (20) Marquez, V. E.; Lim, M.-I. Carbocyclic Nucleosides. *Med. Res. Rev.* **1986**, *6* (1), 1–40. <https://doi.org/10.1002/med.2610060102>.
- (21) Crimmins, M. T. New Developments in the Enantioselective Synthesis of Cyclopentyl Carbocyclic Nucleosides. *Tetrahedron* **1998**, *54* (32), 9229–9272. [https://doi.org/10.1016/S0040-4020\(98\)00320-2](https://doi.org/10.1016/S0040-4020(98)00320-2).
- (22) Trost, B. M.; Van Vranken, D. L. Asymmetric Transition Metal-Catalyzed Allylic Alkylations. *Chem. Rev.* **1996**, *96* (1), 395–422. <https://doi.org/10.1021/cr9409804>.
- (23) Trost, B. M.; Crawley, M. L. Asymmetric Transition-Metal-Catalyzed Allylic Alkylations: Applications in Total Synthesis. *Chem. Rev.* **2003**, *103* (8), 2921–2943. <https://doi.org/10.1021/cr020027w>.
- (24) Trost, B. M.; Zhang, T.; Sieber, J. D. Catalytic Asymmetric Allylic Alkylation Employing Heteroatom Nucleophiles: A Powerful Method for C-X Bond Formation. *Chem. Sci.* **2010**, *1* (4), 427–440. <https://doi.org/10.1039/c0sc00234h>.
- (25) Trost, B. M.; Schultz, J. E. Palladium-Catalyzed Asymmetric Allylic Alkylation Strategies for the Synthesis of Acyclic Tetrasubstituted Stereocenters. *Synth.* **2019**, *51* (1), 1–30. <https://doi.org/10.1055/s-0037-1610386>.
- (26) Trost, B. M. Asymmetric Allylic Alkylation, an Enabling Methodology. *J. Org. Chem.* **2004**, *69* (18), 5813–5837. <https://doi.org/10.1021/jo0491004>.
- (27) Trost, B. M.; Osipov, M.; Kaib, P. S. J.; Sorum, M. T. Acetoxy Meldrum's Acid: A Versatile Acyl Anion Equivalent in the Pd-Catalyzed Asymmetric Allylic Alkylation. *Org. Lett.* **2011**, *13* (12), 3222–3225. <https://doi.org/10.1021/ol2011242>.
- (28) Crimmins, M. T.; King, B. W.; Zuercher, W. J.; Choy, A. L. An Efficient, General Asymmetric Synthesis of Carbocyclic Nucleosides: Application of an Asymmetric Aldol/Ring-Closing Metathesis Strategy. *J. Org. Chem.* **2000**, *65* (25), 8499–8509. <https://doi.org/10.1021/jo005535p>.
- (29) Herdewijn, P. The Interplay between Antiviral Activity, Oligonucleotide Hybridisation and Nucleic Acids Incorporation Studies. *Antiviral Res.* **2006**, *71* (2-3 SPEC. ISS.), 317–321. <https://doi.org/10.1016/j.antiviral.2006.04.004>.
- (30) Herdewijn, P.; De Clercq, E. The Cyclohexene Ring as Bioisostere of a Furanose Ring: Synthesis and Antiviral Activity of Cyclohexenyl Nucleosides. *Bioorganic Med. Chem. Lett.* **2001**, *11* (12), 1591–1597. [https://doi.org/10.1016/S0960-894X\(01\)00270-0](https://doi.org/10.1016/S0960-894X(01)00270-0).
- (31) Marquez, V. E.; Ben-Kasus, T.; Barchi, J. J.; Green, K. M.; Nicklaus, M. C.; Agbaria, R. Experimental and Structural Evidence That Herpes 1 Kinase and Cellular DNA Polymerase(s) Discriminate on the Basis of Sugar Pucker. *J. Am. Chem. Soc.* **2004**, *126* (2), 543–549.

- <https://doi.org/10.1021/ja037929e>.
- (32) Serpi, M.; Madela, K.; Pertusati, F.; Slusarczyk, M. Synthesis of Phosphoramidate Prodrugs: ProTide Approach. *Curr. Protoc. Nucleic Acid Chem.* **2013**, No. SUPPL.53, 1–15. <https://doi.org/10.1002/0471142700.nc1505s53>.
- (33) Mehellou, Y.; Rattan, H. S.; Balzarini, J. The ProTide Prodrug Technology: From the Concept to the Clinic. *J. Med. Chem.* **2018**, *61* (6), 2211–2226. <https://doi.org/10.1021/acs.jmedchem.7b00734>.
- (34) Pradere, U.; Garnier-Amblard, E. C.; Coats, S. J.; Amblard, F.; Schinazi, R. F. Synthesis of Nucleoside Phosphate and Phosphonate Prodrugs. *Chem. Rev.* **2014**, *114* (18), 9154–9218. <https://doi.org/10.1021/cr5002035>.
- (35) Mehellou, Y.; Balzarini, J.; McGuigan, C. Aryloxy Phosphoramidate Triesters: A Technology for Delivering Monophosphorylated Nucleosides and Sugars into Cells. *ChemMedChem* **2009**, *4* (11), 1779–1791. <https://doi.org/10.1002/cmhc.200900289>.
- (36) Mehellou, Y. The ProTides Boom. *ChemMedChem* **2016**, 1114–1116. <https://doi.org/10.1002/cmhc.201600156>.
- (37) Slusarczyk, M.; Serpi, M.; Pertusati, F. *Phosphoramidates and Phosphonamidates (ProTides) with Antiviral Activity*; 2018; Vol. 26. <https://doi.org/10.1177/2040206618775243>.
- (38) McGuigan, C.; Bourdin, C.; Derudas, M.; Hamon, N.; Hinsinger, K.; Kandil, S.; Madela, K.; Meneghesso, S.; Pertusati, F.; Serpi, M.; Slusarczyk, M.; Chamberlain, S.; Kolykhalov, A.; Vernachio, J.; Vanpouille, C.; Introini, A.; Margolis, L.; Balzarini, J. Design, Synthesis and Biological Evaluation of Phosphorodiamidate Prodrugs of Antiviral and Anticancer Nucleosides. *Eur. J. Med. Chem.* **2013**, *70*, 326–340. <https://doi.org/10.1016/j.ejmech.2013.09.047>.
- (39) Sofia, M. J.; Bao, D.; Chang, W.; Du, J.; Nagarathnam, D.; Rachakonda, S.; Reddy, P. G.; Ross, B. S.; Wang, P.; Zhang, H.-R.; Bansal, S.; Espiritu, C.; Keilman, M.; Lam, A. M.; Steuer, H. M. M.; Niu, C.; Otto, M. J.; Furman, P. A. Discovery of a β -d-2'-Deoxy-2'- α -Fluoro-2'- β - C - Methyluridine Nucleotide Prodrug (PSI-7977) for the Treatment of Hepatitis C Virus. *J. Med. Chem.* **2010**, *53* (19), 7202–7218. <https://doi.org/10.1021/jm100863x>.
- (40) De Clercq, E. Tenofovir Alafenamide (TAF) as the Successor of Tenofovir Disoproxil Fumarate (TDF). *Biochem. Pharmacol.* **2016**, *119*, 1–7. <https://doi.org/10.1016/j.bcp.2016.04.015>.
- (41) Esposito, A.; Giovanni, C.; De Fenza, M.; Talarico, G.; Chino, M.; Palumbo, G.; Guaragna, A.; D'Alonzo, D. A Stereoconvergent Tsuji–Trost Reaction in the Synthesis of Cyclohexenyl Nucleosides. *Chem. – A Eur. J.* **2020**, *26* (12), 2597–2601. <https://doi.org/10.1002/chem.201905367>.
- (42) Herdewijn, P. *Nucleic Acids with a Six-Membered “carbohydrate” Mimic in the Backbone*; 2010; Vol. 7. <https://doi.org/10.1002/cbdv.200900185>.
- (43) Wang, J.; Froeyen, M.; Hendrix, C.; Andrei, G.; Snoeck, R.; De Clercq, E.; Herdewijn, P. The Cyclohexene Ring System as a Furanose Mimic: Synthesis and Antiviral Activity of Both Enantiomers of Cyclohexenylguanidine. *J. Med. Chem.* **2000**, *43* (4), 736–745. <https://doi.org/10.1021/jm991171l>.
- (44) Paoletta, C.; D'Alonzo, D.; Schepers, G.; Van Aerschot, A.; Di Fabio, G.; Palumbo, G.; Herdewijn, P.; Guaragna, A. Oligonucleotides Containing a Ribo-Configured Cyclohexenyl Nucleoside: Probing the Role of Sugar Conformation in Base Pairing Selectivity. *Org. Biomol. Chem.* **2015**, *13* (39), 10041–10049. <https://doi.org/10.1039/c5ob01449b>.
- (45) Nicolaou, K. C.; Montagnon, T.; Baran, P. S.; Zhong, Y. L. Iodine(V) Reagents in Organic

- Synthesis. Part 4. o-Iodoxybenzoic Acid as a Chemospecific Tool for Single Electron Transfer-Based Oxidation Processes. *J. Am. Chem. Soc.* **2002**, *124* (10), 2245–2258. <https://doi.org/10.1021/ja012127+>.
- (46) Oliveira, M. T.; Audisio, D.; Niyomchon, S.; Maulide, N. Diastereodivergent Processes in Palladium-Catalyzed Allylic Alkylation. *ChemCatChem* **2013**, *5* (6), 1239–1247. <https://doi.org/10.1002/cctc.201200644>.
- (47) Ferrer, È.; Alibés, R.; Busqué, F.; Figueredo, M.; Font, J.; De March, P. Enantiodivergent Synthesis of Cyclohexenyl Nucleosides. *J. Org. Chem.* **2009**, *74* (6), 2425–2432. <https://doi.org/10.1021/jo802492g>.
- (48) Bartlett, M. J.; Turner, C. A.; Harvey, J. E. Pd-Catalyzed Allylic Alkylation Cascade with Dihydropyrans: Regioselective Synthesis of Furo[3,2- c]Pyrans. *Org. Lett.* **2013**, *15* (10), 2430–2433. <https://doi.org/10.1021/ol400902d>.
- (49) Gais, H. J.; Bondarev, O.; Hetzer, R. Palladium-Catalyzed Asymmetric Synthesis of Allylic Alcohols from Unsymmetrical and Symmetrical Racemic Allylic Carbonates Featuring C-O-Bond Formation and Dynamic Kinetic Resolution. *Tetrahedron Lett.* **2005**, *46* (37), 6279–6283. <https://doi.org/10.1016/j.tetlet.2005.07.044>.
- (50) McGuigan, C.; Cahard, D.; Sheeka, H. M.; De Clercq, E.; Balzarini, J. Aryl Phosphoramidate Derivatives of D4T Have Improved Anti-HIV Efficacy in Tissue Culture and May Act by the Generation of a Novel Intracellular Metabolite. *J. Med. Chem.* **1996**, *39* (8), 1748–1753. <https://doi.org/10.1021/jm950605j>.
- (51) Uchiyama, M.; Aso, Y.; Noyori, R.; Hayakawa, Y. O-Selective Phosphorylation of Nucleosides without N-Protection. *J. Org. Chem.* **1993**, *58* (2), 373–379. <https://doi.org/10.1021/jo00054a020>.
- (52) McGuigan, C.; Devine, K. G.; O'Connor, T. J.; Kinchington, D. Synthesis and Anti-HIV Activity of Some Haloalkyl Phosphoramidate Derivatives of 3'-Azido-3'-Deoxythymidine (AZT): Potent Activity of the Trichloroethyl Methoxyalaninyl Compound. *Antiviral Res.* **1991**, *15* (3), 255–263. [https://doi.org/10.1016/0166-3542\(91\)90071-X](https://doi.org/10.1016/0166-3542(91)90071-X).
- (53) Marinescu, S. C.; Nishimata, T.; Mohr, J. T.; Stoltz, B. M. Homogeneous Pd-Catalyzed Enantioselective Decarboxylative Protonation. *Org. Lett.* **2008**, *10* (6), 1039–1042. <https://doi.org/10.1021/ol702821j>.

5 SYNTHESIS OF PIPERIDINE-BASED NUCLEOSIDES: MIMICKING THE BIOACTIVE CONFORMATION OF IMMUCILLIN-A

5.1 INTRODUCTION

A key feature for a successful and effective NA-based antiviral therapy is the selectivity that a bioactive NA is able to exert for the target enzymes, i.e. viral/host kinases and viral polymerases. This aspect is even more important than the pharmacological activity, as selectivity is conceived to affect viral DNA/RNA replication machinery without interfering with the host molecular mechanisms. In this context, important findings have been provided by the in-depth study of the structural requirements for the enzyme-substrate recognition processes during nucleoside metabolism. Particularly, it is now well known that the conformation of natural nucleosides and their analogues play a crucial role in these processes,¹ and that this information can be exploited for therapeutic purposes.

5.1.1 THE ROLE OF SUGAR CONFORMATION IN THE ACTIVITY OF NUCLEOSIDE ANALOGUES

At the basis of the design of efficient NAs, there is the idea of obtaining molecules acting as conformational mimics of natural nucleosides.² Indeed, it is widely recognized that the conformation adopted by the sugar unit of NAs plays a crucial role in the enzyme-substrate recognition process. The conformations adopted by the natural furanose ring can be described by the value of the pseudorotation angle (P) in the pseudorotational cycle³ (FIGURE 5.1).

By convention, $P = 0^\circ$ corresponds to a C-2'-*exo*/C-3'-*endo* form (3T_2), also defined as the *North* (N) conformation, while $P = 180^\circ$ corresponds to the C-2'-*endo*/C-3'-*exo* pucker (2T_3 , $P = 180^\circ$), also defined as the *South* (S) conformation.⁴

The interaction of a nucleoside with a kinase or a polymerase involves specific conformational requirements by the sugar ring pucker of the substrate; it is now widely established that the conformation required by kinases is opposite than the one required by (cellular and viral) polymerases. Indeed, while kinases typically host *S*-shaped nucleosides, polymerases require nucleotides in an *N* conformation.⁵ Accordingly, the sugar moieties of NAs are typically devised to mimic both the *N* and *S* forms of natural (deoxy)nucleosides, in order to be recognized by both metabolic enzymes and hence to exert the required pharmacological activity.

In order to obtain an accurate conformational mimicry of natural nucleosides, over the years the design process of artificial nucleosides has involved the development of two main, diverging strategies:

a) *Increase of conformational freedom*: acyclic nucleosides with different side chains have shown powerful antiviral activity,⁶ as exemplified by the acyclic guanosine mimic Acyclovir

(ZoviraxTM) acting as one of the most powerful anti-HSV-1 drugs currently in the market (FIGURE 5.2). This approach is based on the apparent assumption that, among the large panel of possible conformations adopted by acyclic nucleosides, there certainly are those required for recognition with the target enzymes. Acyclovir's inherent flexibility allows to hold optimized interactions with the binding sites of viral kinases and polymerases. Its recognition and incorporation by the viral DNA polymerase have been estimated as 100-fold more efficient as compared to the corresponding host enzyme.⁷

b) *Conformational restriction*: for a molecule with a high degree of conformational freedom, the formation of the enzyme-substrate complex is thermodynamically unlikely due to an entropic loss. Conversely, if a molecule is designed to be structurally “frozen” in the binding conformation, the subsequent formation of the enzyme-substrate complex occurs without entropic penalty, typically leading to an enhanced stability of the resulting complex.¹

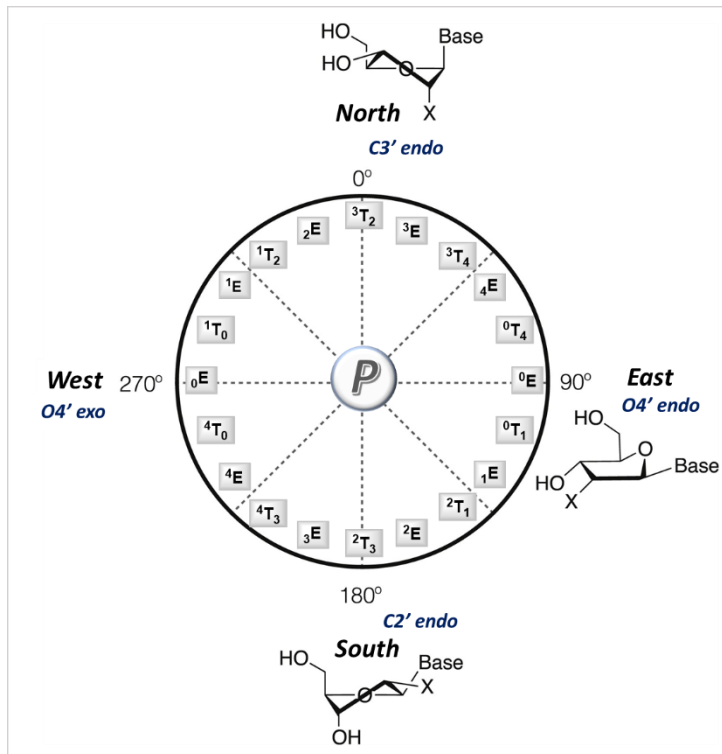


FIGURE 5.1. Pseudorotation cycle of the furanose ring and preferred conformations of a (deoxy)ribonucleoside. The figure was adapted with the permission of ref. 2.

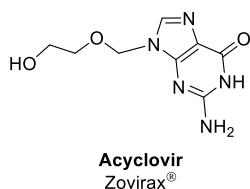


FIGURE 5.2. Acyclovir, as an illustrative example of acyclic nucleosides with antiviral activity

Among conformationally restricted nucleosides,⁸ the most renowned examples are represented by those with a six-membered sugar moiety. In this case, the flexibility of a six-membered ring is significantly reduced due to the large amount of energy required for the rotation of the chair between the two representative conformations (${}^1C_4 \leftrightarrow {}^4C_1$). This explains why six-membered nucleosides do not fluctuate between many conformations, but they are limited in the chair conformation imposed by the thermodynamically most stable positions of the substituents. In this context, 1',5'-anhydro-*arabino*-D-hexitol nucleosides⁹ (hereafter *h*NAs, **FIGURE 5.3**) stand as the most illustrative example of six-membered nucleosides. *h*NAs have been conceived as highly preorganized molecules able to mimic the C3'-*endo* (*N*) conformation of the furanose ring of native (deoxy)ribonucleosides. Indeed, NMR studies first and X-ray crystallographic studies then, demonstrated that the conformation of the *h*NA monomer has the heterocyclic base placed in an axial position, while both the primary and secondary hydroxyl groups are in an equatorial position, the resulting 4C_1 conformation resembling the 3E conformation of deoxynucleosides (**FIGURE 5.3**).

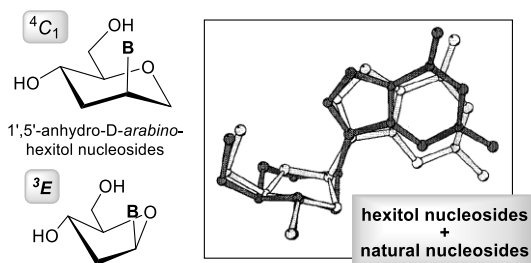


FIGURE 5.3. *h*NAs as mimics of natural deoxyribosyl nucleosides.

*h*NAs with natural and/or modified nucleobases showed a marked and selective activity due to the specific phosphorylation by the virus-encoded thymidine kinase (e.g. HSV-tk), leading to a significant activity¹⁰ against most Human Herpes Viruses (HHV) such as HSV-1, HSV-2, VZV and CMV, comparable *in vitro* to that of acyclovir. Furthermore, because of their conformation, *h*NAs are not incorporated by human kinases (while in presence of HSV-tk they undergo to a conformational change to the 1C_4 conformation), leading to their high selectivity to viral enzymes; for the same reason they did not display activity against HIV-1 and HIV-2.¹⁰

5.1.2 C-NUCLEOSIDES

The replacement of the hemiaminal (O-C-N) glycosidic bond with an O-C-C bond resulted in the so-called C-nucleosides (**FIGURE 5.4**), a class of NAs showing interesting and promising biological properties.^{11–13} As carbocyclic nucleosides (in which the hemiaminal bond is replaced by a C-C-N bond, see Chapter 4), these compounds were conceived to overcome issues related to the fragile stability of the glycosidic bond that often stands as one of the most limiting factors in the *in vivo* development of NAs.¹⁴

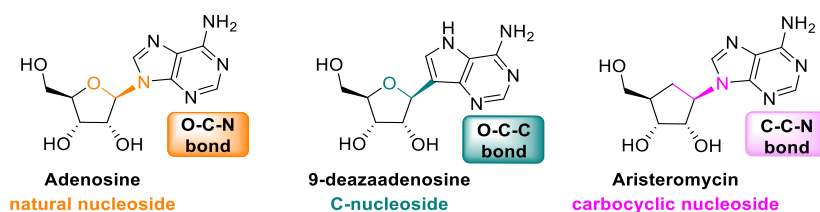


FIGURE 5.4. Structural motif of natural nucleoside compared with C-nucleosides and carbocyclic nucleosides.

The first reported C-nucleoside was the naturally occurring Pseudouridine (**FIGURE 5.5**), discovered in 1950s and most commonly found in both transfer RNA and ribosomal RNA.¹⁵ No significant biological activity was associated to pseudouridine while Showdomycin, another naturally derived C-nucleoside isolated from *Streptomyces showdonensis*, exhibited antibiotic potential against several Gram-positive and negative bacteria by inhibition of nucleoside transport in the cell.¹⁶

Starting from these findings, over the years the advancement in synthetic methodologies has led to the preparation of novel C-nucleoside analogues,^{12,13} revealing an interesting and effective pharmacological potential of this class of NAs, as exemplified by the case of the antiviral C-nucleosides GS-6620 and GS-5734 developed by Gilead Sciences (**FIGURE 5.5**). GS-6620 was the first C-nucleosides HCV polymerase inhibitor with demonstrated antiviral response in HCV patients.^{17,18} Even more interesting biological properties were exhibited by GS-5734 (Remdesivir), that was found to exert broad-spectrum activity against RNA viruses such as West Nile virus, Lassa fever virus, Middle East respiratory syndrome coronavirus *in vitro* and in animal models and has been tested in a clinical trial for Ebola virus.¹⁹ In addition, clinical antiviral activity exhibited by Remdesivir against SARS-CoV-2 by inhibition of viral RNA-dependent RNA polymerase (RdRp) has recently led to its emergency-use authorization by Food and Drug Administration (FDA), while the European Medicines Agency (EMA) granted its conditional marketing authorization, letting it to become the first approved antiviral drug for COVID-19 treatment.^{20–22}

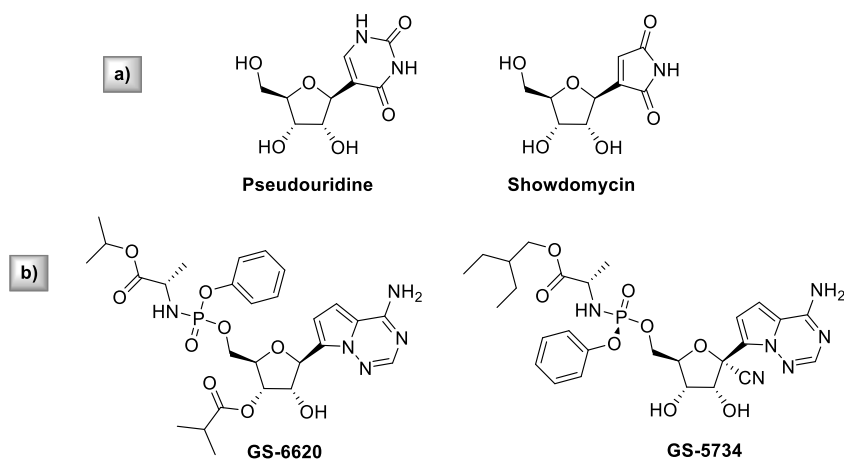


FIGURE 5.5. a) Naturally occurring C-nucleosides and b) C-nucleosides of therapeutic interest.

Replacement of the O-C-C bond with a N-C-C bond led to the class of highly promising C-nucleosides, defined to as aza-C-Nucleosides²³ (FIGURE 5.6).

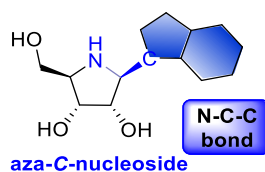


FIGURE 5.6. General structure of Aza-C-nucleosides.

This class of NAs provided attractive therapeutic candidates because they combine the high resistance to phosphorylases and hydrolases with the biological efficacy of nitrogen-containing biomimetics,^{24–28} resulting into NAs with considerably high pharmacological potential in diverse therapeutic areas.²³ The most promising example of aza-C-nucleosides is represented by Immucillins (FIGURE 5.7). In its earliest version, this class of compounds was characterized by the substitution of the natural furanose ring with an iminoribitol core, while natural nucleobases are replaced by 9-deazapurines for the construction of N-C-C bond.

5.1.2.1 PYRROLIDINE-BASED NUCLEOSIDE ANALOGUES: IMMUCILLINS

Immucillins are chemically stable 9-deazapurine C-nucleoside analogues endowed with a variety of therapeutic applications, ranging from the treatment of leukemias and autoimmune disorders to parasitic and viral infections.^{29,30} The most successful examples of Immucillins of therapeutic interest are Immucillin H and Immucillin A.

Immucillin H (Imm-H), also known as Forodesine or Mundesine (FIGURE 5.7), is a powerful inhibitor of bovine ($K_i = 23$ pM) and human ($K_i = 56$ pM) purine nucleoside phosphorylases

(PNP).^{31,32} PNPs are nucleoside processing enzymes belonging to the family of *N*-ribosyltransferases that catalyze the cleavage of the *N*-glycosidic bond of natural purine nucleosides to corresponding bases and ribose(deoxyribose)- α -1-phosphate.³³ As several studies highlighted that PNP inhibition takes down the growth of activated T-cells, Immucillin-H is a valid candidate for the treatment of leukemia and autoimmune diseases and is currently in use in Japan for the treatment of PTCL (Peripheral T-Cell Lymphomas).³⁴

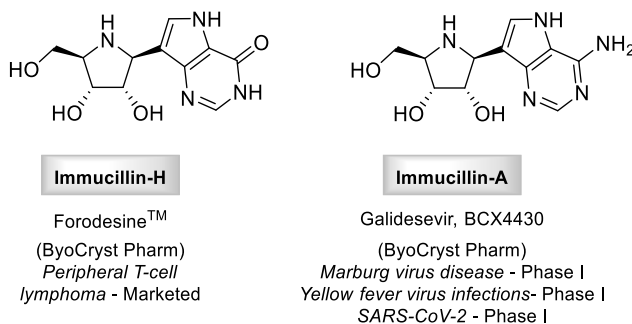


FIGURE 5.7. Immucillin H and Immucillin A.

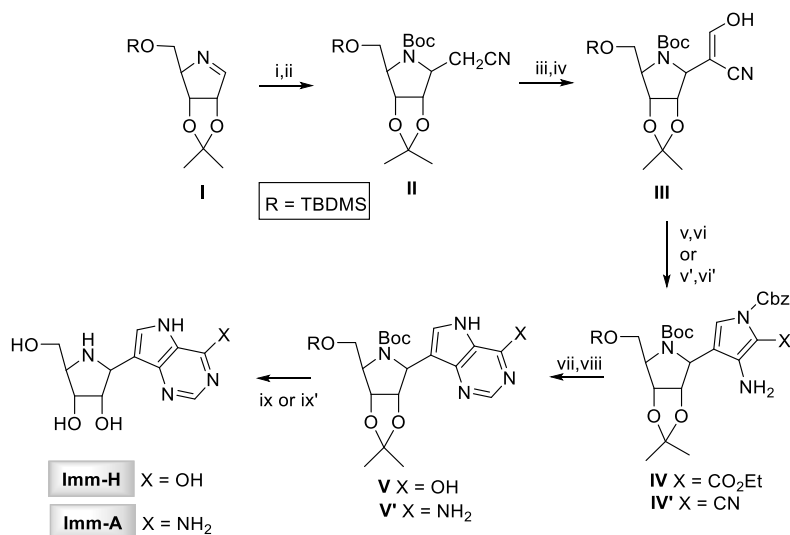
On the other hand, Immucillin A, also known as BCX4430 or as Galidesivir® (**FIGURE 5.7**), has shown a powerful broad-spectrum antiviral activity as RNA-dependent RNA polymerase inhibitor. Originally developed as potential antibiotic against *Trichomonas vaginalis*,³² Imm-A exhibited antiviral activity *in vitro* (in some cases confirmed in animal models) against more than 20 RNA viruses in nine different families including *coronaviruses*, *filoviruses*, *togaviruses*, *bunyaviruses*, *arenaviruses* and *flaviviruses*. The most powerful activity was found for *filoviruses* (including Ebola and Marburg viruses) with EC₅₀ values ranging from 3.4 to 11.8 μ M.³⁵ To exert its pharmacological activity, Immucillin-A, as the other antiviral NAs, must be converted into the corresponding triphosphate in position 5' by the cellular kinases (probably adenosine kinase) in order to compete with natural nucleotides. Imm-A-triphosphate inhibits viral RNA polymerase function acting as non-obligate chain terminator as its incorporation permits the addition of a few additional encoded bases and then terminates viral RNA chain elongation.³⁶ Immucillin-A is currently in early-stage clinical studies (Phase I) evaluating its safety in healthy individuals for the treatment of Marburg³⁷ and Yellow Fever³⁸ disease, as well as for its safety and antiviral properties in patients with COVID-19.^{22,38}

5.1.2.1 SYNTHETIC ROUTES TO IMMUCILLINS

Due to the interesting pharmacological potential exhibited by Immucillins, several synthetic strategies were investigated over the years for their preparation. Particularly, for the synthesis of Immucillin-H and A, the crucial step is the introduction of the unnatural 9-deazapurine onto

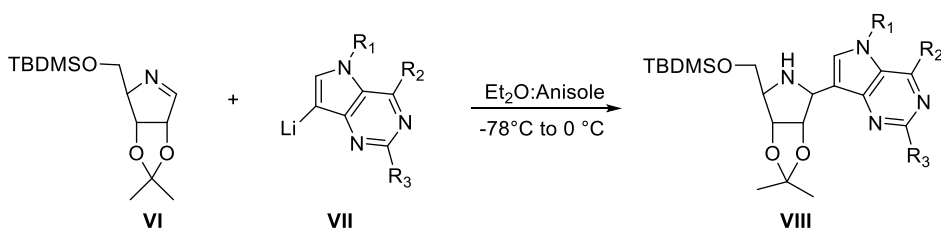
iminoribitol ring. Among the several procedures explored so far, the most efficient are reported below (SCHEMES 5.1 and 5.2).

The first approach consisted of a linear sequence of over 20 steps³⁹ (linear synthesis; SCHEME 5.1). Addition of lithiated acetonitrile to imine **I** provided the cyanomethyl *C*-glycoside derivative, whose assembly with unnatural deazahypoxanthine is then accomplished to give the target Imm-H and Imm-A. Although this route provided a first access to Imm-H and A, it was not suitable for large scale synthesis.



SCHEME 5.1. Linear route to Imm-H and A: (i) CH₂CNLi; (ii) (Boc)₂O, DCM; (iii) BuOCH(NMe)₂, DMF, 70°C; (iv) THF, HOAc, H₂O; (v) H₂NCH₂CO₂Et·HCl, NaOAc, MeOH; (v') H₂NCH₂CN, NaOAc, MeOH; (vi) ClCO₂Bn, DBU, DCM, reflux; (vi') ClCO₂Bn, DBU, DCM, reflux (vii) H₂, Pd/C, EtOH; (viii) H₂NCH=NH·HOAc, EtOH, reflux; (ix) TFA; (ix') a) TFA, b) aq H₂O₂, DMSO.

An improved synthetic methodology then involved the addition of 9-deazahypoxanthine, in turn prepared in a separate procedure, to the iminoribitol scaffold⁴⁰ (convergent synthesis; SCHEME 5.2). The coupling reaction represented the synthetic challenge of this approach being involved the generation of the lithiated deazapurine **VII** for the construction of C-C bond. Particularly, the longevity of lithiated deazapurines in different solvents and different temperature conditions was investigated. The treatment of the properly protected 9-deazahypoxanthine in an ether/anisole mixture at -78 °C, resulted the more suitable choice for both the generation of the lithiated specie and for the subsequent coupling reaction. This procedure allowed the large-scale preparation of both Imm-H and Imm-A.^{35,40}

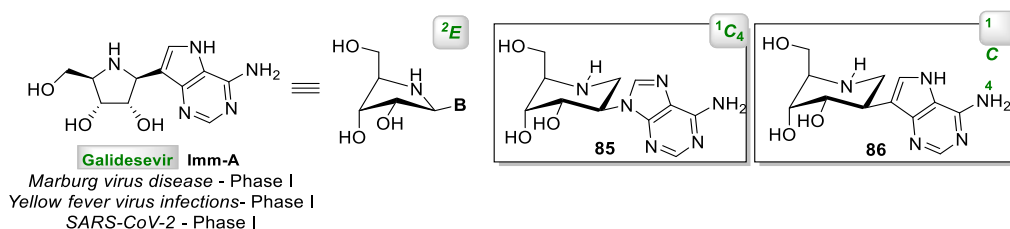


SCHEME 5.2. Convergent route to Immucillin H and A.

5.2 RESULTS AND DISCUSSION

5.2.1 SYNTHESIS OF PIPERIDINYL NUCLEOSIDES AS ANALOGUES OF BIOACTIVE IMMUCILLIN A

Based on the considerations discussed in the previous section on the importance of the conformation of NAs for their efficacy and selectivity in the treatment of viral infections and on the excellent properties exhibited by the iminosugar-based nucleosides, a synthetic approach aimed at the preparation of novel aza-*C*-nucleosides, **85** and **86**, has been herein studied. These compounds have been conceived as analogues of the bioactive Immucillin A, mimicking its structure and conformational properties (FIGURE 5.8). Particularly, compared to Immucillins, azanucleosides **85** and **86** are characterized by the replacement of the pyrrolidine ring with a piperidine moiety in order to obtain conformationally constrained analogues. Indeed, according to the concept of structural preorganization, freezing the substrate in the conformation adopted by the natural substrate in the enzyme-substrate complex could lead to improved enzymatic selectivity and increased pharmacological activity.¹

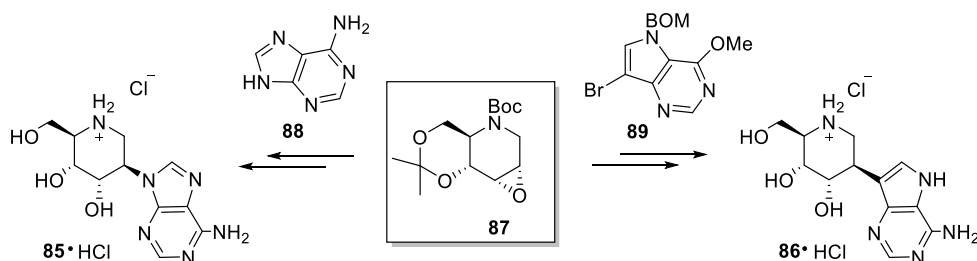
FIGURE 5.8. Imm-A and the corresponding piperidine-based analogues **85** and **86**.

Particularly in early studies, nucleoside **85**, bearing the natural adenine as nucleobase, was synthesized in order to tune up the synthetic strategy aimed at the preparation of the more complex analogues equipped with the unnatural 9-deazapurine (e.g **86**), as well as to study the conformational behavior of our piperidine-based nucleosides. Indeed, these analogues were

conceived to be frozen in a 1C_4 conformation closely related to the 2E Immucillin bioactive conformation.

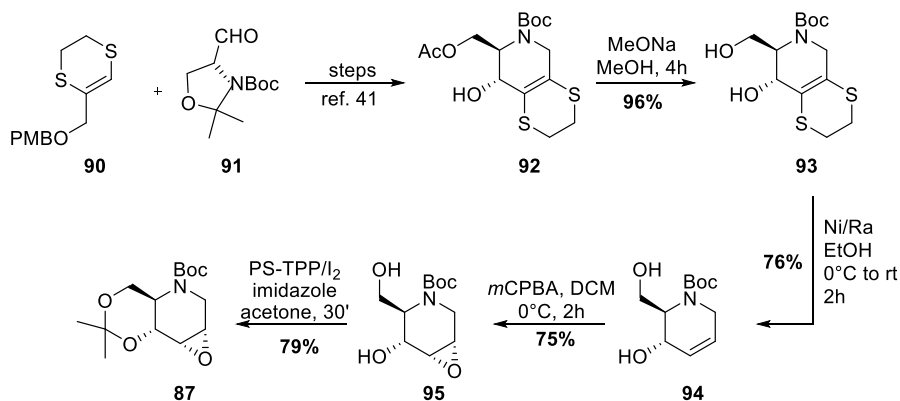
5.2.2 SYNTHESIS OF IMMUCILLIN A ANALOGUE BEARING NATURAL ADENINE

With the aim to obtain our piperidinyl purine nucleosides, a synthetic procedure was finely tuned in order to obtain the *cis*-configured epoxide **87**, key intermediate endowed with the suitable configuration for the introduction of the axially oriented modified nucleobase at the desired C2 position. Indeed, coupling reaction of the latter with the natural adenine **88**, or the suitably protected modified nucleobase **89** would enable access to both Immucillin A analogues **85** and **86** (SCHEME 5.3).



SCHEME 5.3. Synthetic path to piperidine-based analogues **85** and **86**.

Preparation of epoxide **87** was accomplished through a *de novo* strategy, already used for the synthesis of unnatural iminosugars,^{41–43} involving the use of the homologating agent **90** and (*R*)-Garner aldehyde (**91**) whose coupling reaction, followed by few steps,⁴¹ allowed to obtain the bicyclic compound **92** (SCHEME 5.4).

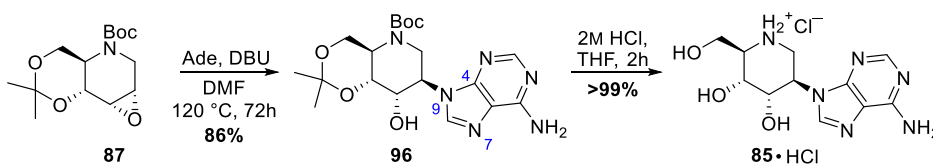


SCHEME 5.4. *De novo* route to *cis*-epoxide **87**.

Acetyl group removal under Zemplén conditions (NaOMe, MeOH) afforded the alcohol **93**, in turn subjected to desulfuration by Raney-Ni in EtOH to provide the olefin **94** in good yield (76%). Treatment of this latter with *m*CPBA in CH₂Cl₂ led to the formation of epoxide **95** (75% yield) with the desired *cis* configuration thanks to the presence of the OH group at C4 position.

The hydroxyl functions at C6 and C4 were then protected through a regioselective isopropylideneation exploiting the polymer supported triphenyl phosphine (PS-TPP)_I₂/imidazole system as the activating agent and acetone as the acetonide source.⁴⁴ Protected epoxide **87** was obtained in 79% yield without needing of extractive work-up procedures (SCHEME 5.4).

With the epoxide **87** in hand, synthesis of piperidine nucleoside was accomplished by coupling reaction with adenine **88** using 1,8-diazabicyclo[5.4.0]undec-7-ene (DBU) in anhydrous DMF at 120 °C (SCHEME 5.5).



SCHEME 5.5. Synthesis of Immucillin A analogue **85**.

Nucleophilic attack of the nucleobase occurred only at C2 and correctly oriented in an axial disposition, providing the desired nucleoside **96** in an excellent 86% yield. Removal of Boc and isopropylidene protecting groups was quantitatively performed by treatment of **96** with 2M HCl solution to reflux temperature affording free immucillin A analogue **85** as HCl salt (SCHEME 5.5).

5.2.2.1 CONFORMATIONAL ANALYSIS OF IMMUCILLIN A ANALOGUE

¹H NMR analysis allowed to obtain indications on the conformation adopted by the piperidinyl nucleoside **85**. High values of the coupling constants related to the H1'_{ax}-H2' and H2'-H3' (10.2 Hz) interactions were observed, as well as, a small coupling constant between H4'-H5' (3.1 Hz). In addition, NOESY analysis revealed dipolar interactions between the axially oriented H-1' and H-6'a. These data clearly suggest that our piperidine nucleoside adopt a ¹C₄ conformation mimicking the bioactive ₃E conformation of Immucillin A (FIGURE 5.9).

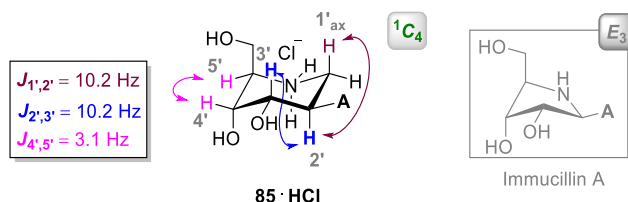


FIGURE 5.9. ¹C₄ conformation adopted by **85**.

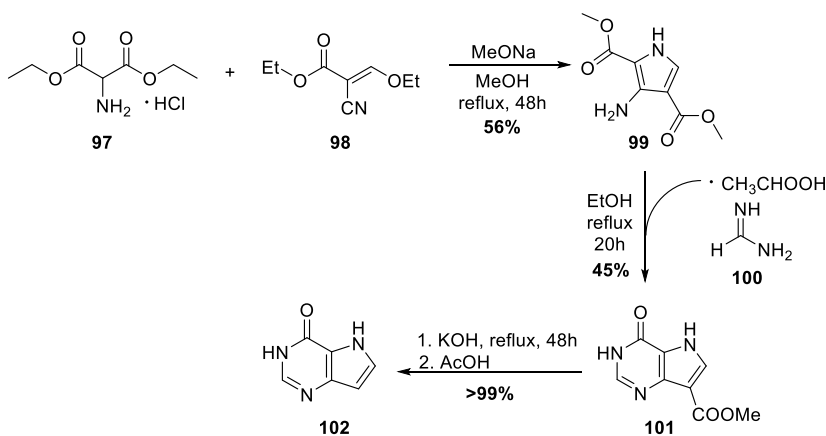
In addition, HMBC correlations between H-2' piperidine proton and the C-4 purine carbons indicated the formation of the N9-C2' bond confirming that nucleophilic attack of the nucleobase at C2 occurred with the desired N9 regioselectivity (SCHEME 5.5).

5.2.3 SYNTHESIS OF IMMUCILLIN ANALOGUE BEARING 9-DEAZAPURINE

Based on the findings described above on the conformational behavior adopted by piperidine-based nucleoside **85**, the synthesis of Immucillin A analogue **86** bearing unnatural nucleobase (9-deazaadenine) was then approached. Exploiting the synthetic route described above, **86** was synthesized by convergent synthesis *via* coupling reaction of epoxide **87** with the protected 9-deazahypoxanthine **89** (SCHEME 5.3).

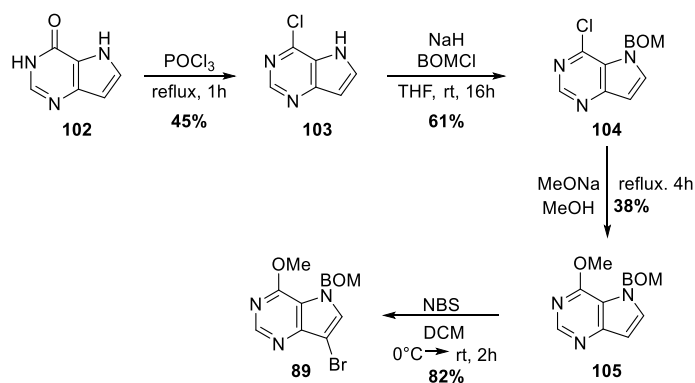
Over the last years, several efforts have been devoted to the identification of a suitable synthetic strategy for the preparation of unnatural and commercially unavailable 9-deazahypoxanthine **89**. Most of the approaches reported in the literature involve laborious procedures, with several reaction steps and low yields, and consequently are not suitable for large-scale preparations. Herein, a synthetic procedure, currently in use for the synthesis of multikilogram quantities,⁴⁵ was exploited for the synthesis of the desired protected 9-deazahypoxanthine **89**. This approach relies on a modification of the synthesis of Knorr's pyrroles⁴⁶ and involves a one-pot reaction mechanism, starting from ethyl(ethoxymethylene) cyanoacetate **97** and diethyl aminomalonate **98** (SCHEME 5.6).

The treatment of **97** and **98** in refluxing MeOH in presence of sodium methoxide enabled a sequence of transformations involving, at first, the formation of an enamine followed by intramolecular cyclization, hydrolysis of the ethoxide, decarboxylation, and finally the replacement of the ethyl ester with the methyl ester providing the substitute pyrrole **99**.



SCHEME 5.6. Synthesis of 9-deazahypoxanthine **102**.

The pyrrole **99** was then reacted with formamidine acetate **100** in ethanol under reflux conditions to facilitate the closure of the second cycle giving the compound **99** (45% yield). Base-catalyzed decarboxylation of the latter (refluxing KOH) followed by neutralization under acid condition (AcOH) quantitatively provided the 9-deazahypoxanthine **102** (SCHEME 5.6). The modified base **102** was then properly protected for the subsequent coupling reaction with the iminosugar moiety. Therefore, chlorination by treatment with refluxing POCl₃ enabled the conversion of **102** into 6-chloro-9-deazahypoxanthine **103** (SCHEME 5.7). Protection of the amine function with a benzyloxymethyl group (BomCl/THF) followed by treatment with MeONa in MeOH to replace the chlorine atom at C6 position with a methoxyl group and then bromination of C9 position (*N*-bromosuccinimide/DCM) eventually afforded the appropriately protected 9-deazahypoxanthine **89** (SCHEME 5.7).

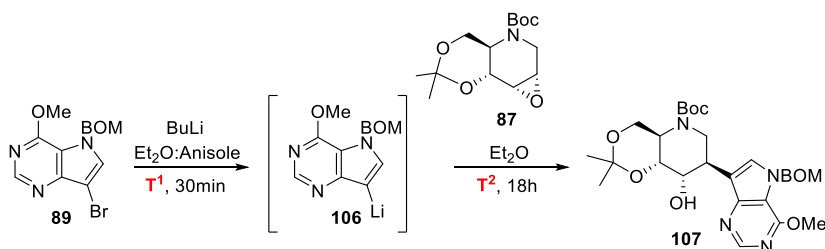


SCHEME 5.7. Synthesis of protected modified nucleobase **87**.

With both the nucleobase **89** and the epoxide **87** in hand, our attention was then turned to the coupling step, enabling access to desired piperidine-based Immucillin A analogue. As mentioned above, this step represents the synthetic challenge of the convergent approach involving the generation of a lithiated deazapurine for the construction of C-C bond. Herein, the studies reported in literature for the coupling step were exploited in order to identify the suitable reaction conditions for the addition of the modified nucleobase to our six-membered epoxide **87**.

The reaction conditions examined are summarized below (TABLE 5.1). The first attempts were realized generating the lithiated nucleobase **106** by treatment of the protected 9-deazahypoxanthine **89** with butyl lithium (BuLi), in an anisole/ethyl ether mixture at -78 °C, while after the addition of the epoxide **87**, the reaction mixture was allowed to warm slowly to -20 °C (entry 1) or to 0 °C (entry 2). In both cases, the reaction did not provide the desired coupling product. As the debrominated nucleobase **105** and the unreacted epoxide **87** were recovered from the reaction mixture. We supposed that, the lower reactivity of our epoxide, compared to those of an imine (usually used in these procedures for the synthesis of Immucillins)³⁰, toward nucleophilic attack, could be responsible for the lack of reactivity of our system.

TABLE 5.1. Coupling reaction.



Entry	T ¹ (°C) ^a	Lewis Acid	T ² (°C) ^b	Yield %
1	-78	/	-20	/
2	-78	/	0	/
3	-78	Ti(O <i>i</i> Pr) ₄	-20	/
4	-78	Ti(O <i>i</i> Pr) ₄	0	/
5	-45	Ti(O <i>i</i> Pr) ₄	-20	30
6	-45	BF ₃ (OEt ₂)	-20	68

^aTemperature for the formation of **106**;

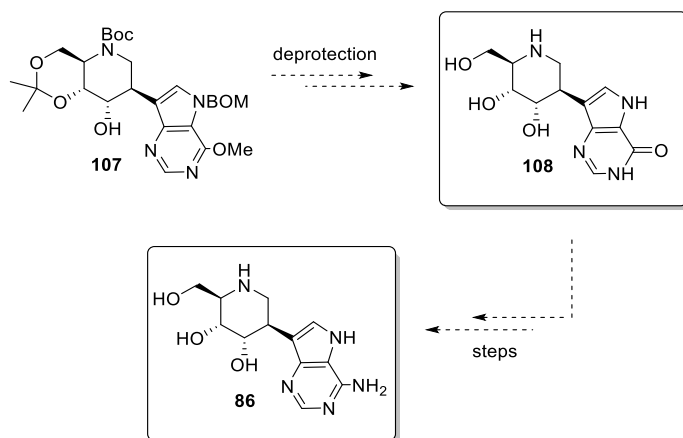
^bTemperature whose the reaction mixture was warmed after epoxide addition.

Therefore, the electrophilic character of the epoxide **87** was increased using Ti(O*i*Pr)₄ as activating agent for the epoxide-ring opening (entries 3 and 4). However, also in this case, **105** and the unreacted epoxide were recovered from the reaction mixture, without formation of the desired coupling product.

Based on the literature data about the stability of the lithiated specie also for temperatures above -78 °C, last experiments were carried out generating the lithiated nucleobase at -45 °C and using Ti(O*i*Pr)₄ as activating agents and warming the reaction mixture up to -20 °C after epoxide addition (entry 5). In this case, the formation of the desired compound **107** was observed, albeit in low yield (30%). Finally, best results were observed when the same reaction was performed using BF₃(OEt₂),⁴⁷ as promoters (entry 6) providing the coupling product **107** with satisfying yield (68%). Starting from these results, future studies will be focused on a deeper study of the reaction in order to identify the best reaction conditions in terms of temperature and activating agents.

With piperidine-based nucleosides **107** in hand, removal of protecting groups will afford Immucillin-H analogue **108** whose few synthetic manipulation³⁵ will provide Immucillin-A analogue **86** (SCHEME 5.8).

The synthesized nucleosides **85** and **86** will be evaluated for their potential as RNA polymerase inhibitors against a wide range of RNA viruses, including SARS-CoV-2, at Rega Institute for Medical Research in Belgium.



SCHEME 5.8. Synthesis of Immucillin A analogue **86**.

5.3 CONCLUDING REMARKS

Over the last decades, the study of the conformational requirements of the NAs for the process of recognition as natural counterparts by the corresponding hosts has proved to be essential in the design of bioactive NAs, leading to the discovery of the concept of structural pre-organization. In this context, replacement of furanose ring with a six-membered system is conceived to limit the conformation of nucleosides only to those required for the binding with the target enzymes. On the other hand, replacement of endocyclic oxygen of the natural ribose with a nitrogen atom and natural hypoxanthine or guanine with the corresponding 9-deazapurine have allowed to develop a new class of nucleoside analogues named “Immucillins” exhibiting high and broad pharmacological potential.

Based on these findings, a synthetic approach aimed at the preparation of novel piperidine-based aza-*C*-nucleosides **85** and **86**, has been herein studied. These compounds have been conceived as analogues of the antiviral agent Immucillin A, mimicking its structure and conformational properties. Particularly in early studies, nucleoside **85**, bearing the natural adenine as nucleobase, was synthesized in order to tune up the synthetic strategy aimed at the preparation of the more complex analogues equipped with the unnatural 9-deazapurine (e.g. **86**), as well as, to study the conformational behavior of these piperidine-based nucleosides. In both cases, the synthesis relied on the preparation of the *cis*-configured epoxide **87**, in turn obtained by a *de novo* strategy. Coupling reaction of the latter with the natural adenine or the suitably protected modified nucleobase deazapurine enable access to both Immucillin A analogues **85** and **86** that will be

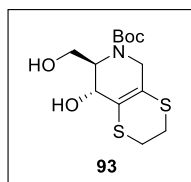
evaluated for their potential as RNA polymerase inhibitors against a wide range of RNA viruses, including SARS-CoV-2, at Rega Institute for Medical Research in Belgium.

5.4 EXPERIMENTAL SECTION

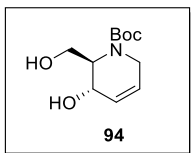
CHEMICAL SYNTHESIS: GENERAL METHODS

All commercially available reagents and solvents were purchased at the highest degree of purity from commercial sources and used without purification. TLC analysis was carried out on precoated silica gel plate F254 (Merck), and products were visualized under UV radiation or by exposure to iodine vapor and chromic mixture. Column chromatography was performed with silica gel (70–230 mesh, Merck Kiesegel 60). CHNS analysis was performed to assess the purity of compounds and was $\geq 95\%$ in all cases. NMR spectra were recorded on NMR spectrometers operating at 400 MHz (Bruker AVANCE) or 500 MHz (Varian Inova equipped with a VnmrJ 4.0 software). Coupling constant values (J) were reported in Hz.

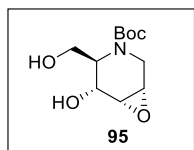
PREPARATION OF THE *CIS*-EPOXIDE



Bicyclic Compound 93. MeONa (16 mg, 0.30 mmol) was added to a stirring solution of **92**⁴¹ (0.12 g, 0.30 mmol) in MeOH (3 mL). The mixture was stirred for 4 h at room temperature and then neutralized with few drops of acetic acid. Then solvent removal under reduced pressure and chromatography of the crude residue over silica gel (hexane/EtOAc = 6/4) provided the pure **93** (92 mg, 96% yield) as a colorless oil. $[\alpha]^{25}_D +47.2$ (*c* 0.22, MeOH). ¹H NMR (200 MHz): δ 1.48 (s, 9H), 1.68 (bs, 2H), 3.19–3.26 (m, 4H), 3.56–3.68 (m, 3H), 3.90 (bs, 1H), 4.19–4.32 (m, 1H), 4.48–4.56 (m, 1H). ¹³C NMR (50 MHz): ppm 27.8, 28.2, 44.8, 58.3, 60.6, 68.0, 81.0, 119.9, 121.5, 145.9, 155.7. Anal. calcd for C₁₃H₂₁NS₂O₄: C 48.88, H 6.63, N 4.38, S 20.07. Found: C 48.98, H 6.61, N 4.39, S 20.02.

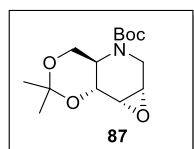


Diol 94. A suspension of Raney-Ni (W2) (0.90 g, wet) in EtOH (1 mL), was added to a stirring solution of bicycle piperidine **91** (90 mg, 0.28 mmol) in the same solvent (3 mL) at 0 °C. The suspension was stirred for 2 h at room temperature, then the solid was filtered off and washed with EtOH. The filtrate was concentrated under reduced pressure providing the crude residue whose chromatography over silica gel (hexane/acetone = 6/4) gave the pure **94** (49 mg, 76% yield) as a colorless oil. $[\alpha]^{25}_D +87.8$ (*c* 0.85, CHCl₃). NMR data for **94** were consistent with those reported elsewhere.⁴⁸



Epoxide 95. To a stirred solution of diol **94** (49 mg, 0.21 mmol) in anhydrous CH_2Cl_2 (2 mL), *m*-CPBA (43 mg, 0.25 mmol) was added at 0 °C. The mixture was stirred for 2 h at room temperature and then, aq. NaHCO_3 was added and the mixture was extracted with CH_2Cl_2 ; the organic layer was dried (Na_2SO_4) and the solvent evaporated under reduced pressure.

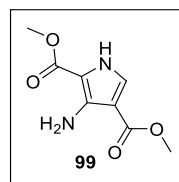
Chromatography of the crude residue over silica gel (hexane/EtOAc = 1:9) afforded the pure **95** (40 mg, 75% yield): oily, $[\alpha]^{25}_{\text{D}} +14.3$ (*c* 1.0, CHCl_3). ^1H NMR (400 MHz): δ 1.46 (s, 9H), 3.31 (bs, 1H), 3.39 (bd, $J = 3.8$, 1H), 3.46 (t, $J = 4.5$, 1H), 3.59 (d, $J = 8.0$, 11.3, 1H), 3.68 (dd, $J = 6.0$, 11.3, 1H), 3.94 (dd, $J = 1.4$, 4.5, 1H), 4.18 (bt, $J = 6.0$, 1H), 4.28 (bs, 1H). ^{13}C NMR (100 MHz): ppm 24.3, 47.5, 48.3, 52.9, 56.4, 58.5, 7.2, 76.9, 152.4. Anal. calcd for $\text{C}_{11}\text{H}_{19}\text{NO}_5$: C 53.87, H 7.81, N 5.71. Found: C 53.96; H 7.79, N 5.72.



Protected Epoxide 87. To a magnetically stirred solution of triphenyl phosphine (PS-TPP; 100-200 mesh, extent of labeling: ~3 mmol/g triphenylphosphine loading) (1.5 equiv) (80 mg, ~0.24 mmol) in anhydrous acetone (0.5 mL) at room temperature, a solution of I_2 (60 mg, 0.24 mmol) in the same solvent (0.7 mL) was added dropwise in the dark and under dry

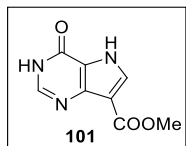
N_2 atmosphere. After 5 min imidazole was added (32 mg, 0.48 mmol) and after additional 10 min **93** (40 mg, 0.16 mmol) was added in one portion to the suspension. TLC monitoring showed the complete consumption of starting sugar within 10 min. The reaction mixture was first treated with sodium thiosulphate then extracted with EtOAc and washed with brine. The organic layer was dried (Na_2SO_4) and evaporated under reduced pressure to give a crude product that after chromatography over silica gel (hexane:EtOAc = 85:15) gave the pure **87** (36 mg, 79% yield) as a colorless oil. $[\alpha]^{25}_{\text{D}} +1.2$ (*c* 2.0, CHCl_3). ^1H NMR (500 MHz, acetone- d_6): δ 1.35 (s, 3H), 1.46 (s, 9H), 1.52 (s, 3H), 3.26 (d, $J = 4.8$, 1H), 3.31 (td, $J = 4.8$, 10.7 1H), 3.41-3.44 (m, 1H), 3.76 (d, $J = 15.3$, 1H), 3.83 (dd, $J = 2.0$, 15.3, 1H), 4.15 (t, $J = 10.7$, 1H), 4.23 (dd, $J = 4.8$, 10.7, 1H) 4.37 (d, $J = 10.7$, 1H). ^{13}C NMR (125 MHz, acetone- d_6): ppm 18.6, 27.5, 29.7, 42.6, 51.0, 51.8, 62.4, 69.5, 79.8, 98.9, 154.4. Anal. calcd for $\text{C}_{14}\text{H}_{23}\text{NO}_5$: C 58.93, H 8.13, N 4.91. Found: C 59.06, H 8.1, N 4.92.

PREPARATION OF THE MODIFIED NUCLEOBASE⁴⁵

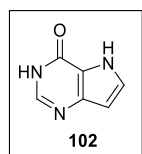


Dimethyl 3-Amino-1H-pyrrolo-2,4-dicarboxylate (99). To a solution of diethyl aminomalonate hydrochloride **97** (3.0 g, 14.0 mmol) in anhydrous MeOH (12 mL), MeONa (2.3 g, 42.0 mmol) and ethyl (ethoxymethylene)cianoacetate **98** (2.37 g, 14.0 mmol) were added and the reaction mixture was heated at reflux temperature. After 48h, the mixture was cooled to room temperature and then quenched with glacial acetic acid. The solvent was removed under reduced pressure to furnish a slurry. Water was added, then the solution was filtered, and the solids were washed with water giving **99** (1.53 g, 56% yield) as a

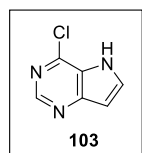
tan solid. ^1H NMR (500 MHz, $\text{DMSO-}d_6$): δ 3.70 (*s*, 3H, CH_3), 3.73 (*s*, 3H, CH_3), 5.63 (*s*, 2H, NH_2), 7.24 (*s*, 1H, H-5), 11.75 (*bs*, 1H, H-1). ^{13}C NMR (100 MHz, $\text{DMSO-}d_6$): ppm 50.7, 50.8, 73.7, 101.8, 103.9, 126.7, 161.3, 165.3.



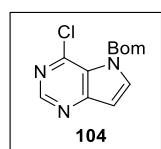
Methyl 4-oxo-4,5-dihydro-3H-pyrrolo[3,2-d]pyrimidine-7-carboxylate (101). To a solution of **99** (1.53 g, 7.7 mmol) in ethanol (13.4 mL), formamidine acetate **100** (3.21 g, 30.8 mmol) were added. The mixture was refluxed for 20h and then water was added. The resulting mixture was filtered to provide **101** (0.69 g, 45% yield) as grey solid. ^1H NMR (500 MHz, $\text{DMSO-}d_6$): δ 3.75 (*s*, 3H, CH_3), 7.90 (*s*, 1H, H-8), 7.91 (*s*, 1H, H-3). ^{13}C NMR (100 MHz, $\text{DMSO-}d_6$): ppm 51.1, 112.1, 119.6, 132.7, 143.7, 144.8, 154.4, 163.5.



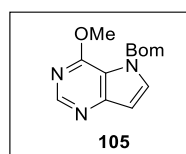
3,5-Dihydro-4H-pyrrolo[3,2-d]pyrimidin-4-one (102). **101** (0.69 g, 3.56 mmol) was dissolved with 10% aqueous KOH (6.9 mL, 14.2 mmol) and refluxed for 48h. Then, the mixture was cooled and neutralized to pH 7 with glacial acetic acid. The solid was filtered and washed with water to furnish **102** (0.48 g, >99% yield). ^1H NMR (500 MHz, $\text{DMSO-}d_6$): δ 6.37 (*s*, 1H, H-9), 7.37 (*s*, 1H, H-8), 7.79 (*s*, 1H, H-3), 11.85 (*bs*, 1H, NH-2), 12.08 (*bs*, 1H, NH-7). ^{13}C NMR (100 MHz, $\text{DMSO-}d_6$): ppm 103.4, 118.3, 127.8, 141.9, 145.10, 154.1.



6-Chloro-9-deazahypoxanthine (103). 9-deazahypoxanthine **102** (0.48 g, 3.56 mmol) was refluxed with POCl_3 (2 mL, 10.7 mmol) for 1h. Ice and 30% ammonium hydroxide were added to quench the solution. The precipitate was filtrated and washed with water to furnish **103** (0.25 g, 45% yield) as a yellow solid. ^1H NMR (500 MHz, $\text{DMSO-}d_6$): δ 6.75 (*d*, 1H, $J_{8,9} = 3.1$ Hz, H-9), 8.00 (*d*, 1H, $J_{8,9} = 3.1$ Hz, H-8), 8.64 (*s*, 1H, H-3). ^{13}C NMR (100 MHz, $\text{DMSO-}d_6$): ppm 102.7, 124.3, 134.8, 142.1, 149.6, 151.3.

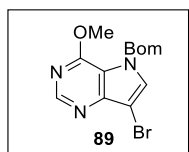


7-((Benzyloxy)methyl)-6-chloro-9-deazahypoxanthine (104). To a solution of **103** (0.25 g, 1.60 mmol) in anhydrous THF (8.2 mL), NaH (90 mg, 2.4 mmol) and BOMCl (0.30 mL, 2.08 mmol) at 0 °C were added. The reaction mixture was stirred at room temperature for 16h. Then, the mixture was extracted with EtOAc and the organic phase was washed with brine, dried (Na_2SO_4), filtered and evaporated under reduced pressure. The crude was chromatographed over silica gel (Hexane/EtOAc = 75:25) to provide compound **104** (0.26 g, 61% yield). ^1H NMR (500 MHz, $\text{DMSO-}d_6$): δ 4.44 (*s*, 2H, CH_2Ph), 5.64 (*s*, 2H, CH_2O), 6.65 (*d*, 1H, $J = 1.5$ Hz, H-8), 7.23-7.35 (*m*, 5H, arom H), 7.93 (*d*, 1H, $J = 1.3$ Hz, H-9), 8.50 (*s*, 1H, H-2).



7-((Benzyloxy)methyl)-6-methoxy-9-deazahypoxanthine (105). MeONa (0.26 g, 4.8 mmol) was added to a solution of **104** (0.26 g, 0.97 mmol) in anhydrous MeOH (4.7 mL) and the reaction mixture was heated at reflux temperature for 4h. The mixture was cooled to room temperature and then washed with brine and extracted with EtOAc. The organic phase is dried

(Na₂SO₄), filtered and concentrated under reduced pressure. The resulting crude was chromatographed over silica gel (Hexane/EtOAc = 6:4) to provide compound **105** (98 mg, 38% yield). ¹H NMR (500 MHz): δ 4.14 (s, 3H, OMe), 4.49 (s, 2H, CH₂Ph), 5.77 (s, 2H, CH₂O), 6.71 (d, 1H, J = 1.9 Hz, H-8), 7.26-7.35 (m, 5H, arom H), 7.43 (d, 1H, J = 1.5 Hz, H-9), 8.56 (s, 1H, H-2). ¹³C NMR (125 MHz): ppm 53.9, 70.5, 104.7, 116.2, 128.4, 128.7, 129.2, 133.4, 133.5, 137.5, 151.1, 152.2, 157.1.

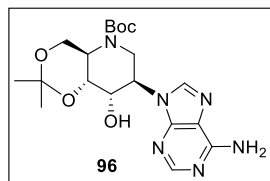


7-((Benzyloxy)methyl)-9-bromo-6-methoxy-9 deazahypoxanthine (**89**).

To a solution of **105** (98 mg, 0.36 mmol) in DCM dry (2 mL) NBS (65 mg, 0.36 mmol) was added at 0 °C. The reaction was stirred at room temperature for 2h. The mixture was then extracted with DCM and washed with brine.

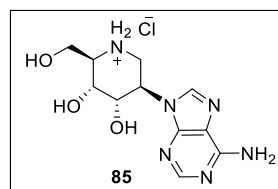
The organic layer was dried (Na₂SO₄) and the solvent was evaporated under reduced pressure. The crude was chromatographed over silica gel (Hexane/Et₂O = 8:2) affording the pure compound **89** (0.10 g, 82% yield). ¹H NMR (400 MHz): δ 4.11 (s, 3H, CH₃), 4.48 (s, 2H, CH₂Ph), 5.71 (s, 2H, CH₂O), 7.21-7.35 (m, 5H, arom H), 7.44 (s, 1H, H-8), 8.60 (s, 1H, H-2). ¹³C NMR (100 MHz): ppm 54.2, 70.8, 92.8, 116.0, 128.0, 128.5, 128.9, 131.9, 136.9, 148.8, 151.4, 156.8.

SYNTHESIS OF IMMUCILLIN-A ANALOGUES



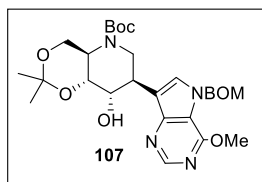
Nucleoside 96. Adenine (**88**; 36 mg, 0.26 mmol) and the epoxide **87** (35 mg, 0.12) were suspended in anhydrous DMF (0.9 mL) for 15 minutes, at room temperature under an Ar atmosphere. Then, 1,8-diazabicyclo[5.4.0]undec-7-ene (DBU, 39 μM, 0.26 mmol) was added and the resulting mixture was heated at 90 °C and stirred for 72 h. The reaction mixture was cooled to rt, quenched with sat.aq.

NH₄Cl and concentrated under reduced pressure. The crude residue was extracted with EtOAc and washed with brine. The organic layers were dried (Na₂SO₄) and the solvent evaporated under reduced pressure. Chromatography of the crude residue over silica gel (EtOAc:MeOH = 9:1) gave the corresponding pure **96** (43 mg, 86% yield): oily, [α]_D²⁵ -21.2 (c 1.0, MeOH). ¹H NMR (400 MHz, CD₃OD): δ 1.44 (s, 3H), 1.47 (s, 9H), 1.60 (s, 3H), 3.78 (td, J = 4.7, 10.5, 1H), 3.98 (dd, J = 5.2, 13.9, 1H), 4.03–4.12 (m, 2H), 4.34 (bt, J = 2.7, 1H), 4.38 (dd, J = 4.7, 10.5 Hz, 1H), 4.60–4.65 (m, 2H), 8.21 (s, 1H), 8.22 (s, 1H). ¹³C NMR (100 MHz, CD₃OD): ppm 19.6, 28.5, 29.4, 42.9, 59.8, 63.9, 70.2, 70.9, 82.4, 100.7, 120.2, 141.5, 150.8, 153.8, 156.6, 157.5. Anal. calcd for C₁₉H₂₈N₆O₅: C 54.27, H 6.71, N 19.99. Found: C 54.27, H 6.73, N 20.05.



Adenine Nucleoside 85. 2 M HCl (11.6 mL) was added to a solution of **96** (40 mg, 0.09 mmol) in THF (0.6 mL) and the reaction mixture was heated to reflux temperature for 1 h. Removal of the volatiles under reduced pressure and subsequent trituration by with Et₂O afforded **85** as chlorohydrate salt (30 mg, quant.)., [α]_D²⁵ 8.25 (c

0.14, H₂O). ¹H NMR (400 MHz, D₂O): δ 3.76 (dd, *J* = 5.2, 13.4, 1H), 3.90 (dt, *J* = 3.5, 8.8, 1H), 4.03 (dd, *J* = 10.5, 13.4, 1H), 4.07 (dd, *J* = 3.5, 12.8, 1H), 4.16 (dd, *J* = 8.8, 12.8, 1H), 4.31 (t, *J* = 3.5 Hz, 1H), 4.62 (dd, *J* = 3.5, 10.5, 1H), 5.19 (td, *J* = 5.2, 10.5, 1H), 8.38 (s, 1H), 8.39 (s, 1H). ¹³C NMR (100 MHz, D₂O): ppm 39.7, 53.3, 55.8, 59.9, 65.9, 66.9, 118.9, 144.2, 144.4, 148.6, 149.9.



Protected Imm-H analogue (107). To a solution of **89** (27 mg, 0.077 mmol) in a mixture of dry Et₂O (0.82 mL) and anisole (0.4 mL), BuLi (35 μL, 0.084 mmol) was added at -45 °C. After 30 min., a solution of epoxide **87** (20 mg, 0.07 mmol) in Et₂O (1 mL) was slowly added dropwise. BF₃·Et₂O (8.6 μL, 0.07 mmol) was added and the resulting mixture was slowly warmed to -20 °C and stirred overnight at the

same temperature. The mixture was extracted with Et₂O and the organic layer was washed with brine and dried (Na₂SO₄). The solvent was evaporated under reduced pressure and the crude residue was chromatographed over silica gel (DCM/MeOH = 95:5) to furnish the pure compound **107** (23 mg, 68% yield). ¹H NMR (500 MHz): δ 1.43 (*s*, 3H, CH₃-ipd), 1.47 (*s*, 9H, *t*-Bu), 1.51 (*s*, 3H, CH₃-ipd), 3.65 (*bs*, 1H, H-2'), 3.70 (*td*, *J*_{5',6'b} = *J*_{5',6'a} = 4.6 Hz, *J*_{5',4'} = 10.5 Hz, 1H, H-5'), 3.93 (*dd*, *J*_{1'a,2'} = 5.2 Hz, *J*_{1'a,1'b} = 13.9 Hz, 1H, H-1'a), 4.09 (*s*, 3H, OCH₃), 4.14–4.18 (*m*, 2H, H-6'b, H-4'), 4.27 (*dd*, *J*_{1'b,2'} = 2.7 Hz, *J*_{1'b,1'a} = 13.9 Hz, 1H, H-1'b), 4.38 (*s*, 1H, H-3'), 4.48 (*s*, 2H, CH₂Ph), 4.52 (*dd*, *J*_{6'a,5'} = 4.7 Hz, *J*_{6'a,6'b} = 11.0 Hz, 1H, H-6'a), 5.73 (*d*, *J* = 10.6 Hz, 1H), 5.65 (*d*, *J* = 10.6 Hz, 1H), 7.35–7.23 (*m*, 5H, arom H), 7.38 (*s*, 1H, H-8), 8.51 (*s*, 1H, H-2).

5.5 BIBLIOGRAPHY

- (1) Kool, E. T. Preorganization of DNA: Design Principles for Improving Nucleic Acid Recognition by Synthetic Oligonucleotides. *Chem. Rev.* **1997**, *97* (5), 1473–1488. <https://doi.org/10.1021/cr9603791>.
- (2) Burai Patrascu, M.; Malek-Adamian, E.; Damha, M. J.; Moitessier, N. Accurately Modeling the Conformational Preferences of Nucleosides. *J. Am. Chem. Soc.* **2017**, *139* (39), 13620–13623. <https://doi.org/10.1021/jacs.7b07436>.
- (3) Deleavey, G. F.; Damha, M. J. Designing Chemically Modified Oligonucleotides for Targeted Gene Silencing. *Chem. Biol.* **2012**, *19* (8), 937–954. <https://doi.org/10.1016/j.chembiol.2012.07.011>.
- (4) Thibaudeau, C.; Acharya, P.; Chattopadhyaya, J. *Stereoelectronic Effects in Nucleosides & Nucleotides and Their Structural Implications*; Uppsala University Press: Uppsala, 2005.
- (5) Marquez, V. E.; Ben-Kasus, T.; Barchi, J. J.; Green, K. M.; Nicklaus, M. C.; Agbaria, R. Experimental and Structural Evidence That Herpes 1 Kinase and Cellular DNA Polymerase(s) Discriminate on the Basis of Sugar Pucker. *J. Am. Chem. Soc.* **2004**, *126* (2), 543–549. <https://doi.org/10.1021/ja037929e>.
- (6) Li, G.; Fan, Y.; Lai, Y.; Han, T.; Li, Z.; Zhou, P.; Pan, P.; Wang, W.; Hu, D.; Liu, X.; Zhang, Q.; Wu, J. Coronavirus Infections and Immune Responses. *J. Med. Virol.* **2020**, *92* (4), 424–432. <https://doi.org/10.1002/jmv.25685>.

- (7) Alvarez-Ros, M.; Palafox, M. Conformational Analysis, Molecular Structure and Solid State Simulation of the Antiviral Drug Acyclovir (Zovirax) Using Density Functional Theory Methods. *Pharmaceuticals* **2014**, *7* (6), 695–722. <https://doi.org/10.3390/ph7060695>.
- (8) Herdewijn, P. The Interplay between Antiviral Activity, Oligonucleotide Hybridisation and Nucleic Acids Incorporation Studies. *Antiviral Res.* **2006**, *71* (2-3 SPEC. ISS.), 317–321. <https://doi.org/10.1016/j.antiviral.2006.04.004>.
- (9) Verheggen, I.; Van Aerschot, A.; Toppet, S.; Snoeck, R.; Janssen, G.; Balzarini, J.; De Clercq, E.; Herdewijn, P. Synthesis and Antiherpes Virus Activity of 1,5-Anhydrohexitol Nucleosides. *J. Med. Chem.* **1993**, *36* (14), 2033–2040. <https://doi.org/10.1021/jm00066a013>.
- (10) Ostrowski, T.; Wroblowski, B.; Busson, R.; Rozenski, J.; De Clercq, E.; Bennett, M. S.; Champness, J. N.; Summers, W. C.; Sanderson, M. R.; Herdewijn, P. 5-Substituted Pyrimidines with a 1,5-Anhydro-2,3-Dideoxy- D - *Arabino* -Hexitol Moiety at N-1: Synthesis, Antiviral Activity, Conformational Analysis, and Interaction with Viral Thymidine Kinase. *J. Med. Chem.* **1998**, *41* (22), 4343–4353. <https://doi.org/10.1021/jm980287z>.
- (11) De Clercq, E. C-Nucleosides to Be Revisited. *J. Med. Chem.* **2016**, *59* (6), 2301–2311. <https://doi.org/10.1021/acs.jmedchem.5b01157>.
- (12) Temburnikar, K.; Seley-Radtke, K. L. Recent Advances in Synthetic Approaches for Medicinal Chemistry of C-Nucleosides. *Beilstein J. Org. Chem.* **2018**, *14*, 772–785. <https://doi.org/10.3762/bjoc.14.65>.
- (13) Hocek, M. C -Nucleosides: Synthetic Strategies and Biological Applications. *Chem. Rev.* **2009**, *109* (12), 6729–6764. <https://doi.org/10.1021/cr9002165>.
- (14) Seley-Radtke, K. L.; Yates, M. K. The Evolution of Nucleoside Analogue Antivirals: A Review for Chemists and Non-Chemists. Part 1: Early Structural Modifications to the Nucleoside Scaffold. *Antiviral Res.* **2018**, *154* (March), 66–86. <https://doi.org/10.1016/j.antiviral.2018.04.004>.
- (15) Hamma, T.; Ferré-D'Amaré, A. R. Pseudouridine Synthases. *Chem. Biol.* **2006**, *13* (11), 1125–1135. <https://doi.org/10.1016/j.chembiol.2006.09.009>.
- (16) Yosh Imasa Uehara; Fisher, J. M.; Rabinovitz, M. Showdomycin and Its Reactive Moiety, Maleimide. *Biochem. Pharmacol.* **1980**, *29* (16), 2199–2204. [https://doi.org/10.1016/0006-2952\(80\)90198-7](https://doi.org/10.1016/0006-2952(80)90198-7).
- (17) Cho, A.; Zhang, L.; Xu, J.; Lee, R.; Butler, T.; Metobo, S.; Aktoudianakis, V.; Lew, W.; Ye, H.; Clarke, M.; Doerffler, E.; Byun, D.; Wang, T.; Babusis, D.; Carey, A. C.; German, P.; Sauer, D.; Zhong, W.; Rossi, S.; Fenaux, M.; McHutchison, J. G.; Perry, J.; Feng, J.; Ray, A. S.; Kim, C. U. Discovery of the First C -Nucleoside HCV Polymerase Inhibitor (GS-6620) with Demonstrated Antiviral Response in HCV Infected Patients. *J. Med. Chem.* **2014**, *57* (5), 1812–1825. <https://doi.org/10.1021/jm400201a>.
- (18) Coats, S. J.; Garnier-Amblard, E. C.; Amblard, F.; Ehteshami, M.; Amiralaei, S.; Zhang, H.; Zhou, L.; Boucle, S. R. L.; Lu, X.; Bondada, L.; Shelton, J. R.; Li, H.; Liu, P.; Li, C.; Cho, J. H.; Chavre, S. N.; Zhou, S.; Mathew, J.; Schinazi, R. F. Chutes and Ladders in Hepatitis C Nucleoside Drug Development. *Antiviral Res.* **2014**, *102*, 119–147. <https://doi.org/10.1016/j.antiviral.2013.11.008>.
- (19) Warren, T. K.; Jordan, R.; Lo, M. K.; Ray, A. S.; Mackman, R. L.; Soloveva, V.; Siegel, D.; Perron, M.; Bannister, R.; Hui, H. C.; Larson, N.; Strickley, R.; Wells, J.; Stuthman, K. S.; Van Tongeren, S. A.; Garza, N. L.; Donnelly, G.; Shurtleff, A. C.; Retterer, C. J.; Gharaibeh, D.; Zamani, R.; Kenny, T.; Eaton, B. P.; Grimes, E.; Welch, L. S.; Gomba, L.; Wilhelmsen, C. L.; Nichols, D. K.; Nuss, J. E.; Nagle, E. R.; Kugelman, J. R.; Palacios, G.; Doerffler, E.; Neville, S.; Carra, E.; Clarke,

- M. O.; Zhang, L.; Lew, W.; Ross, B.; Wang, Q.; Chun, K.; Wolfe, L.; Babusis, D.; Park, Y.; Stray, K. M.; Trancheva, I.; Feng, J. Y.; Barauskas, O.; Xu, Y.; Wong, P.; Braun, M. R.; Flint, M.; McMullan, L. K.; Chen, S.-S.; Fearn, R.; Swaminathan, S.; Mayers, D. L.; Spiropoulou, C. F.; Lee, W. A.; Nichol, S. T.; Cihlar, T.; Bavari, S. Therapeutic Efficacy of the Small Molecule GS-5734 against Ebola Virus in Rhesus Monkeys. *Nature* **2016**, *531* (7594), 381–385. <https://doi.org/10.1038/nature17180>.
- (20) Malin, J. J.; Suárez, I.; Priesner, V.; Fätkenheuer, G.; Rybniker, J. Remdesivir against COVID-19 and Other Viral Diseases. *Clin. Microbiol. Rev.* **2020**, *34* (1), 1–21. <https://doi.org/10.1128/CMR.00162-20>.
- (21) Robson, F.; Khan, K. S.; Le, T. K.; Paris, C.; Demirbag, S.; Barfuss, P.; Rocchi, P.; Ng, W.-L. Coronavirus RNA Proofreading: Molecular Basis and Therapeutic Targeting. *Mol. Cell* **2020**, *79* (5), 710–727. <https://doi.org/10.1016/j.molcel.2020.07.027>.
- (22) Li, G.; De Clercq, E. Therapeutic Options for the 2019 Novel Coronavirus (2019-NCoV). *Nat. Rev. Drug Discov.* **2020**, *19* (3), 149–150. <https://doi.org/10.1038/d41573-020-00016-0>.
- (23) Merino, P.; Tejero, T.; Delso, I. Current Developments in the Synthesis and Biological Activity of Aza-C-Nucleosides: Immucillins and Related Compounds. *Curr. Med. Chem.* **2008**, *15* (10), 954–967. <https://doi.org/10.2174/092986708784049612>.
- (24) Nash, R. J.; Kato, A.; Yu, C. Y.; Fleet, G. W. Iminosugars as Therapeutic Agents: Recent Advances and Promising Trends. *Future Med. Chem.* **2011**, *3* (12), 1513–1521. <https://doi.org/10.4155/fmc.11.117>.
- (25) Cox, T. M.; Platt, F. M.; Aerts, J. M. F. G. Medicinal Use of Iminosugars. In *Iminosugars*; John Wiley & Sons, Ltd: Chichester, UK, 2008; pp 295–326. <https://doi.org/10.1002/9780470517437.ch13>.
- (26) Cipolla, L.; Asano, N. Iminosugars: The Potential of Carbohydrate Analogs. *Carbohydr. Chem. State Art Challenges Drug Dev.* **2015**, No. 2, 279–301. https://doi.org/10.1142/9781783267200_0011.
- (27) Compain, Philippe; Martin, O. *Iminosugars: From Synthesis to Therapeutic Applications*; Compain, P., Martin, O. R., Eds.; John Wiley & Sons, Ltd: Chichester, UK, 2007. <https://doi.org/10.1002/9780470517437>.
- (28) Esposito, A.; D’Alonzo, D.; De Fenza, M.; De Gregorio, E.; Tamanini, A.; Lippi, G.; Dececchi, M. C.; Guaragna, A. Synthesis and Therapeutic Applications of Iminosugars in Cystic Fibrosis. *Int. J. Mol. Sci.* **2020**, *21* (9), 3353. <https://doi.org/10.3390/ijms21093353>.
- (29) Schramm, V.; Tyler, P. Imino-Sugar-Based Nucleosides. *Curr. Top. Med. Chem.* **2003**, *3* (5), 525–540. <https://doi.org/10.2174/1568026033452465>.
- (30) Evans, G.; Schramm, V.; Tyler, P. The Immucillins: Design, Synthesis and Application of Transition-State Analogues. *Curr. Med. Chem.* **2015**, *22* (34), 3897–3909. <https://doi.org/10.2174/0929867322666150821100851>.
- (31) Evans, G. B.; Furneaux, R. H.; Lewandowicz, A.; Schramm, V. L.; Tyler, P. C. Exploring Structure-Activity Relationships of Transition State Analogues of Human Purine Nucleoside Phosphorylase. *J. Med. Chem.* **2003**, *46* (15), 3412–3423. <https://doi.org/10.1021/jm030145r>.
- (32) Evans, G. B.; Tyler, P. C.; Schramm, V. L. Immucillins in Infectious Diseases. *ACS Infect. Dis.* **2018**, *4* (2), 107–117. <https://doi.org/10.1021/acsinfecdis.7b00172>.
- (33) Bzowska, A.; Kulikowska, E.; Shugar, D. Purine Nucleoside Phosphorylases: Properties, Functions, and Clinical Aspects. *Pharmacol. Ther.* **2000**, *88* (3), 349–425.

- [https://doi.org/10.1016/S0163-7258\(00\)00097-8](https://doi.org/10.1016/S0163-7258(00)00097-8).
- (34) Kicska, G. A.; Long, L.; Hörig, H.; Fairchild, C.; Tyler, P. C.; Furneaux, R. H.; Schramm, V. L.; Kaufman, H. L. Immucillin H, a Powerful Transition-State Analog Inhibitor of Purine Nucleoside Phosphorylase, Selectively Inhibits Human T Lymphocytes. *Proc. Natl. Acad. Sci. U. S. A.* **2001**, *98* (8), 4593–4598. <https://doi.org/10.1073/pnas.071050798>.
- (35) Warren, T. K.; Wells, J.; Panchal, R. G.; Stuthman, K. S.; Garza, N. L.; Van Tongeren, S. A.; Dong, L.; Retterer, C. J.; Eaton, B. P.; Pegoraro, G.; Honnold, S.; Bantia, S.; Kotian, P.; Chen, X.; Taubenheim, B. R.; Welch, L. S.; Minning, D. M.; Babu, Y. S.; Sheridan, W. P.; Bavari, S. Protection against Filovirus Diseases by a Novel Broad-Spectrum Nucleoside Analogue BCX4430. *Nature* **2014**, *508* (7496), 402–405. <https://doi.org/10.1038/nature13027>.
- (36) Taylor, R.; Kotian, P.; Warren, T.; Panchal, R.; Bavari, S.; Julander, J.; Dobo, S.; Rose, A.; El-Kattan, Y.; Taubenheim, B.; Babu, Y.; Sheridan, W. P. BCX4430 - A Broad-Spectrum Antiviral Adenosine Nucleoside Analog under Development for the Treatment of Ebola Virus Disease. *J. Infect. Public Health* **2016**, *9* (3), 220–226. <https://doi.org/10.1016/j.jiph.2016.04.002>.
- (37) <https://Clinicaltrials.gov/Ct2/Show/NCT03800173>.
- (38) <https://clinicaltrials.gov/ct2/show/NCT03891420>.
- (39) Evans, G. B.; Furneaux, R. H.; Gainsford, G. J.; Schramm, V. L.; Tyler, P. C. Synthesis of Transition State Analogue Inhibitors for Purine Nucleoside Phosphorylase and N-Riboside Hydrolases. *Tetrahedron* **2000**, *56* (19), 3053–3062. [https://doi.org/10.1016/S0040-4020\(00\)00194-0](https://doi.org/10.1016/S0040-4020(00)00194-0).
- (40) Evans, G. B.; Furneaux, R. H.; Hutchison, T. L.; Kezar, H. S.; Morris, P. E.; Schramm, V. L.; Tyler, P. C. Addition of Lithiated 9-Deazapurine Derivatives to a Carbohydrate Cyclic Imine: Convergent Synthesis of the Aza- C -Nucleoside Immucillins. *J. Org. Chem.* **2001**, *66* (17), 5723–5730. <https://doi.org/10.1021/jo0155613>.
- (41) Guaragna, A.; D’Errico, S.; D’Alonzo, D.; Pedatella, S.; Palumbo, G. A General Approach to the Synthesis of 1-Deoxy-L-Iminosugars. *Org. Lett.* **2007**, *9* (17), 3473–3476. <https://doi.org/10.1021/ol7014847>.
- (42) Guaragna, A.; D’Alonzo, D.; Paoletta, C.; Palumbo, G. Synthesis of 1-Deoxy-l-Gulonojirimycin and 1-Deoxy-l-Talonojirimycin. *Tetrahedron Lett.* **2009**, *50* (18), 2045–2047. <https://doi.org/10.1016/j.tetlet.2009.02.111>.
- (43) D’Alonzo, D.; De Fenza, M.; Porto, C.; Iacono, R.; Huebecker, M.; Cobucci-Ponzano, B.; Priestman, D. A.; Platt, F.; Parenti, G.; Moracci, M.; Palumbo, G.; Guaragna, A. N-Butyl-l-Deoxynojirimycin (l-NBDNJ): Synthesis of an Allosteric Enhancer of α -Glucosidase Activity for the Treatment of Pompe Disease. *J. Med. Chem.* **2017**, *60* (23), 9462–9469. <https://doi.org/10.1021/acs.jmedchem.7b00646>.
- (44) Pedatella, S.; Guaragna, A.; D’Alonzo, D.; De Nisco, M.; Palumbo, G. Triphenylphosphine Polymer-Bound/Iodine Complex: A Suitable Reagent for the Preparation of O -Isopropylidene Sugar Derivatives. *Synthesis (Stuttg)*. **2006**, No. 2, 305–308. <https://doi.org/10.1055/s-2005-918521>.
- (45) Kamath, V. P.; Juarez-Brambila, J. J.; Morris, C. B.; Winslow, C. D.; Morris, P. E. Development of a Practical Synthesis of a Purine Nucleoside Phosphorylase Inhibitor: BCX-4208. *Org. Process Res. Dev.* **2009**, *13* (5), 928–932. <https://doi.org/10.1021/op9001142>.
- (46) Paal-Knorr Pyrrole Synthesis. In *Comprehensive Organic Name Reactions and Reagents*; John Wiley & Sons, Inc.: Hoboken, NJ, USA, 2010. <https://doi.org/10.1002/9780470638859.conrr475>.

- (47) Evans, G. B.; Furneaux, R. H.; Hausler, H.; Larsen, J. S.; Tyler, P. C. Imino- C -Nucleoside Synthesis: Heteroaryl Lithium Carbanion Additions to a Carbohydrate Cyclic Imine and Nitro. *J. Org. Chem.* **2004**, *69* (6), 2217–2220. <https://doi.org/10.1021/jo035744k>.
- (48) Takahata, H.; Banba, Y.; Sasatani, M.; Nemoto, H.; Kato, A.; Adachi, I. Asymmetric Synthesis of 1-Deoxynojirimycin and Its Congeners from a Common Chiral Building Block. *Tetrahedron* **2004**, *60* (37), 8199–8205. <https://doi.org/10.1016/j.tet.2004.06.112>.

6 SYNTHESIS OF PROPARGYLATED NUCLEOSIDE ANALOGUES FOR VISUALIZATION OF VIRAL REPLICATION

6.1 INTRODUCTION

As widely described in the previous chapters, nucleosides analogues (NAs) are the largest and most successful class of antiviral therapeutics targeting viral enzymes¹⁻⁴. The great pharmacological potential of these compounds relies on their ability to mimic naturally occurring nucleosides and thereby to be recognized by the viral transcriptional machinery. Analogously, owing to this unique feature, NAs have been also employed in several DNA/RNA labelling techniques to track viral genome and proteins during viral infection.⁵

6.1.1 TRACKING VIRAL GENOME

The viral life cycle within host cells includes key events such as attachment, penetration, uncoating, genomic replication and expression, assembly and release, that involve numerous interactions between viral and cellular factors.⁶ As highlighted by the recent COVID-19 pandemic, uncovering the molecular mechanisms beyond these events is crucial for preventing the spread of a certain virus, as well as for a full understanding of virus pathogenesis, that for most viruses remains unclear, and to develop vaccines or therapeutics. In this context, tracking viral genomes during virus infection *via* fluorescent labels has emerged as a valid and powerful approach to elucidate viral biology.⁷

Over the last few decades, several viral labelling techniques for virus tracking in live cells have been developed.⁸ Among these, metabolic incorporation of modified nucleosides into viral genomes or replication intermediates has proven to be a powerful strategy to elucidate virus biology.⁷ The first approach used for the analysis of *in vivo* DNA synthesis involved the incorporation of 5-bromo-2'-deoxyuridine (BrdU; **FIGURE 6.1**) and its detection through recognition by specific antibodies. Since its early applications, this method provided significant advancement in elucidation of the molecular mechanism involved in the virus replication. For example, in 1988 this method highlighted that DNA viruses like herpes simplex virus 1 (HSV-1) form replication compartments and recruit cellular replication machinery.⁹ However, this approach requires specific steps for BrdU detection, including extensive denaturation of the samples to enable the reaction of the incorporated BrdU with the specific antibodies.¹⁰ These limitations were overcome with the DNA/RNA-labelling approaches based on the incorporation into the viral genome of (deoxy)nucleosides bearing a small alkyne moiety. In this context, the first and most successful example is represented by 5-ethynyl-2'-deoxyuridine (EdU; **FIGURE 6.1**), used for the first time in 2008 for the detection of viral DNA replicational activity by Salic and Mitchison.¹¹

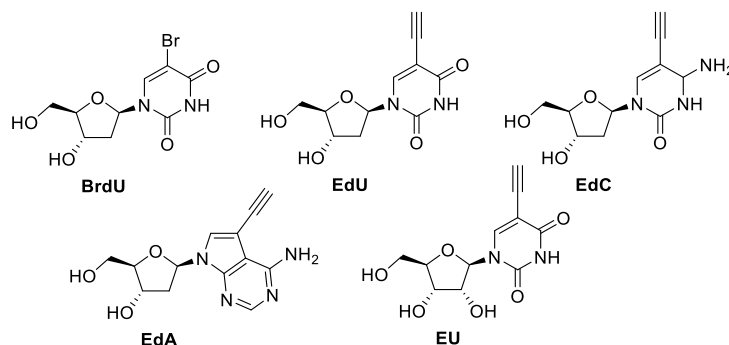


Figure 6.1. Alkyne-containing (deoxy)nucleosides used for DNA/RNA labelling approaches.

On the example of EdU, other alkyne-containing nucleosides were developed such as deoxy-5-ethynylcytidine¹² (EdC) that is the close and less toxic analogue of EdU, 7-deaza-7-ethynyl-2'-deoxyadenosine¹³ (EdA) or the ribonucleoside equivalent of EdU, 5-ethynyl-2'-uridine (EU), developed to label nascent RNA¹⁴ (**FIGURE 6.1**).

6.1.1.1 VIRAL GENOME VISUALIZATION BY CLICK CHEMISTRY

Visualization of DNA/RNA replication by incorporation of EdU and congeners relies on the possibility to introduce fluorescent markers on the triple bond *via* click chemistry.^{15,16}

Indeed, nucleosides bearing an alkyne moiety, as their natural counterparts, are readily recognized by nucleoside kinases. Once converted in their triphosphate form, they are incorporated by polymerases into growing DNA (or RNA) chains (**FIGURE 6.2**). Then, the coupling reaction of the alkyne moiety with an azide-coupled fluorophore (click reaction) through Cu(I)-catalyzed cycloaddition reaction allows the formation of a stable covalent triazole ring conjugate and enables the detection of viral genome.^{7,11}

The major advantage of this DNA/RNA labelling approach relies on the unique features of the click chemistry. Indeed, as the components of this reaction are not found in biological systems, they can proceed in the presence of complex biological mixtures, resulting in low background and high sensitivity in the detection reaction.¹⁷

Over the last years, this approach has been successfully applied to elucidate the biology of several viruses. As mentioned above, in early studies, click labelling technique was employed to visualize HSV-1 and provided novel and important insights into replication of this virus including knowledges about the state of the viral capsid,¹⁸ as well as about the strategy adopted by host cell to counteract HSV-1.¹⁹ Analogously, click labelling also significantly advanced understanding of biology of other DNA viruses such as adenovirus (AdV),²⁰ human papillomaviruses (HPV),²¹ Vaccinia virus,²² as well as click labelling with EdU was exploited to track HIV-1 reverse transcription.^{23,24} In addition, although it has not yet been used as frequently as for DNA viruses, click labeling technology was also used to provide important advancement into understanding of the biology of some family of RNA viruses including filoviruses,²⁵ coronaviruses²⁶ and

arenaviruses.²⁷ As proof of the high potential and versatility of this approach, very recently it was also successful applied to *E. coli*, highlighting the potential of this technique also to study RNA biology in bacterial species.²⁸

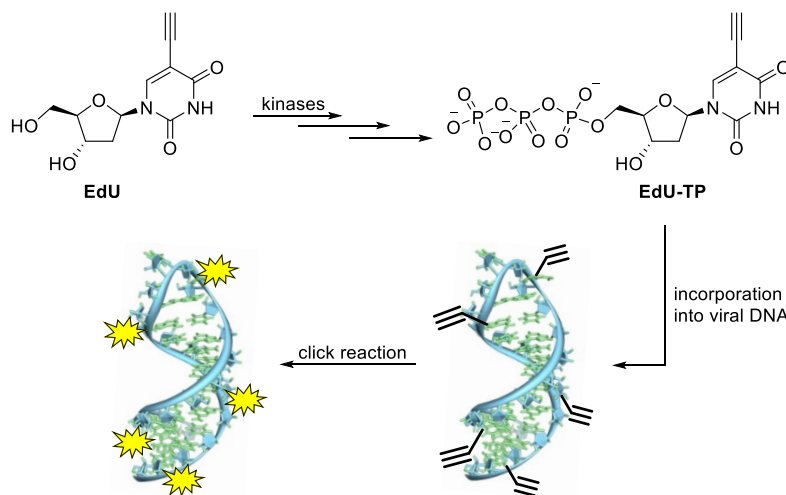


FIGURE 6.2. Phosphorylation and incorporation of EdU and ligation to a fluorophore *via* click reaction.

Despite the great potential of metabolic incorporation of clickable nucleosides for *in vivo* visualization of viral genome, the major limitation of this technique is the lack of selectivity for tracking of viral replication.²⁹ Indeed, EdU (and EdC) is also substrate for cellular polymerases and other metabolic enzymes exhibiting cytotoxicity and causing off-target labelling, resulting in non-specific visualization for the viral processes due to the detection of all nascent DNA (or RNA) molecules.

6.1.1.2. PROPARGYLATED PURINE DEOXYNUCLEOSIDES FOR VISUALIZATION OF HIV-1 REPLICATION

With the aim to obtain virus-specific nucleoside analogues for *in vivo* replication visualization, very recently, Prof. A. Van Aerschot (Medicinal Chemistry, Rega Institute for Medical Research, Department of Pharmaceutical and Pharmacological Sciences, KU Leuven) with his group reported the synthesis of a series of propargylated purine deoxynucleosides **109-116** (FIGURE 6.3). These nucleosides have been conceived to obtain clickable nucleosides able to be selectively incorporated by HIV-1 reverse transcriptase (RT) with the ultimate goal to visualize replicating HIV single particles.³⁰ Biological assays revealed that on one hand, these compounds showed no remarkable cytotoxicity and no antiviral effects against HIV-1 at concentrations below the cytotoxic ones resulting therefore in valid candidates to be used for visualization of viral replication through click chemistry. On the other hand, *in-depth* studies were performed revealing

that none of the analogues negatively affected HIV-1 infectivity, as well as the feasibility of the click reaction and their ability to be incorporated by HIV-1 RT.³¹

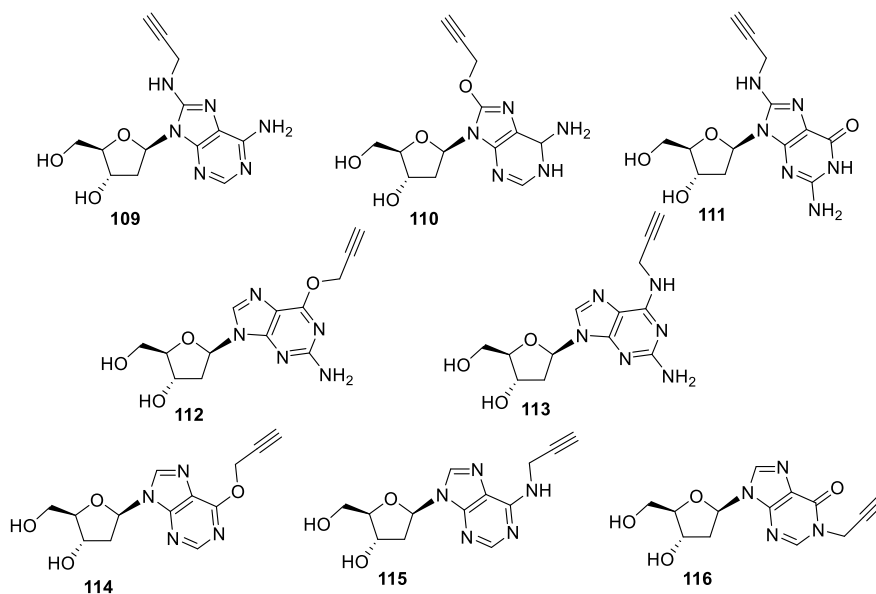


Figure 6.3. Propargyl-containing deoxynucleosides for selective HIV replication visualization developed by Van Aerschot's group [ref 30,31].

Driven by the encouraging results obtained for the propargylated purine deoxynucleosides, the corresponding *ribo*- analogues were herein synthesized in order to extend the potential of these class of nucleosides to the visualization of RNA virus replication. Indeed, the low fidelity of RNA polymerases of some viruses such as HCV and *flaviviruses*, as well as the lack of a proofreading function,^{32,33} should hopefully enable their selective incorporation by viral enzymes without being recognized by cellular polymerases.

6.2 RESULTS AND DISCUSSION

6.2.1 SYNTHESIS OF PROPARGYL-CONTAINING NUCLEOSIDES

Tracking the viral genome by *in vivo* visualization techniques represents a powerful strategy to elucidate and understand virus biology. On these bases, a set of novel propargyl-containing nucleosides (**117-124**; **FIGURE 6.4**) was herein prepared with the aim to obtain clickable nucleoside analogues which would be selectively incorporated into the viral genome without causing off-target labelling of cellular DNA/RNA. Indeed, inspired by the example of EdU and EdC (see **FIGURE 6.1**, **INTRODUCTION**), the introduction of the propargyl group on the nucleobase moiety was conceived to enable viral RNA visualization by insertion of an azide-labeled fluorescent dye through azide-alkyne cycloaddition (click reaction).^{7,15,16}

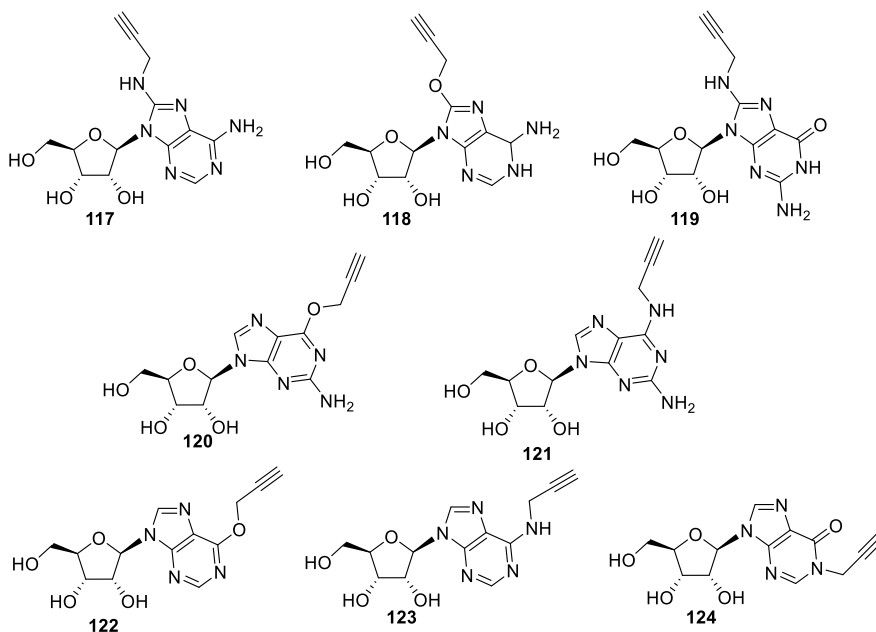


Figure 6.4. Propargyl-containing nucleosides for RNA replication visualization.

This study is part of a research project developed by Prof. Arthur Van Aerschot (Medicinal Chemistry, Rega Institute for Medical Research, Department of Pharmaceutical and Pharmacological Sciences, KU Leuven) and therefore the experiments described below were carried out under his supervision at Rega Institute, KU Leuven in Belgium. Indeed, as briefly described in the previous section, Prof. Van Aerschot with his group reported the synthesis of a series of propargylated purine deoxynucleosides (see **FIGURE 6.3**, **INTRODUCTION**) with the aim

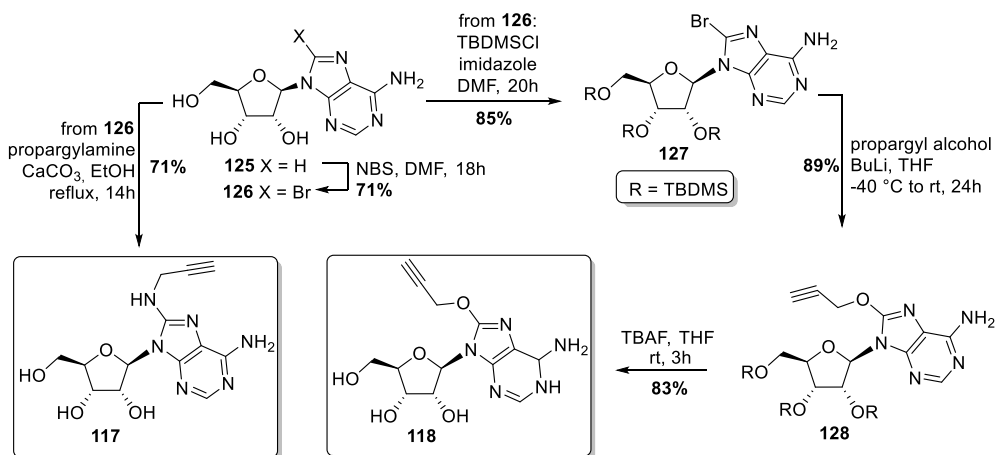
to develop clickable nucleoside able to be selectively incorporated into HIV-DNA thus enabling visualization of replicating single particles.^{30,31}

Driven by the encouraging results obtained for the propargylated purine deoxynucleosides, the corresponding *ribo*- analogues were herein synthesized in order to extend the potential of this class of nucleosides to the visualization of RNA virus replication. Particularly, propargyl moiety was introduced at C8 or C6 position of the nucleobase through either C-N or C-O bond, starting from adenosine, guanosine and inosine as described below. Preliminary biological data to assess the cell cytotoxicity and antiviral properties of the compounds are also provided.

This research was in part supported by University of Napoli Federico II “Programma di Scambi Internazionali con Università ed Istituti di Ricerca Stranieri per la Mobilità di Breve Durata di Docenti, Ricercatori e Studiosi” and KU Leuven (in the frame of Erasmus exchange agreement between University of Napoli and KU Leuven).

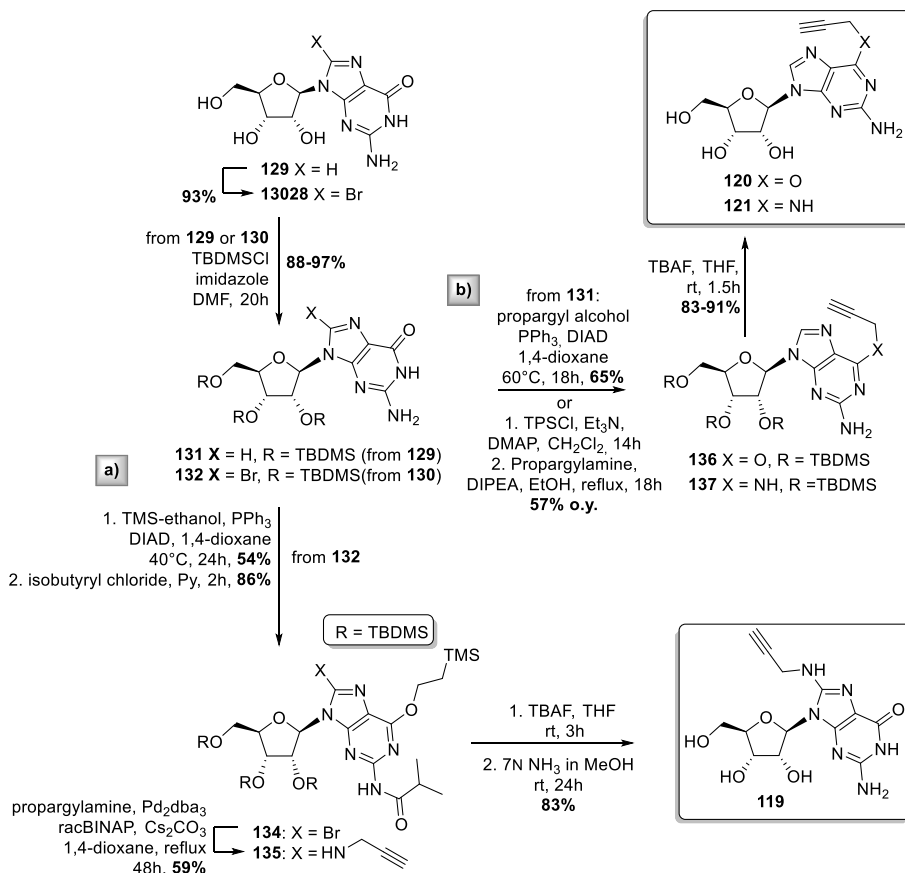
6.2.1.1 SYNTHESIS OF PROPARGYLATED ADENOSINE AND GUANOSINE ANALOGUES

As reported in SCHEMES 6.1 and 6.2A, the synthesis of C8-modified adenosine (**117** and **118**) and guanosine (**119**) analogues required the conversion of the naturally occurring ribonucleosides **125** and **129** in the corresponding 8-bromo derivatives **126** and **130** (NBS/DMF) in order to introduce, *via* nucleophilic substitution, the C-N or C-O bond at the C8 position of the nucleobase. Accordingly, treatment of **126** with propargyl amine in presence of CaCO₃ in refluxing EtOH, gave direct access to the adenosine analogue **117** (SCHEME 6.1).



Scheme 6.1. Synthesis of C8 modified adenosine derivatives **117-118**.

Conversely, the 8-propyloxy-adenosine **118** was obtained by coupling reaction between the *in situ* prepared (nBuLi/THF, -40 °C) propargyl alkoxide and the protected 8-bromo-adenosine **127** (89% yield) followed by treatment with TBAF in THF to remove the TBDMS protective groups (83%). Differently from adenosine analogues **117** and **118**, in the case of the 8-propynylamino-guanosine **119** (SCHEME 6.2A), the introduction of the propynyl moiety at C8 position was achieved by palladium-catalyzed cross coupling reaction³⁴ (Buchwald-Hartwig amination). After protection of the hydroxyl functions (TBDMS/imidazole/DMF), TMS ether group was introduced at *O*⁶ position by Mitsunobu reaction, while the exocyclic amino function was protected by treatment with isobutyryl chloride in pyridine affording the fully protected derivative **134** in 86% yield.

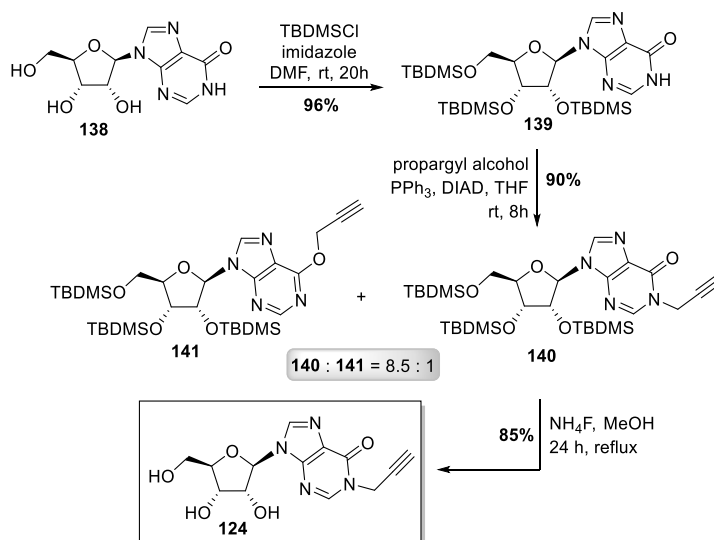


Scheme 6.2. Synthesis of C8 and C6 modified guanosine derivatives **119-121**.

Then, treatment of the latter with propargyl amine in presence of $\text{Pd}_2(\text{dba})_3$, *rac*BINAP (2,2'-bis(diphenylphosphino)-1,1'-binaphthyl) and Cs_2CO_3 in refluxing dioxane yielded, after 48 h, the corresponding C8 propargylated derivative **135** in 59%. Finally, protecting groups removal (TBAF/THF and then 7N NH_3 in MeOH) afforded the desired 8-propynylamino-guanosine **119** in 83% yield. Synthesis of C6 propargylated guanosine analogues **120** and **121** was performed starting from TBDMS-protected guanosine **131** as depicted in SCHEME 6.2B. On one hand, propynyloxy moiety at O^6 position was introduced by Mitsunobu reaction. Treatment of **131** with propargyl alcohol in presence of triphenyl phosphine (PPh_3) and diisopropyl azodicarboxylate (DIAD), in dioxane at 60 °C, provided the derivative **136** (65% yield); subsequent TBDMS groups removal (TBAF/THF) afforded the desired guanosine analogue **120**. On the other hand, access to 6-propynylamino analogue **121** was achieved by C6 activation of **131** with 2,4,6-triisopropyl benzenesulfonyl chloride (TPSCl) and subsequent nucleophilic substitution with propargyl amine in refluxing EtOH in presence of *N,N*-diisopropylethylamine (DIPEA) (57% o.y.) followed by TBDMS groups removal (SCHEME 6.2B).

6.2.1.2 SYNTHESIS OF PROPARGYLATED INOSINE ANALOGUES

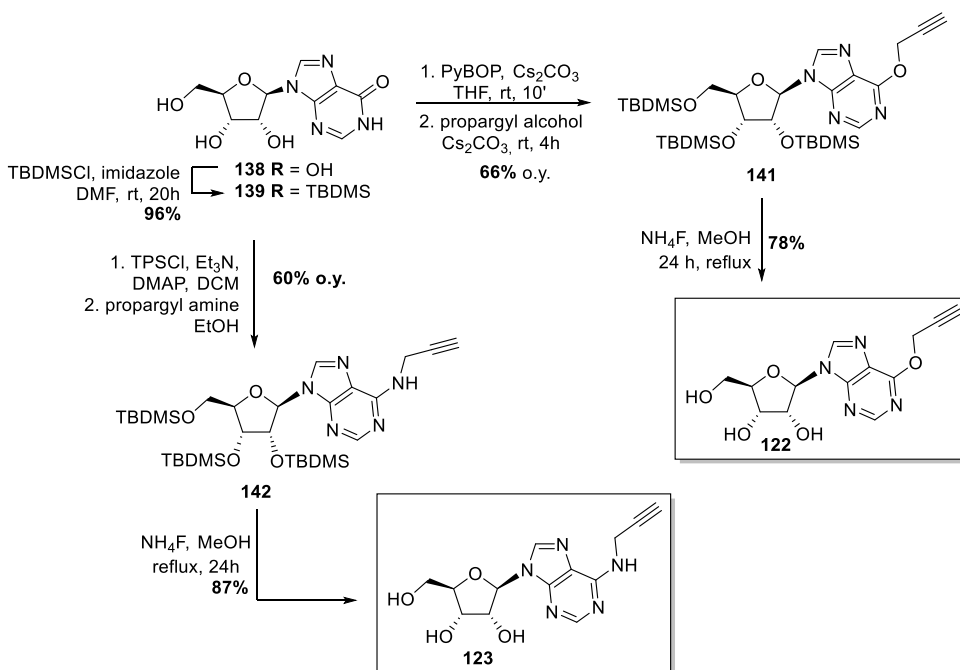
The same synthetic path described above for the synthesis of C6 modified guanosine derivatives **120** and **121** was then exploited to obtain the corresponding inosine analogues. However, when Mitsunobu reaction was performed on the protected inosine **139** (SCHEME 6.3), propargyl moiety was introduced at N^7 position while O^6 -propargylated derivative **141** was obtained in low amount (**140**:**141** = 8.5:1).



Scheme 6.3. Synthesis of inosine derivatives **124**.

Conversely, selective *O*-alkylation was accomplished by *in situ* activation of **139** using benzotriazol-1-yl-oxytripyrrolidinophosphonium hexafluorophosphate (PyBOP) in presence of Cs_2CO_3 followed by coupling reaction with propargyl alcohol (90% yield, (SCHEME 6.4).

The synthesis of the corresponding 6-propynylamino derivative **142** was instead accomplished as previously described for the guanosine analogue (TPSCl/TEA/DMAP and then propargyl amine/DIPEA). Finally, treatment of the protected derivatives **138**, **141**, and **142** with NH_4F in MeOH, used in this case to enable an easier and more efficient purification of the final compounds, led to *N*¹- and *O*⁶-propargylated nucleosides **122**, **123**, and **124** (SCHEMES 6.3 and 6.4).



Scheme 6.4. Synthesis of C6 propargylated derivatives **122** and **123**.

6.2.2 PRELIMINARY BIOLOGICAL ASSAYS

In order to assess the potential of the synthesized nucleosides as tools for visualization of RNA virus replication, preliminary biological assays aimed to evaluate their cell cytotoxicity and potential antiviral effect were performed at Rega Institute for Medical Research by Dr. Suzanne Kaptein. Indeed, lack of cytotoxicity, as well as no inhibitory effect against the target viruses are

essential requirements for the development of successful candidates for visualization of viral replication.

In early studies, cell viability and antiviral properties were evaluated against Zika virus (ZIKV), an RNA virus belonging to the *Flavivirus* genus.³² Previously considered a neglected virus, ZKV has re-emerged more recently for its ability to cause severe neurological disorders, such as microcephaly in newborn babies and Guillain-Barré syndrome in adults.^{35,36} As shown in **TABLE 6.1**, all the compounds showed no remarkable cell toxicity (in all cases CC₅₀ values were >60 μ M) and for concentrations below the cytotoxic one, no antiviral activity against ZIKV MR766 strain was observed, exception made for analogue **120** that exhibited a very interesting activity with an EC₅₀ value of 2.88 μ M.

TABLE 6.1 Cytotoxicity and anti-ZKV activity

Entry	Compound	CC ₅₀ (μ M)	EC ₅₀ (μ M)
1	117	>60	>60
2	118	>60	>60
3	119	>60	>60
4	120	>60	2.88
5	121	>60	>60
6	122	>60	>60
7	123	>60	>60
8	124	>60	>60

CC₅₀: cytotoxic concentration required to reduce cell growth by 50%

EC₅₀: effective concentration required to reduce virus plaque formation by 50%

Starting from these data, further experiments are currently ongoing at Rega Institute for Medical Research. Particularly, studies aimed to evaluate the ability of the synthesized nucleoside analogues to be selectively incorporated by viral polymerases, as well as the feasibility of the click reaction, in order to assess their effective potential as tools for *in vivo* visualization of RNA replication.

6.3 CONCLUDING REMARKS

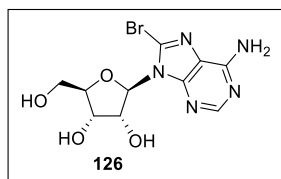
Tracking the viral genome by incorporation of clickable nucleosides represents a powerful strategy to elucidate and understand virus biology. However, the major disadvantage of this approach is the off-target labeling of cellular DNA/RNA that prevents specific visualization of viral genome. Looking for more selective and non-toxic clickable nucleosides for RNA virus life

cycle visualization, a novel set of propargylated ribonucleosides has been herein synthesized. Particularly, propargyl moiety was introduced at C8 or C6 position of the nucleobase through either C-N or C-O bond, starting from natural adenosine, guanosine and inosine. Preliminary biological data to assess the cell cytotoxicity and antiviral properties of the synthesized compounds against Zika virus (ZKV, as an example for *flavivirus*) were also performed. All compounds showed no remarkable cytotoxicity and did not inhibit ZKV virus (exception made for the analogue **118**) and therefore further experiments are currently ongoing in order to assess their effective potential as tools for *in vivo* visualization of RNA replication.

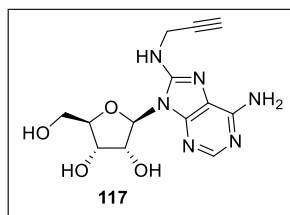
6.4 EXPERIMENTAL SECTION

CHEMICAL SYNTHESIS: GENERAL METHODS

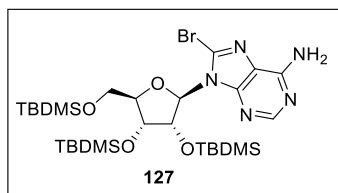
All commercially available reagents and solvents were purchased at the highest degree of purity from commercial sources and used without purification. TLC analysis was carried out on precoated silica gel plate F254 (Merck), and products were visualized under UV radiation or by exposure to iodine vapor and chromic mixture. Column chromatography was performed with silica gel (70–230 mesh, Merck Kiesegel 60). CHNS analysis was performed to assess the purity of compounds and was $\geq 95\%$ in all cases. NMR spectra were recorded on a Bruker 300 MHz. Coupling constant values (J) were reported in Hz.



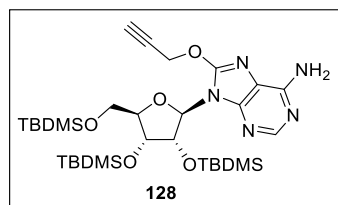
8-Bromo-adenosine (126). To a stirred solution of **125** (2.0 g, 7.48 mmol) in dry DMF (25 mL), NBS (2.63 g, 14.9 mmol) was added in two portions. The suspension was stirred for 24 h at rt turning to red-brown and then the solvent was removed under reduced pressure. Chromatography of the crude residue over silica gel (DCM:MeOH = 92:8) gave the pure **126** (2.0 g, 78% yield) as a white solid. ^1H NMR (300 MHz, DMSO- d_6): δ 3.48-3.59 (m, 1H, H-5'a), 3.64-3.73 (m, 1H, H-5'b), 3.98 (d, J = 2.1, 1H, H-4'), 4.19 (bs, 1H, H-3'), 5.06-5.12 (m, 1H, H-2'), 5.26 (d, J = 4.1, 1H, OH) 5.43-5.56 (m, 2H, OH), 5.83 (d, J = 6.7, 1H, H-1'), 7.59 (bs, 2H, NH₂), 8.1 (s, 1H, H-2). ^{13}C NMR (75 MHz, DMSO- d_6): ppm 62.2, 71.0, 71.2, 86.8, 90.6, 119.8, 127.2, 150.0, 152.5, 155.3; HR-ESI MS (m/z): $[\text{M}+\text{H}]^+$ calcd for C₁₀H₁₃BrN₅O₄, 346.0151; found 346.0138.



8-Propynylamino-adenosine (117). Propargyl amine (0.81 mL, 12.7 mmol) and CaCO_3 (0.13 g, 1.28 mmol) were added to a stirred solution of **126** (0.22 g, 0.63 mmol) in EtOH (17 mL) under nitrogen atmosphere. The mixture was warmed to reflux and stirred for 14 h; afterwards the solution was cooled to rt, filtered and concentrated under reduced pressure. Chromatography of the crude residue over silica gel (DCM:MeOH = 9:1) gave the desired compound **117** as a pale-yellow solid (0.14 g, 71% yield). ^1H NMR (300 MHz, CD_3OD): δ 2.64 (t, $J = 2.5$ Hz, 1H, CH), 3.80 (dd, $J = 1.6, 11.9$, 1H, H-5'a), 3.88 (dd, $J = 2.1, 11.9$, 1H, H-5'b), 4.16 (m, NHCH_2 , H-4'), 4.31 (dd, $J = 1.5, 5.3$, 1H, H-3'), 4.77 (dd, $J = 5.3, 7.3$, 1H, H-2'), 6.03 (d, $J = 7.3$, 1H, H-1'), 8.00 (s, 1H, H-2). ^{13}C NMR (75 MHz, MeOD): ppm 31.0, 61.4, 70.6, 71.0, 71.5, 79.4, 86.0, 87.2, 116.1, 148.4, 149.3, 151.2 152.0. HR-ESI MS (m/z): $[\text{M}+\text{H}]^+$ calcd for $\text{C}_{13}\text{H}_{17}\text{N}_6\text{O}_4$, 321.1311; found 321.1305.

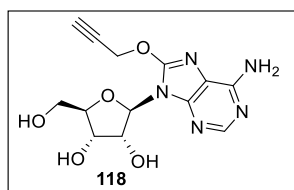


8-Bromo-2',3',5'-O-tri(tert-butyldimethylsilyl)-adenosine (127). To a stirred solution of **125** (0.45 g, 1.3 mmol) in anhydrous DMF (8 mL), TBDMSCl (1.17 g, 7.8 mmol) and imidazole (0.89 g, 13.0 mmol) were added under nitrogen atmosphere. After stirring for 20 h at rt, the reaction mixture was extracted with AcOEt and washed with brine. The organic layer was dried over Na_2SO_4 and the solvent evaporated under reduced pressure. Chromatography of the crude residue over silica gel (hex:AcOEt = 85:15) gave the pure **127** (0.75 g, 85% yield) as a white solid. ^1H NMR (300 MHz, CDCl_3): δ -0.35 (s, 3H, CH_3 -Si), -0.07 (s, 3H, CH_3 -Si), -0.03 (s, 3H, CH_3 -Si), 0.01 (s, 3H, CH_3 -Si), 0.14 (s, 3H, CH_3 -Si), 0.15 (s, 3H, CH_3 -Si), 0.79 (s, 9H, *t*-Bu), 0.83 (s, 9H, *t*-Bu), 0.95 (s, 9H, *t*-Bu), 3.66-3.74 (m, 1H, H-5'a), 4.01-4.10 (m, 2H, H-5'b, H-4'), 4.56 (dd, $J = 2.5, 4.4$, 1H, H-3'), 5.50 (dd, $J = 4.4, 5.6$, 1H, H-2'), 5.58 (bs, 2H, NH_2), 5.93 (d, $J = 5.6$, 1H, H-1'), 8.24 (s, 1H, H-2). ^{13}C NMR (75 MHz): ppm -5.3, -5.1, -4.9, -4.3, -4.2, 18.1, 18.4, 18.6, 25.9, 26.1, 26.2, 62.6, 71.2, 72.1, 72.6, 85.9, 90.9, 120.9, 129.3, 151.2, 152.9, 154.5; HR-ESI MS (m/z): $[\text{M}+\text{H}]^+$ calcd for $\text{C}_{28}\text{H}_{55}\text{BrN}_5\text{O}_4\text{Si}_3$, 688.2745; found 688.2737.



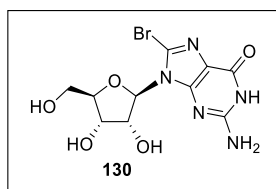
2',3',5'-O-tri(tert-butyldimethylsilyl)-8-propynoxyadenosine (128). To a stirred solution of propargyl alcohol (0.50 mL, 8.60 mmol) in dry THF (10 mL) BuLi (2.5 M solution, 2.5 mL, 6.11 mmol) was slowly added at -40°C under argon atmosphere. In a separate flask, **127** (0.35 g, 0.51 mmol) was dissolved in THF (15 mL) at rt and was slowly added to the in situ generated propargyl alkoxide ion. The resulting mixture was stirred at rt for 24 h and then aq NH_4Cl was added. The solution was extracted with EtOAc and washed with brine. The organic layer was dried over Na_2SO_4 and the solvent

evaporated under reduced pressure. Chromatography of the crude residue over silica gel (hex:AcOEt = 85:15) gave the pure **128** (0.30 g, 89% yield) as a white solid. ^1H NMR (300 MHz, CDCl_3): δ -0.29 (s, 3H, $\text{CH}_3\text{-Si}$), -0.06 (s, 3H, $\text{CH}_3\text{-Si}$), 0.01 (s, 3H, $\text{CH}_3\text{-Si}$), 0.03 (s, 3H, $\text{CH}_3\text{-Si}$), 0.14 (s, 3H, $\text{CH}_3\text{-Si}$), 0.79 (s, 9H, t-Bu), 0.86 (s, 9H, t-Bu), 0.95 (s, 9H, t-Bu), 2.57 (bs, 1H, CH), 3.71 (dd, $J = 4.1, 10.1$, H-5'a), 3.93-4.10 (m, 2H, H-4', H-5'a), 4.51 (bs, 1H, H-3'), 5.12 (d, $J = 2.0$, 1H, OCH_2), 5.19-5.32 (m, 2H, H-2', NH_2), 5.90 (d, $J = 5.8$, 1H, H-1'), 8.21 (s, 1H, H-2). ^{13}C NMR (75 MHz): ppm -5.2, -5.1, -4.8, -4.3, -4.2, 4.1, 18.2, 18.4, 18.6, 26.0, 26.1, 26.2, 57.7, 72.4, 72.7, 76.5, 85.5, 87.3, 116.2, 150.4, 151.5, 153.5, 154.4; HR-ESI MS (m/z): $[\text{M}+\text{H}]^+$ calcd for $\text{C}_{31}\text{H}_{58}\text{N}_5\text{O}_5\text{Si}_3$, 664.3745; found 664.3760.



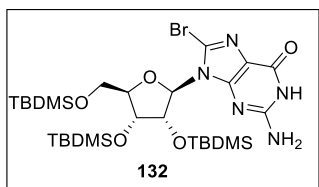
8-Propynyloxy-adenosine (118). To a stirred solution of **128** (0.30 g, 0.45 mmol) in THF (10 mL), tetrabutylammonium fluoride (1M solution in THF, 1.80 mL, 1.80 mmol) was added at 0°C . The reaction mixture was warmed to rt and stirred for 3 h; afterwards the solvent was removed under reduced pressure.

Chromatography of the crude residue over silica gel (DCM:MeOH = 93:7) gave the pure **118** (0.12 g, 83% yield) as a white solid. ^1H NMR (300 MHz, $\text{DMSO-}d_6$): δ 3.45-3.56 (m, 1H, H-5'a), 3.59-3.69 (m, 1H, H-5'b), 3.75 (t, $J = 2.3$ Hz, 1H, CH), 3.91 (dd, $J = 4.0, 6.9$, 1H, H-4'), 4.13 (dd, $J = 4.8, 6.9$, 1H, H-3'), 4.88-4.96 (m, 1H, H-2'), 5.20 (d, $J = 4.8$, 1H, OH), 5.20-5.22 (m, 2H, OCH_2), 5.32-5.43 (m, 2H, OH), 5.73 (d, $J = 6.7$, 1H, H-1'), 7.04 (bs, 1H, NH_2), 8.05 (s, 1H, H.2). ^{13}C NMR (125 MHz, $\text{DMSO-}d_6$): ppm 57.6, 62.3, 71.0, 71.1, 78.0, 79.3, 86.1, 86.8, 114.8, 148.8, 150.9, 152.9, 154.2. HR-ESI MS (m/z): $[\text{M}+\text{H}]^+$ calcd for $\text{C}_{13}\text{H}_{16}\text{N}_5\text{O}_5$, 322.1151; found 322.1152.



8-Bromo-guanosine (130). To a stirred solution of **129** (0.60 g, 2.11 mmol) in ACN (24 mL) and H_2O (6 mL), NBS (0.56 g, 3.17 mmol) was added in two portions. The orange suspension was stirred for 30 min at rt and then the solvent was removed under reduced pressure. Cold acetone (20 mL) was added and the resulting suspension was stirred for 1h at rt. The residual solid was filtered, washed with cold

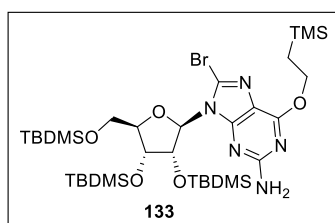
acetone and dried under reduced pressure to give the pure **130** (0.71 g, 93% yield) as an orange solid. ^1H NMR (300 MHz, $\text{DMSO-}d_6$): 3.51 (dd, $J = 5.6, 11.7$, 1H, H-5'a), 3.66 (dd, $J = 4.9, 11.7$, 1H, H-5'b), 3.81-3.90 (m, 1H, H-4'), 4.13 (dd, $J = 3.4, 5.1$, 1H, H-3'), 5.01 (t, $J = 5.7$, 1H, H-2'), 5.69 (d, $J = 6.0$, 1H, H-1'), 6.52 (bs, 2H, NH_2), 10.8 (bs, 1H, NH). ^{13}C NMR (75 MHz): ppm 62.1, 70.5, 70.6, 86.0, 89.9, 117.6, 121.3, 152.2, 153.6, 155.6. HR-ESI MS (m/z): $[\text{M}+\text{H}]^+$ calcd for $\text{C}_{10}\text{H}_{13}\text{BrN}_5\text{O}_5$, 362.0100; found 362.0104.



8-Bromo-2',3',5'-O-tri(tert-butyldimethylsilyl)- guanosine

(132). To a stirred solution of **130** (0.54 g, 1.50 mmol) in anhydrous DMF (8 mL), TBDMSCl (1.13 g, 7.5 mmol) and imidazole (1.02 g, 15.0 mmol) were added under nitrogen atmosphere. After stirring for 20 h at rt, the reaction mixture was diluted with EtOAc and washed with brine until neutral. The

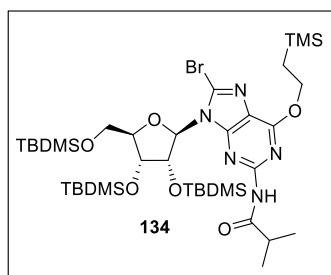
organic layer was dried with Na₂SO₄ and the solvent evaporated under reduced pressure. Chromatography of the crude residue over silica gel (DCM:MeOH = 98:2) gave the pure **132** (1.00 g, 97% yield) as a yellow solid. ¹H NMR (300 MHz, CDCl₃): δ -0.23 (s, 3H, CH₃-Si), -0.26 (s, 3H, CH₃-Si), 0.03 (s, 3H, CH₃-Si), 0.06 (s, 3H, CH₃-Si), 0.16 (s, 3H, CH₃-Si), 0.82 (s, 9H, *t*-Bu), 0.88 (s, 9H, *t*-Bu), 0.96 (s, 9H, *t*-Bu), 3.75 (dd, *J* = 2.9, 9.7, 1H, H-5'a), 3.93-4.1 (m, 2H, H-4', H-5'b), 4.47 (bs, 1H, H-3'), 5.33 (t, *J* = 5.5, 1H, H-2'), 6.01 (d, *J* = 5.5, 1H, H-1'), 6.42 (bs, 2H, NH₂), 11.9 (bs, 1H, NH). ¹³C NMR (75 MHz): ppm -5.3, -5.2, -4.9, -4.4, -4.3, -4.2, 18.0, 18.2, 18.5, 25.9, 26.0, 62.7, 71.6, 72.5, 85.7, 90.4, 118.4, 123.4, 152.7, 153.3, 157.9; HR-ESI MS (*m/z*): [M+H]⁺ calcd for C₂₈H₅₅BrN₅O₅Si₃, 704.2694; found 704.2717.



8-Bromo-2',3',5'-O-tri(tert-butyldimethylsilyl)-6-O-(trimethylsilylethyl)-guanosine (133).

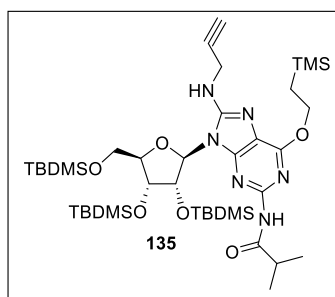
To a stirred solution of **132** (1.7 g, 2.46 mmol) in anhydrous 1,4 dioxane (28 mL) triphenylphosphine (0.97 g, 3.7 mmol) and 2-(trimethylsilyl)ethanol (0.53 mL, 3.7 mmol) were added under nitrogen atmosphere. The mixture was stirred for 10 min, cooled to 0 °C and then, DIAD (0.73 mL, 3.7 mmol) was

added. The reaction mixture was stirred at 40 °C for 24 h, and then the solvent was removed under reduced pressure. The crude was diluted with EtOAc and washed with brine. The organic layer was dried with Na₂SO₄, filtered and the solvent evaporated under reduced pressure. Chromatography of the crude residue over silica gel (hexane:EtOAc = 95:5) gave the pure **133** (1.16 g, 59% yield) as a yellow solid. ¹H NMR (300 MHz, CDCl₃): δ -0.28 (s, 3H, CH₃-Si), -0.06 (s, 3H, CH₃-Si), -0.01 (s, 3H, CH₃-Si), 0.03 (s, 3H, CH₃-Si), 0.08 (s, 9H, CH₃-Si), 0.15 (s, 3H, CH₃-Si), 0.16 (s, 3H, CH₃-Si), 0.81 (s, 9H, *t*-Bu), 0.86 (s, 9H, *t*-Bu), 0.96 (s, 9H, *t*-Bu), 1.17-1.27 (m, 2H, CH₂Si), 3.72 (dd, *J* = 3.1, 9.6, 1H, H-5'a), 3.93-4.0 (m, 2H, H-4', H-5'b), 4.48-4.59 (m, 3H, H-3', OCH₂), 4.70 (bs, 1H, NH₂), 5.40 (dd, *J* = 4.6, 5.6, 1H, H-2'), 5.87 (d, *J* = 5.6, 1H, H-1'). ¹³C NMR (75 MHz): ppm -5.3, -5.2, -4.9, -4.4, -4.3, -4.2, -1.3, 17.7, 18.0, 18.2, 18.5, 25.8, 26.0, 26.1, 62.6, 65.2, 71.6, 72.4, 85.3, 90.3, 116.9, 126.5, 154.3, 158.8, 160.5; HR-ESI MS (*m/z*): [M+H]⁺ calcd for C₃₃H₆₇BrN₅O₅Si₄, 804.3402; found 804.3400.



8-Bromo-2',3',5'-O-tri(tert-butyl dimethylsilyl)-2-N-isobutyryl-6-O-(trimethylsilylethyl)guanosine (134). To a stirred solution of **133** (0.87 g, 1.08 mmol) in anhydrous pyridine (9 mL) isobutyrylchloride (0.23 mL, 2.16 mmol) was added at 0 °C under nitrogen atmosphere. The mixture was stirred for 10 min, cooled at rt for 2 h and then saturated NaHCO₃ was added. The resulting solution was extracted with DCM and washed with brine. The combined organic layers were dried (Na₂SO₄) and the solvent evaporated under reduced

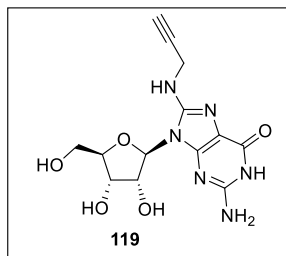
pressure. Chromatography of the crude residue over silica gel (hexane:EtOAc = 9:1) gave the pure **134** (0.81 g, 86% yield) as a white solid. ¹H NMR (300 MHz, CDCl₃): δ -0.39 (s, 3H, CH₃-Si), -0.08 (s, 3H, CH₃-Si), 0.05 (s, 6H, CH₃-Si), 0.09 (s, 9H, CH₃-Si), 0.14 (s, 3H, CH₃-Si), 0.16 (s, 3H, CH₃-Si), 0.75 (s, 9H, *t*-Bu), 0.87 (s, 9H, *t*-Bu), 0.96 (s, 9H, *t*-Bu), 1.21-1.29 (m, 8H, CH₂Si, CH₃*i*Pr), 3.02-1.17 (m, 1H, CH*i*Pr), 3.75 (dd, *J*=9.0, 15.1 Hz, 1H, H-5'*a*), 4.01-4.12 (m, 2H, H-4', H-5'*b*), 4.41 (d, *J*=4.6, 1H, H-3'), 4.55-4.62 (m, 2H, OCH₂), 5.51 (dd, *J*=4.6, 6.8, 1H, H-2'), 5.98 (d, *J*=6.8 Hz, 1H, H-1'), 7.63 (bs, 1H, NH). ¹³C NMR (75 MHz): ppm -5.2, -5.1, -5.0, -4.2, -4.1, -1.2, 17.8, 18.1, 18.3, 18.6, 19.5, 19.6, 25.9, 26.1, 26.2, 35.9, 63.2, 66.2, 71.5, 72.9, 86.5, 90.1, 119.2, 129.3, 151.8, 153.7, 160.3, 175.4. HR-ESI MS (*m/z*): [M+H]⁺ calcd for C₃₇H₇₃BrN₅O₆Si₄, 874.3821; found 874.3795.



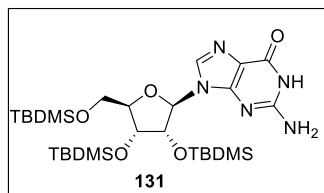
2',3',5'-O-tri(tert-butyl dimethylsilyl)-2-N-isobutyryl 8-propynylamino-6-O-(trimethylsilylethyl)guanosine (135). To a stirred solution of **134** (0.75 g, 0.86 mmol) in dry 1,4 dioxane (23 mL), propargyl amine (79 μL, 1.21 mmol), Pd₂dba₃ (75 mg, 0.10 mmol), *rac*BINAP (0.15 g, 0.24 mmol) and Cs₂CO₃ (0.4 g, 1.21 mmol) were added under nitrogen atmosphere. The mixture was heated to reflux. After 48 h the solution was cooled to rt, NaHCO₃ was added and the mixture was extracted with EtOAc. The organic layer was dried with

Na₂SO₄, filtered and the solvent evaporated under reduced pressure. Chromatography of the crude residue over silica gel (hexane:EtOAc = 85:15) gave the pure **135** (0.43 g, 59% yield) as a white solid. ¹H NMR (300 MHz, CDCl₃): δ -0.41 (s, 3H, CH₃-Si), -0.11 (s, 3H, CH₃-Si), 0.01 (s, 9H, CH₃-Si), 0.09 (s, 3H, CH₃-Si), 0.11 (s, 3H, CH₃-Si), 0.17 (s, 3H, CH₃-Si), 0.19 (s, 3H, CH₃-Si), 0.67 (s, 9H, *t*-Bu), 0.94 (s, 9H, *t*-Bu), 0.97 (s, 9H, *t*-Bu), 1.20-1.28 (m, 8H, CH₂Si, CH₃*i*Pr), 2.18 (t, *J*=2.5, 1H, CH), 3.75-3.80 (m, 1H, CH*i*Pr), 3.81 (dd, *J*=2.3, 11.6, 1H, H-5'*a*), 3.92 (dd, *J*=2.5, 11.6, 1H, H-5'*b*), 4.07 (bs, 1H, H-4'), 4.12 (bd, *J*=4.8, 1H, H-3'), 4.19 (ddd, *J*=2.5, 4.6, 16.8, 1H, CHNH), 4.41 (dd, *J*=2.5, 7.1, 16.8, 1H, CHNH), 4.47-4.61 (m, 3H, H-3', OCH₂), 5.85 (dd, *J*=4.6, 7.1, 1H, NH), 6.05 (d, *J*=7.0, 1H, H-1'), 7.65 (bs, 1H, HN). ¹³C NMR (75 MHz): ppm -5.2, -5.1, -4.7, -4.3, -4.2, -1.2, 18.0, 18.1, 18.3, 19.0, 19.4, 19.5, 25.8, 26.1, 26.4, 32.7,

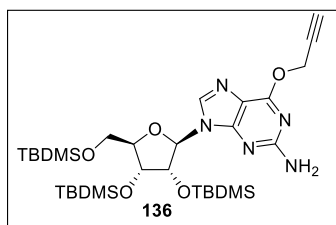
33.7, 63.8, 65.4, 71.5, 72.2, 72.7, 81.0, 85.9, 86.9, 90.1, 115.6, 149.5, 151.8, 154.2, 158.1, 178.6. HR-ESI MS (m/z): $[M+H]^+$ calcd for $C_{40}H_{77}N_6O_6Si_4$, 849.4981; found 849.4961.



8-Propynylamino-guanosine (119). TBAF (1 M solution in THF, 3.04 mL, 3.04 mmol) was added to a stirred solution of **133** (0.43 g, 0.51 mmol) in THF (16 mL) at 0 °C. The mixture was stirred at rt for 3 h and then the solvent was removed under reduced pressure. Chromatography of the crude residue over silica gel (EtOAc:MeOH = 9:1) gave the pure intermediate. The latter was dissolved in 7 N NH_3 in MeOH and was stirred for 24h at rt; afterwards the solvent was removed under reduced pressure and the white solid was suspended in EtOAc:MeOH: NH_3 = 7:2.5:0.5 and filtered with the same solvents. The filtrate was concentrated under reduced pressure and the crude residue triturated with acetone to give the pure **119** (0.14 g, 84% overall yield). 1H NMR (300 MHz, $DMSO-d_6$): δ 3.05 (bs, 1H, CH), 3.63 (bs, 2H, H-5'), 3.90 (bs, 1H, H-4'), 3.98 (bs, 2H, $NHCH_2$), 4.08 (d, J = 3.6, 1H, H-3'), 4.51 (t, J = 6.5, 1H, H-2'), 5.73 (d, J = 6.5, 1H, H-1'), 6.27 (bs, 1H, NH_2), 6.75 (t, J = 5.5, 1H, NH). ^{13}C NMR (75 MHz): ppm 31.7, 61.5, 70.5, 71.0, 72.6, 82.2, 85.4, 86.3, 112.7, 147.8, 150.7, 152.3, 155.5. HR-ESI MS (m/z): $[M+H]^+$ calcd for $C_{13}H_{17}N_6O_5$, 337.1260; found 337.1254.

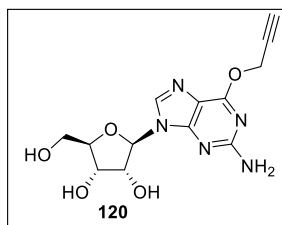


2',3',5'-O-tri(tert-butyldimethylsilyl)-guanosine (131). TBDMSCl (2.23 g, 14.8 mmol) and imidazole (1.68 g, 24.7 mmol) were added to a stirred solution of **129** (0.7 g, 2.47 mmol) in anhydrous DMF (13 mL) under nitrogen atmosphere. After 24 h, the mixture was diluted with EtOAc and aq. NH_4Cl . The resulting solution was extracted with EtOAc and washed with brine. The combined organic layers were dried (Na_2SO_4) and the solvent evaporated under reduced pressure. Chromatography of the crude residue over silica gel (DCM:MeOH = 96:4) gave the pure **131** (1.36 g, 88% yield) as a white solid. 1H NMR (300 MHz, $CDCl_3$): δ -0.04 (s, 3H, CH_3-Si), 0.02 (s, 3H, CH_3-Si), 0.09 (s, 3H, CH_3-Si), 0.10 (s, 3H, CH_3-Si), 0.13 (s, 3H, CH_3-Si), 0.14 (s, 3H, CH_3-Si), 0.86 (s, 9H, $t-Bu$), 0.92 (s, 9H, $t-Bu$), 0.96 (s, 9H, $t-Bu$), 3.77 (dd, J = 2.2, 11.5, 1H, H-5'a), 4.0 (dd, J = 3.5, 11.5, 1H, H-5'b), 4.04-4.12 (m, 1H, H-4'), 4.29 (t, J = 4.1, 1H, H-3'), 4.44 (t, J = 3.8, 1H, H-2'), 5.82 (d, J = 4.0, 1H, H-1'), 6.05-6.23 (m, 2H, NH_2); 7.90 (s, 1H, H.8). ^{13}C NMR (75 MHz): -5.1, -4.5, -4.4, -4.0, 0.2, 18.2, 18.3, 18.8, 26.0, 26.1, 26.4, 62.5, 71.7, 76.4, 84.9, 88.5, 117.9, 136.4, 151.9, 153.7, 159.5. HR-ESI MS (m/z): $[M+H]^+$ calcd for $C_{28}H_{56}N_5O_5Si_3$, 626.3589; found 626.3600.

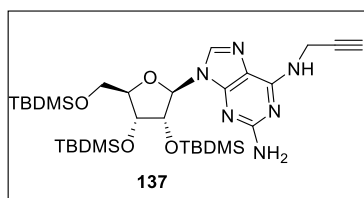


2',3',5'-O-tri(tert-butyldimethylsilyl)-6-O-propynyl-guanosine (136). To a solution of **131** (0.50 g, 0.80 mmol) in anhydrous 1,4 dioxane (32 mL) triphenylphosphine (0.25 g, 0.95 mmol) was added under nitrogen atmosphere. The mixture was heated at 60 °C to allow a complete solubilization of nucleoside **131** and after stirring for 30 min propargyl alcohol (69 μ L, 1.20 mmol) was added. The solution was

stirred for 30 min and then, DIAD (0.24 mL, 1.20 mmol) was added. The reaction mixture was stirred at 60 °C for 18 h, and then the solvent was removed under reduced pressure. The crude residue was chromatographed over silica gel (hexane:EtOac = 85:15) to give the pure **136** (0.34 g, 65% yield) as a white solid. ^1H NMR (300 MHz, CDCl_3): δ -0.14 (s, 3H, CH_3 -Si), -0.02 (s, 3H, CH_3 -Si), 0.09 (s, 3H, CH_3 -Si), 0.12 (s, 6H, CH_3 -Si), 0.13 (s, 3H, CH_3 -Si), 0.82 (s, 9H, *t*-Bu), 0.92 (s, 9H, *t*-Bu), 0.94 (s, 9H, *t*-Bu), 2.46 (t, $J = 2.4$, 1H, CH), 3.79 (dd, $J = 2.5$, 11.4, 1H, H-5'a), 3.98 (dd, $J = 3.7$, 11.4, 1H, H-5'b), 4.07-4.12 (m, 1H, H-4'), 4.29 (t, $J = 4.6$ Hz, 1H, H-3'), 4.47 (t, $J = 4.6$, 1H, H-2'), 4.94 (bs, 2H, NH_2), 5.11 (d, $J = 2.4$, 2H, OCH_2), 5.91 (d, $J = 4.6$, 1H, H-1'), 8.01 (s, 1H, H.8). ^{13}C NMR (75 MHz): -5.1, -4.6, -4.5, -4.4, -4.0, 18.2, 18.4, 18.8, 26.0, 26.1, 26.4, 54.0, 62.7, 72.0, 75.0, 76.3, 78.7, 85.2, 88.3, 138.7, 138.9, 154.4, 159.2, 160.1. HR-ESI MS (m/z): $[\text{M}+\text{H}]^+$ calcd for $\text{C}_{31}\text{H}_{58}\text{N}_5\text{O}_5\text{Si}_3$, 664.3745; found 664.3766.

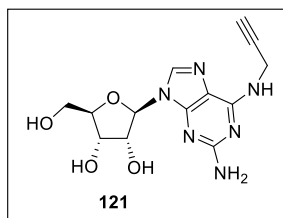


6-O-Propynyl-guanosine (120). To a solution of **136** (0.32 g, 0.49 mmol) in THF (15 mL), tetrabutylammonium fluoride (1M solution in THF, 1.96 mL, 1.96 mmol) was added at 0°C. The reaction mixture was warmed to rt and stirred for 1.5 h; afterwards the solvent was removed under reduced pressure. Chromatography of the crude residue over silica gel (DCM:MeOH = 95:5) gave the pure **120** (0.13 g, 83% yield) as a white solid. ^1H NMR (300 MHz, CDCl_3): δ 2.98 (t, $J = 2.1$ Hz, 1H, CH), 3.76 (dd, $J = 2.1$, 12.2, 1H, H-5'a), 3.91 (dd, $J = 2.1$, 12.4, 1H, H-5'b), 4.12-4.18 (m, 1H, H-4'), 4.33 (dd, $J = 2.7$, 4.7, 1H, H-3'), 4.74 (t, $J = 5.8$, 1H, H-2'), 5.15 (s, 2H, OCH_2), 5.88 (d, $J = 5.8$, 1H, H-1'), 8.07 (s, 1H, H.8). ^{13}C NMR (75 MHz): ppm 53.1, 61.8, 70.9, 73.4, 74.8, 77.5, 86.1, 89.2, 114.3, 139.0, 152.8, 159.5. HR-ESI MS (m/z): $[\text{M}+\text{H}]^+$ calcd for $\text{C}_{13}\text{H}_{16}\text{N}_5\text{O}_5$, 322.1151; found 322.1152.



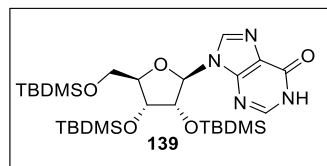
2',3',5'-O-tri(tert-butyldimethylsilyl)-6-N-propynyl -2,6-diaminopurine-ribose (137). To a stirred solution of **129** (1.2 g, 1.92 mmol) in dry DCM (30 mL) triethylamine (0.52 mL, 3.06 mmol), 2,4,6-triisopropylphenylsulfonyl chloride (0.93 g, 3.06 mmol) and DMAP (0.02 g, 0.24 mmol) were added under nitrogen atmosphere. The reaction mixture was stirred for 48 h and then was diluted with DCM. The organic

layer was washed with brine, dried over Na_2SO_4 and the solvent evaporated under reduced pressure. The crude mixture was dissolved in EtOH (45 mL) and propargylamine (0.61 mL, 9.37 mmol) and DIPEA (1.68 mL, 9.37 mL) were added. The solution was heated to reflux. After 18 h, the reaction mixture was cooled to rt, quenched with water and EtOH was removed under reduced pressure. The aqueous layer was extracted with EtOAc. The organic layer was washed with brine, dried over Na_2SO_4 and the solvent evaporated under reduced pressure. Chromatography of the crude residue over silica gel (hex/EtOAc = 85:15) gave the pure **137** (0.72 g, 57% yield over two steps) as a white solid. ^1H NMR (300 MHz, CDCl_3): δ -0.15 (s, 3H, CH_3 -Si), -0.03 (s, 3H, CH_3 -Si), 0.09 (s, 3H, CH_3 -Si), 0.11 (s, 6H, CH_3 -Si), 0.12 (s, 3H, CH_3 -Si), 0.82 (s, 9H, *t*-Bu), 0.92 (s, 9H, *t*-Bu), 0.94 (s, 9H, *t*-Bu), 2.23 (t, $J = 2.5$, 1H, CH), 3.75 (dd, $J = 3.8$, 11.3, 1H, H-5'a), 3.98 (dd, $J = 4.2$, 11.3, 1H, H-5'b), 4.03-4.11 (m, 1H, H-4'), 4.28 (t, $J = 4.2$, 1H, H-3'), 4.36 (bs, 2H, NH_2), 4.56 (t, $J = 4.9$, 1H, H-2'), 4.77 (bs, 2H, NHCH_2), 5.78 (bs, 1H, NH), 5.86 (d, $J = 4.9$, 1H, H-1'), 7.83 (s, 1H, H-8). ^{13}C NMR (125 MHz): ppm -5.1, -4.6, -4.3; -4.4, -4.0, 18.2, 18.4, 18.8, 26.0, 26.2, 26.4, 30.5, 62.8, 71.6, 72.1, 75.9, 80.6, 85.2, 88.2, 115.4, 136.8, 151.6, 154.6, 159.9. HR-ESI MS (m/z): $[\text{M}+\text{H}]^+$ calcd for $\text{C}_{31}\text{H}_{59}\text{N}_6\text{O}_4\text{Si}_3$, 663.3905; found 663.3907.



6-*N*-Propynyl-2,6-diaminopurine-ribose (121). To a stirred solution of **137** (0.7 g, 1.05 mmol) in THF (33 mL), tetrabutylammonium fluoride (1M solution in THF, 4.22 mL, 4.22 mmol) was added at 0°C . The reaction mixture was warmed to rt and stirred for 1.5 h; afterwards the solvent was removed under reduced pressure. Chromatography of the crude residue over silica gel (DCM:MeOH = 93:7) gave the pure **121** (0.30 mg, 91% yield) as a white solid.

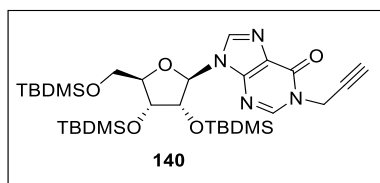
^1H NMR (300 MHz, MeOD): 2.62 (t, $J = 2.5$ Hz, 1H, CH), 3.75 (dd, $J = 2.2$, 12.4, 1H, H-5'a), 3.91 (dd, $J = 2.2$, 12.4, 1H, H-5'b), 4.16 (d, $J = 2.2$, 1H, H-4'), 4.30 (dd, $J = 1.9$, 5.0, 1H, H-3'), 4.34 (bs, 2H, NHCH_2), 4.77 (dd, $J = 3.7$, 6.7, 1H, H-2'), 5.87 (d, $J = 6.7$, 1H, H-1'), 7.89 (s, 1H, H-8). ^{13}C NMR (75 MHz): 70.0, 70.3, 71.2, 73.1, 79.7, 86.4, 89.5, 114.0, 137.2, 149.8, 154.3, 159.7. HR-ESI MS (m/z): $[\text{M}+\text{H}]^+$ calcd for $\text{C}_{13}\text{H}_{17}\text{N}_6\text{O}_4$, 321.1311; found 321.1307



2',3',5'-*O*-tri(tert-butyldimethylsilyl)-inosine (139). To a stirred solution of **138** (0.60 g, 2.24 mmol) in anhydrous DMF (12 mL), TBDMSCl (2.02 g, 13.4 mmol) and imidazole (1.52 g, 22.4 mmol) were added under nitrogen atmosphere. After stirring for 20 h at rt, the reaction mixture was extracted with EtOAc and washed with brine. The organic layer was dried over

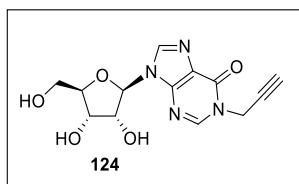
Na_2SO_4 and the solvent evaporated under reduced pressure. Chromatography of the crude residue over silica gel (DCM:MeOH = 98:2) gave the pure **139** (1.31 g, 96% yield) as a white solid. ^1H NMR (300 MHz, CDCl_3): δ -0.17 (s, 3H, CH_3 -Si), -0.01 (s, 3H, CH_3 -Si), 0.10 (s, 3H, CH_3 -Si),

0.11 (s, 3H, CH₃-Si), 0.14 (s, 3H, CH₃-Si), 0.16 (s, 3H, CH₃-Si), 0.82 (s, 9H, *t*-Bu), 0.93 (s, 9H, *t*-Bu), 0.96 (s, 9H, *t*-Bu), 3.80 (dd, *J* = 2.5, 11.4, 1H, H-5'a), 4.0 (dd, *J* = 3.7, 11.4, 1H, H-5'b), 4.10-4.15 (m, 1H, H-4'), 4.30 (t, *J* = 4.0, 1H, H-3'), 4.50 (t, *J* = 4.8 Hz, 1H, H-2'), 6.01 (d, *J* = 4.8, 1H, H-1'), 8.18 (s, 1H, H.8), 8.25 (s, 1H, H-2). ¹³C NMR (75 MHz): ppm -5.3, -4.9, -4.6, -4.3, 17.9, 18.2, 18.6, 27.8, 25.9, 26.2, 62.6, 71.9, 76.7, 85.6, 88.5, 125.2, 139.2, 144.8, 149.2, 159.5; HR-ESI MS (*m/z*): [M+H]⁺ calcd for C₂₈H₅₅N₄O₅Si₃, 611.3480; found 611.3438.

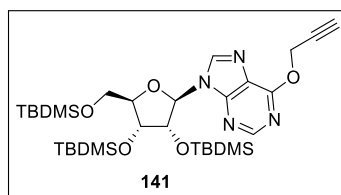


***N*¹-Propynyl-2',3',5'-*O*-tri(*tert*-butyldimethylsilyl) inosine (140).** To a solution of **139** (0.20 g, 0.33 mmol) in anhydrous THF (15 mL) at rt and under nitrogen atmosphere, triphenylphosphine (0.10 g, 0.39 mmol) and propargyl alcohol (28 μL, 0.49 mmol) were added. The solution was stirred for 30 min and then, DIAD (96 μL,

0.49 mmol) was added. The reaction mixture was kept at rt for 8 h, and then the solvent was removed under reduced pressure. The crude residue was chromatographed over silica gel to give **141** (hexane:EtOAc = 9:1; 0.02 g, 10% yield) as a white solid and **140** (hexane:EtOAc = 7:3, 0.17 g, 81% yield) as a white solid (o.y. 90%, **140**:**141** = 8.5:1). Data for **140**. ¹H NMR (500 MHz, CDCl₃): δ -0.17 (s, 3H, CH₃-Si), -0.02 (s, 3H, CH₃-Si), 0.09 (s, 3H, CH₃-Si), 0.10 (s, 3H, CH₃-Si), 0.13 (s, 3H, CH₃-Si), 0.14 (s, 3H, CH₃-Si), 0.81 (s, 9H, *t*-Bu), 0.93 (s, 9H, *t*-Bu), 0.95 (s, 9H, *t*-Bu), 2.51 (t, *J* = 2.6, 1H, CH), 3.79 (dd, *J* = 2.5, 11.4, 1H, H-5'a), 3.97 (dd, *J* = 3.8, 11.4, 1H, H-5'b), 4.13 (td, *J* = 2.5, 3.6, 1H, H-4'), 4.29 (t, *J* = 3.8, 1H, H-3'), 4.46 (t, *J* = 4.6, 1H, H-2'), 4.88 (d, *J* = 2.5, 2H, NCH₂), 5.99 (d, *J* = 4.9, 1H, H-1'), 8.19 (s, 1H, H-8), 8.29 (s, 1H, H-2). ¹³C NMR (125 MHz): ppm -5.4, -5.0, -4.7, -4.7, -4.4, 17.8, 18.1, 18.5, 25.6, 25.8, 26.1, 34.9, 62.4, 71.7, 75.6, 76.7, 76.8, 85.5, 88.1, 124.4, 138.9, 145.7, 147.4, 155.9; HR-ESI MS (*m/z*): [M+H]⁺ calcd for C₃₁H₅₇N₄O₅Si₃, 649.3636; found 649.3647.

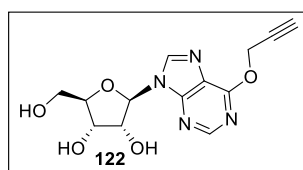


***N*¹-Propynyl-inosine (124).** To a stirred solution of **140** (0.30 g, 0.46 mmol) in MeOH (18 mL), ammonium fluoride (0.17 g, 4.60 mmol) was added at rt. The reaction mixture was warmed to reflux and stirred for 24 h; afterwards the solvent was removed under reduced pressure. Chromatography of the crude residue over silica gel (EtOAc:MeOH = 97:3 gave the pure **124** (0.12 g, 85% yield) as a white solid. ¹H NMR (300 MHz, CDCl₃): δ 2.95 (bs, 1H, CH), 3.77 (dd, *J* = 1.6, 11.8, 1H, H-5'a), 3.90 (dd, *J* = 2.5, 11.8, 1H, H-5'b), 4.12-4.18 (m, 1H, H-4'), 4.35 (, *J*_T = 3.9, 1H, H-3'), 4.64 (t, *J* = 5.0, 1H, H-2'), 4.93 (s, 2H, NHCH₂), 6.02 (d, *J* = 5.0, 1H, H-1'), 8.38 (s, 1H, H.8), 8.47 (s, 1H, H-2). ¹³C NMR (75 MHz): ppm 34.6, 61.0, 70.2, 74.0, 73.8, 74.5, 76.2, 85.8, 88.8, 123.4, 139.5, 146.9, 155.5. HR-ESI MS (*m/z*): [M+Na]⁺ calcd for C₁₃H₁₄N₄O₅Na, 329.0862; found 329.0854.



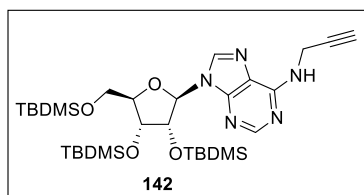
6-O-Propynyl-2',3',5'-O-tri(tert-butyldimethylsilyl)-inosine (141). PyBOP (1.36 g, 2.62 mmol) and Cs_2CO_3 (0.85 g, 2.62 mmol) were added to a stirred solution of **139** (0.80 g, 1.31 mmol) in dry THF (17 mL) under nitrogen atmosphere. The solution was kept to rt for 20 min and then the solvent was removed under reduced pressure. The crude mixture was

dissolved in propargyl alcohol (1.5 mL) and Cs_2CO_3 (0.85 g, 2.62 mmol) was added at rt under nitrogen atmosphere. After 4h the solution was extracted with EtOAc and washed with brine. The organic layer was dried over Na_2SO_4 and the solvent evaporated under reduced pressure. Chromatography of the crude residue over silica gel (hexane/EtOAc = 85:15) gave the pure **141** (0.56 g, 66% yield; 95% yield on recovered starting material) as a white solid. ^1H NMR (300 MHz, CDCl_3): δ -0.21 (s, 3H, CH_3 -Si), -0.03 (s, 3H, CH_3 -Si), 0.09 (s, 3H, CH_3 -Si), 0.10 (s, 3H, CH_3 -Si), 0.13 (s, 3H, CH_3 -Si), 0.14 (s, 3H, CH_3 -Si), 0.80 (s, 9H, *t*-Bu), 0.93 (s, 9H, *t*-Bu), 0.95 (s, 9H, *t*-Bu), 2.50 (t, J = 2.3 Hz, 1H, CH), 3.79 (dd, J = 2.5, 11.4, 1H, H-5'a), 4.03 (dd, J = 3.6, 11.4, 1H, H-5'b), 4.13 (td, J = 3.5, 6.1, 1H, H-4'), 4.32 (t, J = 4.0, 1H, H-3'), 4.59 (t, J = 4.8, 1H, H-2'), 5.23 (d, J = 2.3, 2H, OCH_2), 6.09 (d, J = 4.8, 1H, H-1'), 8.37 (s, 1H, H-8), 8.55 (s, 1H, H-2). ^{13}C NMR (125 MHz): ppm -5.1, -4.7, -4.4, -4.1, 18.1, 18.3, 18.8, 25.9, 26.1, 26.4, 54.4, 62.7, 72.1, 75.3, 76.4, 78.4, 85.7, 88.8, 122.2, 141.8, 152.0, 152.5, 159.7; HR-ESI MS (m/z): $[\text{M}+\text{H}]^+$ calcd for $\text{C}_{31}\text{H}_{57}\text{N}_4\text{O}_5\text{Si}_3$, 649.3636; found 649.3657.



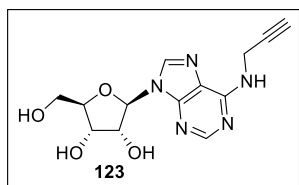
6-O-Propynyl-inosine (122). To a stirred solution of **141** (0.30 g, 0.46 mmol) in MeOH (18 mL), ammonium fluoride (0.17 g, 4.60 mmol) was added at rt. The reaction mixture was warmed to reflux and stirred for 24 h; afterwards the solvent was removed under reduced pressure. Chromatography of the crude residue over silica gel (AcOEt:MeOH = 98:2) gave the pure **122** (110 mg, 78% yield) as a white solid.

^1H NMR (300 MHz, MeOD): δ 3.01 (t, J = 2.4, 1H, CH), 3.78 (dd, J = 3.0, 12.4, 1H, H-5'a), 3.91 (dd, J = 3.6, 12.4, 1H, H-5'b), 4.18-4.21 (m, 1H, H-4'), 4.38 (dd, J = 3.5, 5.6, 1H, H-3'), 4.74 (t, J = 5.6, 1H, H-2'), 5.29 (d, J = 2.4 Hz, 2H, OCH_2), 6.11 (d, J = 5.6, 1H, H-1'), 8.55 (s, 1H, H-8), 8.58 (s, 1H, H-2). ^{13}C NMR (75 MHz, MeOD): ppm 61.4, 70.5, 74.0, 75.1, 77.1, 86.0, 89.3, 121.1, 142.5, 151.2, 159.1. HR-ESI MS (m/z): $[\text{M}+\text{H}]^+$ calcd for $\text{C}_{13}\text{H}_{15}\text{N}_4\text{O}_5$, 307.1042; found 307.1042.



6-N-Propynyl-2',3',5'-O-tri(tert-butyldimethylsilyl) - adenosine (142). To a stirred solution of **139** (1.2 g, 1.96 mmol) in dry DCM (70 mL) triethylamine (0.54 mL, 3.92 mmol), 2,4,6-triisopropylphenylsulfonyl chloride (1.19 g, 3.92 mmol) and DMAP (0.03 g, 0.25 mmol) were added under nitrogen atmosphere. The reaction mixture was stirred

for 14 h and then was diluted with DCM. The organic layer was washed with brine, dried over Na_2SO_4 and the solvent evaporated under reduced pressure. The crude mixture was dissolved in EtOH (90 mL) and propargylamine (0.63 mL, 9.8 mmol) and DIPEA (1.7 mL, 9.8 mL) were added. The solution was heated to reflux. After 18 h, the reaction mixture was cooled to rt, quenched with water and EtOH was removed under reduced pressure. The aqueous layer was extracted with EtOAc. The organic layer was washed with brine, dried over Na_2SO_4 and the solvent evaporated under reduced pressure. Chromatography of the crude residue over silica gel (hexane/EtOAc = 85:15) gave the pure **142** (0.76 g, 60% yield) as a white solid. ^1H NMR (300 MHz, CDCl_3): δ -0.23 (s, 3H, $\text{CH}_3\text{-Si}$), -0.05 (s, 3H, $\text{CH}_3\text{-Si}$), 0.08 (s, 3H, $\text{CH}_3\text{-Si}$), 0.09 (s, 3H, $\text{CH}_3\text{-Si}$), 0.11 (s, 3H, $\text{CH}_3\text{-Si}$), 0.12 (s, 3H, $\text{CH}_3\text{-Si}$), 0.79 (s, 9H, *t*-Bu), 0.92 (s, 9H, *t*-Bu), 0.94 (s, 9H, *t*-Bu), 2.25 (t, $J = 2.5$, 1H, CH), 3.76 (dd, $J = 2.8$, 11.3, 1H, H-5'a), 4.03 (dd, $J = 4.1$, 11.3, 1H, H-5'b), 4.09-4.12 (m, 1H, H-4'), 4.31 (t, $J = 3.9$, 1H, H-3'), 4.47 (bs, 1H, CH_2NH), 4.68 (t, $J = 5.0$, 1H, H-2'), 6.01 (d, $J = 5.0$, 1H, H-1'), 6.08 (bt, $J = 5.0$, 1H, NH), 8.13 (s, 1H, H-8), 8.41 (s, 1H, H-2). ^{13}C NMR (125 MHz): ppm -5.1, -4.8, -4.4, -4.1, 18.1, 18.3, 18.4, 26.0, 26.1, 26.3, 30.8, 62.8, 71.8, 72.3, 75.9, 80.3, 85.7, 88.7, 120.8, 139.7, 149.7, 153.1, 154.2. HR-ESI MS (m/z): $[\text{M}+\text{H}]^+$ calcd for $\text{C}_{31}\text{H}_{58}\text{N}_5\text{O}_4\text{Si}_3$, 648.3796; found 648.3801.



6-*N*-Propynyl-adenosine (123). To a solution of **142** (0.54 g, 0.83 mmol) in MeOH (32 mL), NH_4F (0.31 g, 8.30 mmol) was added at rt. The reaction mixture was warmed to reflux and stirred for 24 h; afterwards the solvent was removed under reduced pressure. Chromatography of the crude residue over silica gel (DCM:MeOH = 9:1) gave the pure **123** (0.22 g, 87% yield) as a white solid. ^1H NMR (300 MHz, MeOD): δ 2.63 (t, $J = 2.5$ Hz, CH), 3.78 (dd, $J = 2.5$, 12.6, 1H, H-5'a), 3.91 (dd, $J = 2.5$, 12.4, 1H, H-5'b), 4.19 (d, $J = 2.5$, 1H, H-4'), 4.34 (dd, $J = 2.5$, 5.0, 1H, H-3'), 4.42 (bs, 2H, NHCH_2), 4.76 (dd, $J = 5.0$, 6.0, 1H, H-2'), 5.98 (d, $J = 6.0$, 1H, H-1'), 8.29 (s, 1H, H-8), 8.30 (s, 1H, H-2). ^{13}C NMR (75 MHz, $\text{DMSO-}d_6$): ppm 29.4, 61.7, 70.7, 72.5, 73.8, 81.8, 85.9, 88.0, 119.9, 140.2, 149.1, 152.3, 154.1; HR-ESI MS (m/z): $[\text{M}+\text{H}]^+$ calcd for $\text{C}_{13}\text{H}_{16}\text{N}_5\text{O}_4$, 306.1202; found 306.1197.

6.5 BIBLIOGRAPHY

- (1) Debing, Y.; Neyts, J.; Delang, L. The Future of Antivirals. *Curr. Opin. Infect. Dis.* **2015**, *28* (6), 596–602. <https://doi.org/10.1097/QCO.0000000000000212>.
- (2) De Clercq, E.; Li, G. Approved Antiviral Drugs over the Past 50 Years. *Clin. Microbiol. Rev.* **2016**, *29* (3), 695–747. <https://doi.org/10.1128/CMR.00102-15>.
- (3) Jordheim, L. P.; Durantel, D.; Zoulim, F.; Dumontet, C. Advances in the Development of Nucleoside and Nucleotide Analogues for Cancer and Viral Diseases. *Nat. Rev. Drug Discov.* **2013**,

- 12 (6), 447–464. <https://doi.org/10.1038/nrd4010>.
- (4) Martinez, J. P.; Sasse, F.; Brönstrup, M.; Diez, J.; Meyerhans, A. Antiviral Drug Discovery: Broad-Spectrum Drugs from Nature. *Nat. Prod. Rep.* **2015**, *32* (1), 29–48. <https://doi.org/10.1039/c4np00085d>.
 - (5) Liu, X.; Ouyang, T.; Ouyang, H.; Ren, L. Single Particle Labeling of RNA Virus in Live Cells. *Virus Res.* **2017**, *237* (March), 14–21. <https://doi.org/10.1016/j.virusres.2017.05.007>.
 - (6) Smith, A. E. How Viruses Enter Animal Cells. *Science (80-.)*. **2004**, *304* (5668), 237–242. <https://doi.org/10.1126/science.1094823>.
 - (7) Müller, T.; Sakin, V.; Müller, B. A Spotlight on Viruses—Application of Click Chemistry to Visualize Virus-Cell Interactions. *Molecules* **2019**, *24* (3), 481. <https://doi.org/10.3390/molecules24030481>.
 - (8) Liu, S.-L.; Wang, Z.-G.; Xie, H.-Y.; Liu, A.-A.; Lamb, D. C.; Pang, D.-W. Single-Virus Tracking: From Imaging Methodologies to Virological Applications. *Chem. Rev.* **2020**, *120* (3), 1936–1979. <https://doi.org/10.1021/acs.chemrev.9b00692>.
 - (9) Kops, A. de B.; Knipe, D. M. Formation of DNA Replication Structures in Herpes Virus-Infected Cells Requires a Viral DNA Binding Protein. *Cell* **1988**, *55* (5), 857–868. [https://doi.org/10.1016/0092-8674\(88\)90141-9](https://doi.org/10.1016/0092-8674(88)90141-9).
 - (10) Ligasová, A.; Strunin, D.; Liboska, R.; Rosenberg, I.; Koberna, K. Atomic Scissors: A New Method of Tracking the 5-Bromo-2'-Deoxyuridine-Labeled DNA In Situ. *PLoS One* **2012**, *7* (12), e52584. <https://doi.org/10.1371/journal.pone.0052584>.
 - (11) Salic, A.; Mitchison, T. J. A Chemical Method for Fast and Sensitive Detection of DNA Synthesis in Vivo. *Proc. Natl. Acad. Sci. U. S. A.* **2008**, *105* (7), 2415–2420. <https://doi.org/10.1073/pnas.0712168105>.
 - (12) Qu, D.; Wang, G.; Wang, Z.; Zhou, L.; Chi, W.; Cong, S.; Ren, X.; Liang, P.; Zhang, B. 5-Ethynyl-2'-Deoxycytidine as a New Agent for DNA Labeling: Detection of Proliferating Cells. *Anal. Biochem.* **2011**, *417* (1), 112–121. <https://doi.org/10.1016/j.ab.2011.05.037>.
 - (13) Neef, A. B.; Samain, F.; Luedtke, N. W. Metabolic Labeling of DNA by Purine Analogues in Vivo. *ChemBioChem* **2012**, *13* (12), 1750–1753. <https://doi.org/10.1002/cbic.201200253>.
 - (14) Jao, C. Y.; Salic, A. Exploring RNA Transcription and Turnover in Vivo by Using Click Chemistry. *Proc. Natl. Acad. Sci. U. S. A.* **2008**, *105* (41), 15779–15784. <https://doi.org/10.1073/pnas.0808480105>.
 - (15) Best, M. D. Click Chemistry and Bioorthogonal Reactions: Unprecedented Selectivity in the Labeling of Biological Molecules. *Biochemistry* **2009**, *48* (28), 6571–6584. <https://doi.org/10.1021/bi9007726>.
 - (16) Kolb, H. C.; Finn, M. G.; Sharpless, K. B. Click Chemistry: Diverse Chemical Function from a Few Good Reactions. *Angew. Chemie Int. Ed.* **2001**, *40* (11), 2004–2021. [https://doi.org/10.1002/1521-3773\(20010601\)40:11<2004::AID-ANIE2004>3.0.CO;2-5](https://doi.org/10.1002/1521-3773(20010601)40:11<2004::AID-ANIE2004>3.0.CO;2-5).
 - (17) Buck, S. B.; Bradford, J.; Gee, K. R.; Agnew, B. J.; Clarke, S. T.; Salic, A. Detection of S-Phase Cell Cycle Progression Using 5-Ethynyl-2'- Deoxyuridine Incorporation with Click Chemistry, an Alternative to Using 5-Bromo-2'-Deoxyuridine Antibodies. *Biotechniques* **2008**, *44* (7), 927–929. <https://doi.org/10.2144/000112812>.
 - (18) Sekine, E.; Schmidt, N.; Gaboriau, D.; O'Hare, P. Spatiotemporal Dynamics of HSV Genome

- Nuclear Entry and Compaction State Transitions Using Bioorthogonal Chemistry and Super-Resolution Microscopy. *PLOS Pathog.* **2017**, *13* (11), e1006721. <https://doi.org/10.1371/journal.ppat.1006721>.
- (19) Alandijany, T.; Roberts, A. P. E.; Conn, K. L.; Loney, C.; McFarlane, S.; Orr, A.; Boutell, C. Correction: Distinct Temporal Roles for the Promyelocytic Leukaemia (PML) Protein in the Sequential Regulation of Intracellular Host Immunity to HSV-1 Infection. *PLOS Pathog.* **2018**, *14* (2), e1006927. <https://doi.org/10.1371/journal.ppat.1006927>.
- (20) Wang, I.-H.; Suomalainen, M.; Andriasyan, V.; Kilcher, S.; Mercer, J.; Neef, A.; Luedtke, N. W.; Greber, U. F. Tracking Viral Genomes in Host Cells at Single-Molecule Resolution. *Cell Host Microbe* **2013**, *14* (4), 468–480. <https://doi.org/10.1016/j.chom.2013.09.004>.
- (21) Aydin, I.; Weber, S.; Snijder, B.; Samperio Ventayol, P.; Kühbacher, A.; Becker, M.; Day, P. M.; Schiller, J. T.; Kann, M.; Pelkmans, L.; Helenius, A.; Schelhaas, M. Large Scale RNAi Reveals the Requirement of Nuclear Envelope Breakdown for Nuclear Import of Human Papillomaviruses. *PLoS Pathog.* **2014**, *10* (5), e1004162. <https://doi.org/10.1371/journal.ppat.1004162>.
- (22) Yakimovich, A.; Huttunen, M.; Zehnder, B.; Coulter, L. J.; Gould, V.; Schneider, C.; Kopf, M.; McInnes, C. J.; Greber, U. F.; Mercer, J. Inhibition of Poxvirus Gene Expression and Genome Replication by Bisbenzimidazole Derivatives. *J. Virol.* **2017**, *91* (18). <https://doi.org/10.1128/JVI.00838-17>.
- (23) Xu, H.; Franks, T.; Gibson, G.; Huber, K.; Rahm, N.; De Castillia, C.; Luban, J.; Aiken, C.; Watkins, S.; Sluis-Cremer, N.; Ambrose, Z. Evidence for Biphasic Uncoating during HIV-1 Infection from a Novel Imaging Assay. *Retrovirology* **2013**, *10* (1), 70. <https://doi.org/10.1186/1742-4690-10-70>.
- (24) Peng, K.; Muranyi, W.; Glass, B.; Laketa, V.; Yant, S. R.; Tsai, L.; Cihlar, T.; Müller, B.; Kräusslich, H.-G. Quantitative Microscopy of Functional HIV Post-Entry Complexes Reveals Association of Replication with the Viral Capsid. *Elife* **2014**, *3*. <https://doi.org/10.7554/eLife.04114>.
- (25) Hoenen, T.; Shabman, R. S.; Groseth, A.; Herwig, A.; Weber, M.; Schudt, G.; Dolnik, O.; Basler, C. F.; Becker, S.; Feldmann, H. Inclusion Bodies Are a Site of Ebolavirus Replication. *J. Virol.* **2012**, *86* (21), 11779–11788. <https://doi.org/10.1128/JVI.01525-12>.
- (26) Hagemeyer, M. C.; Vonk, A. M.; Monastyrska, I.; Rottier, P. J. M.; de Haan, C. A. M. Visualizing Coronavirus RNA Synthesis in Time by Using Click Chemistry. *J. Virol.* **2012**, *86* (10), 5808–5816. <https://doi.org/10.1128/JVI.07207-11>.
- (27) Baird, N. L.; York, J.; Nunberg, J. H. Arenavirus Infection Induces Discrete Cytosolic Structures for RNA Replication. *J. Virol.* **2012**, *86* (20), 11301–11310. <https://doi.org/10.1128/JVI.01635-12>.
- (28) Meng, L.; Guo, Y.; Tang, Q.; Huang, R.; Xie, Y.; Chen, X. Metabolic RNA Labeling for Probing RNA Dynamics in Bacteria. *Nucleic Acids Res.* **2020**, *48* (22), 12566–12576. <https://doi.org/10.1093/nar/gkaa1111>.
- (29) Ligasová, A.; Liboska, R.; Friedecký, D.; Mičová, K.; Adam, T.; Ozdian, T.; Rosenberg, I.; Koberna, K. Dr Jekyll and Mr Hyde: A Strange Case of 5-Ethynyl-2'-Deoxyuridine and 5-Ethynyl-2'-Deoxycytidine. *Open Biol.* **2016**, *6* (1). <https://doi.org/10.1098/rsob.150172>.
- (30) Venkatesham, A.; Pillalamarri, S. R.; De Wit, F.; Lescrinier, E.; Debyser, Z.; Van Aerschot, A. Propargylated Purine Deoxynucleosides: New Tools for Fluorescence Imaging Strategies.

- Molecules* **2019**, *24* (3), 1–16. <https://doi.org/10.3390/molecules24030468>.
- (31) De Wit, F.; Pillalamarri, S. R.; Sebastián-Martín, A.; Venkatesham, A.; Van Aerschot, A.; Zeger Debyser, X. Design of Reverse Transcriptase–Specific Nucleosides to Visualize Early Steps of HIV-1 Replication by Click Labeling. *J. Biol. Chem.* **2019**, *294* (31), 11863–11875. <https://doi.org/10.1074/jbc.RA118.007185>.
- (32) Boldescu, V.; Behnam, M. A. M.; Vasilakis, N.; Klein, C. D. Broad-Spectrum Agents for Flaviviral Infections: Dengue, Zika and Beyond. *Nat. Rev. Drug Discov.* **2017**, *16* (8), 565–586. <https://doi.org/10.1038/nrd.2017.33>.
- (33) Robson, F.; Khan, K. S.; Le, T. K.; Paris, C.; Demirbag, S.; Barfuss, P.; Rocchi, P.; Ng, W.-L. Coronavirus RNA Proofreading: Molecular Basis and Therapeutic Targeting. *Mol. Cell* **2020**, *79* (5), 710–727. <https://doi.org/10.1016/j.molcel.2020.07.027>.
- (34) Böge, N.; Gräsl, S.; Meier, C. Synthesis and Properties of Oligonucleotides Containing C8-Deoxyguanosine Arylamine Adducts of Borderline Carcinogens †. *J. Org. Chem.* **2006**, *71* (26), 9728–9738. <https://doi.org/10.1021/jo061803t>.
- (35) Lazear, H. M.; Stringer, E. M.; de Silva, A. M. The Emerging Zika Virus Epidemic in the Americas. *JAMA* **2016**, *315* (18), 1945. <https://doi.org/10.1001/jama.2016.2899>.
- (36) Bassetto, M.; Cima, C. M.; Basso, M.; Salerno, M.; Schwarze, F.; Friese, D.; Bugert, J. J.; Brancale, A. Novel Nucleoside Analogues as Effective Antiviral Agents for Zika Virus Infections. *Molecules* **2020**, *25* (20). <https://doi.org/10.3390/molecules25204813>.

APPENDIX A

Publications

-
1. De Fenza, M.; D'Alonzo, D.; Esposito, A.; Munari, S.; Loberto, N.; Santangelo, A.; Lampronti, I.; Tamanini, A.; Rossi, A.; Ranucci, S.; De Fino, I.; Bragonzi, A.; Aureli, M.; Bassi, R.; Tironi, M.; Lippi, G.; Gambari, R.; Cabrini, G.; Palumbo, G.; Dehecchi, M. C.; Guaragna, A. Exploring the Effect of Chirality on the Therapeutic Potential of N-Alkyl-Deoxyiminosugars: Anti-Inflammatory Response to *Pseudomonas Aeruginosa* Infections for Application in CF Lung Disease. *Eur. J. Med. Chem.* **2019**, *175*, 63–71. <https://doi.org/10.1016/j.ejmech.2019.04.061>.
 2. Esposito, A.; De Gregorio, E.; De Fenza, M.; D'Alonzo, D.; Satawani, A.; Guaragna, A. Expedient Synthesis and Preliminary Antimicrobial Activity of Deflazacort and Its Precursors. *RSC Adv.* **2019**, *9* (37), 21519–21524. <https://doi.org/10.1039/C9RA03673C>.
 3. Esposito, A.; Giovanni, C.; De Fenza, M.; Talarico, G.; Chino, M.; Palumbo, G.; Guaragna, A.; D'Alonzo, D. A Stereoconvergent Tsuji–Trost Reaction in the Synthesis of Cyclohexenyl Nucleosides. *Chem. – A Eur. J.* **2020**, *26* (12), 2597–2601. <https://doi.org/10.1002/chem.201905367>.
 4. Esposito, A.; Vollaro, A.; Esposito, E. P.; D'Alonzo, D.; Guaragna, A.; Zarrilli, R.; De Gregorio, E. Antibacterial and Antivirulence Activity of Glucocorticoid PYED-1 against *Stenotrophomonas Maltophilia*. *Antibiotics* **2020**, *9* (3), 105. <https://doi.org/10.3390/antibiotics9030105>.
 5. Vollaro, A.; Esposito, A.; Antonaki, E.; Iula, V. D.; D'Alonzo, D.; Guaragna, A.; De Gregorio, E. Steroid Derivatives as Potential Antimicrobial Agents against *Staphylococcus Aureus* Planktonic Cells. *Microorganisms* **2020**, *8* (4), 468. <https://doi.org/10.3390/microorganisms8040468>.
 6. De Fenza, M.; Eremeeva, E.; Troisi, R.; Yang, H.; Esposito, A.; Sica, F.; Herdewijn, P.; D'Alonzo, D.; Guaragna, A. Structure–Activity Relationship Study of a Potent α -Thrombin Binding Aptamer Incorporating Hexitol Nucleotides. *Chem. - A Eur. J.* **2020**, *26* (43), 9589–9597. <https://doi.org/10.1002/chem.202001504>.
 7. Vollaro, A.; Esposito, A.; Esposito, E. P.; Zarrilli, R.; Guaragna, A.; De Gregorio, E. PYED-1 Inhibits Biofilm Formation and Disrupts the Preformed Biofilm of *Staphylococcus Aureus*. *Antibiotics* **2020**, *9* (5), 240. <https://doi.org/10.3390/antibiotics9050240>.
 8. De Gregorio, E.; Esposito, A.; Vollaro, A.; De Fenza, M.; D'Alonzo, D.; Migliaccio, A.; Iula, V. D.; Zarrilli, R.; Guaragna, A. N-Nonyloxypentyl-l-Deoxynojirimycin Inhibits Growth, Biofilm Formation and Virulence Factors Expression of *Staphylococcus Aureus*. *Antibiotics* **2020**, *9* (6), 362. <https://doi.org/10.3390/antibiotics9060362>.
 9. Esposito, A.; D'Alonzo, D.; De Fenza, M.; De Gregorio, E.; Tamanini, A.; Lippi, G.; Dehecchi, M. C.; Guaragna, A. Synthesis and Therapeutic Applications of Iminosugars in Cystic Fibrosis. *Int. J. Mol. Sci.* **2020**, *21* (9), 3353. <https://doi.org/10.3390/ijms21093353>.
 10. Esposito, A.; D'Alonzo, D.; D'Errico, S.; De Gregorio, E.; Guaragna, A. Toward the Identification of Novel Antimicrobial Agents: One-Pot Synthesis of Lipophilic Conjugates of N-Alkyl d- and l-Iminosugars. *Mar. Drugs* **2020**, *18* (11), 572. <https://doi.org/10.3390/md18110572>.
-

